

UC Davis

Research Reports

Title

Preliminary Study on Developing a Surrogate Performance-Related Test for Fatigue Cracking of Asphalt Pavements

Permalink

<https://escholarship.org/uc/item/52d1d1q5>

Authors

Jiao, Liya
Harvey, John
Wu, Rongzong
et al.

Publication Date

2023-04-01

DOI

10.7922/G2TM78D9

Preliminary Study on Developing a Surrogate Performance-Related Test for Fatigue Cracking of Asphalt Pavements

Authors:

Liya Jiao, John Harvey, Rongzong Wu, Mohamed Elkashef, David Jones, and Yanlong Liang

Partnered Pavement Research Center (PPRC) Project Number 3.40 (DRISI Task 3187):
Performance-Related Testing in Superpave

PREPARED FOR:

California Department of Transportation
Division of Research, Innovation, and System Information
Office of Materials and Infrastructure

PREPARED BY:

University of California
Pavement Research Center
UC Davis, UC Berkeley




TECHNICAL REPORT DOCUMENTATION PAGE

1. REPORT NUMBER UCPRC-RR-2021-02	2. GOVERNMENT ASSOCIATION NUMBER	3. RECIPIENT'S CATALOG NUMBER
4. TITLE AND SUBTITLE Preliminary Study on Developing a Surrogate Performance-Related Test for Fatigue Cracking of Asphalt Pavements		5. REPORT PUBLICATION DATE April 2023
		6. PERFORMING ORGANIZATION CODE
7. AUTHOR(S) Liya Jiao (ORCID 0000-0003-0648-693X) John Harvey (ORCID 0000-0002-8924-6212) Rongzong Wu (ORCID 0000-0001-7364-7583) Mohamed Elkashef (0000-0002-8028-1935) David Jones (ORCID 0000-0002-2938-076X) Yanlong Liang (ORCID 0000-0002-7538-9757)		8. PERFORMING ORGANIZATION REPORT NO. UCPRC-RR-2021-02 UCD-ITS-RR-21-52
9. PERFORMING ORGANIZATION NAME AND ADDRESS University of California Pavement Research Center Department of Civil and Environmental Engineering, UC Davis 1 Shields Avenue Davis, CA 95616		10. WORK UNIT NUMBER
		11. CONTRACT OR GRANT NUMBER 65A0628
12. SPONSORING AGENCY AND ADDRESS California Department of Transportation Division of Research, Innovation, and System Information P.O. Box 942873 Sacramento, CA 94273-0001		13. TYPE OF REPORT AND PERIOD COVERED Research Report October 2017 to October 2020
		14. SPONSORING AGENCY CODE
15. SUPPLEMENTAL NOTES DOI:10.7922/G2TM78D9		
16. ABSTRACT Currently, no performance-related test exists for fatigue cracking for use in routine asphalt mix design to approve job mix formula (JMF) and quality control and quality assurance (QC/QA) in California. The existing four-point bending (4PB) test was developed to evaluate the fatigue performance of asphalt pavement, but it is not necessarily appropriate for use in routine JMF and it is too slow for QC/QA. The objective of this study is to evaluate potential surrogate fatigue performance-related testing methods and identify a test that is simple and easy to perform but also able to provide guidance for asphalt mix design on routine projects and QC/QA on all projects. This report compares potential performance-related tests with 4PB tests for simplicity, repeatability (variability), and their relationship to stiffness and fatigue life. Tests evaluated in this study included the semicircular bend (SCB) test, indirect tensile asphalt cracking test (IDEAL-CT), and fatigue testing on fine aggregate matrix (FAM) mixes with linear amplitude sweep (LAS) analysis. These tests were conducted on a variety of asphalt mixtures. Fracture parameters obtained from SCB and IDEAL-CT tests and fatigue parameters from FAM mixes were included as potential fatigue cracking indicators. Linear regression analysis was used to correlate these indicators with the stiffness and fatigue life from 4PB tests. The comparison analysis demonstrates that SCB and IDEAL-CT tests are providing the same fracture information. Fracture parameters from SCB and IDEAL-CT tests are well correlated with the initial flexural stiffness from 4PB tests, and the initial flexural stiffness has a moderate inverse nonlinear correlation with the fatigue life from the controlled-strain 4PB tests. As the IDEAL-CT test is faster and requires less specimen preparation, the recommendation is that attention focus on this test. All the fracture tests indicate that the <i>Strength</i> parameter has low variability and good correlation with 4PB flexural stiffness and a moderate correlation with flexural fatigue, and it is proposed as a surrogate indicator for flexural stiffness and an indication of fatigue life. The FAM test showed promise regarding matching 4PB fatigue life as well as stiffness. The relationships identified in this study between flexural stiffness and flexural fatigue life and between flexural stiffness and the <i>Strength</i> parameter from the IDEAL-CT tests were used to develop a preliminary approach to using the <i>Strength</i> parameter to place upper and lower boundary limits on the stiffness of mixes for use in routine mix design and QC/QA. Examples of this approach are presented in the appendices based on flexural fatigue testing and on setting of those limits without 4PB tests. The sensitivity of performance for both approaches is demonstrated by mechanistic-empirical simulation using <i>CalME</i> . Recommendations are made to further develop the IDEAL-CT <i>Strength</i> parameter for routine mix design and QC/QA, with limits set following the approach developed in this study. Review of pavement management system field cracking data and indirect tensile strength from the AASHTO T 283 test in Caltrans databases is recommended to help this development. Further development of FAM mixes LAS testing is also recommended.		
17. KEY WORDS fatigue cracking, SCB, IDEAL-CT, FAM mixes, performance-related testing, 4PB fatigue test	18. DISTRIBUTION STATEMENT No restrictions. This document is available to the public through the National Technical Information Service, Springfield, VA 22161	
19. SECURITY CLASSIFICATION (of this report) Unclassified	20. NUMBER OF PAGES 148	21. PRICE None

Reproduction of completed page authorized

UCPRC ADDITIONAL INFORMATION

1. DRAFT STAGE Final	2. VERSION NUMBER 1				
3. PARTNERED PAVEMENT RESEARCH CENTER STRATEGIC PLAN ELEMENT NUMBER 3.40	4. DRISI TASK NUMBER 3187				
5. CALTRANS TECHNICAL LEAD AND REVIEWER(S) Raghubar Shrestha	6. FHWA NUMBER CA223187A				
7. PROPOSALS FOR IMPLEMENTATION No recommendation for immediate implementation based on results from this report. Recommend further evaluation of use of recommended test, its variability, and the effectiveness of the recommended parameter for use in design and QC/QA, through pilot projects, moving toward implementation. Further development of FAM testing is also recommended.					
8. RELATED DOCUMENTS None					
9. LABORATORY ACCREDITATION The UCPRC laboratory is accredited by AASHTO re:source for the tests listed in this report.					
10. SIGNATURES					
L. Jiao FIRST AUTHOR	J.T. Harvey TECHNICAL REVIEW	C. Fink EDITOR	J.T. Harvey PRINCIPAL INVESTIGATOR	R. Shrestha CALTRANS TECH. LEAD	T.J. Holland CALTRANS CONTRACT MANAGER

Reproduction of completed page authorized

DISCLAIMER

This document is disseminated in the interest of information exchange. The contents of this report reflect the views of the authors who are responsible for the facts and accuracy of the data presented herein. The contents do not necessarily reflect the official views or policies of the State of California or the Federal Highway Administration. This publication does not constitute a standard, specification, or regulation. This report does not constitute an endorsement by the Department of any product described herein.

For individuals with sensory disabilities, this document is available in alternate formats. For information, call (916) 654-8899, TTY 711, or write to California Department of Transportation, Division of Research, Innovation and System Information, MS-83, P.O. Box 942873, Sacramento, CA 94273-0001.

ACKNOWLEDGMENTS

This project was funded by the California Department of Transportation, Division of Research, Innovation, and System Information. The authors would like to acknowledge the support, assistance, and direction of Raghubar Shrestha and T. Joseph Holland of Caltrans. The technical reviews and comments on this report from Caltrans reviewers are greatly appreciated. Special thanks to the UCPRC laboratory staff for help with material preparation and testing. The authors would also like to acknowledge UCPRC Senior Editor Camille Fink for providing detailed editing of the content of this report.

PROJECT OBJECTIVES

The objective of this project is to develop a surrogate test for asphalt mixture design and quality control/quality assurance (QC/QA) to evaluate fatigue cracking performance. Preliminary research on this topic has been completed in this study. The focus of this report includes the following tasks:

1. A literature review on research related to the topic, with special emphasis on the work of fatigue and fracture properties of asphalt material, fatigue and fracture testing on asphalt mixtures, and testing methods of asphalt material at small scales.
2. Selection of candidate surrogate fatigue cracking tests and identification of representative parameters based on the literature review.
3. Design of an experimental plan for a range of asphalt mixtures with varying material properties for four-point bend (4PB) fatigue tests and candidate surrogate tests in the University of California Pavement Research Center (UCPRC) laboratory.
4. Completion of tests and interpretation of testing results.
5. Recommendation of the surrogate test along with an index and the corresponding acceptance criteria determination process.
6. Preparation of a summary report detailing the study.

This report covers all tasks.

EXECUTIVE SUMMARY

Fatigue cracking in asphalt pavements is a nationwide problem faced by every highway agency on roads that carry heavy vehicles (trucks and buses). Increasing numbers of trucks and more usage of recycled materials (reclaimed asphalt pavement [RAP] and recycled asphalt shingles [RAS]) may make current situations even worse. Therefore, there is an urgent need to develop a performance-related test for routine asphalt mix design and quality control and quality assurance (QC/QA) to minimize fatigue cracking problems. Age-related cracking is a top-down distress that is related to environmental conditions and eventually occurs on all asphalt pavements, regardless of the vehicle traffic. This study includes a literature review of research on the fatigue and fracture properties of asphalt material; selection of candidate surrogate tests; testing of fracture and fatigue performance for asphalt material varying in RAP and RAS content, binder types, and preparation methods of mixtures; and evaluation of these surrogate testing methods for use in routine mix design and QC/QA.

Key points from the literature review include the following:

- The fatigue life of asphalt pavement consists of three stages: crack initiation, crack propagation and ultimate failure. Fatigue damage theory is a typical method to model crack initiation, and fracture mechanics is often applied to describe the cracking propagation. Fracture mechanics consists of linear elastic fracture mechanics and elastic plastic fracture mechanics, depending on the fracture state (brittle/ductile) and yielding scale.
- While recently developed fracture testing methods, including semicircular bend (SCB) testing (producing the Illinois Flexibility Index Test [I-FIT] and Louisiana Semicircular Bend Test [LOU-SCB] parameters) and indirect tensile asphalt cracking testing (IDEAL-CT), are simple and rank the cracking performance of asphalt materials based on fracture parameters, they are not focused on the repeated load effects that cause fatigue and reflective cracking. Fracture parameters can be related to age-related cracking (transverse and longitudinal cracking leading to block cracking), which is caused by oxidation of the asphalt mix and thermal contraction, whether a single event or repeated day/night and seasonal temperature changes. They have been related to fatigue and reflective cracking of surface mixes as well as age-related cracking by other researchers. Age-related cracking is top-down from the surface and occurs regardless of the thickness of the new asphalt layer or layers. However, fatigue and reflective cracking are primarily bottom-up from the bottom of the new asphalt layers, and the performance is related not just to mix properties but also the interaction of mix properties and the thickness of the asphalt layers.
- For routine asphalt mix design and/or QC/QA implementation, the surrogate cracking test method requires minimal operator training time, easy specimen fabrication, straightforward interpretation of testing results, and representative indicators for cracking performance. More importantly, this surrogate cracking

test should be able to provide a reasonable estimate of the flexural stiffness and flexural fatigue life from four-point bending (4PB) testing.

- SCB and IDEAL-CT testing have been validated against a limited amount of field cracking data and the ranking comparison implies that these tests are applicable to mix design or QC/QA implementation. However, a more comprehensive study of these testing methods on a wider range of asphalt material types and a large correlation study with fatigue testing have not yet been conducted.
- In previous studies, cracking resistance indicators from SCB and IDEAL-CT tests showed good sensitivities to asphalt material mix variables, primarily binder type (including conventional, polymer-modified, rubberized), and inclusion of RAP, which is critical in providing guidance in mix design procedures. Air void content and aggregate gradation variance were not variables that were examined.
- Linear amplitude sweep (LAS) fatigue testing on fine aggregate matrix (FAM) mixes also stands out as a good candidate for a surrogate fatigue cracking test. It is capable of capturing the fatigue properties of the FAM mix portion of the full asphalt mixture. Understanding the damage and cracking mechanisms in the FAM portion will help characterize asphalt pavement fatigue performance and may provide a faster and easier test than the 4PB test. However, this test will not be as fast and easy as SCB and IDEAL-CT testing.
- Based on the literature review, I-FIT, LOU-SCB, and IDEAL-CT testing and LAS testing of FAM mixes were chosen for surrogate performance-related testing to serve the function of 4PB fatigue tests for routine mix design and QC/QA implementation.

An experimental design was developed for each candidate testing method. Cracking parameters, including the ones recommended in the corresponding standard and potential ones from the literature review, were calculated from the testing results. Each testing method was then evaluated in terms of repeatability (variability) and correlation with stiffness and fatigue performance obtained from 4PB fatigue tests.

Key observations and findings from the I-FIT test on 36 asphalt mixtures include the following:

- Loading versus displacement curves from three loading rates (0.5 in./min [12.5 mm/min], 1 in./min [25 mm/min], 2 in./min [50 mm/min]) show that asphalt mixtures fracture in a brittle form at higher loading rates, as expected. They also show that the flexibility index (*FI*) value decreases as the loading rate increases. However, the Tukey's honestly significant difference (HSD) testing results indicate no significant difference among these three loading rates. In evaluating pairs of mixtures, the Tukey's HSD test results show that the loading rate of 2 in./min (50 mm/min) outperforms the two slower loading rates.
- Previous verification of the I-FIT test with field data from the University of Illinois suggests a strong relationship between *FI* from the I-FIT test and early-age transverse cracking. Age-related cracking is more important for asphalt pavements that do not have significant heavy vehicle traffic. However, the

fatigue cracking performance at an intermediate temperature is the main focus of this study because it is the primary mode of structural failure for asphalt surfaced pavements in California that carry heavy vehicles. The relationship between the I-FIT test and fatigue cracking performance was explored by comparing the I-FIT parameters against the 4PB fatigue parameters.

- Seven fracture parameters—including slope parameters (post-peak slope [S_{pp}] and ascending slope [S_{asc}]), flexibility index (FI), flexibility index calculated using ascending slope (FI_{asc}), fracture toughness (KIC), *Strength*, and fracture energy (G_f)—were reviewed in this study. The variability of each parameter was evaluated using coefficient of variance (COV) values. FI and S_{pp} had the highest variability while KIC and *Strength* demonstrate the best repeatability, with COV values of 11%.
- Fatigue performance from the 4PB tests is represented by the strain value for fatigue life of one million cycles (*StrainNfIM*) and initial flexural stiffness ($E50$). The relationship between fatigue performance and fracture performance was examined by comparing the *StrainNfIM* and $E50$ with fracture parameters. Both KIC and *Strength* show a moderate linear positive correlation with the initial flexural stiffness ($E50$), but no significant correlation was found between *StrainNfIM* and any fracture parameter.

LOU-SCB testing was conducted on seven asphalt mixtures. The fracture properties obtained from two SCB testing configurations (LOU-SCB and I-FIT) were compared. The relationship between the fracture parameters of LOU-SCB and fatigue parameters from 4PB tests was also investigated. The following conclusions can be drawn from this analysis:

- There is a strong linear correlation between the critical J -integral (J_c) from the LOU-SCB test and the area of load-displacement curve before peak load (*AreaBefore*) from the I-FIT test. KIC from the I-FIT test also correlates well with J_c . These findings indicate that the I-FIT and LOU-SCB tests provide the same fracture information for these materials.
- A comparison of LOU-SCB parameters with parameters from 4PB testing shows that J_c is strongly correlated with the initial flexural stiffness ($E50$), while the correlation between J_c and *StrainNfIM* is not noticeable.
- These results indicate that, at least for these mixes, the LOU-SCB and I-FIT tests are providing similar information and that the information correlates well with flexural stiffness but not flexural fatigue life.

The IDEAL-CT test was performed on 13 asphalt mixtures. The variability of fracture parameters from the IDEAL-CT test was evaluated. In addition, the IDEAL-CT test was compared to the I-FIT test and then correlated with the fatigue results from the 4PB test. The following conclusions can be drawn from this analysis:

- The fracture parameters from the IDEAL-CT test display lower variability compared with those from the I-FIT test. *Strength* and fracture energy (G_f) show the lowest COV values.

- There are strong correlations between the parameters from the IDEAL-CT test and the ones from the I-FIT test. The cracking tolerance index (*CTindex*) is proposed as a representative fracture resistance parameter in the IDEAL-CT test, which shows a significantly strong linear relationship with *FI*, the cracking indicator developed in the I-FIT test.
- The *Strength* parameter from the IDEAL-CT test (*IDT_Strength*) shows a strong linear correlation with the initial stiffness (*E50*) from the 4PB test, which matches the finding of the strong correlation between *Strength* from the I-FIT test and *E50* from the 4PB test. However, there is no significant relationship between fracture parameters from the IDEAL-CT test and fatigue life from the 4PB tests.

The LAS fatigue testing was conducted on FAM mixes specimens for four types of mixtures, all with 20% or more RAP content, with two different silo hours (without silo hours versus with silo hours). The viscoelastic continuum damage (VECD) model was used to analyze these FAM mixes testing results. The fatigue performance of FAM mixes was then compared with the I-FIT fracture results as well as the 4PB fatigue results. The following observations were made based on this analysis:

- The variability analysis shows that fatigue parameters from FAM mixes LAS testing—including the strain value corresponding to the fatigue failure (*FailureStrain*), damage value at the failure (*DamageLevel*), and the power coefficient *B* in the Wohler’s law—have low average COV values: 11.19%, 3.81% and 3.1%, respectively.
- The comparison between FAM mixes LAS testing and I-FIT testing indicates a good relationship between the power coefficient *B* from Wohler’s law of the LAS testing on FAM mixes and most of the fracture parameters from the I-FIT test.
- The relationship between fatigue life and strain values was analyzed for four types of asphalt material (HRAP_1, HRAP_2, HRAP_3, HRAP_4) of full mixtures and FAM mixes with different silo hours. The VECD analysis of the LAS testing results of FAM mixes shows that the HRAP_1 and HRAP_4 mixtures became stiffer after short-term silo hours (5 silo hours for HRAP_1 and 6 silo hours for HRAP_4). In addition, the fatigue performance of HRAP_1 and HRAP_4 with silo hours is inferior to the mixes without silo hours. However, long-term silo hours did not result in a noteworthy impact on fatigue performance as observed from the comparison between HRAP_0H_2 (HRAP_2 without silo hours) and HRAP_16H_2 (HRAP_2 with 16 silo hours) and the comparison between HRAP_0H_3 (HRAP_3 without silo hours) and HRAP_16H_3 (HRAP_3 with 16 hours). On the other hand, the fatigue results from the 4PB tests indicate that short-term silo hours increased fatigue life, based on the comparison between HRAP_0H_4 (HRAP_4 without silo hours) and HRAP_6H_4 (HRAP_4 with 6 silo hours) and the comparison between HRAP_0H_1 (HRAP_1 without silo hours) and HRAP_5H_1 (HRAP_1 with 5 silo hours). This conclusion matches the findings from the FAM mixes LAS testing results. In terms of the effect of longer

silo hours, comparable fatigue performance was found between HRAP_0H_2 and HRAP_16H_2 while 16 silo hours for HRAP_16H_3 resulted in decreased fatigue life at higher strain values, which are greater than values encountered in the pavement.

- Both the FAM mixes and full mixes fatigue tests reveal that the fatigue performance of HRAP_4, which contains the highest amount of RAP material, is inferior to the fatigue performance of all the other materials. Among all these mixtures, HRAP_1 without silo hours has the most promising fatigue performance at both the FAM and full mixture scales.
- The correlation analysis between FAM mixes fatigue parameters and the 4PB parameters indicates a strong linear correlation between the strain value at fatigue failure (*FailureStrain*) for FAM mixes LAS testing and fatigue life (*StrainNfIM*) for 4PB testing, with an R^2 value of 0.84. As stated previously, the stiffness of asphalt mixtures plays an important role in determining the fatigue cracking resistance of asphalt pavements and also serves as a key property input in the *CalME* fatigue damage model. However, a weak linear relationship exists between the initial shear stiffness from LAS testing and initial elastic stiffness from 4PB testing for the four high RAP/RAS asphalt materials included in this study, with an r value of 0.49.

The ability to distinguish the fatigue cracking resistance between asphalt materials is an important criterion when selecting a surrogate fatigue performance-related test for the asphalt mix design and QC/QA. The following is a summary of the sensitivity of potential tests and corresponding parameters for asphalt mixtures based on the findings reviewed in this report:

- The boxplot of 4PB testing results, including initial stiffness (*E50*) and *StrainNfIM*, provides an overview of the distribution of fatigue properties for different asphalt material types. The distribution of *StrainNfIM* indicates that mixtures of 0% RAP with asphalt rubber (AR) binder and 15% RAP with polymer-modified (PM) binder have the best fatigue cracking resistance and also the softest *E50*. In addition, the mixtures in the category of 50% RAP with recycling agent (RA) have the lowest *StrainNfIM* values and highest *E50* values—although some mixtures in other categories that are much stiffer have better fatigue life, indicating that variables other than stiffness play an important role in fatigue performance.
- The Tukey’s HSD analysis shows that the softest mixtures have better fatigue performance and that stiffer mixtures have lower fatigue cracking resistance among the mixture types containing low RAP content. However, *StrainNfIM* values show that mixtures with RAP content higher than 25% have noticeably weaker fatigue performance, while *E50* could not distinguish these mixes from the rest of the materials.
- The boxplots of the I-FIT test results show that mixtures of 0% RAP with AR binder and 40% RAP with neat binder have the highest *FI* values and are notably different from the rest of the mixtures, while it is difficult to distinguish between the rest of the mixtures based on the *FI* values. The 15% RAP with PM

binder mixtures show the lowest strength, the lowest *E50* value, and the highest *StrainNfIM* value of all the materials.

- The Tukey's HSD grouping results indicate that both *FI* and *Strength* display a fair ability to distinguish between asphalt mixtures. The grouping results of *FI* highly match the fatigue grouping results of *StrainNfIM*, though the grouping primarily separates rubberized and polymer binder mixtures from the rest of the mixtures. Meanwhile, the grouping result of *Strength* is consistent with the *E50* grouping results.
- The analysis of sensitivity to material types using the Tukey's HSD method demonstrates that *Strength* distinguishes between asphalt materials, and the grouping results match the stiffness grouping of asphalt material with low RAP or RAS content.
- In conclusion, *Strength* from the I-FIT test is recommended as the representative indicator for fatigue performance because it provides sensitivity to different materials similar to the stiffness (*E50*) and fatigue life (*StrainNfIM*) measured from the 4PB testing. *Strength* from IDEAL-CT testing might have the same sensitivity to different material types as a strong linear correlation has been found between the IDEAL-CT and I-FIT tests.

A summary and comparison of the surrogate tests is presented as well as a procedure for determining the criteria value for a specific material to implement the *Strength* criteria in practice for QC/QA. Different criteria for the stiffness and fatigue life of materials need to be satisfied depending on the asphalt material application in the pavement structure—for example, in a thin surface layer or in a thick surface layer, intermediate layer, or bottom layer. The general procedure recommended considers the minimum stiffness and the fatigue life (minimum strain value of one million cycles to failure) determined from flexural beam testing (either project-specific requirements or from the *CalME* standard materials library). The material used in the mechanistic-empirical (ME) pavement design using *CalME* provides the input to determination of the *Strength* criteria. Criteria for capital preventive maintenance mixes can be developed using the same approach. The following are the detailed steps to calculate the upper and lower *Strength* criteria:

- Based on the relationship between stiffness and *Strength* from the IDEAL-CT test, the criterion of *Strength_{min}* will be determined to meet the minimum stiffness requirement obtained from the stiffness value at the same temperature and loading rate used in the ME rehabilitation structural design. For maintenance projects where ME design is not used, a reasonable stiffness value for each mix type will need to be determined, which will be used to determine the lowest value for *Strength*.
- The minimum fatigue life requirement will be satisfied by meeting the criterion of *Strength_{max}*, which is the upper bound of *Strength* from the relationship between *Strength* and *StrainNfIM*.

- To help obtain good fatigue and reflective cracking performance of asphalt pavement, the *Strength* value of asphalt material from the IDEAL-CT test needs to fall in the range of $Strength_{min}$ to $Strength_{max}$.

The appendices include a detailed example for deciding the *Strength* range for projects with performance-related specifications as well as validation from *CalME* simulations of the efficacy of the proposed approach. An alternative approach is also shown for determining the upper and lower limits for the *Strength* criteria based on mean stiffness for those projects without performance-related specifications, also with validation from *CalME* simulations.

The following are final conclusions from this study:

- The four testing methods included in this study (three monotonic fracture tests: I-FIT [semicircular notched beam], LOU-SCB [semicircular notched beam], and IDEAL-CT [indirect tensile]; one repetitive fatigue test with increasing strain value: fine aggregate mixes [FAM] mixes with linear amplitude sweep [LAS] test) have simple sample preparation processes and testing operations as well as short testing times compared to the benchmark 4PB test.
- The three fracture testing methods (I-FIT, LOU-SCB and IDEAL-CT) showed good correlations with the initial flexural stiffness for the range of asphalt mixes included in the study (conventional, rubberized, polymer-modified, high RAP), while no strong correlation was found between these tests and flexural fatigue life. The results from the three tests are very well correlated linearly with each other for both the strength and fracture parameters. Considering that they produced very similar results, but the IDEAL-CT test is simpler and faster, the IDEAL-CT test is the recommended test among the three.
- The *Strength* parameter obtained from both I-FIT and IDEAL-CT tests has low variability compared with the respective fracture parameters (*CTindex* from IDEAL-CT and *FI* from I-FIT) and shows a good positive linear correlation with the initial stiffness from the 4PB test. *Strength* from the IDEAL-CT test also has a moderate negative correlation with the fatigue life (*StrainNfIM*) from 4PB. In addition, the initial flexural stiffness from the 4PB fatigue test was found to be nonlinearly well correlated with the fatigue life. Thus, it is proposed that *Strength* be a representative indicator for predicting the initial stiffness of asphalt mixtures. The moderate relationship between *Strength* from IDEAL-CT and 4PB fatigue life, and the good inverse nonlinear correlation between 4PB stiffness and 4PB fatigue life, leads to a conclusion that mix stiffness as measured from IDEAL-CT *Strength* provides a weak inverse indication of the fatigue life.
- A strong correlation exists between the strain at failure from LAS fatigue testing of FAM mixes and the strain value for fatigue life of one million cycles from 4PB fatigue testing of full mixtures, indicating that FAM LAS testing may serve as a good candidate fatigue test for mix design and QC/QA. However, due

to the limited data set in this study, more experiments on various asphalt materials should be conducted. The FAM LAS test is more expensive, time consuming, and complex than IDEAL-CT, but it is less expensive, faster, and simpler than conventional full mix flexural beam testing.

- A procedure for determining the criteria value for a specific material to implement the *Strength* criteria in practice for QC/QA was developed based on the relationships found in this study between flexural stiffness and flexural fatigue, and flexural stiffness and *Strength* from I-FIT and IDEAL-CT tests:
 - Different criteria for the stiffness and fatigue life of materials need to be satisfied depending on the asphalt material application in the pavement structure—for example, in a thin surface layer or in a thick surface layer, intermediate layer, or bottom layer.
 - The general procedure developed in this study considers both the minimum stiffness to provide resistance to bending and a maximum stiffness to provide adequate fatigue life at a given strain (minimum strain value of one million cycles to failure).
 - The criterion of $Strength_{min}$ will be determined to meet the minimum stiffness requirement obtained from the stiffness value at the same temperature and loading rate used in the ME rehabilitation structural design. For maintenance projects where ME design is not used, a reasonable value for each mix type will need to be determined, which will be the lowest value for *Strength*. Thin overlays on existing asphalt or concrete pavement, and thin layers of new asphalt placed on granular or recycled bases, may not require a minimum stiffness (from $Strength_{min}$), while layers in thicker sections will (generally asphalt layers thicker than about 0.2 to 0.3 ft.).
 - The minimum fatigue life requirement will be satisfied by meeting the criterion of $Strength_{max}$, which is the upper bound of *Strength* from the moderately correlated relationship between *Strength* and *StrainNfIM*. To help obtain good fatigue and reflective cracking performance of asphalt pavement, the *Strength* value of asphalt material from the IDEAL-CT test needs to fall in the range of $Strength_{min}$ to $Strength_{max}$.

The following recommendations are made based on the conclusions of this study:

- Further development of the IDEAL-CT *Strength* parameter is recommended for potential use in routine mix design and QC/QA, where use of a performance-related test is warranted by the value of the project and the cost of testing. The main developments needed are a material aging procedure for preparation of test methods and identification of minimum and maximum values for different applications.
- Further development and potential use in piloting for evaluation for implementation of the procedure developed in this study for determining the criteria value for $Strength_{min}$ and $Strength_{max}$ for different applications (asphalt layer thickness, reflective or fatigue cracking, heavy traffic level) are recommended.

- In parallel with development and piloting, it is recommended that a search be done for mix test records from the AASHTO T 283 testing (similar to IDEAL-CT *Strength*) done over the past 10 years by Caltrans and compared with field cracking performance data in the Caltrans Pavement Management System database. The Automated Pavement Condition Survey (APCS) will not distinguish between top-down age-related and bottom-up reflective cracking from previous age-related cracking, which will mostly be transverse, longitudinal, and block cracking. Identification of bottom-up reflective cracking of previous fatigue cracking will be easier to identify because it can only be bottom-up. Consideration will need to be given to new asphalt layer thickness, underlying pavement cracking and thickness, climate, and traffic in analysis of the data, if a sufficient number of mix test results are available.
- Further development of the FAM mixes LAS test for potential application in the practice of routine asphalt mix design or QC/QA is recommended. This work has not been advanced for the past four years at UCPRC due to other priorities.

TABLE OF CONTENTS

DISCLAIMER.....	iii
PROJECT OBJECTIVES.....	iv
EXECUTIVE SUMMARY.....	v
TABLE OF CONTENTS.....	xiv
LIST OF FIGURES.....	xvi
LIST OF TABLES.....	xviii
LIST OF ABBREVIATIONS.....	xix
LIST OF TEST METHODS AND SPECIFICATIONS USED IN THE REPORT.....	xxi
1 INTRODUCTION.....	1
1.1 Background.....	1
1.2 Problem Statement.....	4
1.3 Study Objectives and Tasks.....	5
2 LITERATURE REVIEW.....	6
2.1 Introduction.....	6
2.2 Fatigue and Fracture Models.....	6
2.3 Overview of Current Cracking Tests.....	10
2.4 Literature Review Summary.....	19
3 SUMMARY OF PERFORMANCE-RELATED TESTS.....	20
3.1 Flexural Fatigue Testing.....	21
3.2 SCB Testing.....	23
3.2.1 I-FIT Testing.....	23
3.2.2 LOU-SCB Testing.....	27
3.3 IDEAL-CT Testing.....	28
3.4 FAM Mixes LAS Testing.....	30
4 MATERIAL AND EXPERIMENTAL DESIGN.....	36
5 RESULTS AND ANALYSIS FOR I-FIT.....	43
5.1 I-FIT Testing Results.....	43
5.1.1 Loading Rate Study.....	43
5.1.2 Variability of I-FIT Parameters.....	46
5.2 Comparison Between I-FIT and 4PB Testing.....	47
5.2.1 Stiffness Comparison.....	48
5.2.2 Fatigue Life Comparison.....	52
5.3 Summary.....	54
6 RESULTS AND ANALYSIS for LOU-SCB TESTING.....	56
6.1 LOU-SCB Testing Results.....	56
6.2 Comparison Between I-FIT and LOU-SCB Testing.....	58
6.3 Comparison Between LOU-SCB and 4PB Testing.....	60
6.3.1 Stiffness Comparison.....	61
6.3.2 Fatigue Life Comparison.....	61
6.4 Summary.....	62
7 RESULTS AND ANALYSIS FOR IDEAL-CT.....	63
7.1 IDEAL-CT Testing Results.....	63
7.2 Comparison of I-FIT and IDEAL-CT Testing.....	63
7.3 Comparison Between IDEAL-CT and 4PB Testing.....	65
7.3.1 Stiffness Comparison.....	66
7.3.2 Fatigue Life Comparison.....	67
7.4 Summary.....	71
8 RESULTS ANALYSIS OF FAM MIXES LAS TESTING.....	73

8.1	FAM Mixes LAS Testing Results	73
8.2	Comparison Between FAM Mixes LAS and I-FIT Tests	78
8.3	Comparison Between FAM Mixes LAS and 4PB Tests	79
8.4	Summary	85
9	SENSITIVITY OF TESTS TO MATERIAL TYPE.....	86
9.1	4PB Testing.....	86
9.2	I-FIT Testing.....	89
9.3	Summary	91
10	SUMMARY AND PRELIMINARY CRITERIA DEVELOPMENT.....	93
10.1	Summary and Comparison of Surrogate Tests.....	93
10.2	Preliminary Development of Criteria	96
11	CONCLUSIONS AND RECOMMENDATIONS.....	102
	REFERENCES.....	105
	APPENDIX A EXAMPLE FOR DETERMINING STRENGTH CRITERIA FOR USE WITH A PERFORMANCE-RELATED SPECIFICATION BASED ON FLEXURAL BEAM TESTING.....	112
A.1	Strength Criteria Range for PRS Projects	112
A.2	Validation of Strength Criteria in CalME	116
	APPENDIX B EXAMPLE FOR DETERMINING STRENGTH CRITERIA FOR PROJECTS WITH NO PERFORMANCE-RELATED SPECIFICATION.....	119

LIST OF FIGURES

Figure 1.1: Generalized Maxwell model.....	2
Figure 1.2: Stiffness evolution curve along cycles.....	3
Figure 1.3: General principle of asphalt mixture stiffness, structural thickness, and fatigue performance.	4
Figure 2.1: Stress intensity factor for brittle and quasi-brittle material.	9
Figure 2.2: 4PB test configuration.	11
Figure 2.3: TOL test configuration.	11
Figure 2.4: I-FIT fixture and test specimen (dimensions in mm).	12
Figure 2.5: IDT test configuration.....	14
Figure 3.1: 4PB testing apparatus with a beam specimen.....	22
Figure 3.2: Stiffness curve and fatigue failure determination.	22
Figure 3.3: Schematic I-FIT specimen preparation.....	24
Figure 3.4: I-FIT machine with a specimen.	24
Figure 3.5: Example load-displacement curve from I-FIT.....	25
Figure 3.6: Typical result curve from LOU-SCB method (notch depth in in.) (40).	27
Figure 3.7: Testing machine for IDEAL-CT testing with a specimen.	28
Figure 3.8: Example load-displacement curve from IDEAL-CT testing.	29
Figure 3.9: A cylinder of FAM mix after cutting and coring.....	31
Figure 3.10: DSR equipment for FAM mixes LAS testing with a specimen.....	32
Figure 4.1: Air void information for I-FIT and 4PB specimens.	42
Figure 5.1: Loading versus displacement curve under different loading rates for (a) RAP15%AR_1 and (b) RAP15%_7.....	44
Figure 5.2: Flexibility index under different loading rates for two mixtures.....	45
Figure 5.3: Average coefficient of variance for all parameters from I-FIT test.....	47
Figure 5.4: Correlation matrix between all parameters from 4PB and I-FIT tests.....	48
Figure 5.5: Linear relationship between flexural stiffness and I-FIT parameters.	51
Figure 5.6: Linear relationship between <i>StrainNfIM</i> and I-FIT parameters.	54
Figure 6.1: Air void content for LOU-SCB mixtures.	56
Figure 6.2: Linear regression curves between notch depth and strain energy to failure.....	57
Figure 6.3: Correlation matrix between LOU-SCB and I-FIT parameters.	59
Figure 6.4: Linear regression analysis between $\ln(Jc)$ and <i>AreaBefore</i>	59
Figure 6.5: Linear regression analysis between $\ln(Jc)$ and <i>KIC</i>	60
Figure 6.6: Correlation matrix between LOU-SCB and 4PB parameters.	60
Figure 6.7: Linear regression analysis between <i>Jc</i> and <i>E50</i>	61
Figure 6.8: Linear regression analysis between <i>Jc</i> and <i>StrainNfIM</i>	62
Figure 7.1: Average coefficient of variance for all parameters from IDEAL-CT test.	63
Figure 7.2: Correlation matrix between IDEAL-CT and I-FIT parameters.	64
Figure 7.3: Linear regression between <i>CTindex</i> from IDEAL-CT test and <i>FI</i> from I-FIT test.....	64
Figure 7.4: Correlation matrix between IDEAL-CT and 4PB parameters.....	65
Figure 7.5: Linear regression between <i>IDT_Strength</i> and <i>E50</i>	66
Figure 7.6: Linear regression between <i>IDT_Strength</i> and <i>E50</i> for conventional asphalt mixtures (RAP binder replacement lower than or equal to 25% and without modified binder).	67
Figure 7.7: Linear regression between <i>IDT_Strength</i> and <i>E50</i> for unconventional asphalt mixtures (RAP binder replacement higher than 25% or with modified binder).....	67
Figure 7.8: Linear regression between <i>IDT_Ctindex</i> and <i>StrainNfIM</i>	68
Figure 7.9: Linear regression between <i>IDT_Strength</i> and <i>StrainNfIM</i>	69
Figure 7.10: Linear regression between <i>IDT_Strength</i> and <i>StrainNfIM</i> for conventional asphalt mixtures (RAP binder replacement lower than or equal to 25% and without modified binder).	69

Figure 7.11: Linear regression between <i>IDT_Strength</i> and <i>StrainNfIM</i> for unconventional asphalt mixtures (RAP binder replacement higher than 25% or with modified binder).....	70
Figure 7.12: Linear regression between <i>IDT_Ctindex</i> and <i>StrainNf0.25M</i>	71
Figure 7.13: Linear regression between <i>IDT_Strength</i> and <i>StrainNf0.25M</i>	71
Figure 8.1: Air void content for FAM mix specimens.....	73
Figure 8.2: An example of LAS testing result on FAM mixes.....	74
Figure 8.3: LAS testing results for HRAP_1.....	75
Figure 8.4: LAS testing results for HRAP_2.....	75
Figure 8.5: LAS testing results for HRAP_3.....	76
Figure 8.6: LAS testing results for HRAP_4.....	76
Figure 8.7: Summary of FAM mixes LAS testing results.....	77
Figure 8.8: Averaged coefficient of variance for fatigue parameters from FAM mixes LAS testing.....	78
Figure 8.9: Correlation matrix between FAM mixes LAS testing parameters and I-FIT parameters.....	79
Figure 8.10: Wohler’s curve for HRAP_0H_1 and HRAP_5H_1.....	80
Figure 8.11: Wohler’s curve for HRAP_0H_2 and HRAP_16H_2.....	81
Figure 8.12: Wohler’s curve for HRAP_0H_3 and HRAP_16H_3.....	82
Figure 8.13: Wohler’s curve for HRAP_0H_4 and HRAP_6H_4.....	83
Figure 8.14: Correlation matrix between FAM mixes LAS testing parameters and 4PB testing parameters.....	84
Figure 8.15: Linear regression between <i>FailureStrain</i> from FAM mixes fatigue testing and <i>StrainNfIM</i> from 4PB testing.....	85
Figure 9.1: <i>E50</i> sensitivity to material types.....	87
Figure 9.2: <i>StrainNfIM</i> sensitivity to material types.....	87
Figure 9.3: <i>FI</i> sensitivity to material types.....	89
Figure 9.4: <i>Strength</i> sensitivity to material types.....	90
Figure 10.1: Relationship between <i>Strength</i> from IDEAL-CT test and <i>E50</i> from 4PB test.....	98
Figure 10.2: Fitted relationship between <i>E50</i> and <i>StrainNfIM</i> from 4PB test.....	99
Figure 10.3: Fitted relationship between <i>E50</i> and <i>StrainNf0.25M</i> from 4PB test.....	99
Figure 10.4: Relationship between <i>Strength</i> from IDEAL-CT with <i>StrainNfIM</i> from 4PB test.....	100
Figure 10.5 : Flowchart for determining criteria for fatigue cracking based on <i>Strength</i>	101
Figure A.1: Determination of <i>Strength_{min}</i> based on the stiffness requirement for surface layer.....	113
Figure A.2: Determination of <i>Strength_{max}</i> based on the fatigue life requirement for surface layer.....	114
Figure A.3: Determination of <i>Strength_{min}</i> based on the fatigue stiffness requirement for intermediate layer.....	115
Figure A.4: Determination of <i>Strength_{max}</i> based on the fatigue life requirement for intermediate layer.....	116
Figure B.1 Histogram of HMA stiffness from <i>CalME</i> material library.....	119
Figure B.2 Histograms of HMA stiffness (ksi) with different base binder PGs from <i>CalME</i> material library.....	120
Figure B.3 Determination of <i>Strength_{min}</i>	121
Figure B.4 Determination of <i>Strength_{max}</i>	121
Figure B.5 Histogram of RHMA stiffness from <i>CalME</i> material library.....	123
Figure B.6 Determination of <i>Strength_{min}</i> based on mean stiffness of RHMA.....	123
Figure B.7 Determination of <i>Strength_{max}</i> based on mean stiffness of RHMA.....	124

LIST OF TABLES

Table 2.1: Summary of Semicircular Bend Test Methods	13
Table 2.2: Calibration Information for Fatigue and Fracture Tests	16
Table 3.1: Fracture Parameters for I-FIT Testing	26
Table 3.2: Fracture Parameters from IDEAL-CT Testing	30
Table 3.3: Fatigue Parameters from FAM Mixes LAS Testing	34
Table 4.1: Asphalt Mixture Information	38
Table 4.2: Experimental Design.....	41
Table 5.1: Tukey’s HSD Test for Loading Rate	46
Table 5.2: Tukey’s HSD Test for Different Mixtures	46
Table 5.3: R ² Values for Correlation of I-FIT Parameters with Flexural Stiffness (E50).....	51
Table 5.4: R ² Values for Correlation of I-FIT Parameters with 4PB Fatigue Performance (StrainNf1M).....	52
Table 9.1: Tukey’s HSD Analysis Result for 4PB Testing.....	88
Table 9.2: Tukey’s HSD Analysis Result for I-FIT	91
Table 10.1: Summary of I-FIT Testing Parameters	93
Table 10.2: Summary of LOU-SCB Testing Parameters.....	93
Table 10.3: Summary of IDEAL-CT Parameters.....	94
Table 10.4: Summary of FAM Mixes LAS Testing Parameters.....	94
Table 10.5: Comparison of Surrogate Tests.....	95
Table 10.6: Regression Model Summary for Strength from IDEAL-CT at 77°F (25°C) and E50 from 4PB at 68°F (20°C).....	97
Table 10.7: Regression Model Summary for E50 and StrainNf1M from 4PB	98
Table 10.8: Regression Model Summary for IDT_Strength and StrainNf1M from 4PB Test.....	100
Table A.1: HMA-LL Performance Requirements.....	112
Table A.2: Asphalt Mixtures Passing Strength Criteria Range for HMA-LL Surface Layer	114
Table A.3: Asphalt Mixtures Passing Strength Criteria Range for HMA-LL Intermediate Layer	116
Table A.4: Inputs for CalME Simulation with Changing Surface Materials	117
Table A.5: Fatigue Cracking Simulation in CalME for Surface Layer.....	117
Table A.6: Inputs for CalME Simulation with Changing Intermediate Materials	118
Table A.7: Fatigue Cracking Simulation in CalME for Intermediate Layer	118
Table B.1: Inputs for CalME Simulation of New AC Pavement	122
Table B.2: Fatigue Cracking Simulation Results from CalME of New AC Pavement.....	122
Table B.3: Inputs for CalME Simulation of RHMA Over Cracked AC Pavement	124
Table B.4: Reflective Cracking Simulation Results from CalME of RHMA Over Cracked AC Pavement.....	125

LIST OF ABBREVIATIONS

AASHTO	American Association of State Highway and Transportation Officials
AB	Aggregate base
ABR	Asphalt binder replacement
AC	Asphalt concrete
ALF	Accelerated loading facility
APCS	Automated Pavement Condition Survey
AR	Asphalt rubber
COV	Coefficient of variance
CRM	Crumb rubber modified
DSR	Dynamic shear rheometer
EPFM	Elastic plastic fracture mechanics
FAM	Fine aggregate matrix
FEM	Finite element modeling
FI	Flexibility index
FMFC	Field mixed and field compacted
FMLC	Field mixed and lab compacted
HMA	Hot mix asphalt
HRAP	High content of RAP
HSD	Honestly significant difference
HVS	Heavy Vehicle Simulator
ICT	Illinois Center for Transportation
IDEAL-CT	Indirect tensile asphalt cracking test
IDT	Indirect tension test
I-FIT	Illinois Flexibility Index Test
JMF	Job mix formula
LAS	Linear amplitude sweep test
LEFM	Linear elastic fracture mechanics
LMLC	Lab mixed and lab compacted
LOU-SCB	Louisiana Semicircular Bend Test
ME	Mechanistic-empirical

PBS	Performance-based specifications
PG	Performance grade
PM	Polymer modified
PPRC	Partnered Pavement Research Center
PRS	Performance-related specification
QC/QA	Quality control/quality assurance
RA	Recycling agent
RAP	Reclaimed asphalt pavement
RAS	Recycled asphalt shingles
RHMA	Rubberized hot mix asphalt
R-SCB	Repeated semicircular bend test
SCB	Semicircular bend test
SGC	Superpave gyratory compactor
SMA	Stone mastic asphalt
Superpave	Superior Performing Asphalt Pavement
TOL	Texas Overlay Test
UCPRC	University of California Pavement Research Center
VECD	Viscoelastic continuum damage
4PB	Four-point bending test

LIST OF TEST METHODS AND SPECIFICATIONS USED IN THE REPORT

AASHTO M 320	Standard Specification for Performance-Graded Asphalt Binder
AASHTO M 323	Standard Specification for Superpave Volumetric Mix Design
AASHTO R 30	Standard Practice for Mixture Conditioning of Hot Mix Asphalt (HMA)
AASHTO R 35	Standard Practice for Superpave Volumetric Design for Asphalt Mixtures
AASHTO TP 124	Estimating Damage Tolerance of Asphalt Binders Using the Linear Amplitude Sweep
AASHTO TP 124	Standard Method of Test for Determining the Fracture Potential of Asphalt Mixtures Using Semicircular Bend Geometry (SCB) at Intermediate Temperature
AASHTO T 84	Standard Method of Test for Specific Gravity and Absorption of Fine Aggregate
AASHTO T 85	Standard Method of Test for Specific Gravity and Absorption of Coarse Aggregate
AASHTO T 166	Standard Method of Test for Bulk Specific Gravity (Gmb) of Compacted Hot Mix Asphalt (HMA) Using Saturated Surface-Dry Specimens
AASHTO T 209	Standard Method of Test for Theoretical Maximum Specific Gravity (Gmm) and Density of Asphalt Mixtures
AASHTO T 312	Standard Method of Test for Preparing and Determining the Density of Asphalt Mix Specimens by Means of the Superpave Gyratory Compactor
AASHTO T 321	Standard Method of Test for Determining the Fatigue Life of Compacted Asphalt Mixtures Subjected to Repeated Flexural Bending
AASHTO T 331	Standard Method of Test for Bulk Specific Gravity (Gmb) and Density of Compacted Hot Mix Asphalt (HMA) Using Automatic Vacuum Sealing Method
DOTD TR 330	Evaluating of Asphalt Mixture Crack Propagation Using the Semi-Circular Bend Test
ASTM D 6931	Standard Test Method for Indirect Tensile (IDT) Strength of Asphalt Mixtures
EN 12697-24	Bituminous Mixtures- Test Methods for Hot Mix Asphalt Part 24: Resistance to Fatigue
TxDOT Tex-248-F	Test Procedure for Overlay Test

SI* (MODERN METRIC) CONVERSION FACTORS

APPROXIMATE CONVERSIONS TO SI UNITS				
Symbol	When You Know	Multiply By	To Find	Symbol
LENGTH				
in.	inches	25.40	millimeters	mm
ft.	feet	0.3048	meters	m
yd.	yards	0.9144	meters	m
mi.	miles	1.609	kilometers	km
AREA				
in ²	square inches	645.2	square millimeters	mm ²
ft ²	square feet	0.09290	square meters	m ²
yd ²	square yards	0.8361	square meters	m ²
ac.	Acres	0.4047	hectares	ha
mi ²	square miles	2.590	square kilometers	km ²
VOLUME				
fl. Oz.	fluid ounces	29.57	milliliters	mL
gal.	gallons	3.785	liters	L
ft ³	cubic feet	0.02832	cubic meters	m ³
yd ³	cubic yards	0.7646	cubic meters	m ³
MASS				
oz.	ounces	28.35	grams	g
lb.	pounds	0.4536	kilograms	kg
T	short tons (2000 pounds)	0.9072	metric tons	t
TEMPERATURE (exact degrees)				
°F	Fahrenheit	(F-32)/1.8	Celsius	°C
FORCE and PRESSURE or STRESS				
lbf	pound-force	4.448	newtons	N
lbf/in ²	pound-force per square inch	6.895	kilopascals	kPa
APPROXIMATE CONVERSIONS FROM SI UNITS				
Symbol	When You Know	Multiply By	To Find	Symbol
LENGTH				
mm	millimeters	0.03937	inches	in.
m	meters	3.281	feet	ft.
m	meters	1.094	yards	yd.
km	kilometers	0.6214	miles	mi.
AREA				
mm ²	square millimeters	0.001550	square inches	in ²
m ²	square meters	10.76	square feet	ft ²
m ²	square meters	1.196	square yards	yd ²
ha	hectares	2.471	acres	ac.
Km ²	square kilometers	0.3861	square miles	mi ²
VOLUME				
mL	milliliters	0.03381	fluid ounces	fl. Oz.
L	liters	0.2642	gallons	gal.
m ³	cubic meters	35.31	cubic feet	ft ³
m ³	cubic meters	1.308	cubic yards	yd ³
MASS				
g	grams	0.03527	ounces	oz.
kg	kilograms	2.205	pounds	lb.
t	metric tons	1.102	short tons (2000 pounds)	T
TEMPERATURE (exact degrees)				
°C	Celsius	1.8C + 32	Fahrenheit	°F
FORCE and PRESSURE or STRESS				
N	newtons	0.2248	pound-force	lbf
kPa	kilopascals	0.1450	pound-force per square inch	lbf/in ²

*SI is the abbreviation for the International System of Units. Appropriate rounding should be made to comply with Section 4 of ASTM E380.
(Revised April 2021)

1 INTRODUCTION

1.1 Background

In 2020, about 94% of all state and local pavements in the United States and 95% in California were asphalt pavements (1). Currently, the California state highway system, owned and operated by the California Department of Transportation (Caltrans), is made up of about 37,000 lane miles of asphalt concrete (AC) pavement (also referred to as flexible pavement) and 13,000 lane miles of concrete pavement (also referred to as rigid pavement). In fiscal year 2019–2020, about \$201 million was awarded for pavement maintenance and \$1,038 million for rehabilitation. Asphalt overlays and chip seals, which are the most widely used asphalt maintenance treatments, accounted for nearly 71% of total maintenance funds (\$132 million for overlays and \$10 million for chip seals) (2). Material costs often make up a large part of these overall project costs.

Age-related cracking is a top-down distress that is related to environmental conditions and eventually occurs on all asphalt pavements, regardless of whether there is heavy vehicle traffic (trucks and buses). Age-related cracking is caused by oxidation of the asphalt mix and thermal contraction, whether a single event (typically in locations with subfreezing temperatures) or repeated day/night and seasonal temperature changes (in locations without subfreezing temperatures). Thermal contractions make tensile stresses in the mix larger as oxidation makes the asphalt binder stiffer. Age-related cracking initially appears as transverse and longitudinal cracks that eventually connect to form block cracking.

Fatigue cracking and reflective cracking, which have similar mechanisms and respond to the same material properties, are the most common distresses in asphalt pavements that carry heavy vehicles, and they are caused by repeated traffic loading at intermediate temperatures. The number of cracks and cracked areas grows over time. Subsequent water infiltration into the underlying layers may lead to more distresses, such as underlayer rutting and the pumping of fine materials up from the subgrade. As a result, the loss of pavement functionality is accelerated.

The mechanism of fatigue cracking, referring to both bottom-up fatigue cracking and reflective cracking, of asphalt pavements is related to pavement structure, traffic loading, asphalt mixture properties, and environmental conditions. An asphalt mixture is a complex composite material containing binder, coarse aggregates, fine aggregates, and air voids, and its behavior is dependent on loading time and temperature. Due to the viscoelasticity of asphalt pavements, modeling their fatigue cracking behavior is difficult. Researchers have proposed many analytical viscoelastic models to describe the viscoelastic behavior of asphalt material, including the Maxwell, Kelvin, Burger, generalized Kelvin, and generalized Maxwell models (Figure 1.1). These models are composed

of two basic elements: a spring and a dashpot. The spring describes the elastic part of the asphalt mixture while the dashpot models the viscosity of asphalt material. The elastic-viscoelastic correspondence principle proposed by Schapery suggested that the constitutive relationship of viscoelastic material can be expressed in the same form as the elastic cases with pseudo variables (3). The ratio between stress and pseudo strain is defined as pseudo stiffness. This correspondence principle was then implemented by Kim and Little to describe the nonlinear response of asphalt material under loading (4).

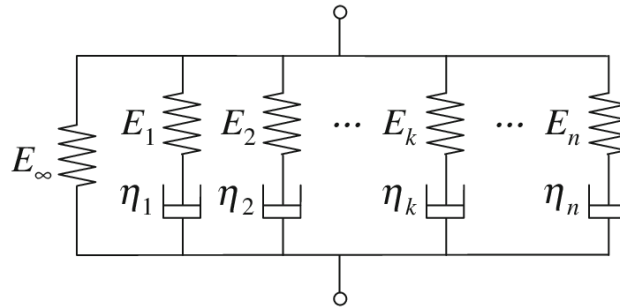
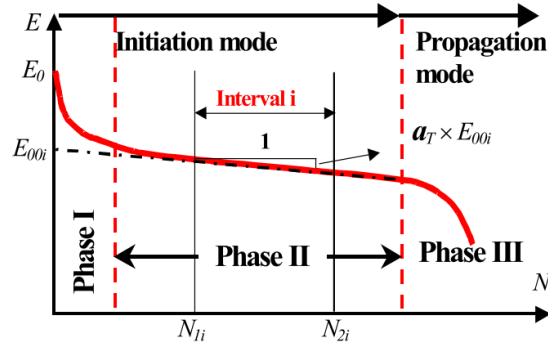


Figure 1.1: Generalized Maxwell model.

At low temperatures and high loading rates, asphalt mixtures tend to behave in a more elastic way and brittle fracture occurs, while viscosity governs material behavior when temperatures increase and/or loading rates decrease. The stiffness of asphalt material in the context of a fatigue study is controlled by the combined mechanisms that occur at intermediate temperatures and loading rates of traffic speeds. Fatigue damage and cracking are related to the energy of bending asphalt pavement under traffic. Fatigue damage is primarily related to tensile strains at the bottom of the asphalt layer or the energy associated with the combined tensile and shear strains that occur when traffic moves over an asphalt layer that has been placed over a layer with discontinuity (a crack or joint), resulting in reflective cracking. Damage is defined with respect to fatigue as the loss of stiffness due to repetitive loading.

Researchers have investigated the fatigue phenomenon through laboratory experiments, numerical simulations, and field evaluations. There are typically three distinct phases for the modulus evolution during a fatigue test in the laboratory, shown in Figure 1.2 (5). Phase I, the adaptation phase, is the combined effect of fatigue, heating, and thixotropy, which contribute to the rapid decrease in stiffness. Phase II, the quasi-stationary phase, is dominated by fatigue damage. Phase III, the failure phase, occurs when damage results in the formation of micro cracks that then propagate as macro cracks. Phases I and II correspond to crack initiation while Phase III represents crack propagation.



Source: Di Benedetto et al., 2003 (5)

Figure 1.2: Stiffness evolution curve along cycles.

Researchers have studied the fatigue performance of asphalt pavements at different levels of scale, including binder, fine aggregate matrix (FAM) mix, and full mixture. The results of many tests over the past 60 years have characterized the cracking resistance of asphalt materials in the laboratory (6). Common tests currently used include the four-point bend (4PB) fatigue test, Texas Overlay (TOL) test, indirect tension (IDT) test, semicircular bend (SCB) test, indirect tensile asphalt cracking test (IDEAL-CT), and FAM mixes fatigue testing.

Researchers developed the 4PB test, also called the flexural bending beam fatigue test, to predict the fatigue performance of asphalt materials (7,8,9). The equipment and procedures have been standardized in Europe (EN 12697-24) and North America (AASHTO T 321 and ASTM D8237), and it a standard test in parts of Europe and for some projects with performance-related specifications in the United States (10,11,12). In 4PB testing, prismatic beam specimens are subjected to repeated strain-controlled or stress-controlled loading until predefined failure. Researchers have proposed multiple parameters from 4PB testing to represent fatigue resistance. The failure criterion may be defined by the reduction in the initial stiffness, peak of phase angle, peak of product of stiffness and loading cycles, or dissipated energy. Wohler's law describes the relationship between applied strain or stress level and the loading repetitions to failure (13). Researchers have identified 4PB testing as appropriately sensitive to the material variables that determine fatigue performance (14,15). However, 4PB testing is not necessarily appropriate for use in the routine job mix formula (JMF) because of its cost and complexity and because it is too slow for routine quality control/quality assurance (QC/QA) (14).

The process of determining criteria for asphalt mixture fatigue performance should include consideration of the pavement structure, traffic loading, and material stiffness, as illustrated in Figure 1.3. The fatigue performance of asphalt pavements is mostly an interaction of the tensile strain in the structure and the asphalt material fatigue damage resistance property. In general, the fatigue performance is primarily related to the energy of tensile deformation under loading with greater energy causing greater damage in the material. The energy of deformation

is a function of the product of strain and stress, which can also be written in elastic mechanics as the product of the stiffness and the strain squared. The tensile strain in the pavement is an interactive function of the material stiffness and structure thickness. Figure 1.3 shows that for the same tensile strain, a mix with a softer binder will have a longer fatigue life because there is less energy of deformation. The figure also shows that a mix with a stiff binder in a thick pavement structure will result in the lowest tensile strain value and highest fatigue life compared with a soft binder in the same thick structure, while a soft binder in a thin pavement structure will result in better fatigue performance than a stiff binder because the stiffness of the thin asphalt layer has a relatively small effect on the tensile strain. The energy and damage relationship and the performance of binders with different stiffnesses in structures of different thicknesses are general principles that show variability for different materials, structures, and other variables, such as traffic loads and support to the asphalt layers from underlying layers.

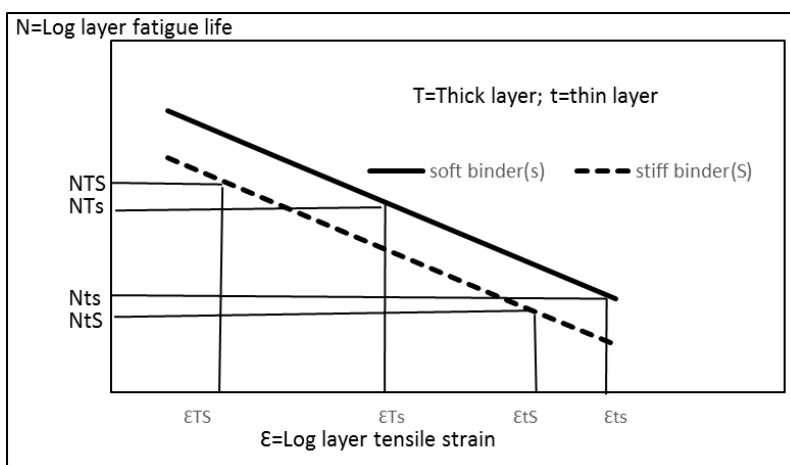


Figure 1.3: General principle of asphalt mixture stiffness, structural thickness, and fatigue performance.

1.2 Problem Statement

Caltrans implemented the Superior Performing Asphalt Pavement (Superpave) mix design procedure for asphalt pavements with initial pilot projects in 2011 and full implementation in 2015, but fatigue cracking performance is not assessed in the Superpave volumetric mix design method (15). Current QC/QA specifications for asphalt pavement design and construction are based on the volumetric properties of compacted asphalt mixtures using parameters such as aggregate gradation, air voids, voids filled with asphalt, and voids in mineral aggregate. However, no fundamental correlation exists between these volumetric parameters and the fatigue cracking field performance of asphalt pavements. The increased use of new pavement materials—such as mixes with high percentages of recycled material, polymer-modified asphalt mixtures, and warm-mix technologies—and the desire to better engineer and produce materials for longer-lasting pavements are some of the motivations to introduce performance-related testing for fatigue cracking of asphalt pavement. The overall goals are less variability of

performance, lower life cycle costs, and fewer construction closures. Therefore, an effective and reliable QC/QA testing method to ensure the as-built pavement meets the as-designed criteria is necessary.

Performance-related specification (PRS) is a promising approach to overcome the shortcomings of current QC/QA methods by measuring fundamental mechanical properties of asphalt mixtures. Repeated load laboratory tests to support PRS, including 4PB and TOL testing, produce results that can improve mix design. The 4PB tests are also used for mechanistic-empirical (ME) design, but they are complex and time consuming for routine use in asphalt mix design and QC/QA activities (10). A more efficient surrogate performance-related test providing results sufficiently correlated with the results of the more complex repeated load tests, and ultimately with field performance, can offer an improvement over the current lack of performance-related tests in mix design and QC/QA.

1.3 Study Objectives and Tasks

The objective of this project is to identify a surrogate test for asphalt mixture design and QC/QA for fatigue performance. This objective is achieved through the following tasks:

1. Completion of a literature review on research related to asphalt material fatigue performance, with special emphasis on work about the fatigue properties of asphalt material, fracture testing of asphalt mixtures, and testing method of multiple scales.
2. Selection of candidate surrogate fatigue cracking tests and identification of representative parameters based on the literature review.
3. Design and execution of an experimental plan for 4PB tests and other candidate testing methods on a range of asphalt mixtures with different material properties at the University of California Pavement Research Center (UCPRC) laboratory.
4. Interpretation of testing results.
5. Preparation of a summary report detailing the study.

This study includes the following results:

- Evaluation of the repeatability of the testing method and variability of cracking parameters proposed for each test.
- Assessment of the correlation among candidate tests and of the relationship between candidate tests and the 4PB test.
- Comparison and evaluation of each candidate testing method and cracking parameters regarding the potential for characterizing fatigue cracking performance.
- Recommendation of a performance-related test along with representative indicators.

This report documents the work completed for each of the project tasks.

2 LITERATURE REVIEW

2.1 Introduction

This literature review includes research related to the fracture and fatigue performance of asphalt pavements, including fatigue and fracture mechanisms of hot mix asphalt (HMA) and current cracking tests.

2.2 Fatigue and Fracture Models

Fatigue is defined as a cumulative, progressive, and permanent damage process that occurs in a material subjected to external cyclic or fluctuating strains or stresses, where the maximum value of the stress is less than the static yield strength of the material (1). The fatigue life of an asphalt mixture consists of crack initiation, crack propagation, and ultimate failure (17). During crack initiation, a microcracking network develops in a diffuse way that decreases the modulus. In the propagation phase, microcracks coalesce into macrocracks and spread inside the material, which leads to the ultimate failure of the material.

Like many other materials, the fatigue performance of asphalt mixtures is expressed by the relationship between strain or stress and loading cycles to failure, also known as Wohler's law, and fatigue behavior is evaluated by the slope of this relationship. Equation 2.1 shows this relationship (18,19):

$$N_f = a \left(\frac{1}{\varepsilon_0} \right)^b \left(\frac{1}{S_0} \right)^c \quad (2.1)$$

Where:

N_f = fatigue life,

ε_0 = applied strain value,

S_0 = initial mix stiffness, and

a, b, c = experimentally determined coefficients.

The fatigue life of an asphalt mixture specimen is normally defined by the stiffness evolution, shown in Figure 1.2. The conventional criterion for fatigue failure is the stiffness modulus reaching a 50% reduction of initial stiffness. Despite its simplicity, this criterion does not include other fatigue-related material properties such as self-heating and thixotropy (20). In addition, no cracking appears for some asphalt materials, particularly polymer- and rubber-modified mixes, when the stiffness decreases to 50% and results in the underestimating of fatigue life (21).

Fatigue damage modeling is an alternative theoretical approach for crack initiation modeling. *CalME*, software, which the UCPRC developed for Caltrans for new asphalt pavements and rehabilitation design, simulates the

fatigue cracking performance of asphalt materials and pavement structures together. It is based on ME principles to model and simulate pavement performance. For fatigue performance, the mechanical part includes calculating pavement response, such as tensile strain based on material stiffness and traffic loading. An incremental-recursive procedure updates the stiffness of asphalt materials after damage, where the output from one increment is the input for the next increment. The relationship between stiffness and damage is shown in the following equation:

$$\log(E) = \delta + \frac{\alpha \times (1 - \omega)}{1 + e^{(\beta + \gamma \log(tr))}} \quad (2.2)$$

Where:

tr = reduced time (s), and

ω = damage, which is a function of number of loads, strain, and stiffness:

$$\omega = \left(\frac{MN}{MN_p}\right)^\alpha \quad (2.3)$$

$$\alpha = \exp\left(\alpha_0 + \alpha_1 \times \frac{t}{1^\circ C}\right) \quad (2.4)$$

$$MN_p = A \times \left(\frac{\mu\varepsilon}{\mu\varepsilon_r}\right)^\beta \times \left(\frac{E}{E_r}\right)^\gamma \times \left(\frac{E_i}{E_r}\right)^\delta \quad (2.5)$$

Where:

MN = number of repeated loadings in millions,

MN_p = allowable repetitions,

$\mu\varepsilon$ = bending strain for bottom-up fatigue, calculated using layer elastic theory,

E = damaged modulus,

E_i = intact modulus,

t = temperature, and

A , α_0 , α_1 , β , γ , δ , $\mu\varepsilon_r$, and E_r are constants.

The fatigue cracking density on the pavement surface can then be calculated with an empirical model based on fatigue damage in the asphalt surface layer. The simulation of reflective cracking performance in *CalME* applies the same damage model Equation 2.2 as fatigue cracking, while the tensile strain in Equation 2.5 for reflective cracking is the one calculated for the bottom of the asphalt overlay using Wu's regression equation through finite element modeling (22).

Viscoelastic continuum damage (VECD) models are based on the elastic-viscoelastic correspondence principle and model the mechanical behavior of asphalt mixtures (23). Correspondence principles establish a simple relationship between mechanical states of elastic and viscoelastic material (3). In VECD models, pseudo stiffness

(C) and the damage parameter (S) describe the deviation of stress from pseudo strain. The relationship between the C and S parameters is used to predict fatigue life. The following are the main elements of this model (5):

$$\text{Pseudo strain energy density function: } W^R = W^R(\varepsilon^R, S) \quad (2.6)$$

$$\text{Constitutive relationship: } \sigma = \frac{\partial W^R}{\partial \varepsilon^R} = C(S)\varepsilon^R \quad (2.7)$$

$$\text{Uniaxial pseudo strain: } \varepsilon^R = \frac{1}{E_R} \int_0^t E(t - \tau) \frac{\partial \varepsilon}{\partial \tau} d\tau \quad (2.8)$$

$$\text{Damage evolution law: } \frac{dS}{dt} = \left(-\frac{\partial W^R}{\partial S}\right)^\alpha \quad (2.9)$$

Where:

W^R = pseudo strain energy density function, a function of pseudo strain and damage parameter S ,

α = material constant, depending on the fracture characteristics of the material,

$\alpha = \frac{1}{m}$ in controlled-stress mode and $\alpha = \frac{1}{m} + 1$ in controlled-strain mode,

t = reduced time, and

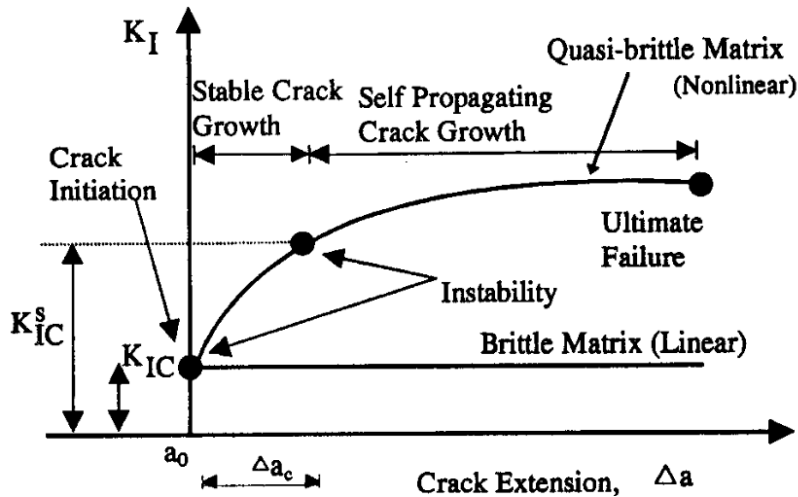
E_R = reference modulus included for dimensional compatibility.

Researchers integrated VECD-based damage and healing models to study fatigue damage and healing characteristics and found that C versus S is a unique material property independent of healing history (24).

One study proposed a viscoelastic method, with dissipated energy criteria, to predict fatigue life during the crack initiation and fitted asphalt mixture properties through a four-Maxwell element model (25). A comparison between the fatigue life to crack initiation from this method and an elastic method found that the elastic analysis overpredicted fatigue life and that the viscoelastic analysis was not as sensitive to pavement thickness as the elastic method.

Monotonic fracture is the failure of a material under constant static loading exceeding the ultimate strength of the material. It differs from fatigue failure mainly in the phases before crack propagation, when the fatigue process exhibits more crack nucleation locations (26). Linear elastic fracture mechanics (LEFM) and elastic plastic fracture mechanics (EPFM) are the main fracture mechanics approaches for assessing the fracture properties of asphalt mixtures. LEFM is more suitable for brittle materials, which have small-scale yielding areas, while EPFM is better for quasi-brittle materials with high-scale yielding areas at the crack tip (27). LEFM uses a single loading level, and common parameters include the stress intensity factor (K), fracture toughness (K_{IC}), and fracture energy (G_{IC}). The stress intensity factor linearly depends on applied stress, and it is a function of the specimen geometry.

When the factor is equal to fracture toughness, the material fails. Figure 2.1 shows the fracture process of different materials.



Source: Mobasher et al., 1997 (28).

Figure 2.1: Stress intensity factor for brittle and quasi-brittle material.

The energy release rate, expressed by the J -integral, is a parameter in EPFM analysis. The J -integral is defined as the work done per unit area of crack growth (29). In one study, a generalized J -integral for viscoelastic materials was developed (3):

$$J = \int \Gamma \left(w dy - T_i \frac{\partial u_i}{\partial x} ds \right) \quad (2.10)$$

$$J_e = \int \Gamma (w^e dy - T_i \frac{\partial u_i^e}{\partial x} ds) \quad (2.11)$$

Where:

Γ = arbitrary counterclockwise path around the crack tip,

T_i = components of the traction vector,

u_i = displacement vector components,

u_i^e = pseudo displacement vector components,

w, w^e = strain energy density and pseudo strain energy density, and

J_e = pseudoelastic J -integral.

Researchers have used fracture mechanics to predict the fatigue life of asphalt pavement (30,31). It presupposes the existence of flaws and their propagation as cracks as the damage mechanism governing fatigue under repeated cyclic loading, until a flaw has developed to an unstable size. Fracture mechanics divides fatigue life into four

phases: (1) a crack nucleation phase associated with cyclic slip on the atomic scale and controlled by the local stress and strain concentrations; (2) a microcrack growth phase, where a crack grows due to void, inclusion, or flaws; (3) a macrocrack growth phase; and (4) final failure. The fracture mechanics approach has successfully correlated and predicted fatigue life in the macrocrack growth and final failure phases (32). Paris's law describes the relationship between crack propagation and the stress intensity factor under repeated loading:

$$\frac{da}{dN} = C(\Delta K)^m \quad (2.12)$$

Where:

$$\Delta K = K_{max} - K_{min},$$

a = crack length,

N = number of cycles, and

C, m = material parameters to be determined experimentally.

Similarly, researchers have applied the J -integral instead of the stress intensity factor in Paris's law in assessing the viscoelasticity of asphalt mixtures (17,33).

2.3 Overview of Current Cracking Tests

The four-point bending (4PB) test (AASHTO T321, ASTM D8237), shown in Figure 2.2, is a widely used repeated-loading beam fatigue test for evaluating the fatigue cracking potential of asphalt materials. This test measures either the load repetitions to the predefined failure or the rate of dissipated strain energy per loading cycle until the rate reaches a constant level. Researchers have verified the 4PB test through field projects and found it is a good predictor of asphalt material stiffness and fatigue performance. In addition, the 4PB test helps the simulation of the fatigue cracking of asphalt pavements in *CalME*. Fitting the stiffness reduction curve from 4PB testing results produces the parameters in the damage models of *CalME*, Equation 2.2 to Equation 2.5. Researchers have calibrated the fatigue damage model in *CalME* against multiple accelerated pavement testing projects (34,35,36). However, 4PB testing has numerous disadvantages, including a complicated specimen preparation procedure, long testing time, high variability (typical of all repeated-loading tests), and an expensive testing apparatus. In the study presented in this report, the 4PB test was the benchmark testing for flexural stiffness and fatigue life performance, and it was used to evaluate potential surrogate fatigue performance-related testing candidates. The final recommended surrogate fatigue performance-related test should provide the same stiffness and fatigue information as the 4PB test without the disadvantages of that test.



Figure 2.2: 4PB test configuration.

The Texas Overlay Test (TxDOT Tex-248-F [TOL]), shown in Figure 2.3, simulates accelerated reflective cracking in asphalt pavement overlays, with the number of cycles measuring crack resistance. Good relationships were found between TOL test results and field fatigue performance (37). The main disadvantages of this test are high variability, typical of repetitive loading tests, and the high cost of the test device (38).

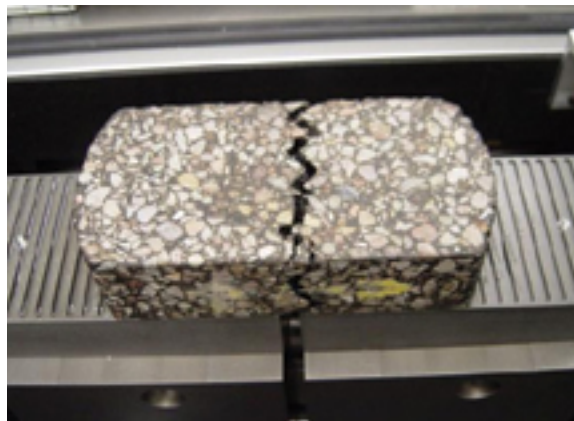


Figure 2.3: TOL test configuration.

The 4PB and TOL repetitive cracking tests share common shortcomings because they are complicated tests and they have high variability. As a result, implementing them for routine mix designs and QC/QA of pavement construction is difficult. Researchers have developed several monotonic fracture tests to characterize the cracking performance of asphalt mixtures intended for practical application, including SCB, IDT, and IDEAL-CT tests.

One study proposed the SCB test as a simple testing method to measure the fracture performance of materials such as rock and concrete (39). The SCB test is a three-point loading configuration on a semicircular specimen with a notch in the center, a simplified approach suggested for use in performance-related specifications (PRS,

sometimes referred to as performance-based specifications [PBS]) that could improve the reliability of current QC/QA specifications. A simplified PRS framework was proposed, with three notch depths for SCB specimens and constant crosshead loadings of 0.5 mm/min until failure fracture (40). This testing is referred to as the Louisiana Semicircular Bend (LOU-SCB) test. The critical value of the energy release rate, the J -integral (J_c), calculated based on the area under the load-displacement test curve, showed a weak correlation with the IDT strength but a relatively good correlation with the IDT toughness index value (41). Another study conducted monotonic SCB tests and repeated SCB (R-SCB) tests at room temperature 77°F (25°C) as a part of a comparison to the TOL test (42). The conclusion was that neither SCB nor R-SCB tests were ready to be used as a routine HMA cracking test because of the poor repeatability and high variability (COV >30%).

Two common SCB testing methods are the Illinois Flexibility Index Test (I-FIT) (AASHTO TP124), developed at the University of Illinois, and the LOU-SCB (DOTD TR330) test, developed at Louisiana State University. Researchers at the Illinois Center for Transportation (ICT) developed the I-FIT test, shown in Figure 2.4, and proposed a cracking parameter called the flexibility index (FI) based on the load-displacement curve to distinguish cracking performance between asphalt concrete (AC) mixtures (43). Table 2.1 compares these two methods in terms of specimen geometries, testing configurations, and cracking parameters.

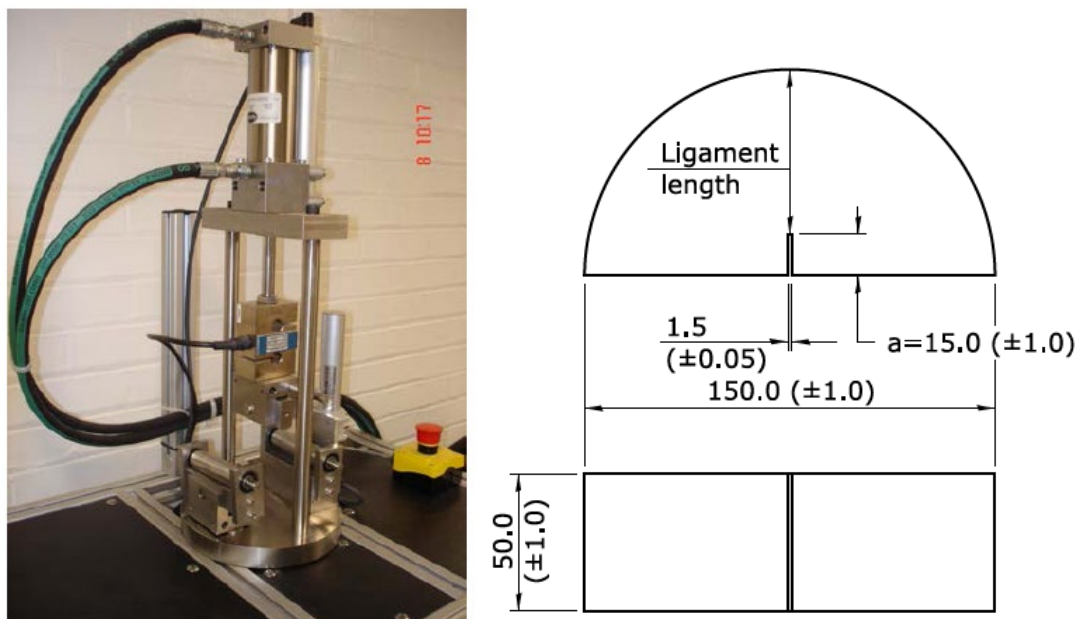


Figure 2.4: I-FIT fixture and test specimen (dimensions in mm).

Table 2.1: Summary of Semicircular Bend Test Methods

Test Method	LOU-SCB (DOTD TR330)	I-FIT (AASHTO TP124)
Parameter	Critical strain energy release rate (Jc)	Flexibility index (FI)
Loading rate (mm/min)	0.5	50
Temperature (°C)	25±1	25
Compaction method	Gyratory	Gyratory
Air voids (%)	7.0±0.5	7.0±0.5
Thickness (mm)	57	50±1
Diameter (mm)	150	150±1
Notch length (mm)	25.4±1.0 31.8±1.0 38.1±1.0	15.0±1.0
Notch width (mm)	3.0±0.5	1.5±0.05

Researchers have used SCB tests to evaluate the fracture behavior of various asphalt materials. Of SCB specimens with three notches tested at 0.5 mm/min, the specimens with crumb rubber asphalt showed higher critical fracture resistance than the specimens without it (44). Researchers have also conducted SCB tests at a constant crack mouth opening displacement of 0.0005 mm/sec to compare the fracture energy for asphalt materials with reclaimed asphalt pavement (RAP) content of 0%, 20%, and 40%. The 20% RAP mixtures had a similar fracture resistance to that of the control mixture without RAP while the addition of 40% RAP resulted in a clear decrease in fracture resistance (45). SCB tests following the I-FIT test procedure on the effect of rejuvenator agents added to RAP showed that the fracture resistance of the asphalt material with rejuvenator improved (43,46).

SCB testing can also assess fatigue performance. One study used SCB tests to study the fracture properties of asphalt mixtures with polymer-modified asphalt binders (41). The specimens had three notches, and the loading speed was 0.5 mm/min. The results showed a moderate correlation between the fracture test results and the combined cracking rate in the field (transverse and alligator cracking). Additional research has shown a good correlation between the FI from I-FIT tests and fatigue cycles from TOL tests for eight asphalt materials with varying RAP and recycled asphalt shingle (RAS) contents and binder types (47). A comparative study of fracture parameters (Jc and K factor) from SCB testing with a loading speed of 0.5 mm/min and fatigue life from 4PB tests for seven mixtures implied a weak correlation between fracture properties and fatigue life (48).

Researchers have also investigated the ability of SCB testing to predict the fracture properties of FAM mixes. They fabricated SCB specimens of FAM mixes (sieve size \leq #50) by slicing Superpave gyratory compactor (SGC) samples and cutting 2.5 mm wide and 25 mm deep notches (49). They then incorporated the material fracture properties obtained from SCB tests into the cohesive-zone fracture model for the finite element modeling (FEM) simulation.

The indirect tension (IDT) test (ASTM D6931 [IDT]), shown in Figure 2.5, is a frequently used monotonic crack test for characterizing the fracture properties of HMA mixes. The loading configuration is similar to SCB testing but with fewer specimen preparation steps. Diametric compression loading of cylindrical specimens induces horizontal tensile stress indirectly and ultimately causes cracking. IDT tests conducted on WesTrack field cores showed the relationship between IDT parameters and field fatigue performance (50). However, tensile strength and horizontal strain at peak stress from IDT tests did not have a strong relationship to fatigue cracking. Only the fracture energy seemed to weakly correlate with the fatigue cracking percentage measured in the field.

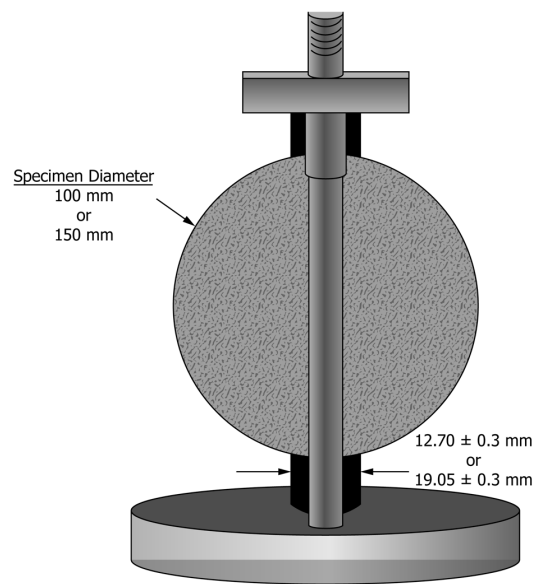


Figure 2.5: IDT test configuration.

The IDEAL-CT test is a newly developed fracture test for mix design and QC/QA from the Texas A&M Transportation Institute that is based on the same loading configuration as IDT testing (6,51). The benefits of this test are simple specimen preparation, fast testing procedure, and accessible testing equipment. Researchers developed a cracking index (*Ctindex*) based on a function of the slopes, displacement, and area under the load-versus-displacement curve. They examined the sensitivity of *Ctindex* with asphalt mixtures containing three different RAP/RAS contents. A comparison study showed that adding a higher percentage of RAP and RAS in the asphalt mixture reduced the *Ctindex* value (51).

The development of cracking tests has expanded to multiple scales of asphalt material. The FAM mix is the portion of a full-gradation asphalt mix consisting of binder, dust, and fine aggregates smaller than a given size. Testing on FAM mixes is an efficient approach for characterizing the performance of asphalt mixtures using substantially less material. Additionally, the FAM portion determines the cracking resistance of asphalt mixtures rather than

the larger aggregate portions since cracks typically initiate and develop in the FAM portion. The performance of full asphalt mixtures can also be predicted through the testing of FAM mixes (52,53,54).

Researchers evaluated the fatigue performance and stiffness of asphalt mixtures with 50% and 100% RAP replacement in the asphalt mix by means of time sweep tests at constant strain values (55). They found the addition of RAP had an adverse effect on fatigue life. In addition, they constructed master curves from frequency sweep tests on FAM mix specimens with varying amounts of RAP replacement (56). Comparisons of the master curves demonstrated that adding RAP to FAM mixes contributed to greater stiffnesses and that testing of FAM mixes distinguished between mixes with varying contents of RAP replacement. These findings also suggest that testing on FAM mixes can be further developed to replace extraction, recovery, and testing of RAP binder to assess the effects of RAP inclusion.

Another study examined the relationship between the fatigue resistance of HMA and the binder (57). The 4PB tests revealed the fatigue behaviors of two asphalt mixtures, one with 35% RAP and one without RAP. The evaluation of binder fatigue occurred through time sweep tests and linear amplitude sweep (LAS) tests. A good relationship was found between the fatigue life of the mixtures and binders at different loading frequencies. A summary report from the Asphalt Institute also noted that the parameter ΔTc of asphalt binder, which is calculated from S and m from the bending beam rheometer tests, can indicate the stiffness and relaxation ability of asphalt at low temperatures and has the potential to predict durability-related cracking performance of aged asphalt pavement (58,59,60,61). The report suggests that ΔTc has a direct effect on block cracking and indirect effects on fatigue cracking and reflective cracking (62).

Table 2.2 summarizes the calibration information for these potential surrogate tests, including the 4PB, I-FIT, LOU-SCB, and IDEAL-CT tests.

Table 2.2: Calibration Information for Fatigue and Fracture Tests

Test	Calibrated Against	Structure Information	Traffic	Replicate	Climate	Mix Type	Crack Type	Recommend Threshold	Correlation Result
4PB	SWK ¹ wheel track device in Nottingham, United Kingdom (63)	50 mm asphalt slabs over a weak thick (92 mm) rubber sheet	Tire pressure of 650 kPa; frequency of loading was 30 passes per minute	2 replicates at each strain value	Tested at 20°C	6 conventional asphalt mixes and 3 asphalt mixes with modifiers	Fatigue cracking	—	Similar ranking results of fatigue life from 4PB and wheel-tracking device for conventional mixes
4PB	LCPC ² circular test track in Nantes, France (63)	Wearing layer of SMA ³ on top of thick AC ⁴ with AB ⁵	Dual tire with 63.6 kN load and 800 kPa tire pressure	2 replicates at each strain value	Nantes, France (northwest of France)	4 conventional asphalt mixes including one high-modulus mix	Surface cracking	—	Not well correlated
4PB	HVS ⁶ sections in Richmond and Davis, California (64)	Structure 1: 2 AC layers with an AB and an ASB ⁷ Structure 2: 2 AC layers with an ATPB ⁸ , AB, and ASB	Dual bias-ply tires with 690 kPa pressure, consisted of 150,000 repetitions of a 40 kN load followed by 50,000 repetitions of an 80 kN load and then by about 1.23 million repetitions of a 100 kN load	More than 2 replicates at each strain value	A constant temperature of 20°C	The surface mix was Caltrans Type A, 19 mm, maximum-size, coarse-graded AC	Fatigue cracking	—	Parameters for <i>CalME</i> fatigue damage model were derived from 4PB tests; deflection simulated from <i>CalME</i> during the fatigue loading process matches well with the measured deflection in the 2 HVS structures
4PB	HVS sections in Richmond and Davis, California (64)	Structure 1: AC overlay on top of cracked existing AC layer with an ATPB, AB, and ASB Structure 2: AC overlay top of cracked AC with AB and ASB	Dual bias-ply tires with 690 kPa pressure, consisted of 150,000 repetitions of a 40 kN load followed by 50,000 repetitions of a 80 kN load and then by about 1.23 million repetitions of a 100 kN load	More than 2 replicates at each strain value	A constant temperature of 20°C	2 AC overlay mixes: an asphalt rubber hot mix gap-graded concrete overlay and a dense-graded AC	Reflective cracking	—	Reflective cracking model in <i>CalME</i> used the fatigue damage model; the predicted resilient deflections agree well with the measured deflection in the HVS sections during all the loading levels

Test	Calibrated Against	Structure Information	Traffic	Replicate	Climate	Mix Type	Crack Type	Recommend Threshold	Correlation Result
4PB	Westrack section in Fallon, Nevada (65)	150 mm AC layer on a 300 mm thick aggregate base with a subgrade below	4 triple-trailer combinations at a speed of 40 mph, 10.3 equivalent single-axle load applications per vehicle pass	3 replicates at each strain value (2 strain values)	Fallon, Nevada	26 conventional asphalt mixes varying in aggregate gradation, asphalt content and air void	Wheelpath fatigue cracking	—	Good correlation between the deflection calculated from <i>CalME</i> and measured from WesTrack sections caused by fatigue loading
I-FIT	9 field sections in Chicago, Illinois (66)	AC overlay on PCC ⁹ , and FD HMA ¹⁰	Speed limit varied from 30 to 50 mph; two-way ADT ¹¹ varied from 1,700 to 22,400	—	Chicago, Illinois	12 asphalt mixes ranging in ABR ¹² from 15% to 60%	Transverse cracking (reflective cracking)	$FI^{13} > 8$ for AC surface	Good linear correlation between log scale of <i>FI</i> and transverse cracking ($R^2 \approx 0.70$); suitable for early-age cracking
I-FIT	ALF ¹⁴ of Federal Highway Administration in McLean, Virginia (67)	AC layer on AB	Super-single tire with pressure of 689 kPa and wheel load of 63 kN	A minimum of 3 replicates	Conditioned at 20°C	8 asphalt mixes ranging in ABR from 0% to 40%	Fatigue cracking (first surface cracking)	—	Good linear correlation between ALF cycles and <i>FI</i> ($R^2 \approx 0.83$)
LOU-SCB	9 field projects in Louisiana (40)	AC overlay on existing AC layer and newly built HMA ¹⁵	Level 2 traffic volume and level 1 traffic volume ¹⁶	4 replicates per single notch depth	Across Louisiana	21 asphalt mixtures varying RAP ¹⁷ from 0% to 30% (PM ¹⁸ binder or CRM ¹⁹ binder)	Random cracking (sum of longitudinal and transverse cracks)	$J_c > 0.5$ kJ/m ²	Moderate linear regression ($R^2 = 0.6$) between RCI ²⁰ and J_c
IDEAL-CT	ALF of Federal Highway Administration in McLean, Virginia (51)	AC layer on aggregate base	Super-single tire with pressure of 689 kPa and wheel load of 63 kN. Speed was 11 mph	3 replicates	Conditioned at 20°C	8 asphalt mixes ranging in ABR from 0% to 40%	Fatigue cracking	$CT_{index} > 80$	Good correlation between ALF cycles to the first crack and CT_{index} (in power function) ($R^2 \approx 0.87$)

Test	Calibrated Against	Structure Information	Traffic	Replicate	Climate	Mix Type	Crack Type	Recommend Threshold	Correlation Result
IDEAL-CT	5 SPS ²¹ test sections in Yukon, Oklahoma (51)	AC layer on existing cracked pavement	—	3 replicates	Yukon, Oklahoma (center of Oklahoma)	5 asphalt mixes with 12% RAP and 3% RAS ²² , varying in WMA ²³ dose and RA ²⁴ dose	Reflective cracking	—	Good correlation between reflective cracking percentage and CT_{index} (in exponential function) ($R^2 = 0.98$); 5 data points of reflective cracking percentage clustered at 100% and 30%
IDEAL-CT	2 field test sections in Perryton, Texas (51)	AC layer on top of milled AC layer	—	3 replicates	Perryton, Texas (north Texas)	2 asphalt mixes with 20% RAP varying in asphalt content	Fatigue cracking	—	Ranking of fatigue cracking rate among 2 sections matches the CT_{index} ranking of 2 mixes
IDEAL-CT	2 field test sections in Childress, Texas (51)	AC layer on top of milled AC layer with severe transverse cracking	—	3 replicates	Childress, Texas (north Texas)	2 asphalt mixes: one is virgin mix, one with 5% RAP and 5% RAS	Reflective cracking	—	Ranking of reflective cracking among 2 sections matches the CT_{index} ranking of 2 mixes

¹ SWK: SWK (Scott Wilson Kirpatrick) Pavement Engineering Ltd.

² LCPC: Laboratoire Central des Ponts et Chaussées

³ SMA: Stone mastic asphalt

⁴ AC: Asphalt concrete

⁵ AB: Aggregate base

⁶ HVS: Heavy Vehicle Simulator

⁷ ASB: Aggregate subbase

⁸ ATPB: Asphalt-treated permeable base

⁹ PCC: Portland cement concrete

¹⁰ FD HMA: Full-depth hot mix asphalt

¹¹ ADT: Average daily traffic

¹² ABR: Asphalt binder replacement

¹³ FI: Flexibility index

¹⁴ ALF: Accelerated loading facility

¹⁵ HMA: Hot mix asphalt

¹⁶ In accordance with the 2006 Louisiana Standard Specifications for Roads and Bridges

¹⁷ RAP: Reclaimed asphalt pavement

¹⁸ PM: Polymer modified

¹⁹ CRM: Crumb rubber modified

²⁰ RCI: Random cracking index

²¹ SPS: Specific pavement studies

²² RAS: Recycled asphalt shingles

²³ WMA: Warm-mix asphalt

²⁴ RA: Recycling agent

Table 2.2 shows that SCB tests (both I-FIT and LOU-SCB tests) have good correlations with transverse cracking, and the calibration with the field cracking data implies the potential of I-FIT and IDEAL-CT tests as surrogate tests for the 4PB test.

2.4 Literature Review Summary

The following are key points from the literature review relevant to this UCPRC research:

- Recently developed fracture testing methods, including SCB tests (producing I-FIT and LOU-SCB parameters) and IDEAL-CT tests, are simple and rank the cracking performance of asphalt materials based on fracture parameters (*FI* or *Ctindex*), but they are not focused exclusively on fatigue and reflective cracking.
- For adoption for routine asphalt mix design or QC/QA implementation, the surrogate cracking test method should require minimal operator training time, easy specimen fabrication, straightforward interpretation of testing results, and representative indicators for cracking performance. More importantly, this surrogate cracking test should be able to provide a reasonable estimate of the stiffness and fatigue life and results similar to the 4PB testing.
- I-FIT, LOU-SCB, and IDEAL-CT testing have been validated against a limited amount of field cracking data, and the ranking comparison implies the applicability of these tests for mix design or QC/QA implementation. However, a more comprehensive study of these testing methods on a wider range of asphalt material types and a correlation study with fatigue testing have not yet been conducted.
- In previous studies, cracking resistance indicators from SCB tests and the IDEAL-CT test showed good sensitivities to asphalt material mix variables, primarily binder type (including conventional, polymer-modified, rubberized), and the inclusion of RAP, which is critical in providing guidance in mix design procedures.
- LAS testing of FAM mixes also stands out as a good candidate for the surrogate fatigue cracking test. It is capable of capturing the fatigue properties of the FAM mix portion in the full asphalt mixture. Understanding the damage and cracking mechanisms in the FAM mixes portion will help characterize asphalt pavement fatigue performance and may provide a faster and easier test than the 4PB test. However, this test will not be as fast and easy as the SCB and IDEAL-CT tests.
- Based on the literature review, I-FIT, LOU-SCB, IDEAL-CT, and LAS tests of FAM mixes were chosen for surrogate performance-related testing to replace 4PB fatigue tests for routine mix design and QC/QA implementation.

3 SUMMARY OF PERFORMANCE-RELATED TESTS

This chapter discusses the performance-related tests conducted in this study. The specific tests and corresponding standards are the following:

- Fatigue cracking resistance of full asphalt mixture: 4PB fatigue testing, also called flexural fatigue testing (AASHTO T 321: Standard Method of Test for Determining the Fatigue Life of Compacted Asphalt Mixtures Subjected to Repeated Flexural Bending), is used as a reference test in this study for stiffness and fatigue cracking performance.
- Fracture performance of full asphalt mixtures: I-FIT testing (AASHTO TP 124: Standard Method of Test for Determining the Fracture Potential of Asphalt Mixtures Using the Flexibility Index Test [FIT]), LOU-SCB testing (DOTD TR 330-14: Evaluation of Asphalt Mixture Crack Propagation Using the Semi-Circular Bend Test [SCB]), and IDEAL-CT testing (ASTM D8225-19: Standard Test Method for Determination of Cracking Tolerance Index of Asphalt Mixture Using the Indirect Tensile Cracking Test at Intermediate Temperature) are used to measure fracture performance.
- Fatigue performance of FAM mixes: LAS testing. Currently, standardized testing for the fatigue performance of FAM mixes does not exist, and the LAS procedure is adopted from the binder fatigue testing standard (AASHTO TP 101: Estimating Damage Tolerance of Asphalt Binders Using the Linear Amplitude Sweep).

These tests used two air void measurement methods: (1) AASHTO T 331: Standard Method of Test for Bulk Specific Gravity (G_{mb}) and Density of Compacted Hot Mix Asphalt (HMA) Using Automatic Vacuum Sealing Method and (2) AASHTO T 166: Standard Method of Test for Bulk Specific Gravity (G_{mb}) of Compacted Hot Mix Asphalt (HMA) Using Saturated Surface-Dry Specimens. The specific method depended on the test method or the UCPRC's standard practice if the method is not outlined in the testing specification. Air voids obtained by vacuum sealing (AASHTO T 331) include those voids connected to surfaces and are not measured by the saturated surface-dry method (AASHTO T 166). Therefore, the vacuum sealing method is suitable for specimens with high air voids. However, sealing the surface is difficult to do for specimens without smooth surfaces because the surface is not cut or a notch is cut in it. As a result, multiple considerations were taken into account when selecting the appropriate air void measuring method for the fatigue and fracture tests and when selecting specimens for testing in the factorial, including the standard specification recommendation, the simplifying of specimen preparation step, and the allowable air void range of the specimens.

3.1 Flexural Fatigue Testing

Specimens for the 4PB tests were compacted using the rolling wheel compactor and cut to 2.5 in. (63.5 mm) wide by 2 in. (50.8 mm) tall by 15 in. (381.0 mm) long. Measurement of the air voids for the 4PB testing specimens followed AASHTO T 331. For those specimens mixed and compacted in the laboratory, target air voids were $7\pm 0.5\%$. The specimens collected in the field did not have air void requirements. Cyclic loading was applied to the HMA beams in the configuration of the four-point bending beam to maintain the same peak strain in each cycle. In this study, specimens for 4PB testing were first conditioned at 68°F (20°C) in the environmental testing chamber. Initial strain values (normally in the range of 250 to 750 microstrain for conventional mixes) were selected depending on the material and performance at 68°F (20°C), with the testing frequency fixed at 10Hz. The testing used three strain values selected by first identifying a high strain that would ensure the specimen would undergo a minimum of 10,000 cycles before failure. The next level was a middle strain. The results of these first two strains were used to extrapolate a log strain versus log fatigue life plot to select the third and lowest strain value where failure would occur after approximately one million cycles. Three replicates were tested for each strain value. Figure 3.1 shows an example of 4PB testing with a beam specimen.

Applied strain, response stress, and loading cycles were recorded during the test, and the stiffness reduction along with loading cycles were calculated based on these measures. Figure 3.2 shows an example of the stiffness master curve and the fatigue failure criterion. In this study, fatigue failure is defined based on the dissipated flexural energy in the material, which is a function of the loading cycles, stiffness, and strain values. As the strain is a controlled value, the function can be simplified to only include loading cycles and stiffness. Therefore, fatigue failure is determined by the peak value of the product of loading cycles and the stiffness reduction ($n \times SR$), shown in Figure 3.2. The stiffness reduction is the ratio of damaged stiffness to initial stiffness, and the initial stiffness is defined as that occurring at the 50th loading cycle.

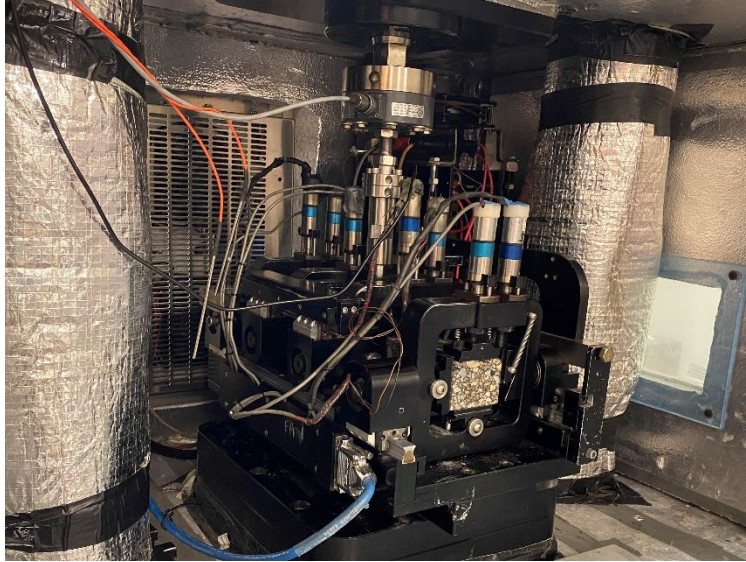


Figure 3.1: 4PB testing apparatus with a beam specimen.

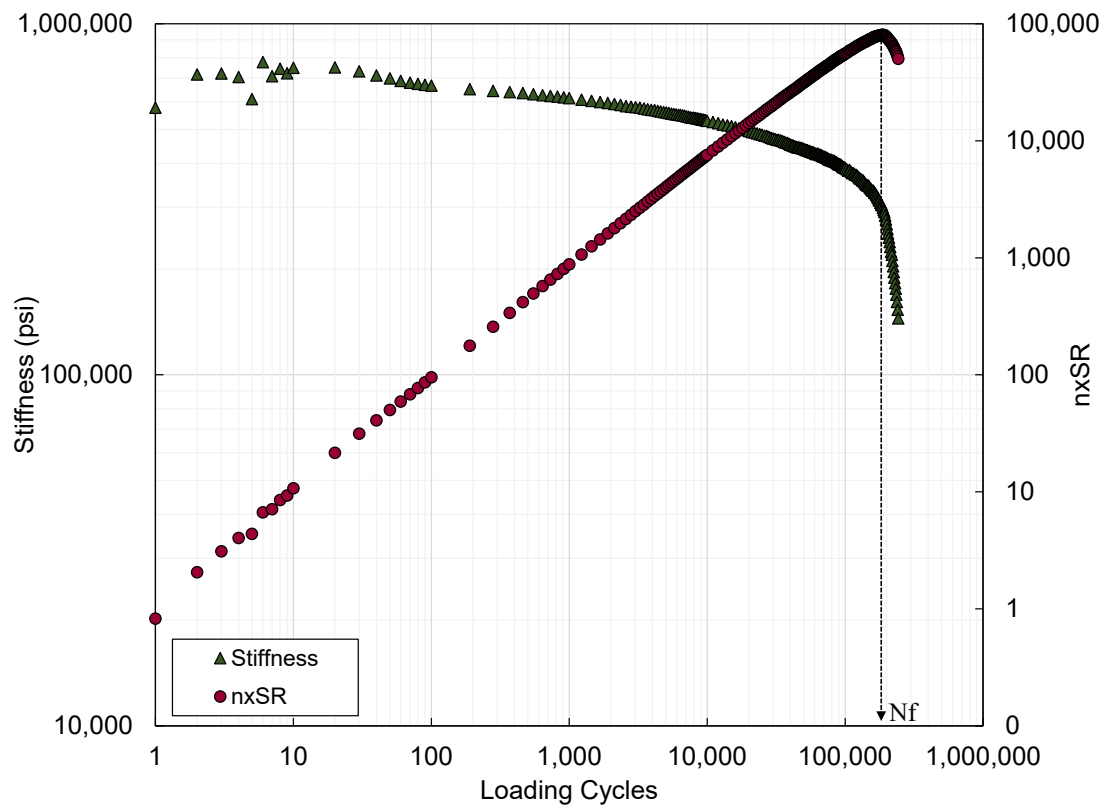


Figure 3.2: Stiffness curve and fatigue failure determination.

Two fatigue parameters were obtained during each fatigue test: initial stiffness (E_{50}) and fatigue life (N_f). The relationship between strain value and fatigue life was expressed with Wohler's law for every mixture, shown in Equation 3.1:

$$N_f = a\varepsilon^b \quad (3.1)$$

Where:

N_f = fatigue cycles,

ε = applied strain value, and

a, b = regression coefficients.

To compare the fatigue performance of all types of asphalt mixtures efficiently, the strain value for fatigue life of one million cycles ($Strain_{N_f=1M}$) was obtained with Wohler's law for each mixture, using Equation 3.2:

$$\varepsilon_{N_f=10^6} = e^{\frac{\ln(10^6) - \ln(a)}{b}} \quad (3.2)$$

Where:

$\varepsilon_{N_f=10^6}$ = strain value when fatigue life is one million cycles.

3.2 SCB Testing

This study used two configurations of SCB testing: I-FIT testing and LOU-SCB testing. The notching depths and the loading rates are the main differences between these two tests.

3.2.1 I-FIT Testing

Specimens prepared in the laboratory for I-FIT testing were fabricated according to AASHTO TP 124. The SGC was used to compact SCB test specimens to a diameter of 5.9 in. (150 mm) and a height of 6.9 in. (175 mm), and the target air void for mixtures prepared in the laboratory was set to $7 \pm 1.0\%$. Compacted specimens were then cut into two disks with a thickness of 2.0 in. (50 mm). The air void for each disk was measured according to AASHTO T166. Then the disk was cut into two halves, a 0.6 in. (15 mm) deep notch was added to each half, and the dimensions—including diameter, notch depth, and thickness—were recorded. At least four replicates were used for the I-FIT testing of each specimen. The specimen preparation and testing apparatus used for the I-FIT testing are shown in Figure 3.3 and Figure 3.4.

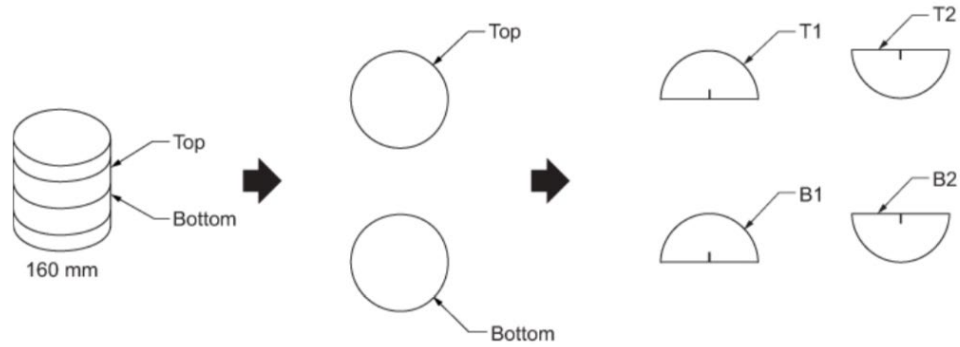
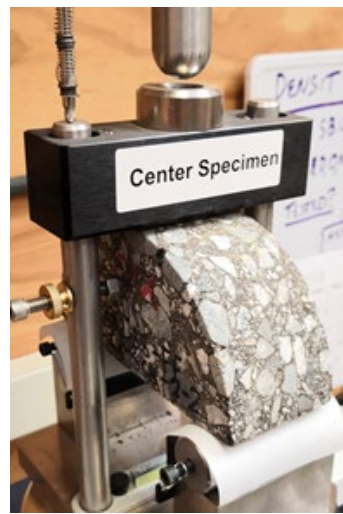


Figure 3.3: Schematic I-FIT specimen preparation.



(a) I-FIT machine



(b) Loading jig with an SCB specimen

Figure 3.4: I-FIT machine with a specimen.

Specimens were conditioned in an oven at 77°F (25°C) for at least two hours prior to testing. The linear variable differential transformer recorded the displacement, and the loading cell measured the concentrated loading force. Specimens deformed under a loading rate of 2 in./min (50 mm/min) until final failure. A typical loading-displacement in I-FIT is shown in Figure 3.5. The load increases as the displacement increases until it reaches the peak load. Prior to reaching the peak load, the nonlinearity between load and displacement indicates both the viscoelasticity of the asphalt mixture and the initiation of microcracks near the notch tip. The peak load point represents the onset of macro crack growth along the notch.

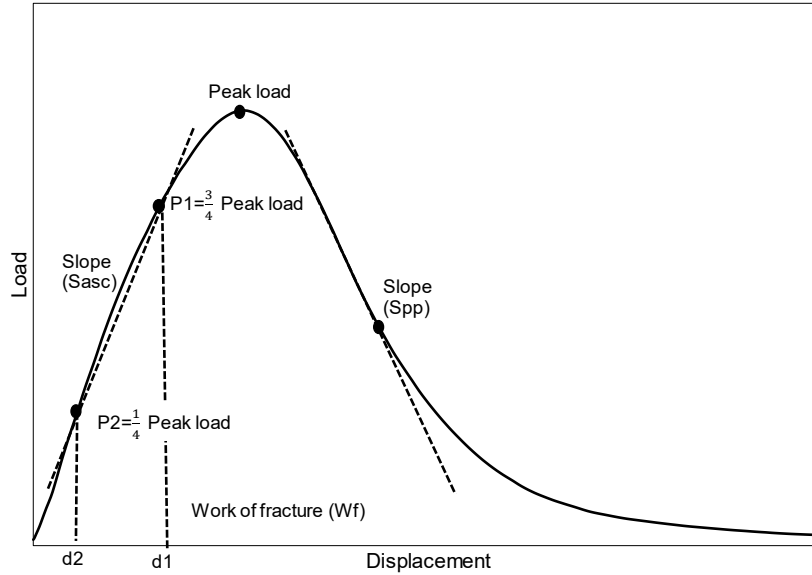


Figure 3.5. Example load-displacement curve from I-FIT.

The displacement versus loading curve was analyzed using I-FIT software developed by ICT, and the analysis results were validated using a MATLAB-based program developed at the UCPRC. The flexibility index (FI), fracture energy (G_f), and post-peak slope (S_{pp}) parameters obtained from I-FIT testing corresponded well with the ones calculated using the UCPRC software. This study also included new parameters based on previous UCPRC research to evaluate the initial stiffness of materials: ascending slope (S_{asc}), flexibility index calculated based on ascending slope (FI_{asc}), and fracture toughness (KIC) (15). Table 3.1 shows a detailed list of the parameters and equations.

Table 3.1: Fracture Parameters for I-FIT Testing

Parameters	Equations
S_{asc} : ascending slope	$S_{asc} = \frac{P1-P2}{d1-d2} \quad (3.3)$ Where: $P1 = \frac{3}{4}$ peak load, $P2 = \frac{1}{4}$ peak load, $d1 =$ deformation at $P1$, and $d2 =$ deformation at $P2$.
S_{pp} : post-peak slope	Tangent slope at inflection point of the curve after peak load
G_f : fracture energy (J/m^2)	$G_f = \frac{W_f}{Area_{lig}} \quad (3.4)$ Where: $W_f =$ area under load-displacement curve, $Area_{lig} = t \times (r - a)$, and $t =$ thickness, $r =$ radius, $a =$ notch depth.
FI : flexibility index	$FI = \frac{W_f \times 0.01}{Area_{lig} \times S_{pp} } \quad (3.5)$
FI_{asc} : flexibility index	$FI_{asc} = \frac{W_f \times 0.01}{Area_{lig} \times S_{asc}} \quad (3.6)$
KIC : fracture toughness ($MPa\sqrt{m}$)	$KIC = Y_{I(0.8)} \sigma_0 \sqrt{\pi a} \quad (3.7)$ Where: $Y_{I(0.8)} = 4.782 + 1.219 \left(\frac{a}{r}\right) + 0.063 \exp(7.045 \left(\frac{a}{r}\right))$.
Strength (Mpa)	$Strength = \frac{Peak\ load}{2rt} \quad (3.8)$

S_{asc} and S_{pp} are indices representing the stiffness information of a specimen. S_{asc} reflects the intact stiffness of a specimen before the crack occurs. S_{pp} is the stiffness of a specimen after the crack initiates and starts to propagate, formulated as the slope of the inflection point after the peak load is reached. For certain specimens, especially brittle materials, it is difficult to locate the inflection point mathematically. Therefore, S_{asc} is defined as the secant slope between two points, unlike S_{pp} , which is defined as the tangent slope of the inflection point. The first point is in the pre-peak curve corresponding to one-quarter of the peak load, and the second point is at three-quarters of the peak load. The corresponding flexibility index is obtained simply by replacing S_{pp} with S_{asc} .

All the I-FIT specimens in this study fractured suddenly from the crack tip under a loading rate of 2 in./min (50 mm/min), implying brittle fracture behavior. Due to such brittle fracture behavior, LEFM is more suitable for describing the testing data and the critical stress intensity K factor from LEFM, also called the fracture toughness (KIC), and the strength of the materials were included as parameters instead of those recommended in AASHTO TP 124. KIC represents the critical stress value at which a crack starts to propagate. It is not only related to the material strength but also associated with the presence of preexisting structural flaws in the material.

3.2.2 LOU-SCB Testing

The same compaction procedure used for I-FIT specimens was used for preparing LOU-SCB specimens. Compacted specimens were cut into two disks with a thickness of 2.2 in. (57 mm). Then each disk was cut into two halves. At least four replicate SCB specimens were prepared for each notch depth. Therefore, there were 12 total SCB specimens for all three notch depths (1.0 in. [25.4 mm], 1.25 in. [31.8 mm], and 1.5 in. [38.1 mm]). Air voids were measured following AASHTO T 166 specifications and the required range of air voids was the same as those used in the I-FIT tests.

Specimens were conditioned in an oven at 77°F (25°C) for at least two hours prior to LOU-SCB testing. The LOU-SCB specimens were tested using the same testing apparatus as the I-FIT tests, shown in Figure 3.4, except that the spacing between the two supports was adjusted from 4.7 in. (120 mm) for the I-FIT test to 5 in. (127 mm) for the LOU-SCB test. A loading rate of 0.5mm/min was applied to specimens until the load diminished to 25% of the peak load. A typical loading versus displacement curve is shown in Figure 3.6.

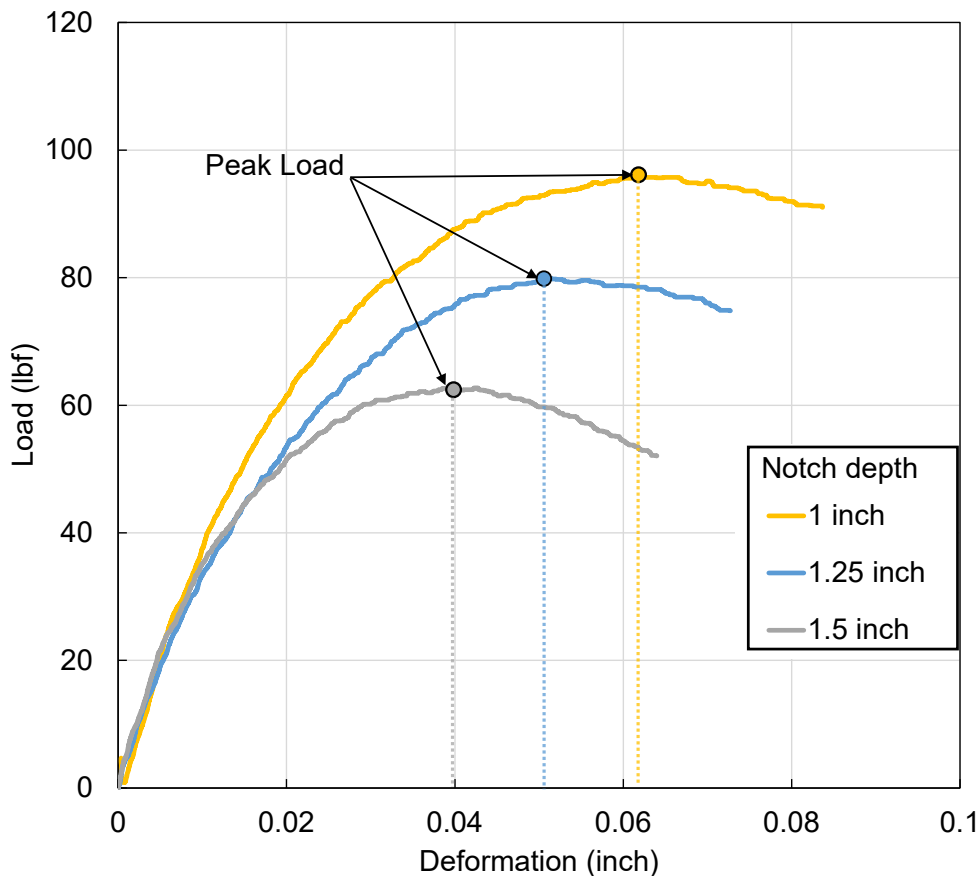


Figure 3.6: Typical result curve from LOU-SCB method (notch depth in in.) (40).

The following Equation 3.9 shows the calculation of the critical J -integral:

$$J_c = -\left(\frac{1}{b}\right) \frac{dU}{da} \quad (3.9)$$

Where:

J_c = critical strain energy release rate (kJ/m²),

b = sample thickness (m),

a = notch depth (m),

U = strain energy to failure (kilo-Joule, kJ), and

$\frac{dU}{da}$ = change of strain energy with notch depth (kJ/m).

To calculate the $\frac{dU}{da}$ in Equation 3.9, a linear regression curve was fitted between the notch depth and the corresponding strain energy to failure. The slope of the fitted curve is equal to the value of $\frac{dU}{da}$.

3.3 IDEAL-CT Testing

Specimens for the IDEAL-CT testing were compacted using the SGC to a diameter of 5.9 in. (150 mm) and a height of 2.4 in. (62 mm). No further cutting process was required for this test. Air voids of specimens were obtained according to AASHTO T 331 specifications, and target air voids for specimens prepared in the laboratory were set to 7±0.5%. At least four replicates were prepared for each mixture, and they were conditioned at 77°F (25°C) for at least two hours prior to testing. The IDEAL-CT testing used the same apparatus as the SCB testing but with a different specimen fixture, shown in Figure 3.7. A loading rate of 2 in./min (50 mm/min) was applied until the tested specimen reached failure. An example of a test result from the IDEAL-CT testing is illustrated in Figure 3.8.

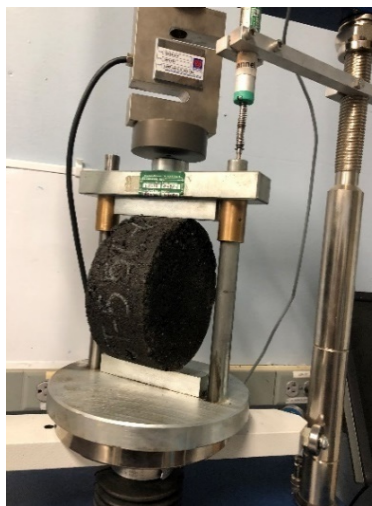


Figure 3.7: Testing machine for IDEAL-CT testing with a specimen.

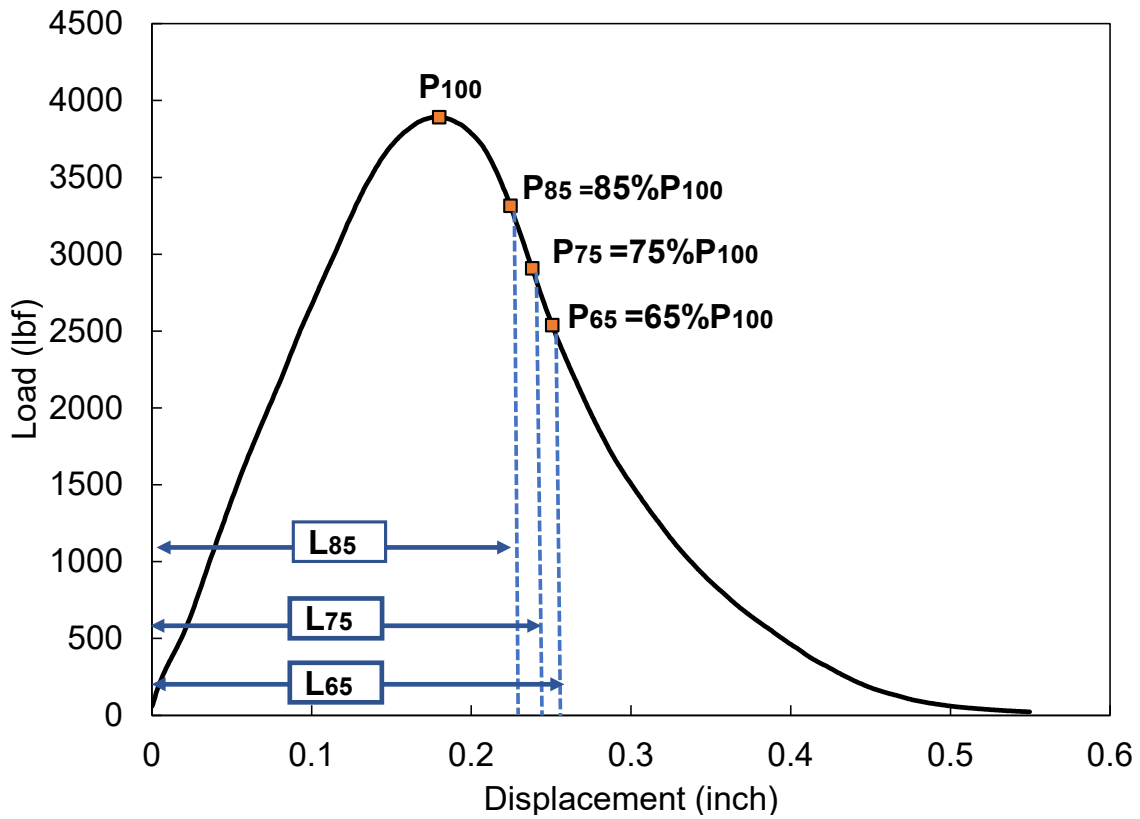


Figure 3.8: Example load-displacement curve from IDEAL-CT testing.

Fracture parameters obtained from the IDEAL-CT testing are shown in Table 3.2 along with definitions. In addition to the parameters suggested in the standard, the strength of a material was also included using the same equation that was used to calculate the same parameter in the I-FIT testing.

Table 3.2: Fracture Parameters from IDEAL-CT Testing

Parameters	Equations
$ m_{75} $: post-peak slope (N/m)	$ m_{75} = \left \frac{P_{85} - P_{65}}{l_{85} - l_{65}} \right \quad (3.10)$ Where: P_{85} = 85% of peak load, P_{65} = 65% of peak load, l_{85} = deformation at P_{85} , and l_{65} = deformation at P_{65} .
l_{75} (mm)	Displacement at 75% of the peak load after the peak
G_f : failure energy (J/m^2)	$G_f = \frac{W_f}{D \times t} \times 10^6 \quad (3.11)$ Where: W_f = area under load-displacement curve (J), and t = thickness (mm), D = diameter (mm).
CT_{index} : cracking tolerance index	$CT_{index} = \frac{t}{62} \times \frac{l_{75}}{D} \times \frac{G_f}{ m_{75} } \times 10^6 \quad (3.12)$
Strength	$Strength = \frac{Peak\ load}{2rt}$

3.4 FAM Mixes LAS Testing

FAM mixes are defined in this study as a homogeneous blend of asphalt binder and fine aggregates that will pass through a No. 8 (0.094 in. [2.36 mm]) sieve. The research team selected the maximum size of 0.094 in. (2.36 mm) to balance the largest size possible with the minimal amount of wasted material while maintaining a representative volume element (56,68,69) and staying within the geometrical and mechanical constraints of the dynamic shear rheometer (DSR) testing device. For mixes designed and prepared in the laboratory, the binder content and aggregate gradation of a FAM mix should reflect the fine portion of the corresponding full-graded mix. The binder content and aggregate gradation of these FAM mixes were determined based on a UCPRC procedure that involves designing a full-graded asphalt mix with optimum binder content using virgin binder, virgin aggregates, and RAP, according to AASHTO R 35 (56). After short-term aging for two hours, the loose mix was sieved through the 0.094 in. (2.36 mm) sieve (AASHTO R 30) using a high-capacity screen shaker. Agglomerations were broken up gently by hand prior to the sieving to ensure that most of the material finer than 0.094 in. (2.36 mm) would be collected. The binder content and aggregate gradation of the FAM portion were then determined through extraction and recovery of the binder (AASHTO T164, Method A) and wet sieving of the recovered aggregate (AASHTO T30). For loose mixes collected in the field, the mix design step was skipped. The same short-term aging and sieving process with the high-capacity screen shaker were performed directly on the loose field samples to obtain the fine portion of the mix.

Mixes for FAM testing were sampled from other laboratory or field experiments used in a number of different research projects. Any project that required flexural beam testing had FAM testing done on the same mixes. None

of the mixes was specifically prepared for FAM testing. Loose FAM mix samples, mixed in the laboratory or field mix collected from the plant, were sieved through a 0.094 in. (2.36 mm) sieve and then compacted using the SGC to a height of 4 in. (100 mm) and a diameter of 6 in. (150 mm). The target air void was set to $9\pm 2\%$. Two ends with a thickness of 0.98 in. (25 mm) were cut off the compacted cylinder to produce a specimen 1.97 in. (50 mm) tall. The cutting minimized air void variations on the compacted specimens and produced smooth parallel end faces. The air void contents of SGC-compacted specimens before and after cutting were determined by measuring the maximum theoretical specific gravity of the mix (AASHTO T 209) and bulk specific gravity of the saturated surface-dry specimens (AASHTO T 166). Small FAM mix specimens for LAS testing with a diameter of approximately 0.47 in. (12 mm) and a height of 1.97 in. (50 mm) were then cored from the compacted cylinder, shown in Figure 3.9. The air void content of the FAM mix specimens was determined according to AASHTO T 166 Method A.



(a) A compacted cylinder with two ends cut off



(b) A FAM specimen cored from the cylinder

Figure 3.9: A cylinder of FAM mix after cutting and coring.

The modified LAS testing procedure was conducted on the FAM mix cores using a solid torsion bar fixture in a DSR, shown in Figure 3.10. Two ends of a FAM specimen were glued to aluminum caps, which were later clamped in the DSR torsion fixture. Each specimen was carefully inspected to ensure that its two ends were clean and undamaged in the clamping zone and that no localized weak areas—such as aggregates torn out during coring—were present that could influence the testing results.

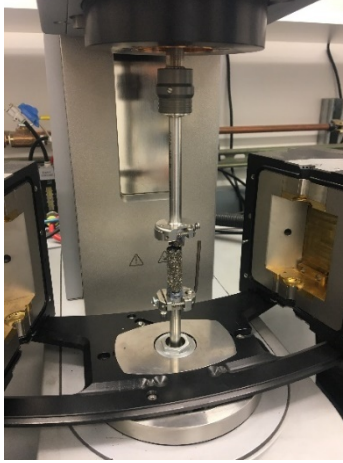


Figure 3.10: DSR equipment for FAM mixes LAS testing with a specimen.

At least three replicates were tested for each FAM mix type. Specimens were conditioned at 77°F (25°C) for one hour in the DSR chamber before testing. At the beginning of a test, a frequency sweep test was performed covering frequencies from 25 Hz to 0.1 Hz at a strain value of 0.002% and a temperature of 77°F (25°C). The strain value of 0.002% was selected to ensure the material would remain in the linear viscoelastic region and the undamaged material properties could be determined. The testing temperature of 77°F (25°C) was determined based on previous research experience to ensure that fatigue damage took place within the DSR torque limit. Based on the frequency sweep testing results, a parameter α was calculated to describe the damage rate relative to undamaged properties as defined in the VECD model. Following the frequency sweep testing, an LAS test was conducted to induce damage to the specimen and the strain amplitude was systematically increased to accelerate damage. The strain amplitude was changed over time, using a linear log scale, from 0.002% to 0.6% at 77°F (25°C) and a constant frequency of 10 Hz. The linear log increased the strain amplitude over time, applying more loading cycles at lower strains and less loading cycles at higher strains. As a result, sufficient damage was induced in the specimen at lower strains before higher strains were applied, which is important because of the limitation on the applied torque in the DSR.

The VECD model was developed based on Schapery's work potential theory shown in Equation 3.13 (3):

$$\frac{dD}{dt} = \left(\frac{dW}{dD}\right)^\alpha \quad (3.13)$$

Where:

D = damage,

t = time,

W = work performed, and

α = material constant.

The work potential theory establishes a relationship between the damage rate and the rate of work performed. Although it has been primarily applied to the fatigue damage behavior in asphalt mixtures as a function of tensile strains, it is formulated in terms of general work of distortion to the internal state of material (4,70,71,72). The FAM LAS testing in this study used sinusoidal torsional loading, and the work energy is purely torsional with minimal tensile force caused by the clamping restraints at the two ends. Therefore, only the torsion-caused energy was considered during the analysis for the VECD model. The material constant α can be directly obtained using the slope of the log-log plot of the storage modulus versus frequency. The relationship between the storage modulus and the frequency is defined by Equation 3.14:

$$\log G'(\omega) = m(\log \omega) + b \quad (3.14)$$

Where:

G' = storage modulus,

ω = test frequency,

m = slope of the regression line, and

b = constant.

The parameter α can then be calculated as:

$$\alpha = \frac{1}{m} \quad (3.15)$$

Using the LAS test results, the accumulation of damage intensity over the loading cycles (N) can be calculated as follows:

$$D(t) \cong \sum_{i=1}^N [\pi I_D \gamma_o^2 (|G^*| \sin \delta_{i-1} - |G^*| \sin \delta_i)]^{\frac{\alpha}{1+\alpha}} (t_i - t_{i-1})^{\frac{1}{1+\alpha}} \quad (3.16)$$

Where:

$D(t)$ = damage intensity at loading time t ,

I_D = initial complex shear modulus, Mpa,

t = loading time, s,

γ_o = applied shear strain, and

$|G^*|$ = complex shear modulus, Mpa.

The relationship between damage intensity and the loss modulus ($|G^*| \sin \delta$) can be fitted using a power law curve as follows (73):

$$|G^*| \sin \delta = C_0 - C_1 D^{C_2} \quad (3.17)$$

Where:

C_0 = averaged $|G^*| \sin \delta$ at the initial strain rate, and

C_1 and C_2 = curve fitting coefficients.

The relationship between fatigue life (N_f) and strain rate can be written as:

$$N_f = A(\gamma_o)^B \quad (3.18)$$

Where the coefficients A and B are given by:

$$A = \frac{f(D_f)^k}{k(\pi I_D C_1 C_2)^\alpha} \quad (3.19)$$

$$B = -2\alpha \quad (3.20)$$

Where:

D_f = damage intensity at failure.

According to AASHTO TP101, failure occurs in a binder when the initial undamaged value of $|G^*| \sin \delta$ decreases by 35%. In this study, the failure criterion was defined as the peak of the phase angle curve, which was identified as a realistic failure criterion for FAM mixes (74). The main fatigue parameters from FAM mixes LAS testing are listed in Table 3.3.

Table 3.3: Fatigue Parameters from FAM Mixes LAS Testing

Parameters	Equations
E_{10}	Initial stiffness from LAS testing on FAM mixes, calculated as the average complex modulus of the first ten loading cycles
$FailureStrain$	Applied shear strain corresponding to the peak of phase angle
A and B : Wohler's law coefficients	$N_f = A(\gamma_o)^B$
$DamageLevel$: damage level at the failure	$DamageLevel = 1 - \frac{G_f^*}{I_D}$ (3.21) Where: G_f^* = complex modulus corresponding to peak phase angle.
D_f : damage intensity at failure	$D(t)_{t=t_f} \cong \sum_{i=1}^N [\pi I_D \gamma_o^2 (G^* \sin \delta_{i-1} - G^* \sin \delta_i)]^{\frac{\alpha}{1+\alpha}} (t_i - t_{i-1})^{\frac{1}{1+\alpha}}$ Where: t_f = test time corresponding to peak phase angle.

As a material is subjected to external loading, the work done on the body will be partially stored as strain energy and part of it will dissipate due to damage growth. Specific VECD models can be developed from the material's

general form for multiaxial loading to other specific forms depending on the applied work (pure tension, pure shear, or mixed mode). In Equation 3.16, fatigue damage is a function of the complex shear stiffness times the shear strain squared ($G^* \gamma_o^2$), which is equivalent to the shear stress times the shear strain, or the simple work of the shear distortion. In *CalME*, the fatigue damage model is defined as a function of the Young's modulus times the tensile strain squared ($E \varepsilon^2$), which is equivalent to the tensile stress times the tensile strain, or the simple work of tensile distortion. In reality, the stress or strain components in asphalt pavements are complex and not pure tension or pure shear. The fatigue failure primarily comes from the sum of normal and shear work caused by the traffic loading. In this study, pure tensile loading or pure torsional loading was performed in the laboratory to evaluate the fatigue damage resistance of asphalt mixtures.

4 MATERIAL AND EXPERIMENTAL DESIGN

To investigate the practical application of surrogate tests and the relationship between fatigue tests and fracture tests, this study tested a varying set of asphalt mixture types (dense gradations unless otherwise noted):

- Rubberized hot mix asphalt with gap gradation
- Hot mix asphalt with 0% RAP and base binder
- Hot mix asphalt with 15% RAP and base binder
- Hot mix asphalt with 15% RAP and rubberized binder
- Hot mix asphalt with 15% RAP and polymer-modified binder
- Hot mix asphalt with 25% RAP and base binder
- Hot mix asphalt with 25% RAP and polymer-modified binder
- Hot mix asphalt with 20% RAP and 3% RAS with base binder
- Hot mix asphalt with 40% RAP with base binder
- Hot mix asphalt with 40% RAP mixed with rejuvenator in base binder
- Hot mix asphalt with 50% RAP mixed with rejuvenator in base binder

The State of California permits the use of RAP material in asphalt mixtures. In 2009, Caltrans started allowing 15% RAP replacement in asphalt pavement by aggregate mass. Caltrans has used up to 25% RAP for AC Long Life mixes since 2012. Recycled asphalt shingles (RAS) are another potentially valuable source of asphalt binder for use in asphalt pavement construction. Caltrans is currently permitting 25% RAP in HMA by aggregate mass for surface course, and it is studying other mixes with more than 25% RAP and small amounts of RAS. Recycled tire rubber has been used in asphalt pavements since the 1960s and used extensively in California since the 1990s. The incorporation of rubber into asphalt pavements has been found to improve the low temperature fracture resistance (75,76). In this study, asphalt materials included various RAP/RAS contents, asphalt binder contents, and asphalt modifier types and were prepared using different mixture methods. These test samples were tested using both the proposed potential surrogate fatigue tests and 4PB test. This diverse set of mixes was expected to exhibit a wide range of stiffness and fatigue properties, which would be used to evaluate the relationships between flexural fatigue and stiffness and the parameters from the potential surrogate tests.

This study included a total of 49 asphalt mixtures. The binder performance grades (PGs) included PG 58-22, PG 64-10, PG 64-28, PG 64-16, PG 64-22, and PG 70-10. Some asphalt binders in the mixtures were polymer-modified (PM) or crumb rubber-modified (CRM) asphalt binders. There were six levels of RAP/RAS content by the total mass of production (TMP: RAP/RAS material + virgin aggregates): 0% RAP, 15% RAP, 25% RAP, 40% RAP, 20% RAP + 3% RAS, and 50% RAP. Table 4.1 shows the detailed information for each mixture. The

Mix Type column groups the 49 asphalt mixtures into 11 categories based on the RAP/RAS content and binder type.

Five asphalt mixtures were collected from paved state highways in California and labeled FMFC in the Preparation Method column. Loose mixes of some asphalt mixtures, labeled FMLC, were sampled from the field plant and then compacted in the UCPRC laboratory. The remaining mixtures, labeled LMLC, were both mixed and compacted in the laboratory.

Among the FMLC materials, the asphalt mixtures labeled with the MIXID label HRAP were collected from plants in Southern California and these mixes contain high percentages of recycled asphalt material. These mixes are produced for private or local government clients and do not necessarily meet Caltrans specifications. The mixes were sampled for the study specifically because of their high RAP content. They were sampled after two different silo storage periods to evaluate the effect of high temperatures over time on their fatigue properties. Previous research has shown that more complete blending of the RAP binder with the virgin binder as well as additional aging occur at high temperatures over longer time periods (77). HRAP_0H_1 and HRAP_5H_1 followed the same mix design but with a different number of storage hours in the silo at the plant (0 hours versus 5 hours). The same identification convention applies to HRAP_0H_2 and HRAP_16H_2 (0 hours versus 16 hours), HRAP_0H_3 and HRAP_16H_3 (0 hours versus 16 hours), and HRAP_0H_4 and HRAP_6H_4 (0 hours versus 6 hours). Different silo times were sampled at the plants during routine mix production for a separate ongoing study investigating the impact of silo hours on these high RAP content mixes. Those mixes were included to study the full range of mixes for which a simple, fast, economical test for routine mix design and construction QC/QA are desired, including conventional mixes, polymer- and rubber-modified mixes, and high RAP and RAS mixes. The purpose of sampling at different amounts of time spent in the silo is to evaluate any changes in stiffness and fatigue performance from the additional aging of virgin binder and recycling agent and additional blending of virgin and RAP binders caused by longer amounts of time at high temperatures. The FMFC materials did not have an air void requirement, while the LMLC and FMLC materials had target air voids of 7%. The asphalt content is calculated as the total virgin binder weight divided by the total weight of the mix.

Table 4.1: Asphalt Mixture Information

MIXID	Mix Type	Mix Category	Gradation Type	Binder Replacement ^a (%)	PG + Modifier	AC ^b (%)	Preparation Method ^c	Mixing/Compaction Temperature (°C)
Virgin_1	0% RAP with AR binder ^d	RHMA-G ^e	Gap	0	PG 64-16 + 20% CRM ^f	7.6	FMFC	—/—
Virgin_2	0% RAP with AR binder	RHMA-G	Gap	0	PG 64-16 + 20% CRM	7.6	FMLC	—/163
Virgin_3	0% RAP with AR binder	RHMA-G	Gap	0	PG 64-16 + 20% CRM	7.7	FMLC	—/152
Virgin_4	0% RAP with AR binder	RHMA-G	Gap	0	PG 64-16 + 20% CRM	7.3	FMLC	—/153
Virgin_5	0% RAP with AR binder	RHMA-G	Gap	0	PG 70-10 + CRM	7.5	FMLC	—/143
Virgin_6	0% RAP with AR binder	RHMA-G	Gap	0	PG 64-16 + CRM	7.5	FMLC	—/152
Virgin_7	0% RAP with AR binder	RHMA-G	Gap	0	PG 64-16 + CRM	7.5	FMLC	—/160
Virgin_8	0% RAP with neat binder	HMA	Dense	0	PG 64-16	5.39	LMLC	144/134
RAP15%_1	15% RAP with neat binder	HMA Type A ^g	Dense	11	PG 64-16	6.4	LMLC	155/144
RAP15%_2	15% RAP with neat binder	HMA Type A	Dense	15	PG 64-16	5.0	FMFC	—/—
RAP15%_3	15% RAP with neat binder	HMA Type A	Dense	15	PG 64-16	5.0	FMFC	—/—
RAP15%_4	15% RAP with neat binder	HMA Type A	Dense	14	PG 64-16	5.0	FMLC	—/146
RAP15%_5	15% RAP with neat binder	HMA Type A	Dense	15	PG 64-16	4.5	FMLC	—/138
RAP15%_6	15% RAP with neat binder	HMA	Dense	12	PG 64-16	5.3	LMLC	150/140
RAP15%_7	15% RAP with neat binder	HMA	Dense	12	PG 70-10	5.3	LMLC	170/155
RAP15%_8	15% RAP with neat binder	HMA	Dense	15	PG 64-22	5.3	LMLC	150/140
RAP15%_9	15% RAP with neat binder	HMA	Dense	13	PG 64-16	5.4	FMLC	—/142
RAP15%_10	15% RAP with neat binder	HMA	Dense	12	PG 64-16	5.4	FMLC	—/143
RAP15%AR_1	15% RAP with AR binder	HMA	Dense	12	PG 64-16 + 5% CRM	5.3	LMLC	150/140
RAP15%AR_2	15% RAP with AR binder	HMA	Dense	12	PG 64-16 + 10% CRM	5.3	LMLC	150/140
RAP15%AR_3	15% RAP with AR binder	HMA	Dense	12	PG 70-10 + 10% CRM	5.3	LMLC	170/155
RAP15%AR_4	15% RAP with AR binder	HMA	Dense	12	PG 64-16 + 5% CRM	5.3	LMLC	150/140
RAP15%AR_5	15% RAP with AR binder	HMA	Dense	15	PG 64-22 + 5% CRM	5.3	LMLC	165/158
RAP15%AR_6	15% RAP with AR binder	HMA	Dense	15	PG 64-22 + 10% CRM	5.3	LMLC	170/166
RAP15%PM_1	15% RAP with PM binder	HMA Type A	Dense	14	PG 64-28 PM ^h	5.2	LMLC	159/152
RAP15%PM_2	15% RAP with PM binder	HMA Type A	Dense	14	PG 64-28 PM	5.0	FMLC	—/147
RAP15%PM_3	15% RAP with PM binder	HMA Type A	Dense	14	PG 64-28 PM	5.2	FMLC	—/149
RAP15%PM_4	15% RAP with PM binder	HMA Type A	Dense	14	PG 64-28 PM	5.2	FMLC	—/149
RAP15%PM_5	15% RAP with PM binder	HMA	Dense	13	PG 64-28 PM	5.09	FMLC	—/141
RAP15%PM_6	15% RAP with PM binder	HMA	Dense	13	PG 64-28 PM	5.09	FMLC	—/141
RAP25%_1	25% RAP with neat binder	HMA Type A	Dense	24	PG 64-16	5.3	LMLC	155/144

MIXID	Mix Type	Mix Category	Gradation Type	Binder Replacement ^a (%)	PG + Modifier	AC ^b (%)	Preparation Method ^c	Mixing/ Compaction Temperature (°C)
RAP25%_2	25% RAP with neat binder	HMA-SP ⁱ	Dense	23	PG 64-10	5.0	FMFC	—/—
RAP25%_3	25% RAP with neat binder	HMA-SP	Dense	24	PG 64-10	5.0	FMLC	—/138
RAP25%_4	25% RAP with neat binder	HMA Type A	Dense	23	PG 64-16	5.2	FMLC	—/143
RAP25%_5	25% RAP with neat binder	HMA	Dense	24	PG 64-16	5.5	LMLC	144/134
RAP25%_6	25% RAP with neat binder	HMA	Dense	22	PG 64-16	5.2	FMLC	—/143
RAP25%_7	25% RAP with neat binder	HMA	Dense	22	PG 64-16	5.2	FMLC	—/143
RAP25%_8	25% RAP with RA	HMA	Dense	19	PG 64-16	5.7	LMLC	144/134
RAP25%PM_1	25% RAP with PM binder	HMA-SP	Dense	20	PG 64-28 PM	3.7	FMFC	—/—
RAP25%PM_2	25% RAP with PM binder	HMA-SP	Dense	20	PG 64-28 PM	3.7	FMLC	—/158
HRAP_0H_1	20% RAP + 3% RAS with neat binder	HMA	Dense	29	PG 58-22	5.2	FMLC	—/134
HRAP_5H_1	20% RAP + 3% RAS with neat binder	HMA	Dense	29	PG 58-22	5.2	FMLC	—/134
HRAP_0H_2	40% RAP with neat binder	HMA	Dense	33	PG 58-22	5.9	FMLC	—/134
HRAP_16H_2	40% RAP with neat binder	HMA	Dense	33	PG 58-22	5.9	FMLC	—/134
HRAP_0H_3	40% RAP with RA ^j	HMA	Dense	33	PG 64-10	5.75	FMLC	—/134
HRAP_16H_3	40% RAP with RA	HMA	Dense	33	PG 64-10	5.75	FMLC	—/134
HRAP_0H_4	50% RAP with RA	HMA	Dense	55	PG 64-10	5.1	FMLC	—/134
HRAP_6H_4	50% RAP with RA	HMA	Dense	55	PG 64-10	5.1	FMLC	—/134
HRAP_5	50% RAP with RA	HMA	Dense	40	PG 64-16	5.5	LMLC	144/134

^a Binder replacement = (weight of binder in RAP or RAS)/(virgin binder + recycled binder)

^b AC = (total binder weight)/(total asphalt mixture weight)

^c FMFC: Field-mixed and field-compacted mixture; FMLC: Field-mixed and lab-compacted mixture; LMLC: Lab-mixed and lab-compacted mixture

^d RAP: Reclaimed asphalt pavement; AR: Asphalt rubber

^e RHMA-G: Rubberized hot mix asphalt (gap graded)

^f PG: Performance grade; CRM: Crumb rubber modified

^g HMA: Hot mix asphalt

^h PM: Polymer modified

ⁱ HMA-SP: Hot mix asphalt (Superpave)

^j RA: Recycling agent content = weight of recycling agent/weight of virgin binder

Due to the time and sample quantity limitations, the selected surrogate tests were not performed on all 49 mixtures. The detailed experimental design is shown in Table 4.2. The I-FIT testing was conducted on 40 asphalt mixtures, 4PB testing on 45 mixtures, LOU-SCB testing on seven mixtures, IDEAL-CT testing on 26 mixtures, and FAM LAS testing on eight mixtures. The testing results and fatigue/fracture parameters from each surrogate test were analyzed and compared against testing results from the 4PB test, which is the benchmark testing method for fatigue cracking performance in this study. All the tests involved in this study were performed at the temperatures recommended in the corresponding specifications, which is 68°F (20°C) for 4PB testing and 77°F (25°C) for I-FIT, LOU-SCB, and IDEAL-CT testing. Although the testing temperature for 4PB testing (68°F [20°C]) is slightly different from the testing temperature of the four surrogate tests (77°F [25°C]), both temperatures can be considered intermediate pavement temperatures associated with fatigue cracking in asphalt pavements. The testing temperature of 77°F (25°C) for the I-FIT fracture test was selected by the University of Illinois during test development to amplify the difference between mixes and eliminate the need for an environmental condition chamber during testing, assuming the room temperature could be maintained at 77°F (25°C) (43).

Table 4.2: Experimental Design

MIXID	Mix Type	Mix Category	4PB	I-FIT	LOU-SCB	IDEAL-CT	FAM LAS
Virgin_1	0% RAP with AR binder	RHMA-G	X	X	X		
Virgin_2	0% RAP with AR binder	RHMA-G	X	X		X	
Virgin_3	0% RAP with AR binder	RHMA-G	X	X			
Virgin_4	0% RAP with AR binder	RHMA-G	X	X			
Virgin_5	0% RAP with AR binder	RHMA-G	X			X	
Virgin_6	0% RAP with AR binder	RHMA-G	X			X	
Virgin_7	0% RAP with AR binder	RHMA-G	X			X	
Virgin_8	0% RAP with neat binder	HMA	X	X		X	
RAP15%_1	15% RAP with neat binder	HMA Type A	X	X			
RAP15%_2	15% RAP with neat binder	HMA Type A	X	X			
RAP15%_3	15% RAP with neat binder	HMA Type A	X	X	X		
RAP15%_4	15% RAP with neat binder	HMA Type A		X		X	
RAP15%_5	15% RAP with neat binder	HMA Type A		X		X	
RAP15%_6	15% RAP with neat binder	HMA	X	X			
RAP15%_7	15% RAP with neat binder	HMA	X	X			
RAP15%_8	15% RAP with neat binder	HMA	X	X			
RAP15%_9	15% RAP with neat binder	HMA	X			X	
RAP15%_10	15% RAP with neat binder	HMA	X			X	
RAP15%AR_1	15% RAP with AR binder	HMA	X	X	X		
RAP15%AR_2	15% RAP with AR binder	HMA	X	X	X		
RAP15%AR_3	15% RAP with AR binder	HMA	X	X	X		
RAP15%AR_4	15% RAP with AR binder	HMA	X	X			
RAP15%AR_5	15% RAP with AR binder	HMA	X	X			
RAP15%AR_6	15% RAP with AR binder	HMA	X	X			
RAP15%PM_1	15% RAP with PM binder	HMA Type A	X	X			
RAP15%PM_2	15% RAP with PM binder	HMA Type A	X	X			
RAP15%PM_3	15% RAP with PM binder	HMA Type A	X	X			
RAP15%PM_4	15% RAP with PM binder	HMA Type A	X	X			
RAP15%PM_5	15% RAP with PM binder	HMA	X			X	
RAP15%PM_6	15% RAP with PM binder	HMA	X			X	
RAP25%_1	25% RAP with neat binder	HMA Type A	X	X			
RAP25%_2	25% RAP with neat binder	HMA-SP	X	X	X		
RAP25%_3	25% RAP with neat binder	HMA-SP		X		X	
RAP25%_4	25% RAP with neat binder	HMA Type A	X	X			
RAP25%_5	25% RAP with neat binder	HMA	X	X		X	
RAP25%_6	25% RAP with neat binder	HMA	X			X	
RAP25%_7	25% RAP with neat binder	HMA	X			X	
RAP25%_8	25% RAP with RA	HMA	X	X		X	
RAP25%PM_1	25% RAP with PM binder	HMA-SP	X	X	X		
RAP25%PM_2	25% RAP with PM binder	HMA-SP		X		X	
HRAP_0H_1	20% RAP + 3% RAS with neat binder; 0 silo storage hours	HMA	X	X		X	X
HRAP_5H_1	20% RAP + 3% RAS with neat binder; 5 silo storage hours	HMA	X	X		X	X
HRAP_0H_2	40% RAP with neat binder; 0 silo storage hours	HMA	X	X		X	X
HRAP_16H_2	40% RAP with neat binder; 16 silo storage hours	HMA	X	X		X	X
HRAP_0H_3	40% RAP with RA; 0 silo storage hours	HMA	X	X		X	X
HRAP_16H_3	40% RAP with RA; 16 silo storage hours	HMA	X	X		X	X
HRAP_0H_4	50% RAP with RA; 0 silo storage hours	HMA	X	X		X	X
HRAP_6H_4	50% RAP with RA; 6 silo storage hours	HMA	X	X		X	X
HRAP_5	50% RAP with RA	HMA	X	X		X	

Figure 4.1 shows a comparison between the air voids for the 4PB and I-FIT specimens with the standard deviation as the error bar for both tests. Most of the air voids scatter along the diagonal identity line, implying comparable specimen volumetrics for the specimens used for the 4PB and I-FIT tests.

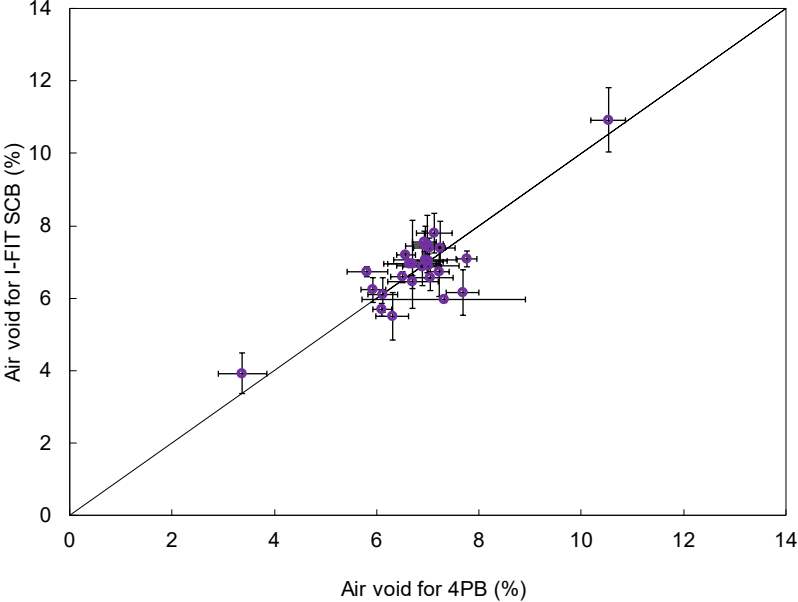


Figure 4.1: Air void information for 4PB and I-FIT specimens.

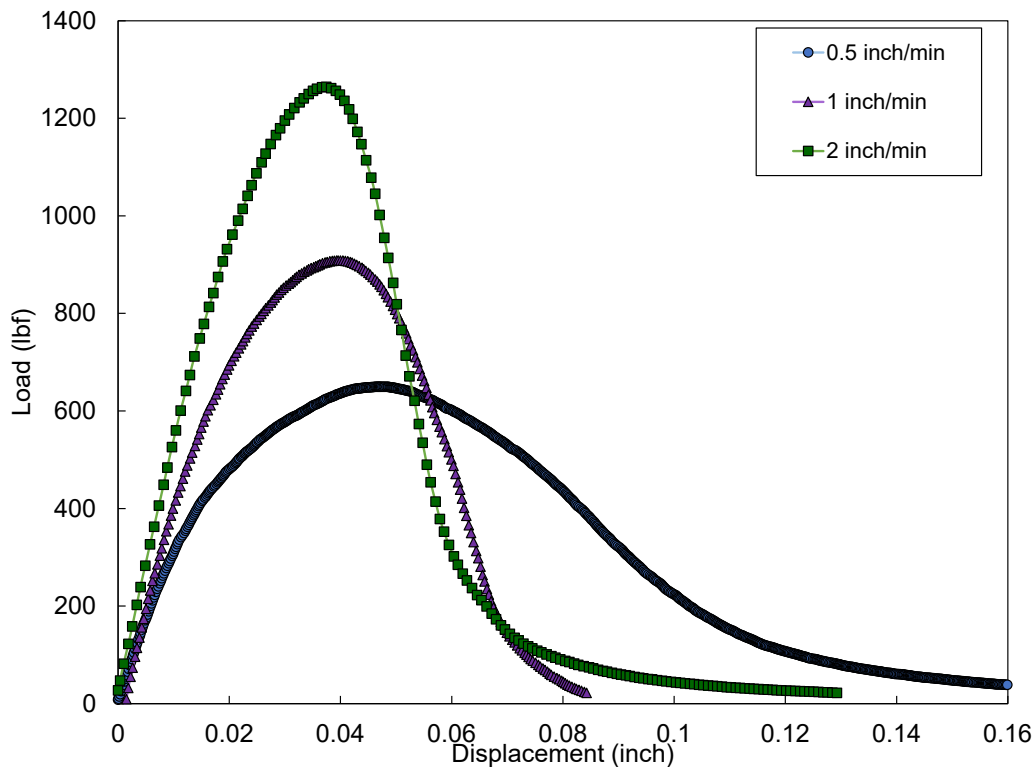
5 RESULTS AND ANALYSIS FOR I-FIT

5.1 I-FIT Testing Results

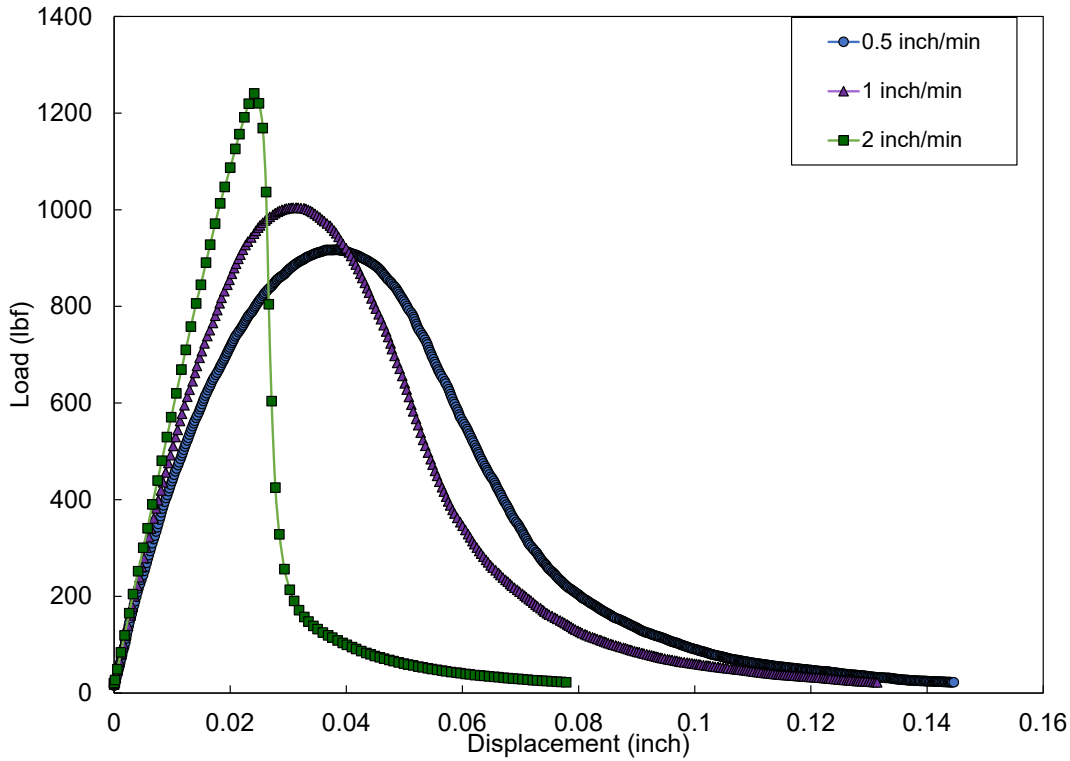
5.1.1 Loading Rate Study

The viscoelastic mechanical behavior of asphalt mixtures leads to the temperature and loading-rate sensitivity. The typical analytical model of asphalt materials consists of springs and dashpots. At a fast loading rate, the characteristics of the asphalt material are determined primarily by the elastic behavior between the stress and strain in the material, modeled using the spring. Due to limited plasticity and viscosity in the material, the specimen will fracture quickly and brittlely. Such behavior can also be observed in asphalt materials at low temperatures or in aged asphalt materials, where the spring/elastic part dominates the response. In contrast, at a slower loading rate, the asphalt material will show more viscous behavior, modeled by the dashpot, which is the same behavior of the material at intermediate and high temperatures.

The effect of loading rate on the fracture results was measured before performing I-FIT testing at the required loading rate of 2 in./min (50 mm/min), following AASHTO TP 124. Two loading rates other than 2 in./min were applied on selected mixtures from Table 4.1 with 15% RAP content: RAP15%AR_1 and RAP15%_7. The loading versus displacement curves at different loading rates are illustrated in Figure 5.1 for both mixtures.



(a) RAP15%AR_1

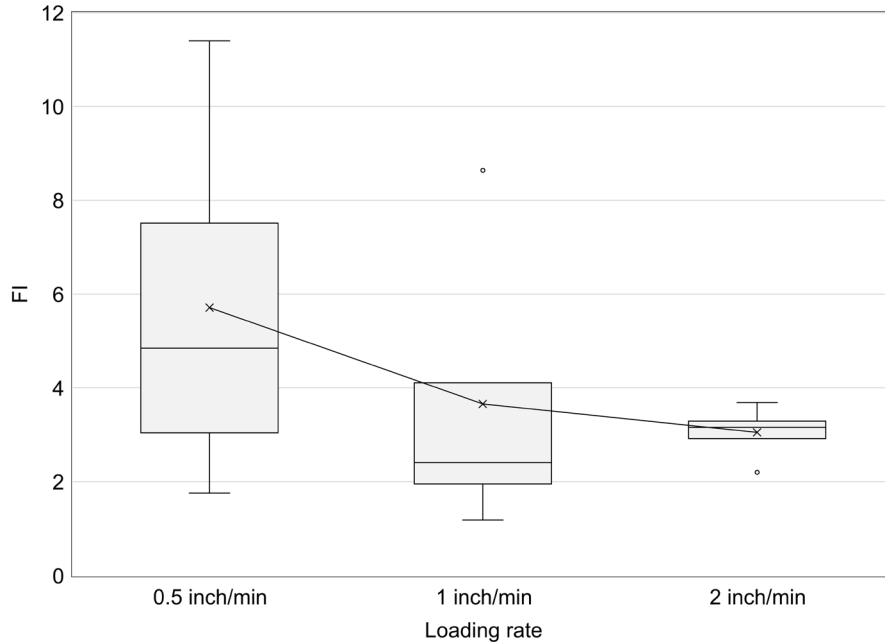


(b) RAP15%_7

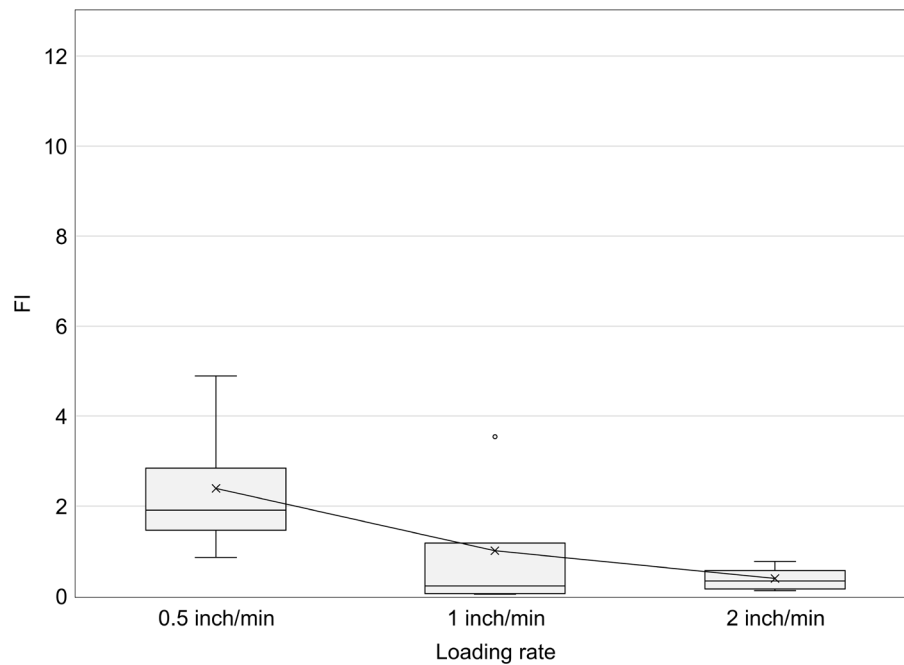
Figure 5.1: Loading versus displacement curve under different loading rates for (a) RAP15%AR_1 and (b) RAP15%_7.

The results show that when the loading rate decreases from 2 in./min (50 mm/min) to 1 in./min (25 mm/min) and 0.5 in./min (12.5 mm/min), the load-displacement curve becomes flatter, the peak load drops, and the initial slope of the curve decreases. At the same time, the curve becomes wider in terms of the displacement at final failure. This phenomenon is due to the mechanical response of the material under different loading rates. Such rate dependence is commonly observed for nearly all materials. In this study, at a faster loading rate, asphalt mixtures tended to behave in an elastic form and end up with brittle fracture failure, while at a lower loading rate the mixtures had more ductile properties and more viscoelasticity.

Figure 5.2 shows a boxplot comparison for both mixtures of *FI* measures obtained for different loading rates. Generally, the averaged *FI* value for both mixtures decreases with an increase in loading rate. However, there is overlap between the *FI* data for different loading rates, particularly between 1 in./min and 2 in./min. The median line of the 2 in./min rate falls between the box boundaries of 1 in./min, implying that there is likely no difference between these two loading rates. In addition, the wider range of the whiskers for the 0.5 in./min loading rate indicates a higher variability of *FI* from this loading rate.



(a) *FI* at different loading rates for RAP15%AR_1



(b) *FI* at different loading rates for RAP15%_7

Figure 5.2: Flexibility index under different loading rates for two mixtures.

A further statistical analysis step investigated the effect of loading rate. The main fracture parameters of I-FIT testing from the same mix at different loading rates were analyzed using the Tukey's honestly significant

difference (HSD) test, which is a statistical method for determining if the two sets of data are statistically different from each other. Table 5.1 shows that there is no significant difference between these three loading rates for the two mixtures, as they share the same group letter *A*. The same analysis method was used to examine the difference between two mixes under the same loading rate, shown in Table 5.2. At the loading rates of 0.5 in./min and 1 in./min, all the I-FIT parameters—including *FI*, *S_{pp}*, and *G_f*—have the same group letter for the two mixtures while the difference is significant between RAP15%AR_1 and RAP15%_7 for all parameters at the loading rate of 2 in./min. Therefore, the loading rate of 2 in./min was selected to provide for differentiation between mixes.

Table 5.1: Tukey’s HSD Test for Loading Rate

Loading Rate	Mix ID	<i>FI</i>	<i>S_{pp}</i>	<i>G_f</i>
0.5 in./min	RAP15%AR_1	A	A	A
1 in./min	RAP15%AR_1	A	A	A
2 in./min	RAP15%AR_1	A	A	A
0.5 in./min	RAP15%_7	A	A	A
1 in./min	RAP15%_7	A	A	AB
2 in./min	RAP15%_7	A	A	B

Note: Tukey’s HSD significance level = 0.1

Table 5.2: Tukey’s HSD Test for Different Mixtures

Loading Rate	Mix ID	<i>FI</i>	<i>S_{pp}</i>	<i>G_f</i>
0.5 in./min	RAP15%AR_1	A	A	A
0.5 in./min	RAP15%_7	A	A	A
1 in./min	RAP15%AR_1	A	A	A
1 in./min	RAP15%_7	A	A	A
2 in./min	RAP15%AR_1	A	A	A
2 in./min	RAP15%_7	B	B	B

Note: Tukey’s HSD significance level = 0.1

5.1.2 Variability of I-FIT Parameters

The repeatability of I-FIT and the variability of parameters—including *FI*, *FI_{asc}*, *S_{pp}*, *S_{asc}*, *G_f*, *Strength*, and *KIC*—are assessed in this section. The coefficient of variation (COV) is a statistical parameter calculated as the ratio of the standard deviation to the mean of the variable that normalizes the variation relative to the mean value and creates a unitless parameter. COV is used in this analysis to describe the variation of each fracture parameter. The higher the COV, the greater the dispersion of the parameter. The average COV values across all mixtures for each parameter are shown in Figure 5.3.

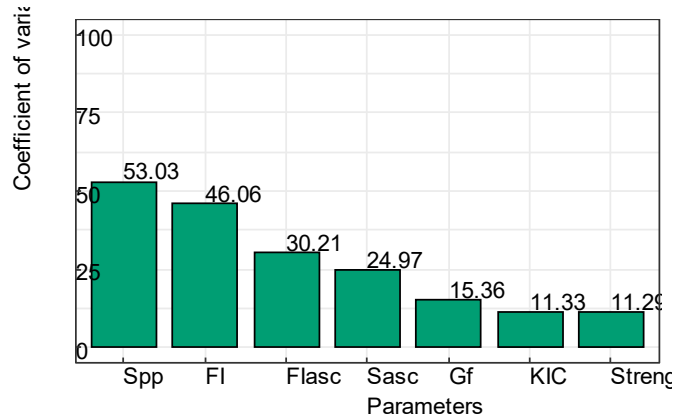


Figure 5.3: Average coefficient of variance for all parameters from I-FIT test.

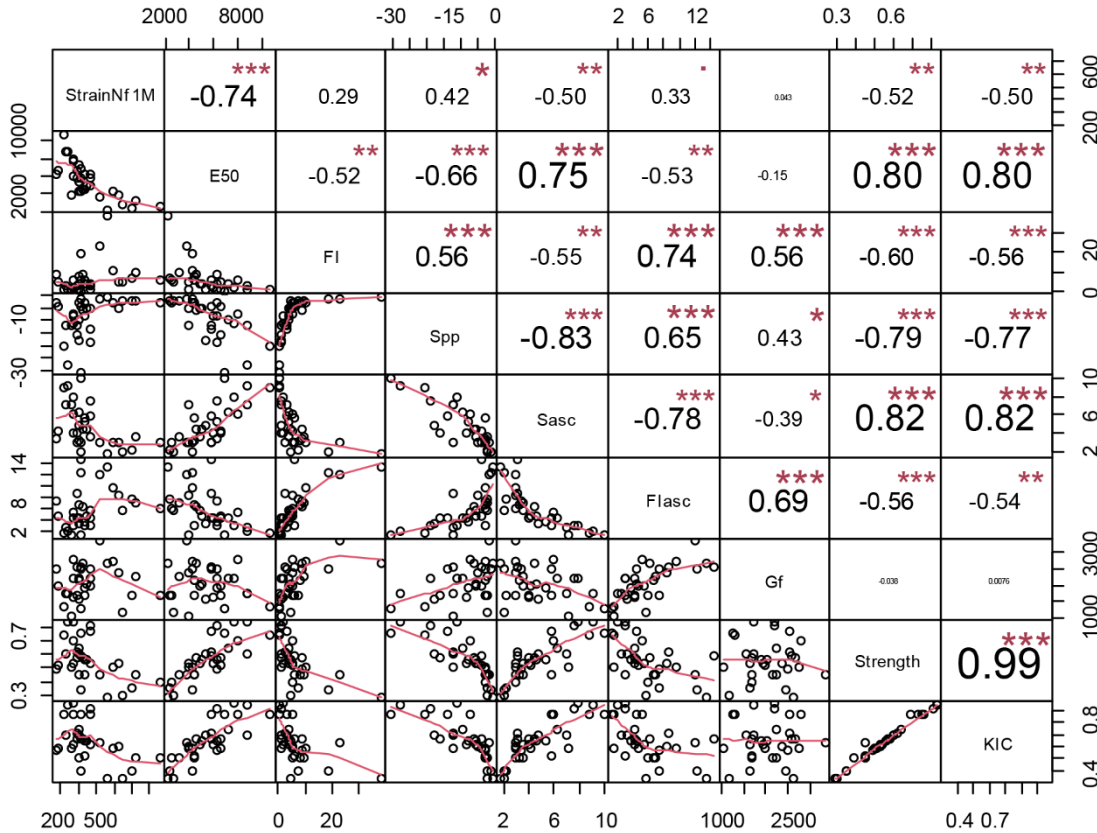
Figure 5.3 shows that post-peak slope (S_{pp}) has the highest variability, 53%, followed by FI with an average COV of 46%. The average COV for FI is much higher than for FI_{asc} (30%) and S_{asc} (25%). The higher variability of S_{pp} can be explained by the brittle fracture failure of the asphalt mixtures included in the study. Such fast brittle failure resulted in difficulties recording load and displacement information during the test. This issue, along with the complex mathematical equation for the inflection point tangent slope, contributes to the low repeatability of S_{pp} . The variability of the slopes (S_{pp} and S_{asc}) is consistent with the variability of the flexibility indexes (FI and FI_{asc}). By definition, the flexibility index (FI) is determined by the slope and fracture energy. As a result, the high variability of S_{pp} contributes to the high COV value of FI when the variability of the fracture energy (G_f) is considerably low (15%). Therefore, the ascending slope (S_{asc}) and the ascending slope-based flexibility index (FI_{asc}) show smaller variability than the post-peak slope (S_{pp}) and post-peak slope-based flexibility index (FI). In addition, KIC and $Strength$ show the best repeatability with COVs as low as 11%.

5.2 Comparison Between I-FIT and 4PB Testing

This section explores the correlation between I-FIT and 4PB testing results and investigates the potential of I-FIT testing at the standard loading rate of 2 in./min (50 mm/min) as a surrogate test for mix design and QC/QA. The analysis of the relationship between fatigue parameters obtained from the 4PB tests and fracture parameters from the SCB tests consists of two parts: stiffness comparison and fatigue life comparison.

First, the correlation comparison between all fatigue parameters and fracture parameters is shown in Figure 5.4. The correlation matrix plot shows the significance levels of the relationship between the parameters. The lower triangular matrix is composed of the bivariate scatter plots with a fitted smooth line. The upper triangular matrix shows the Pearson correlation coefficient (r value) plus significance level (as stars). Each significance level is associated with a symbol: 0.001 (***), 0.01 (**), 0.05 (*), and 0.1(\cdot). Figure 5.4 shows that the 4PB fatigue

performance (*StrainNf1M*) is moderately correlated with the initial stiffness (*E50*) from the 4PB tests (r value = 0.74), but the best correlations with the I-FIT parameters are relatively weak. The r values for the ascending slope (*S_{asc}*), *Strength*, and *KIC* are all approximately 0.5. On the other hand, the flexural stiffness from the 4PB tests (*E50*) is highly correlated with *Strength* and *KIC* from the I-FIT tests, and the rest of the I-FIT parameters have r values greater than 0.5, except for fracture energy (*G_f*).



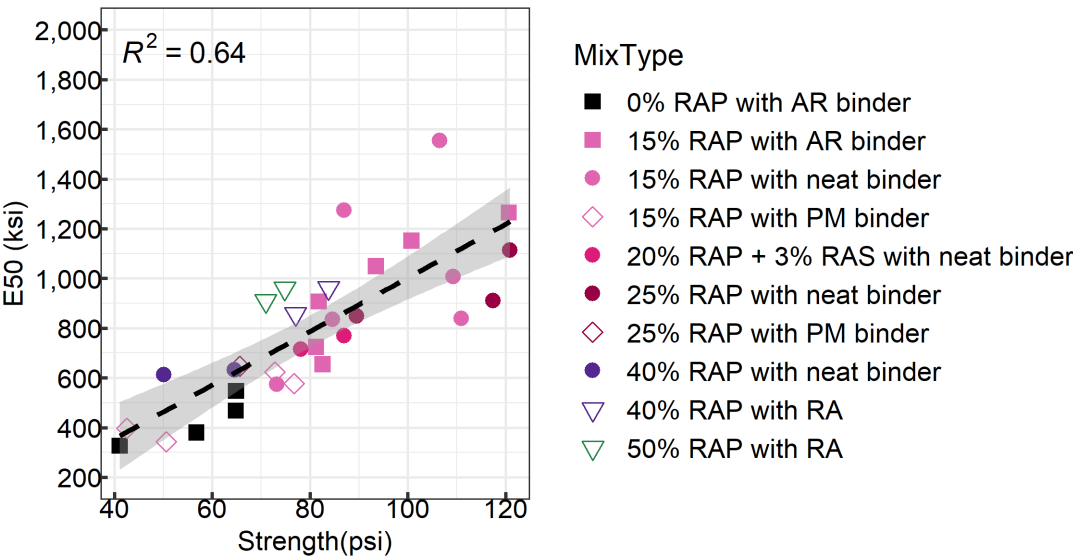
Note: *E50* and *StrainNf1M* tested at 68°F (20°C), all other parameters at 77°F (25°C).

Figure 5.4: Correlation matrix between all parameters from 4PB and I-FIT tests.

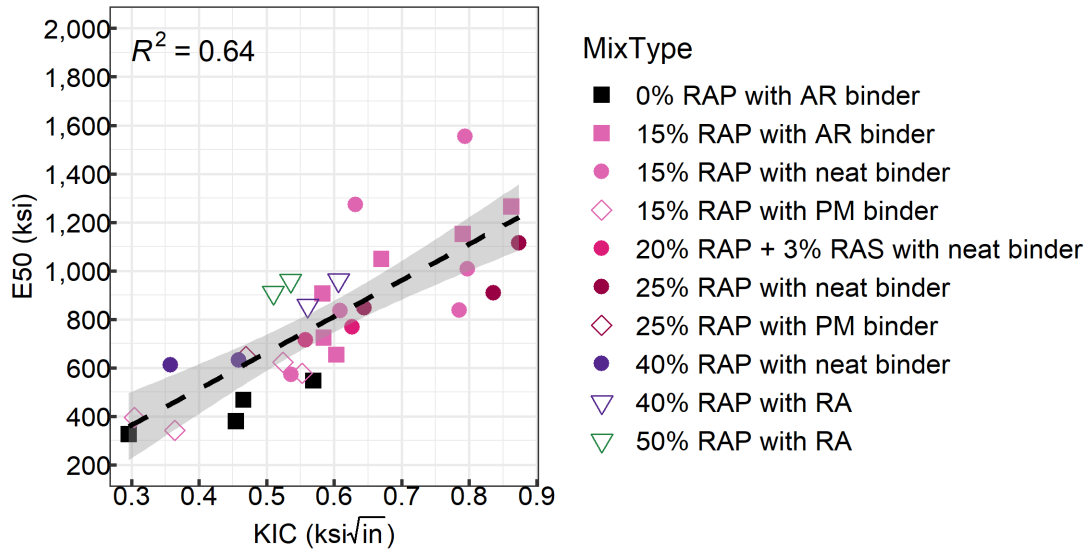
5.2.1 Stiffness Comparison

Fatigue development in asphalt mixtures is reflected in the stiffness evolution curve, and the damage induced in a material is directly related to the reduction in stiffness, including self-heating and thixotropy. These two phenomena are assumed to be reversible, and they cause a greater reduction in stiffness during initial loading than damage. However, the effects also tend to stabilize after the initial repeated load repetitions while damage continues to increase (78). The damage rate with load repetitions in 4PB tests is related to the energy of flexure,

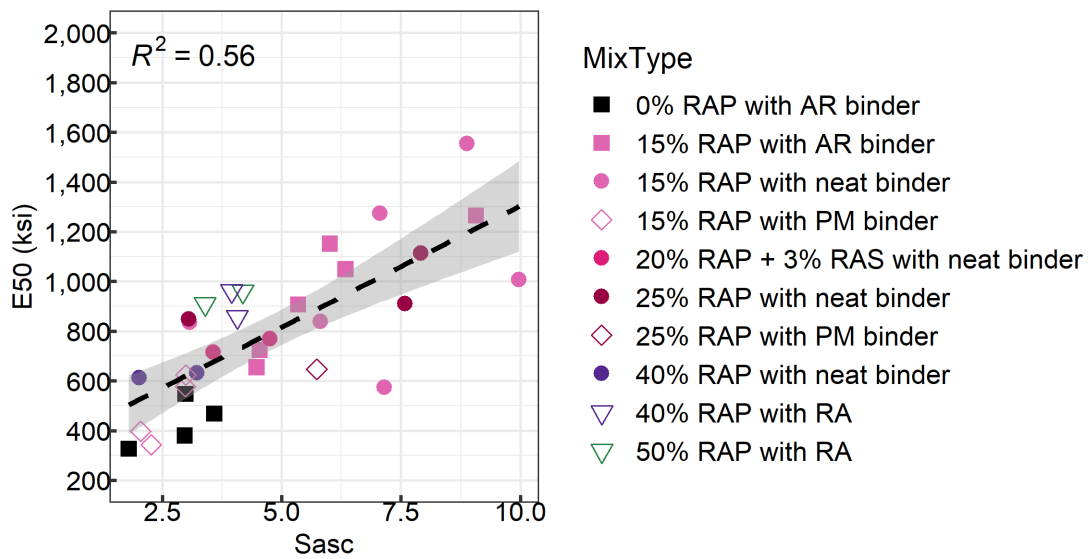
which is dominated by stiffness in the case of the strain-controlled loading configuration. Thus, it is important to investigate the relationship between the stiffness from flexural fatigue testing and the SCB parameters. The initial stiffness from 4PB tests (E_{50}) is defined as the elastic modulus at the 5⁰h cycle at the testing temperature of 68°F (20°C), which is the original stiffness before any damage occurred to the material. According to the definitions of the SCB slope parameters, S_{asc} and S_{pp} also reflect the stiffness information of asphalt mixtures. To fully investigate the relationship between stiffness and the SCB parameters, a simple linear regression analysis was performed on all SCB parameters at the testing temperature of 77°F (25°C). Some cases of the regression results with correlation coefficients are shown in Figure 5.5. The R^2 value and the 95% confidence interval are included for each plot and listed in Table 5.3. In this study, the correlation is considered as “strong” with R^2 higher than 0.8, “moderate” with R^2 between 0.4 and 0.8, and “weak” with R^2 between 0.1 and 0.4.



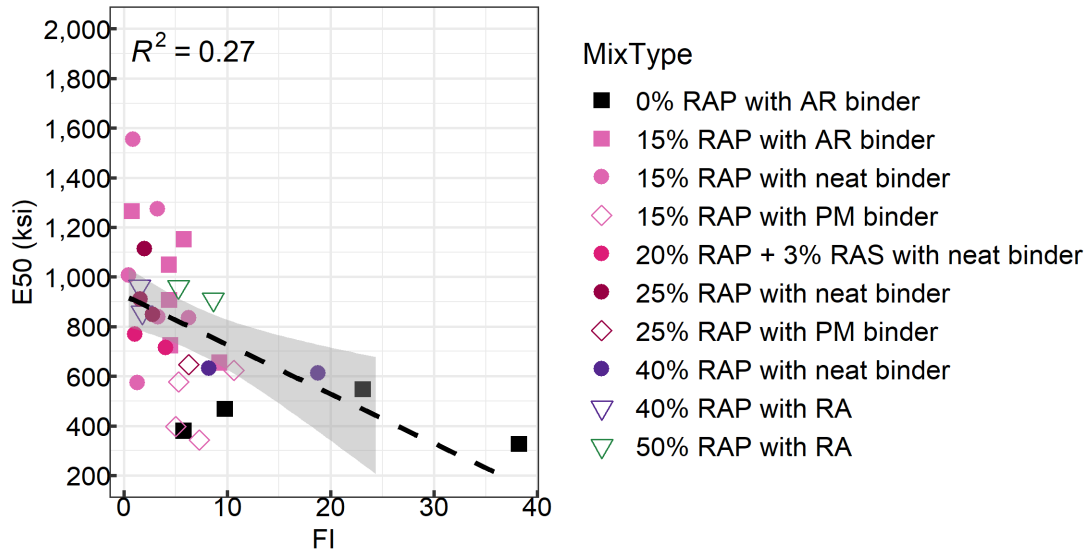
(a) Linear regression between *Strength* and *E50*



(b) Linear regression between KIC and $E50$



(c) Linear regression between S_{asc} and $E50$



Note: Gray area indicates 95% confidence interval.

Figure 5.5: Linear relationship between flexural stiffness and I-FIT parameters.

Table 5.3: R^2 Values for Correlation of I-FIT Parameters with Flexural Stiffness ($E50$)

I-FIT Parameters	S_{asc}	S_{pp}	FI	FI_{asc}	KIC	$Strength$	G_f
R^2	0.56	0.44	0.27	0.28	0.64	0.64	0.022

Figure 5.5 clearly shows that there is a positive relationship between the absolute value of both slopes (S_{pp} and S_{asc}) from the I-FIT test and $E50$ from the flexural test. The correlation is stronger for S_{asc} (R^2 of 0.56) than for S_{pp} . KIC and $Strength$ also demonstrate good positive correlations with $E50$ (R^2 of 0.64). The higher R^2 values for correlations of $E50$ with KIC and $Strength$ may come from the brittle fracture failure of these mixtures, which makes the LFM theory more suitable for the result analysis. As KIC is a function of the strength and geometry of the specimen, KIC and $Strength$ are essentially the same parameter given the consistency of the specimen preparation procedure. The R^2 values of the flexibility indexes (FI and FI_{asc}) and G_f suggest weak relationships with $E50$. Therefore, the initial flexural stiffness ($E50$) could be estimated from the KIC or $Strength$ measures obtained from I-FIT testing.

The SCB curve is composed of two distinct cracking phases: the crack initiation phase (roughly before the peak load) and the crack propagation phase (after the peak load). In the crack initiation phase, material damage resistance plays the major role while fracture resistance dominates the cracking behavior after peak load. The relatively stronger correlations between $E50$ and the front slope (S_{asc}), KIC , and $Strength$ indicate that the crack initiation phase is associated with the initial stiffness of asphalt mixtures. Fracture energy (G_f) captures the

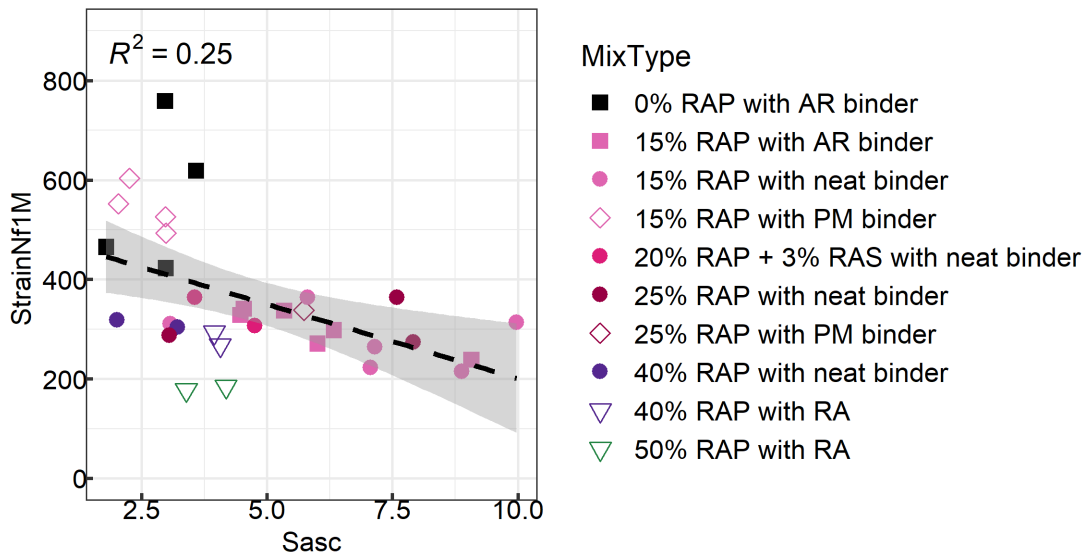
information from both the crack initiation phase and crack propagation phase, and it shows a negligible correlation with initial flexural stiffness. After combining the findings of the weak correlation between $E50$ with G_f and the stronger one between $E50$ and KIC , no noteworthy connection appears to exist between the initial flexural stiffness from the 4PB test and the crack propagation phase from the SCB testing.

5.2.2 Fatigue Life Comparison

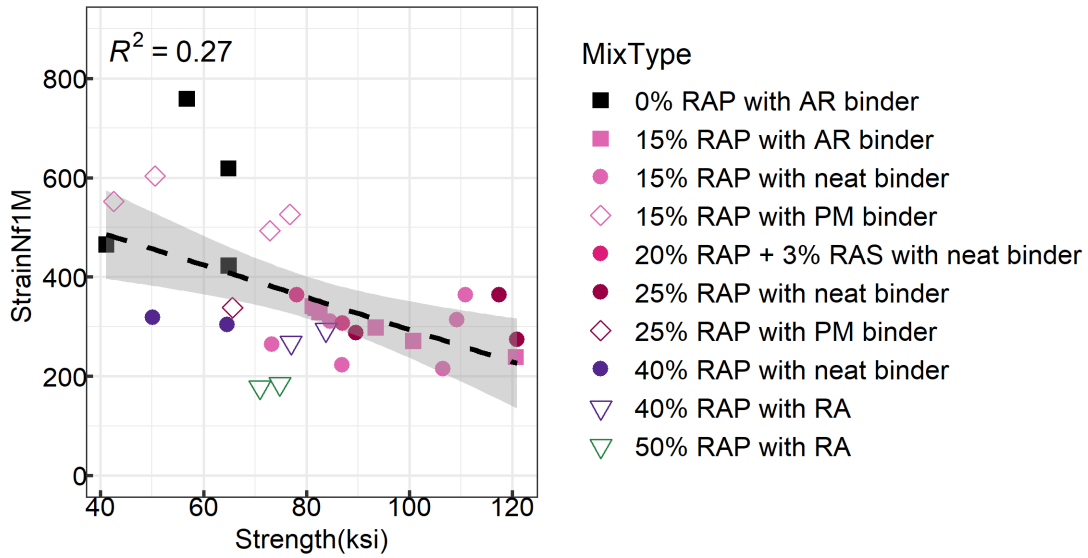
A simple linear regression analysis was performed to examine the correlation between fatigue life performance and SCB parameters. The fatigue life performance is represented by the strain value when fatigue life equals one million cycles ($StrainNf1M$), shown in Equation 3.2. A higher strain value at one million repetitions to failure represents better fatigue performance. According to the table of R^2 values shown in Table 5.4, the correlations between the fatigue performance and SCB parameters are not significant. Figure 5.6 shows some examples of linear regressions. KIC , $Strength$, and S_{asc} have relatively better linear correlations with fatigue life performance compared with the rest of the parameters. As KIC , $Strength$, and S_{asc} increase, $StrainNf1M$ decreases. However, these parameters cannot be used to predict flexural fatigue life due to such low R^2 values. In summary, it is likely not plausible to directly establish a fatigue life prediction model based on the AASHTO TP 124 I-FIT results for asphalt mixtures.

Table 5.4: R^2 Values for Correlation of I-FIT Parameters with 4PB Fatigue Performance ($StrainNf1M$)

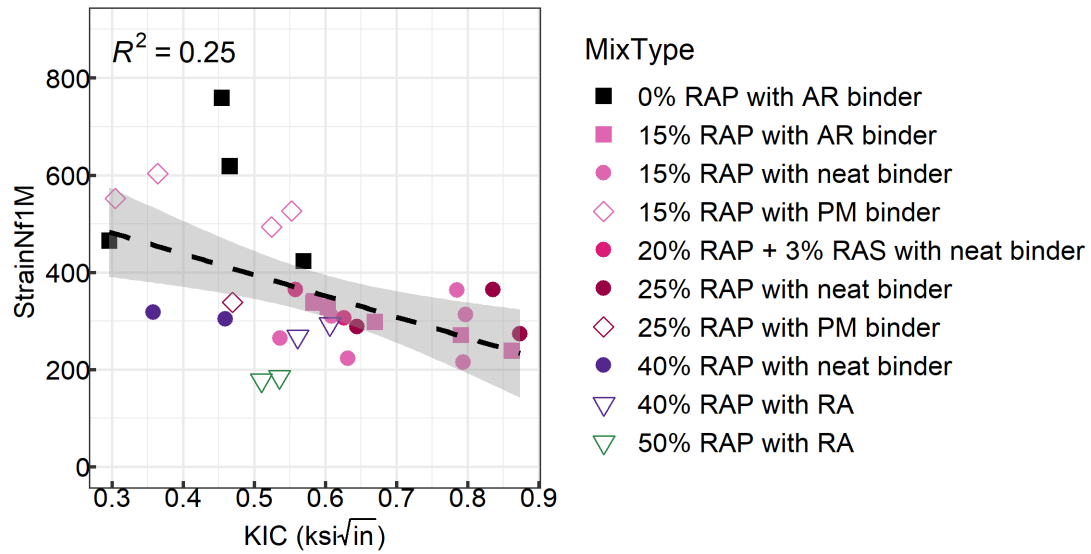
SCB Parameters	S_{asc}	S_{pp}	FI	FI_{asc}	KIC	$Strength$	G_f
R^2	0.25	0.17	0.082	0.11	0.25	0.27	0.0019



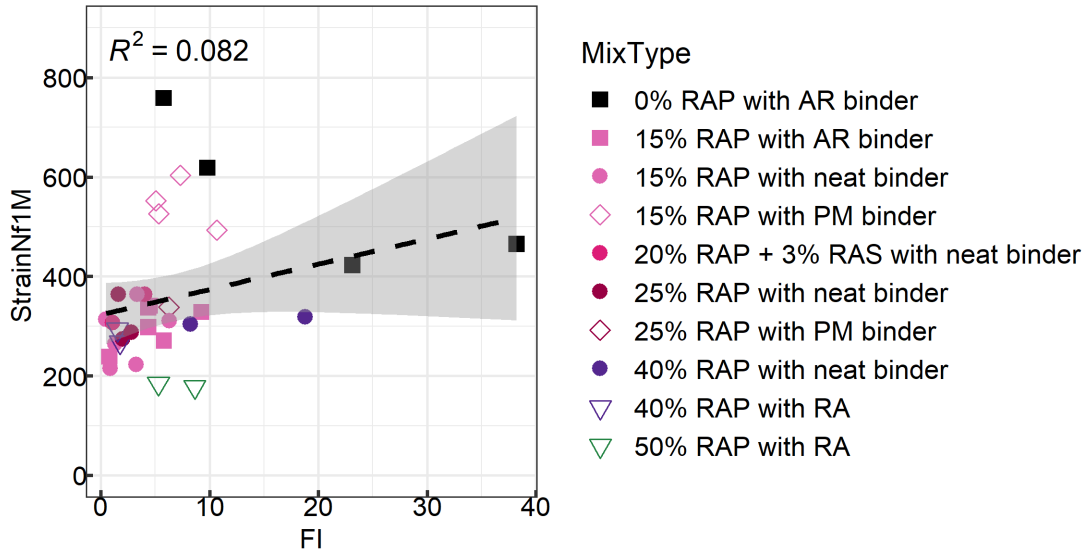
(a) Linear regression between S_{asc} and $StrainNf1M$



(b) Linear regression between *Strength* and *StrainNf1M*



(c) Linear regression between *KIC* and *StrainNf1M*



(d) Linear regression between FI and $StrainNf1M$

Note: Gray area indicates 95% confidence interval.

Figure 5.6: Linear relationship between $StrainNf1M$ and I-FIT parameters.

5.3 Summary

I-FIT testing was conducted at a temperature of 77°F (25°C) on 36 mixtures varying in terms of air voids, RAP/RAS content, binder types, and production methods. For each mixture, seven fracture parameters were calculated from the SCB tests. Three different loading rates were applied to two asphalt mixtures to assess the sensitivity of the loading rate on fracture performance. In addition, the fracture parameters were compared to the 4PB stiffness and fatigue life performance. The analysis results can be summarized as follows:

- Loading versus displacement curves from three loading rates (0.5 in./min, 1 in./min, 2 in./min) show that asphalt mixtures fracture in a brittle form at a higher loading rate, as expected. They also show that the FI value decreases as the loading rate increases. However, the Tukey's HSD testing results indicate no significant difference among these three loading rates. In evaluating pairs of mixtures, the Tukey's HSD results show that the loading rate of 2 in./min outperforms the two slower loading rates.
- Previous verification of I-FIT testing with field data by the University of Illinois suggested a strong relationship between FI from the I-FIT testing and early-age transverse cracking. However, the fatigue cracking performance at an intermediate temperature is the main focus of this study because it is the primary mode of structural failure for asphalt surfaced pavements in California. Age-related cracking is more important for asphalt pavements that do not have significant heavy vehicle traffic. The relationship between I-FIT testing and fatigue cracking performance was explored by comparing the I-FIT parameters against the 4PB fatigue parameters measured at a temperature of 68°F (20°C).

- This study included seven fracture parameters: FI , FI_{asc} , S_{pp} , S_{asc} , KIC , $Strength$ and G_f . The variability of each parameter was evaluated using the COV values. FI and S_{pp} have the highest variability while KIC and $Strength$ demonstrate the best repeatability with COV values of approximately 11%.
- Fatigue performance from the 4PB test is represented by the strain value for fatigue life of one million cycles ($StrainNf1M$) and initial flexural stiffness ($E50$). The relationship between fatigue performance and fracture performance was examined by comparing $StrainNf1M$ and $E50$ with fracture parameters. Both KIC and $Strength$ show a moderate linear positive correlation with the initial flexural stiffness ($E50$), but no significant correlation was found between $StrainNf1M$ and any fracture parameter.

6 RESULTS AND ANALYSIS FOR LOU-SCB TESTING

6.1 LOU-SCB Testing Results

At least three replicates were produced for each notch depth for the LOU-SCB testing. However, due to the limited coring samples collected from the field, the study included only three specimens for the RAP15%_3 mixture. The air voids of LOU-SCB specimens are shown in Figure 6.1. All the asphalt mixtures have air voids falling between $7\pm 1\%$, except the RAP15%_3, which was prepared in the field. The standard deviations for air voids are all less than 1, indicating a narrow dispersion of air voids among replicates.

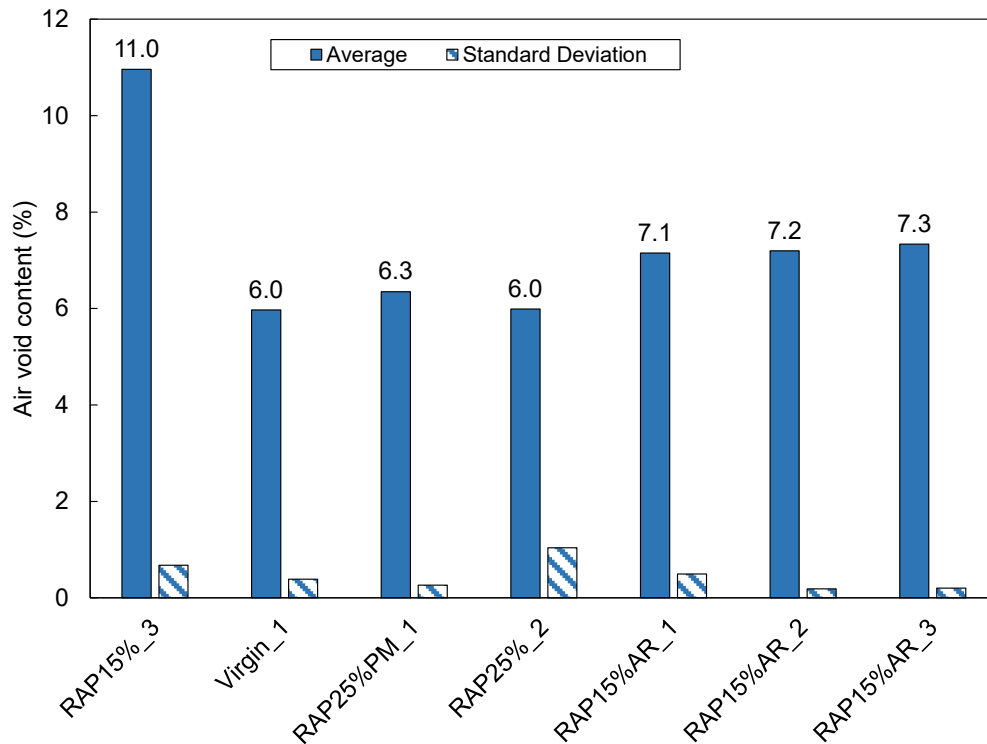


Figure 6.1: Air void content for LOU-SCB mixtures.

The fracture parameter (J_c) from the LOU-SCB test is a function of the change of strain energy to failure (U) with respect to notch depth (a) by definition, which is the slope of a fitted linear regression curve between U and a . The test results, along with the regression curves for all asphalt mixtures, are shown in Figure 6.2. Only three RAP15%_3 mixture specimens were tested, with R^2 values around 0.35. These values are much lower than those of the other asphalt mixtures and may be the result of the sample sizes.

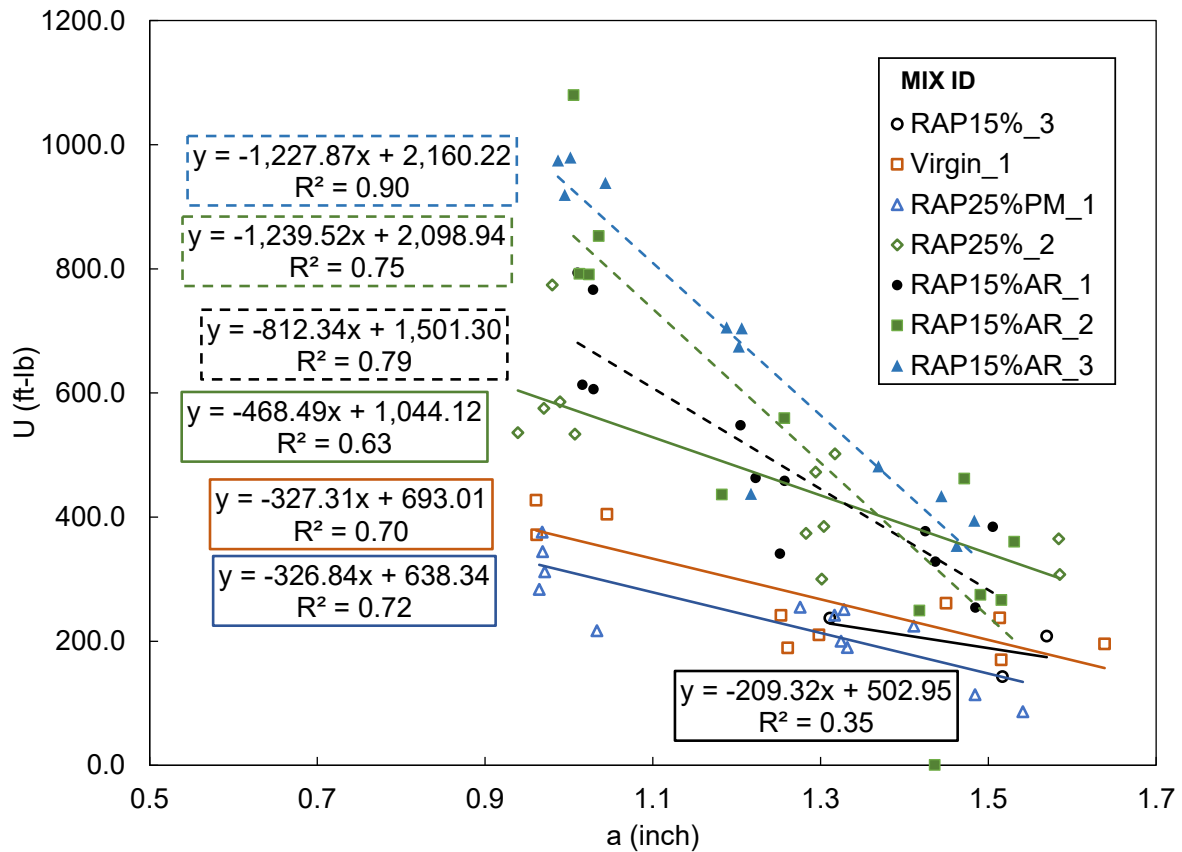


Figure 6.2: Linear regression curves between notch depth and strain energy to failure.

J_c measures the energy required to generate a unit crack surface area, and a higher J_c value indicates better fracture resistance of a material. Comparison of the slopes of these fitted curves shows that RAP15%AR_2 and RAP15%AR_3 have the best fracture resistance while RAP15%_3, Virgin_1, and RAP25%PM_1 show relatively inferior fracture performance. Among the three rubberized asphalt mixtures, RAP15%AR_2 and RAP15%AR_3 have the same slope value, 0.07, while the slope for RAP15%AR_1 is slightly smaller, 0.04. RAP15%AR_1 contains the same RAP and binder contents as the other two rubberized asphalt mixtures and the same virgin binder type as RAP15%AR_2. However, both RAP15%AR_2 and RAP15%AR_3 have 10% CRM while RAP15%AR_1 only has 5% CRM. The difference in the amount of added crumb rubber may result in the slope change of these three mixtures. In addition, by comparing the slopes between RAP25%PM_1 and RAP25%_2, both of which contain the same amount of RAP, similar values were found (0.03 for RAP25%_2 and 0.02 for RAP25%PM_1). The main differences between these two mixtures are the binder content and binder modifier. RAP25%_2 has a higher virgin binder content than RAP25%PM_1 while the polymer modifier was added to RAP25%PM_1. In conclusion, the results indicate that the addition of rubber modifier and polymer modifier in the binder may improve the fracture resistance of asphalt mixtures.

6.2 Comparison Between I-FIT and LOU-SCB Testing

This section compares the fracture parameters from the I-FIT and LOU-SCB testing. For linear elastic solids, the relationship between J_c and KIC (79) is the following:

$$J_c = KIC^2 \frac{(1-\nu^2)}{E} \quad (6.1)$$

Where:

ν = Poisson's ratio, and

E = elastic stiffness.

Because J_c is calculated based on the area before the peak load in a load-displacement curve, a new parameter was included for the I-FIT test, *AreaBefore*, which is the area underlying the I-FIT load-displacement curve before the peak load. A correlation matrix was built to explore the correlation between the parameters from the I-FIT and LOU-SCB testing, shown in Figure 6.3. The first row of the matrix shows that of all the I-FIT parameters, only KIC and *AreaBefore* display good correlations with J_c . A linear regression model was established for the relationship between J_c and *AreaBefore* (Figure 6.4) and between J_c and KIC (Figure 6.5). A natural log scale transformation on J_c was performed based on the trending relationship displayed in the scatter plots of Figure 6.3. The good correlation between J_c and *AreaBefore* implies that, given the constant notch length, the LOU-SCB testing would provide similar fracture information of these materials as the I-FIT testing.

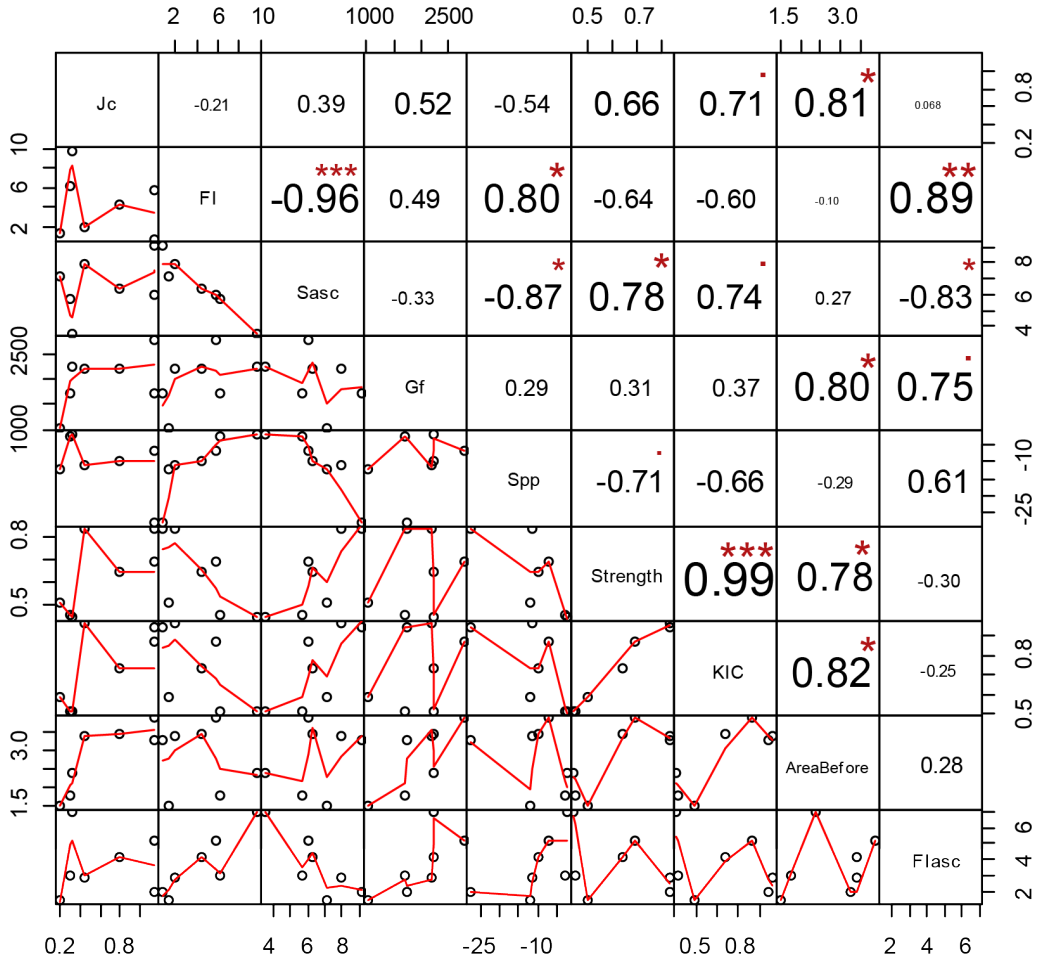
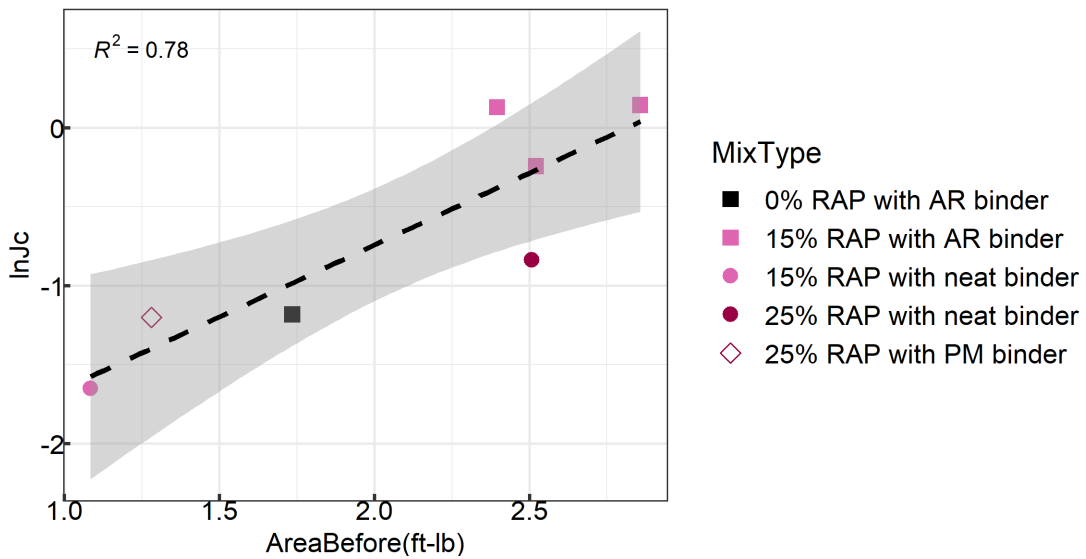
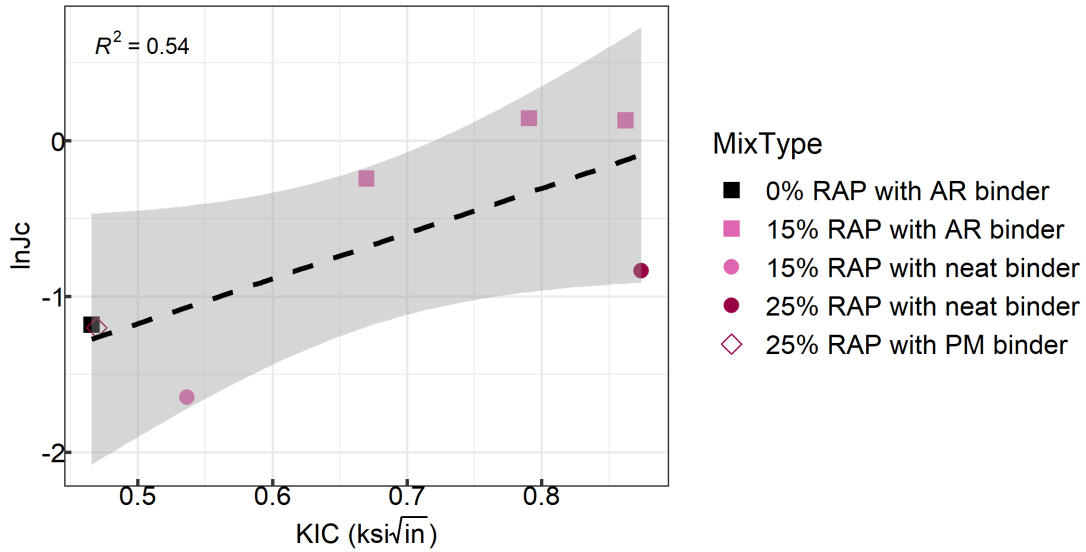


Figure 6.3: Correlation matrix between LOU-SCB and I-FIT parameters.



Note: Gray area indicates 95% confidence interval.

Figure 6.4: Linear regression analysis between $\ln(Jc)$ and $AreaBefore$.



Note: Gray area indicates 95% confidence interval.

Figure 6.5: Linear regression analysis between $\ln(J_c)$ and KIC .

6.3 Comparison Between LOU-SCB and 4PB Testing

This section compares the main parameter (J_c) obtained from the LOU-SCB tests with the testing temperature of 77°F (25°C) and the fatigue parameters (E_{50} and $StrainNfIM$) from the 4PB tests with the testing temperature of 68°F (20°C). The correlation matrix in Figure 6.6 shows that J_c is strongly correlated with E_{50} , with no significant correlation between J_c and $StrainNfIM$.

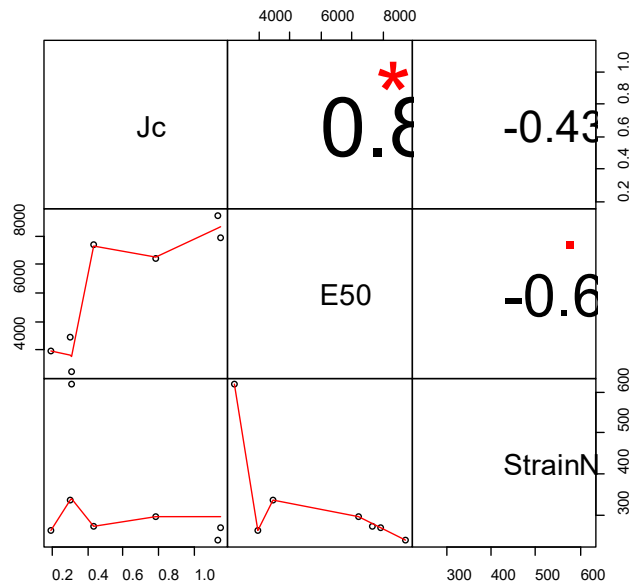
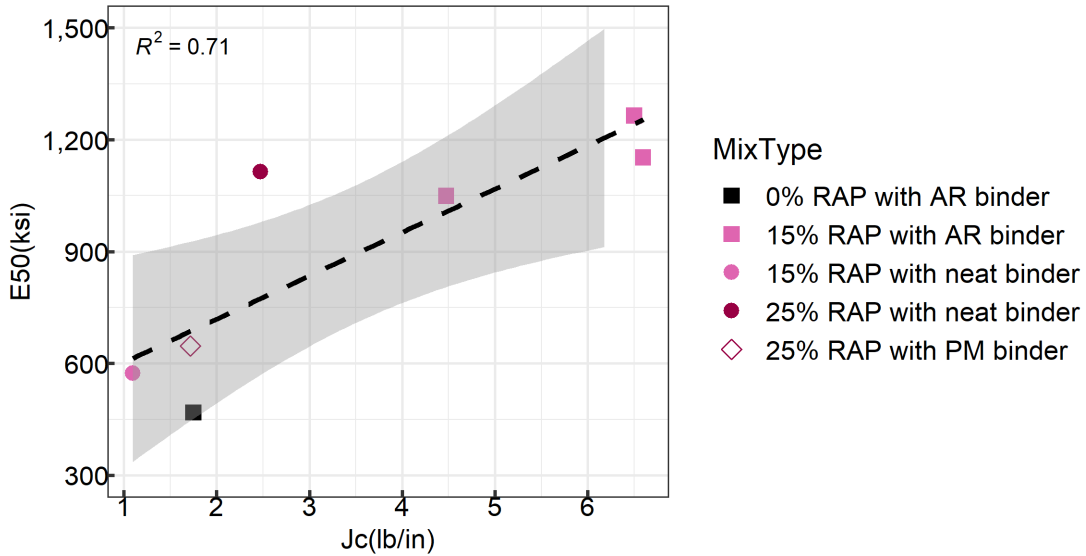


Figure 6.6: Correlation matrix between LOU-SCB and 4PB parameters.

6.3.1 Stiffness Comparison

In a follow-up analysis to the correlation matrix, a linear regression analysis was performed between J_c at 77°F (25°C) and E_{50} at 68°F (20°C), shown in Figure 6.7, with an R^2 value of 0.71. The mixtures with 15% RAP and rubber modifier show relatively higher initial flexural stiffnesses and higher J_c values.

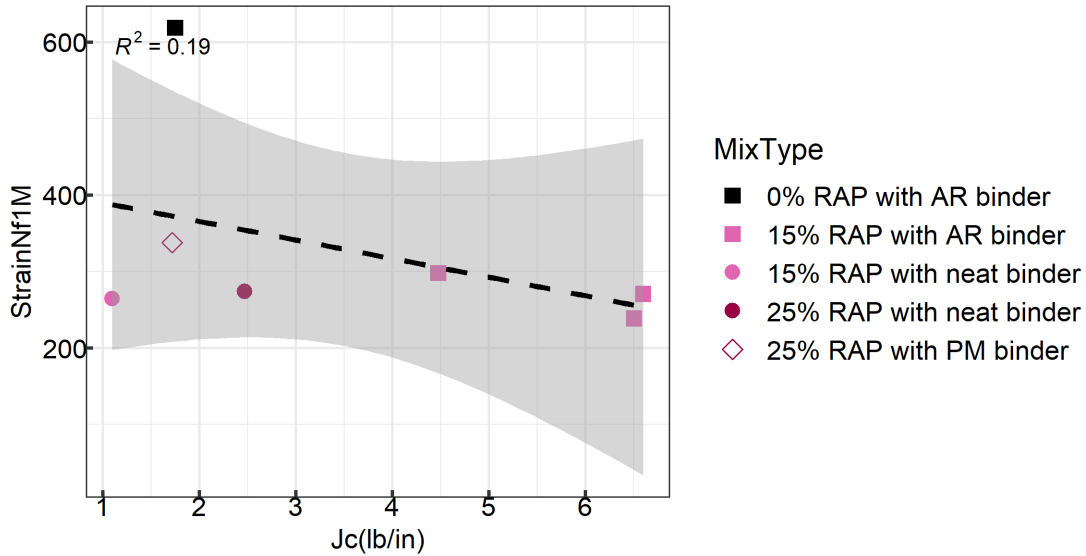


Note: Gray area indicates 95% confidence interval.

Figure 6.7: Linear regression analysis between J_c and E_{50} .

6.3.2 Fatigue Life Comparison

The relationship between the LOU-SCB testing results and fatigue life from the 4PB testing shows a relationship similar to the one from the I-FIT analysis. No significant correlation exists between J_c and $Strain_{NfIM}$, shown in Figure 6.8. The mixture containing 0% RAP and rubber modifier evidently provides the best fatigue performance but has one of the lowest J_c values. The other mixtures do not show much difference in strain values, as they did in the LOU-SCB testing, and the J_c value ranges widely from 0.1 to 1. According to the recommended threshold of 0.5 for J_c (40), only the dense-graded mixtures with 15% RAP and 5% or 10% rubber in the binder have sufficient cracking resistance, which does not correspond to the fatigue testing results.



Note: Gray area indicates 95% confidence interval.

Figure 6.8: Linear regression analysis between J_c and $StrainNf1M$.

6.4 Summary

The LOU-SCB testing was conducted on seven asphalt mixtures at 77°F (25°C). The fracture properties obtained from two SCB testing configurations (LOU-SCB and I-FIT) were compared. The relationship between the fracture parameters of the LOU-SCB test and fatigue performance at 68°F (20°C) were also investigated. The following conclusions are based on these test results:

- There is a strong linear correlation between the J_c parameter from the LOU-SCB test and the *AreaBefore* parameter from the I-FIT test. *KIC* also correlates well with J_c . These findings indicate that the I-FIT and LOU-SCB tests provide the same fracture information for these materials.
- Comparison of LOU-SCB and 4PB testing parameters showed that J_c is strongly correlated with the initial flexural stiffness ($E50$), while the correlation between J_c and $StrainNf1M$ is not noticeable.
- These results indicate that, at least for these mixes, the LOU-SCB and I-FIT tests are providing similar information and that the information correlates well with flexural stiffness but not flexural fatigue.

7 RESULTS AND ANALYSIS FOR IDEAL-CT

7.1 IDEAL-CT Testing Results

This section discusses the repeatability of the IDEAL-CT test as well as the variability of fracture parameters. The coefficient of variance (COV) values for each parameter were averaged across all asphalt mixtures, shown in Figure 7.1. The averaged COV values of all parameters are lower than those from the I-FIT test. The *Strength* and G_f parameters from the IDEAL-CT test show the lowest variability among all these parameters, which matches the findings from the I-FIT analysis.

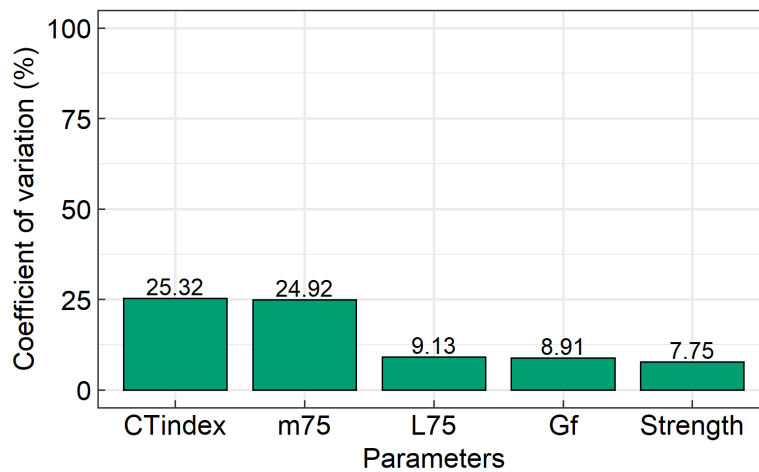


Figure 7.1: Average coefficient of variance for all parameters from IDEAL-CT test.

7.2 Comparison of I-FIT and IDEAL-CT Testing

The most important difference between I-FIT and IDEAL-CT testing is the specimen geometry. The I-FIT test uses a half-circular beam with a notch requiring saw cutting, while the IDEAL-CT test is performed directly on a compacted cylinder. The same analysis was conducted for the IDEAL-CT test results, including the development of a similar loading versus displacement curve. First, a correlation matrix was built with parameters from the I-FIT and IDEAL-CT tests, shown in Figure 7.2. The first five rows are the parameters from the IDEAL-CT test, and these variable names start with *IDT_* to differentiate them from the rest of the rows, which are parameters from the I-FIT test. Most of the IDEAL-CT parameters—including *m75*, *L75*, *IDT_strength*, and *cTindex*—are highly correlated with the I-FIT parameters, especially *cTindex* from the IDEAL-CT test and *FI* from the I-FIT test. A linear regression model between these two parameters is shown in Figure 7.3. The very strong correlation between these I-FIT and IDEAL-CT parameters implies that both tests are providing the same fracture-related information.

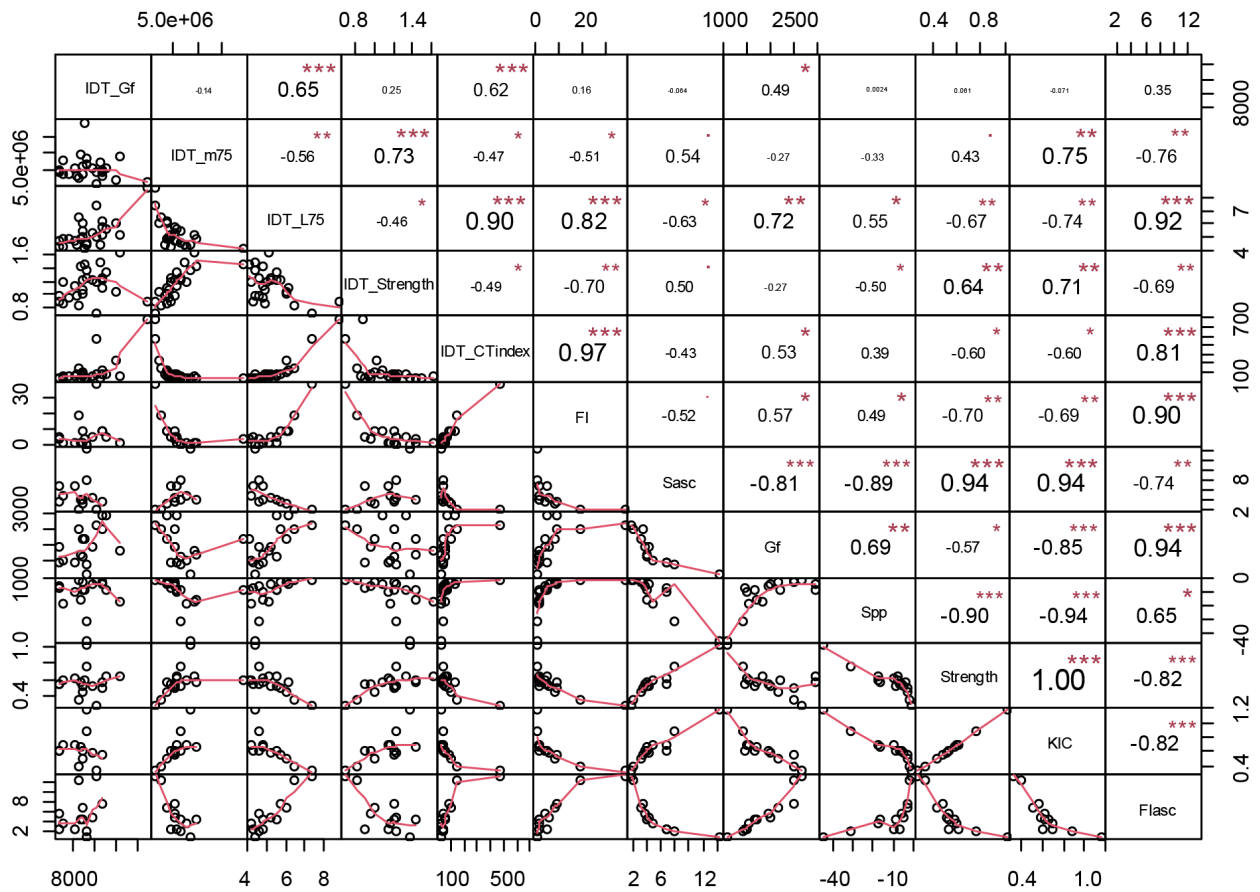
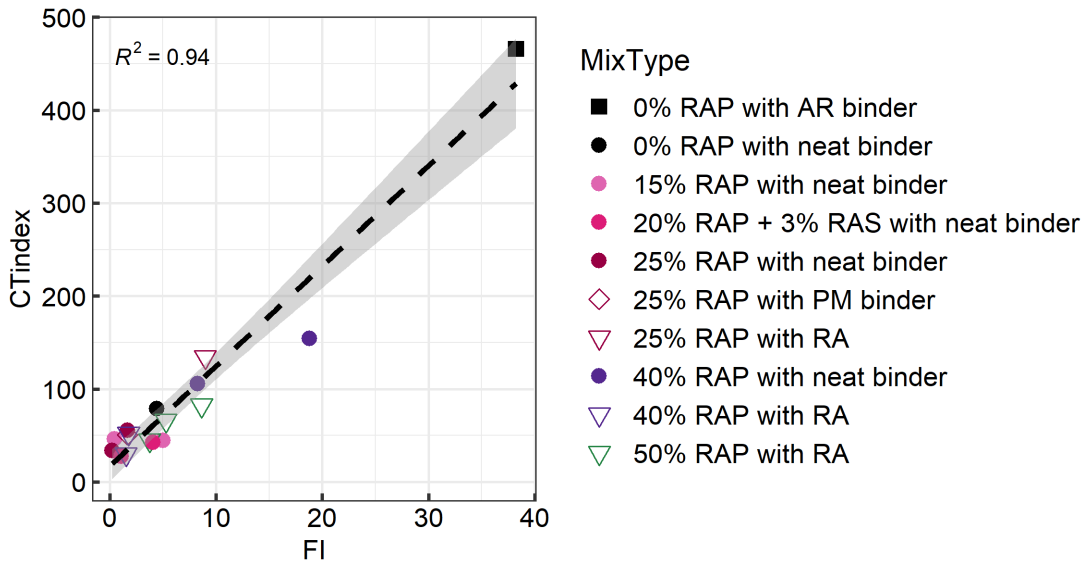


Figure 7.2: Correlation matrix between IDEAL-CT and I-FIT parameters.

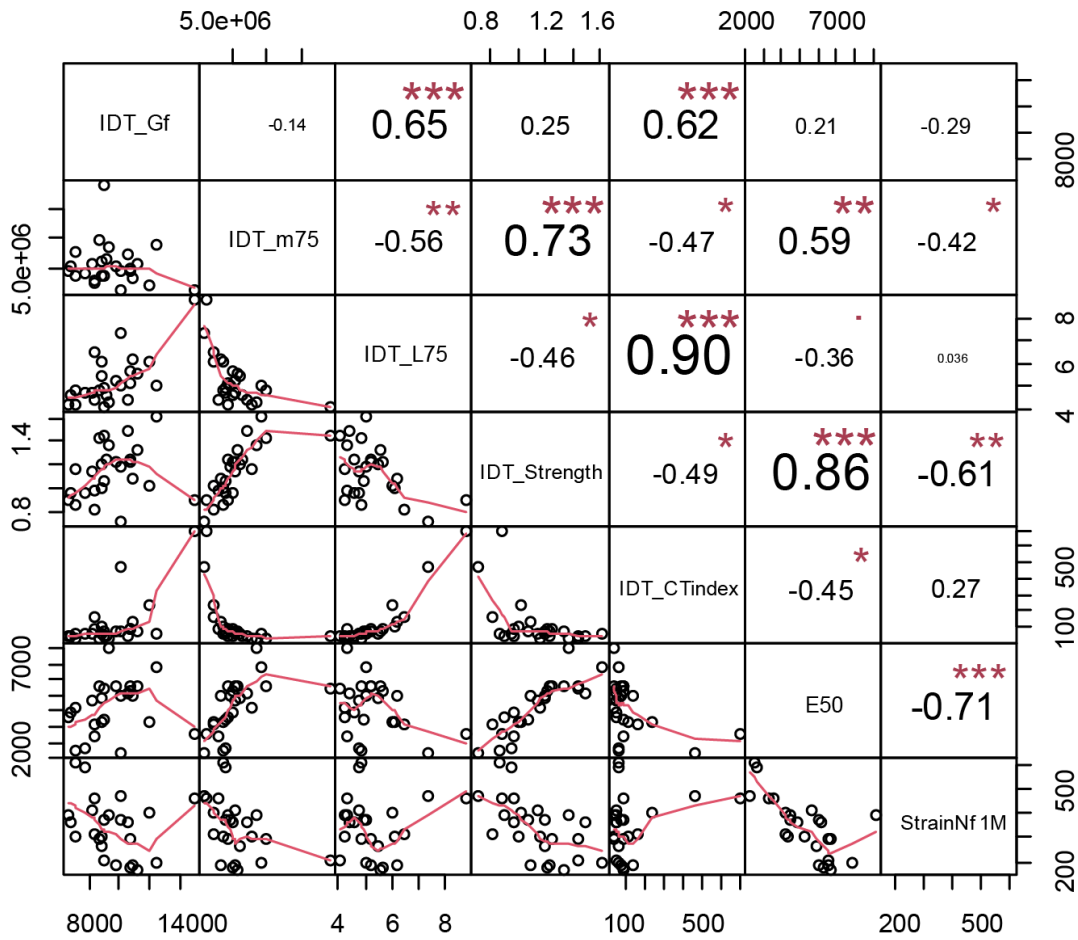


Note: Gray area indicates 95% confidence interval.

Figure 7.3: Linear regression between *cTIndex* from IDEAL-CT test and *FI* from I-FIT test.

7.3 Comparison Between IDEAL-CT and 4PB Testing

The correlation matrix between the 4PB parameters measured at the testing temperature of 68°F (20°C) and fracture parameters from IDEAL-CT testing at the testing temperature of 77°F (25°C) is shown in Figure 7.4. Parameters from the IDEAL-CT test, especially strength (*IDT_Strength*), show good linear correlations with initial flexural stiffness (*E50*), which matches the findings from the comparison between the I-FIT and 4PB tests and between the LOU-SCB and 4PB tests. The *StrainNf1M* does not show any significant correlation with the fracture parameters from the IDEAL-CT test, with the best *r* value being 0.61 for *IDT_Strength*.

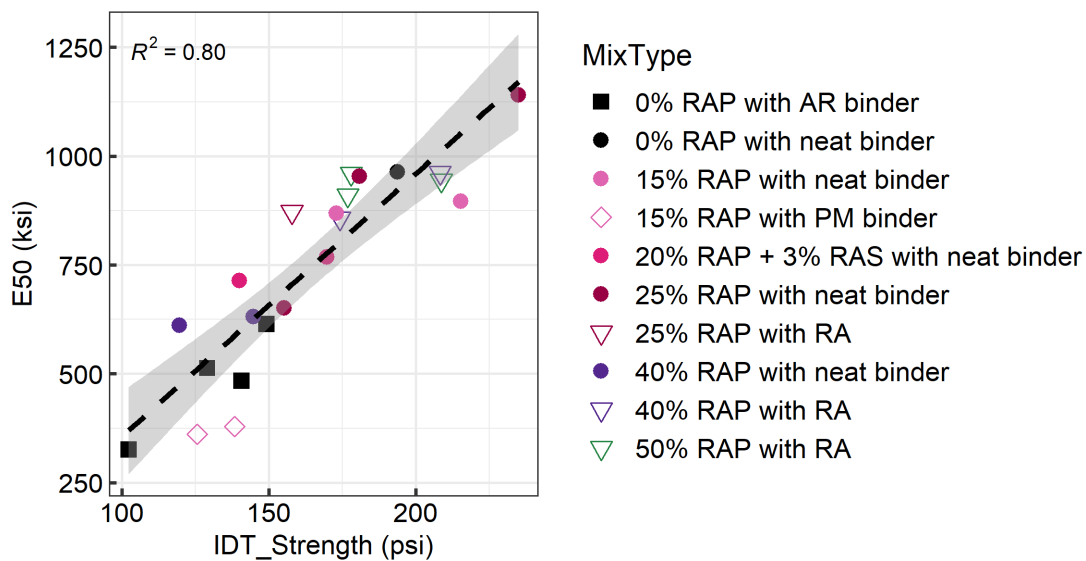


Note: *E50* and *StrainNf1M* at 68°F (20°C) and IDEAL-CT parameters at 77°F (25°C).

Figure 7.4: Correlation matrix between IDEAL-CT and 4PB parameters.

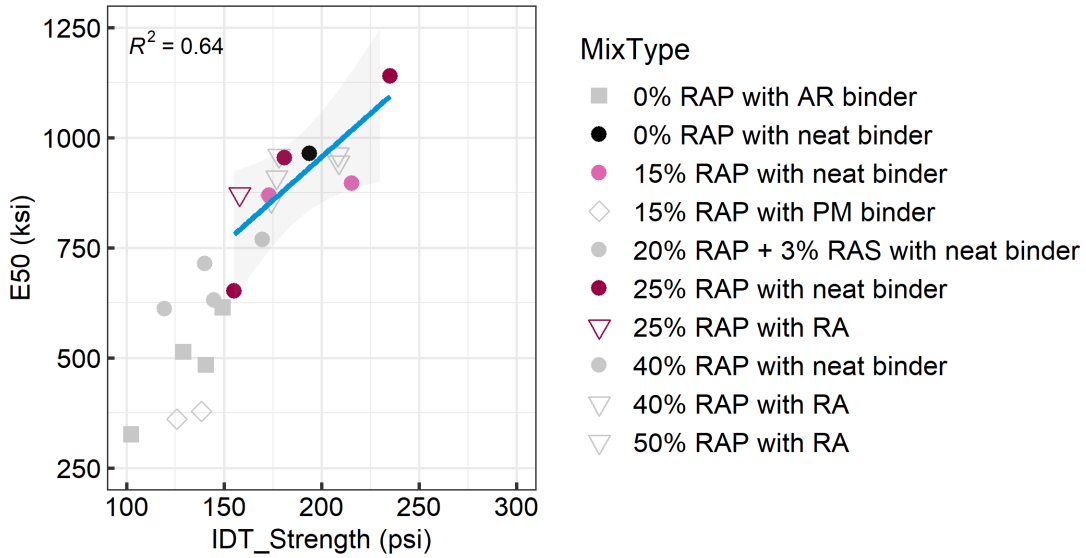
7.3.1 Stiffness Comparison

The correlation results in Figure 7.4 were used to develop a fitted linear regression curve between E_{50} from the 4PB test and $Strength$ from the IDEAL-CT test, shown in Figure 7.5. The R^2 value of 0.80 indicates a strong linear positive relationship between fracture strength and initial flexural stiffness. In addition, the relationship between fracture strength and initial flexural stiffness was examined separately for conventional asphalt mixtures, which contain recycled binder lower than 25% with neat binder, and unconventional mixtures, those that contain a higher content of recycled binder and those with rubber and/or polymer modifiers, shown in Figure 7.6 and Figure 7.7. A strong linear relationship exists for both conventional and unconventional asphalt mixtures when evaluated separately. Therefore, it can be concluded that the parameter $IDT_Strength$ is highly correlated with the flexural stiffness regardless of the asphalt mixture types.



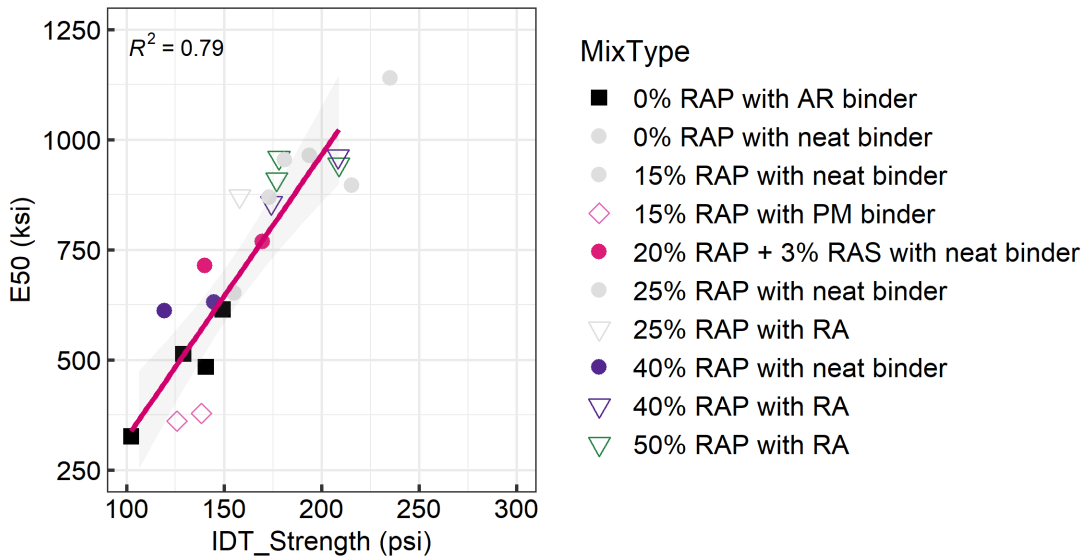
Note: Gray area indicates 95% confidence interval.

Figure 7.5: Linear regression between $IDT_Strength$ and E_{50} .



Note: Gray area indicates 95% confidence interval.

Figure 7.6: Linear regression between *IDT_Strength* and *E50* for conventional asphalt mixtures (RAP binder replacement lower than or equal to 25% and without modified binder).



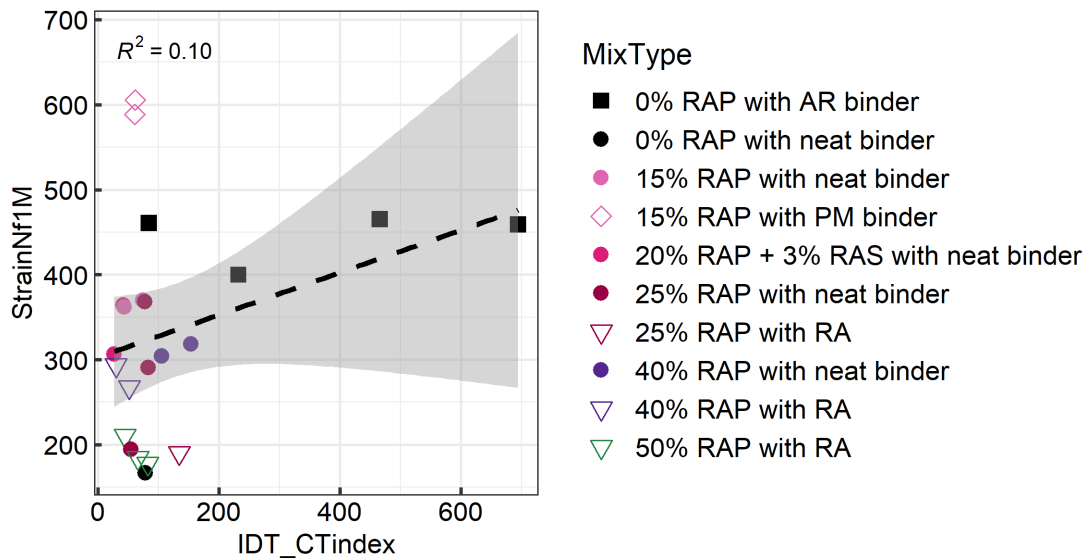
Note: Gray area indicates 95% confidence interval.

Figure 7.7: Linear regression between *IDT_Strength* and *E50* for unconventional asphalt mixtures (RAP binder replacement higher than 25% or with modified binder).

7.3.2 Fatigue Life Comparison

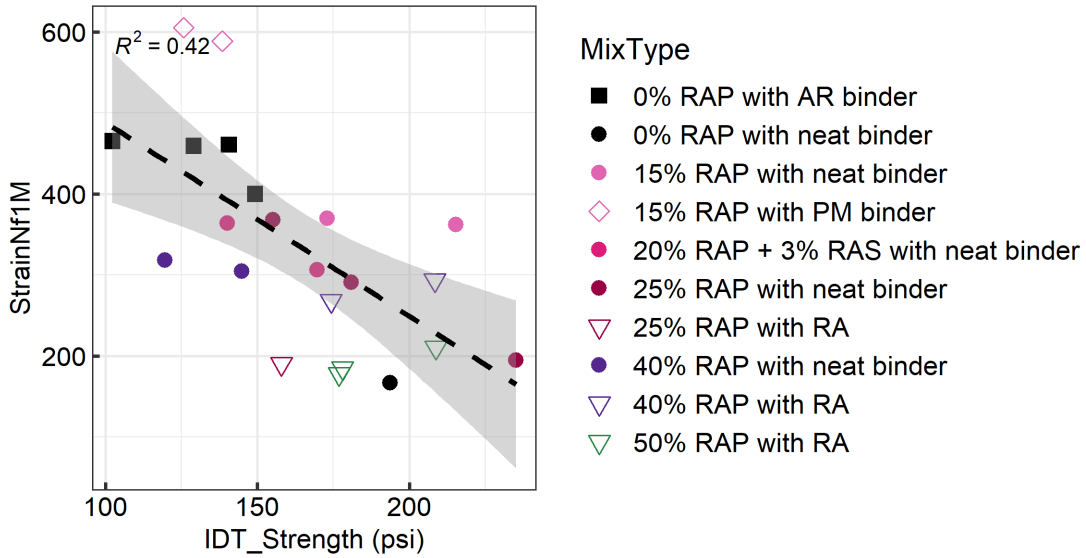
The linear regression analysis between the *StrainNfIM* and *cTindex* parameters is shown in Figure 7.8. The regression indicates a weak positive relationship between the fatigue life performance (*StrainNfIM*) and

IDEAL-CT cracking index ($cTindex$). In addition, the fatigue performance of the mixtures with 20% RAP is better than the mixtures with 50% RAP, recycling agent (RA), and potentially a softer base binder, according to $StrainNfIM$, while the $cTindex$ parameter indicates the opposite. The 40% RAP mixtures with neat binder show higher $cTindex$ values than the mixtures with 20% RAP and 3% RAS with neat binder. Because of the nature of the neat binder and the RAP and RAS binders and use of additives, the 20% RAP mixes are stiffer than the 40% RAP mixes but have similar or better fatigue performance, shown in Figure 7.5. The $IDT_Strength$ parameter has a moderate negative linear correlation with $StrainNfIM$, with an R^2 value of 0.42, shown in Figure 7.9, and the expected trend that stiffer mixes (as indicated by $IDT_Strength$) have shorter fatigue lives in the controlled-strain 4PB fatigue test. The virgin mixture with rubberized asphalt (0% RAP with AR binder) shows the best fatigue performance and lowest strength value while the mixtures with high RAP contents have the weakest fatigue resistance and highest strength values. Figure 7.10 and Figure 7.11 show the linear relationship between $StrainNfIM$ and $IDT_Strength$ for conventional and unconventional asphalt mixtures, respectively. Due to the limited number of conventional mixtures tested in this study and similar fatigue and fracture performance among these mixtures, there is no correlation found between the two parameters. On the other hand, a moderate relationship could be observed from unconventional asphalt mixtures as there is a wider range of fatigue and $IDT_Strength$ performance of these mixtures.



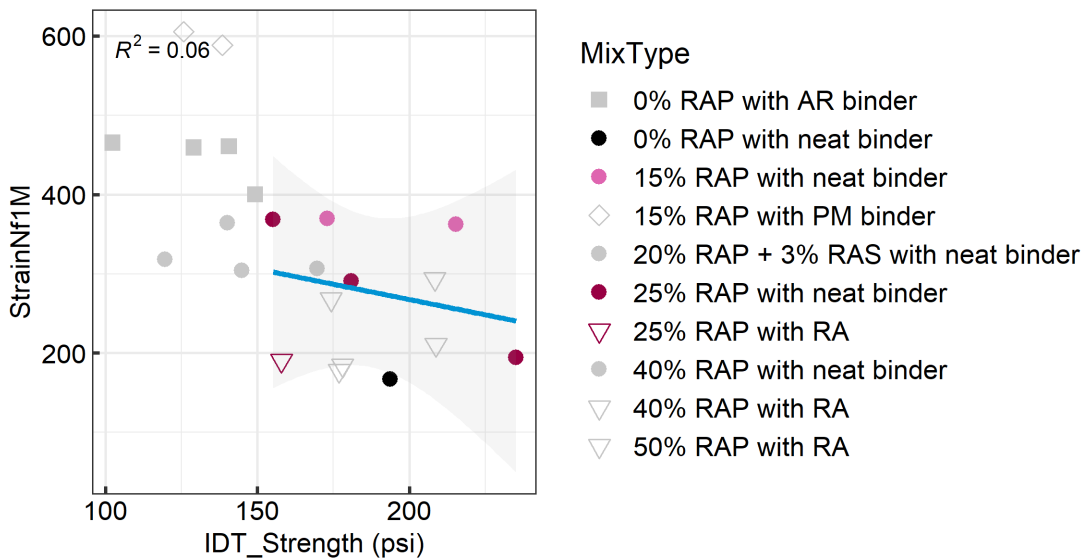
Note: Gray area indicates 95% confidence interval.

Figure 7.8: Linear regression between $IDT_cTindex$ and $StrainNfIM$.



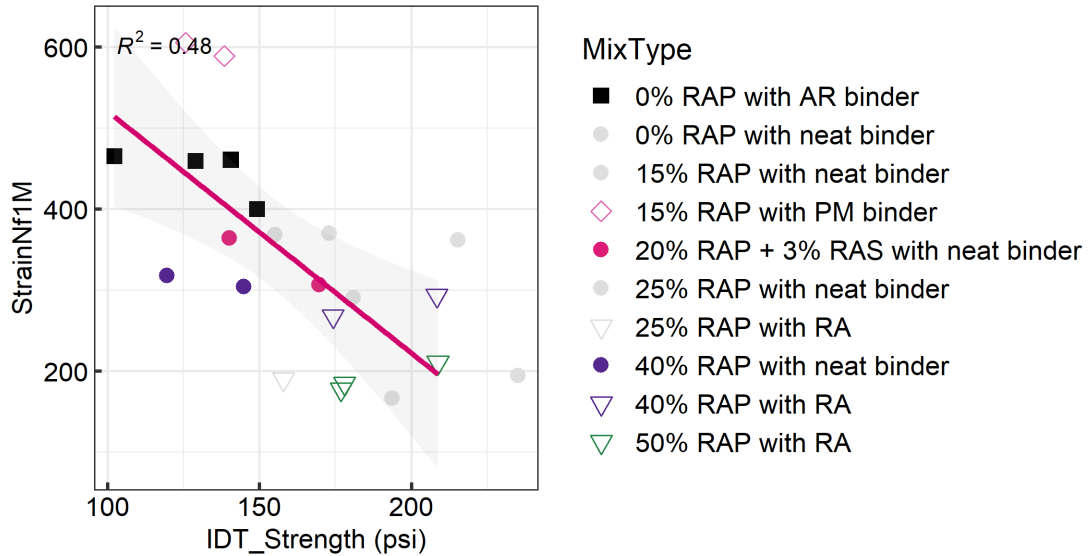
Note: Gray area indicates 95% confidence interval.

Figure 7.9: Linear regression between *IDT_Strength* and *StrainNf1M*.



Note: Gray area indicates 95% confidence interval.

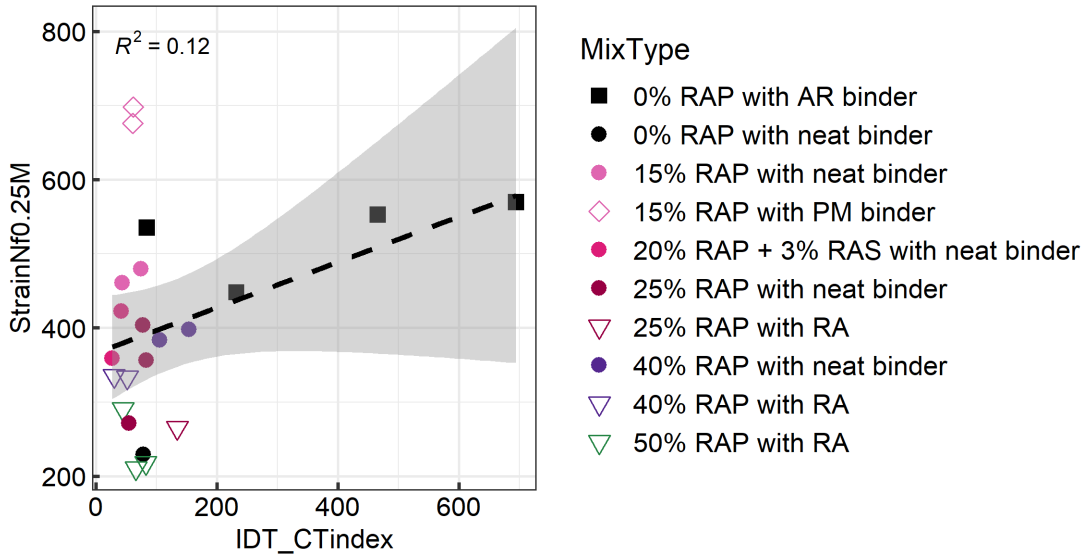
Figure 7.10: Linear regression between *IDT_Strength* and *StrainNf1M* for conventional asphalt mixtures (RAP binder replacement lower than or equal to 25% and without modified binder).



Note: Gray area indicates 95% confidence interval.

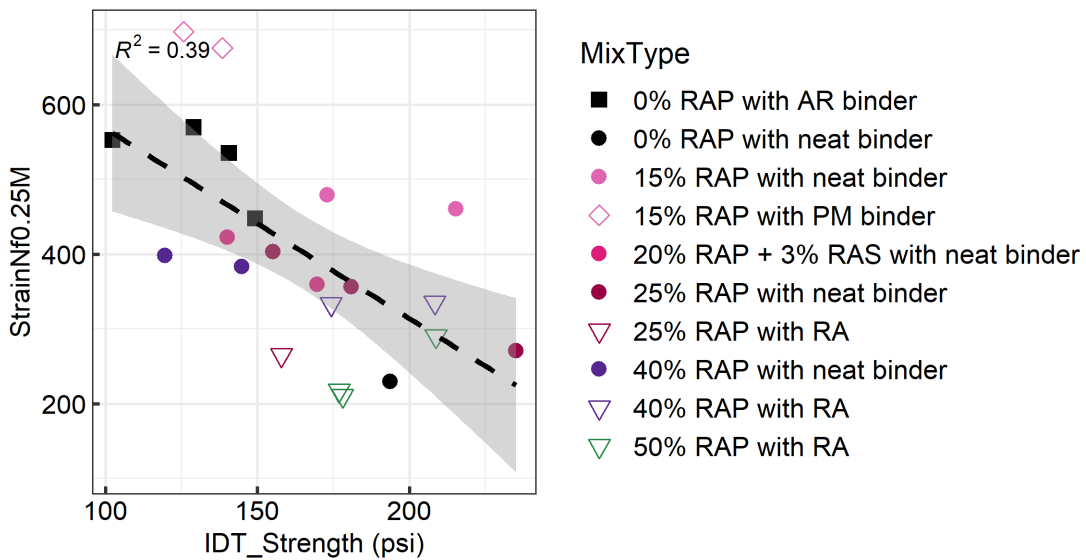
Figure 7.11: Linear regression between *IDT_Strength* and *StrainNf1M* for unconventional asphalt mixtures (RAP binder replacement higher than 25% or with modified binder).

To further explore the relationship between IDEAL-CT testing and the fatigue result from 4PB testing, another fatigue life parameter, *StrainNf0.25M*, which is more related to thin surface layer fatigue performance, is included here. *StrainNf0.25M* is the strain level at which the fatigue life reaches 250,000 cycles, and it is calculated using Equation 3.2 by replacing 10^6 on the right side of the equation with 250,000, resulting in a comparison of fatigue life for higher strain levels in the 4PB testing. As shown in Figure 7.12 and Figure 7.13, the regression analysis between *cTindex* and *StrainNf0.25M*, and *IDT_Strength* and *StrainNf0.25M*, has similar correlation results with *StrainNf1M*.



Note: Gray area indicates 95% confidence interval.

Figure 7.12: Linear regression between *IDT_cTindex* and *StrainNf0.25M*.



Note: Gray area indicates 95% confidence interval.

Figure 7.13: Linear regression between *IDT_Strength* and *StrainNf0.25M*.

7.4 Summary

This chapter reviewed the variability of fracture parameters from the IDEAL-CT test, compared the IDEAL-CT and I-FIT tests, and then correlated these findings with the stiffness and fatigue performance results from 4PB testing. The following conclusions are based on this analysis:

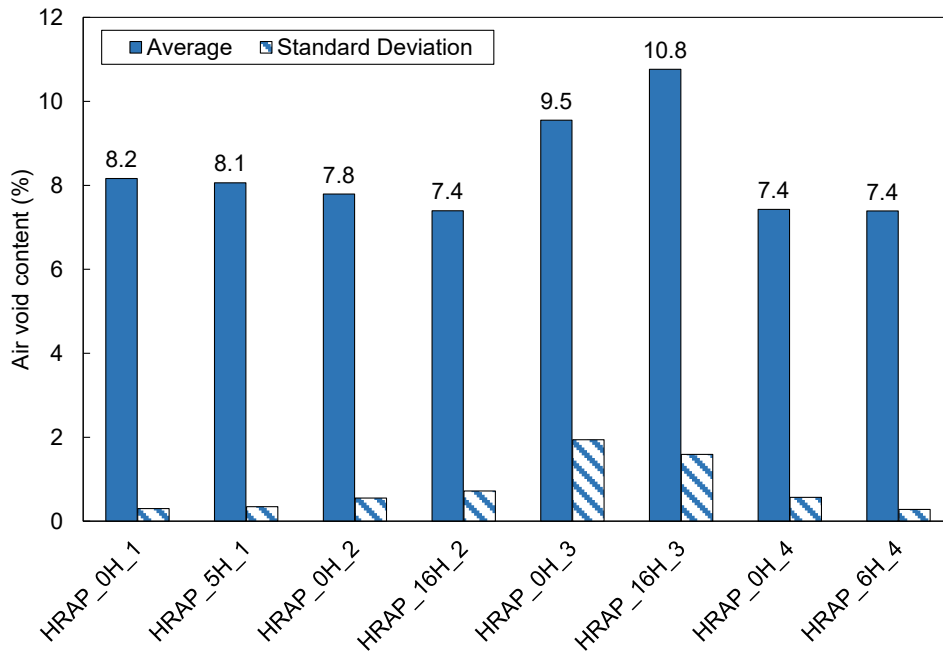
- The fracture parameters from IDEAL-CT display an overall lower variability compared with the I-FIT results, with *IDT_Strength* showing better repeatability than *cTindex* between the two parameters from the IDEAL-CT test.
- The analysis found strong correlations between the IDEAL-CT and I-FIT parameters. *cTindex* was proposed as a representative fracture resistance parameter for the IDEAL-CT test and showed a significantly strong linear relationship with *FI*, the cracking indicator developed in the I-FIT test.
- The analysis showed a strong linear correlation between *IDT_Strength* and the initial stiffness (*E50*) from the 4PB test, which agrees with the previous finding from the comparison between *Strength* from the I-FIT test and stiffness from 4PB test. This result was also separately analyzed considering only conventional asphalt mixtures (RAP binder replacement lower than or equal to 25% and without modified binder) and only unconventional mixes (RAP binder replacement higher than 25% or with rubber- and/or polymer-modified binder), with the same conclusion.
- The analysis showed that there is no significant relationship between *IDT_cTindex* and fatigue life (*StrainNfIM*), and a weak relationship between *IDT_Strength* from the IDEAL-CT test and fatigue life from the 4PB test. This result was also separately analyzed considering only conventional asphalt mixtures (RAP binder replacement lower than or equal to 25% and without modified binder) and only unconventional mixes (RAP binder replacement higher than 25% or with rubber- and/or polymer-modified binder). The results showed no significant correlation for the conventional mixes and a weak positive correlation for the unconventional mixes, which have a wider range of stiffnesses, fatigue lives, and IDEAL-CT values than do the conventional mixes. The weak relationship between *IDT_Strength* and fatigue life is largely influenced by the unconventional mix results.
- An analysis of *IDT_cTindex* and *IDT_Strength* versus the 4PB tensile strain that results in a fatigue life of 250,000 cycles to failure (*StrainNf0.25M*) resulted in the same conclusions found for the lower strain level resulting in one million cycles to failure: no correlation with *IDT_cTindex* and a weak correlation with *IDT_Strength*.
- The results from this chapter and the previous two chapters indicate that, at least for these mixes, the LOU-SCB, I-FIT, and IDEAL-CT tests provide similar information and that information correlates well with flexural stiffness but not flexural fatigue.
- Of the three tests, the IDEAL-CT test is faster and simpler to perform, with fewer cuts in the preparation procedure, and good repeatability. The *IDT_Strength* had lower variability than *IDT_cTindex*.

8 RESULTS ANALYSIS OF FAM MIXES LAS TESTING

The four non-Caltrans high RAP mixes, each sampled in the field at two silo storage times, were used to compare the results of FAM LAS testing for stiffness and fatigue life with results from full mix four-point beam stiffness and fatigue life. Several insights regarding the effects of silo time are also noted in this chapter. A separate report has been written providing more in-depth testing results and analysis for the high RAP mix silo storage study (80)

8.1 FAM Mixes LAS Testing Results

For each asphalt material, at least three replicates were prepared for the LAS testing of FAM mixes. The average air voids content for the FAM mixes specimens is shown in Figure 8.1. The averages range from 7.4% to 10.8%, which is within the target range and considered acceptable for this study.



Note: All are high RAP mixes (see Chapter 4), 0H indicates no silo storage, XH indicates X hours of silo storage, and the last number indicates high RAP mix type.

Figure 8.1: Air void content for FAM mix specimens.

The fatigue criterion for FAM mixes LAS testing is defined as the peak of phase angle curve, shown in Figure 8.2. The multiple localized phase angle peaks observed in some testing results correspond to the transition points between phases in the complex modulus evolution curves and indicate that extra caution is required during the data analysis process. As shown in Figure 8.2, the first peak in the phase angle curve matches the end of the first phase of the modulus curve. A sharp drop after the first peak indicates the second phase, and the second peak in

the phase angle curve occurs at the same time as the beginning of the third stage of the modulus curve. For those mixes showing multiple peaks in the phase angle curves, the first peak reflects the predefined failure criterion. However, the second peak value of the phase angle may be larger than the first peak, resulting in the miscalculation of the fatigue life. As a result, instead of identifying the global maximum phase angle as the failure point, this study located the first local phase angle peak corresponding to the end of the first phase of the complex modulus curve for all testing results.

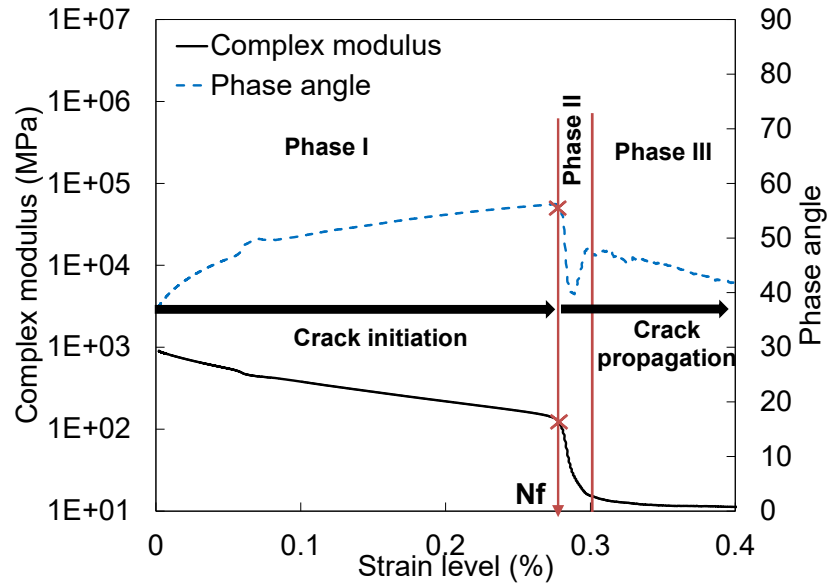


Figure 8.2: An example of LAS testing result on FAM mixes.

The LAS fatigue testing results are shown in Figure 8.3 to Figure 8.6. Three parameters—including initial stiffness, shear strain value at the failure, and the peak value of phase angle—were extracted from the LAS testing results to describe the characteristics of phase angle curves and complex modulus curves. Each parameter was calculated separately for the four field-mixed high RAP mixtures sampled at different amounts of silo time (discussed in Chapter 4), shown in the bar plots with replicate values in Figure 8.7. The fatigue performance of FAM mixes can be represented through the parameter of shear strain at failure. Higher strain value at failure indicates better fatigue resistance of the asphalt material. Figure 8.7 indicates that of all FAM mixes without silo hours, HRAP_0H_4, which has the highest RAP content (50%), shows the worst fatigue performance with the lowest shear strain value at failure. The highest average shear strain value at failure of HRAP_0H_1, which contains the lowest amount of recycled asphalt material (20% RAP and 3% RAS) and a softer binder (PG 58-28), indicates that it has the best fatigue performance. The relatively low content of recycled asphalt material and softer binder in HRAP_0H_1 also results in the softest initial stiffness, shown in Figure 8.7(a). By examining the shear strain values at failure of HRAP_0H_2 and HRAP_0H_3, comparable fatigue performance was found between

these two FAM mixes, with heavily overlapping replicate shear strain values. Both HRAP_0H_2 and HRAP_0H_3 contain 40% RAP in the mixtures, while HRAP_0H_2 uses a softer binder (PG 58-28) in the mix design and recycling agent was added to HRAP_3.

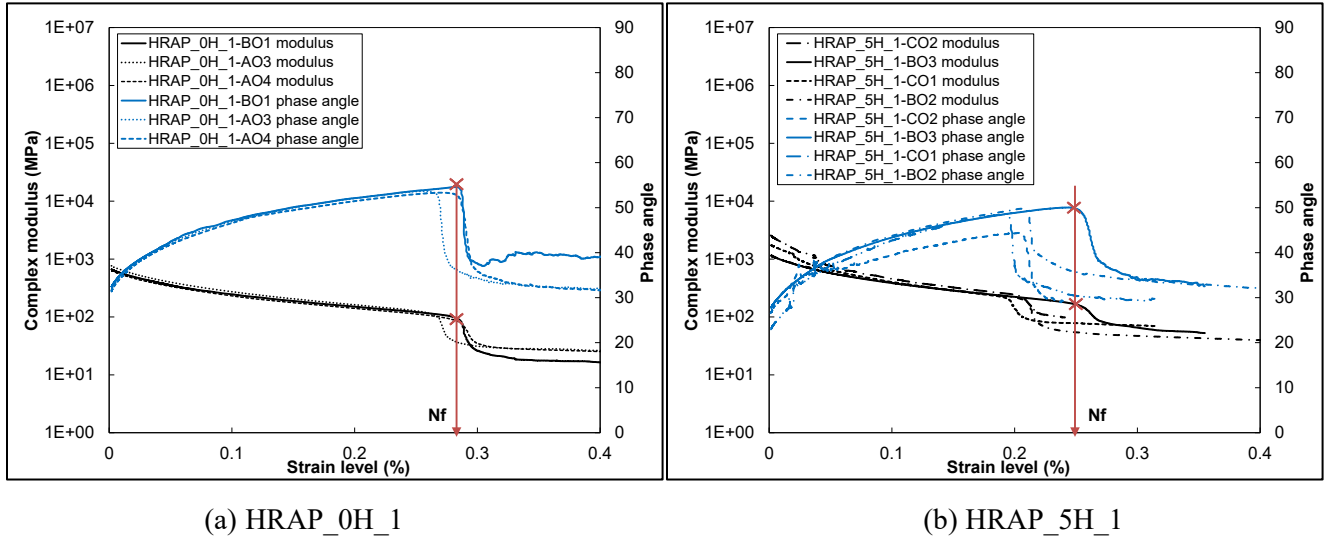


Figure 8.3: LAS testing results for HRAP_1.

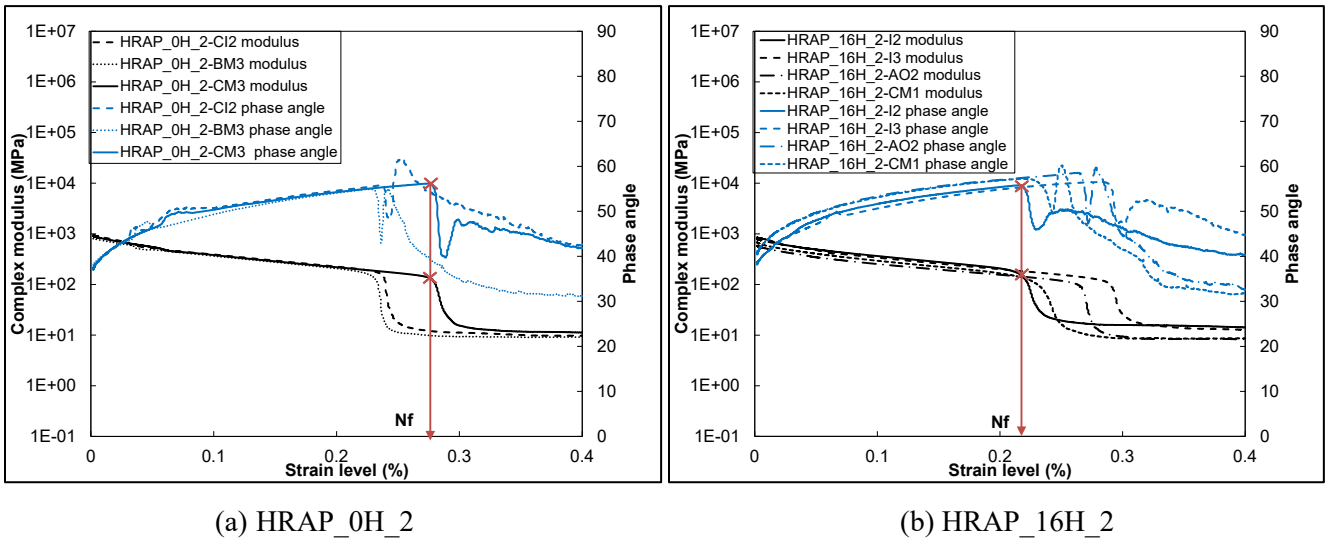
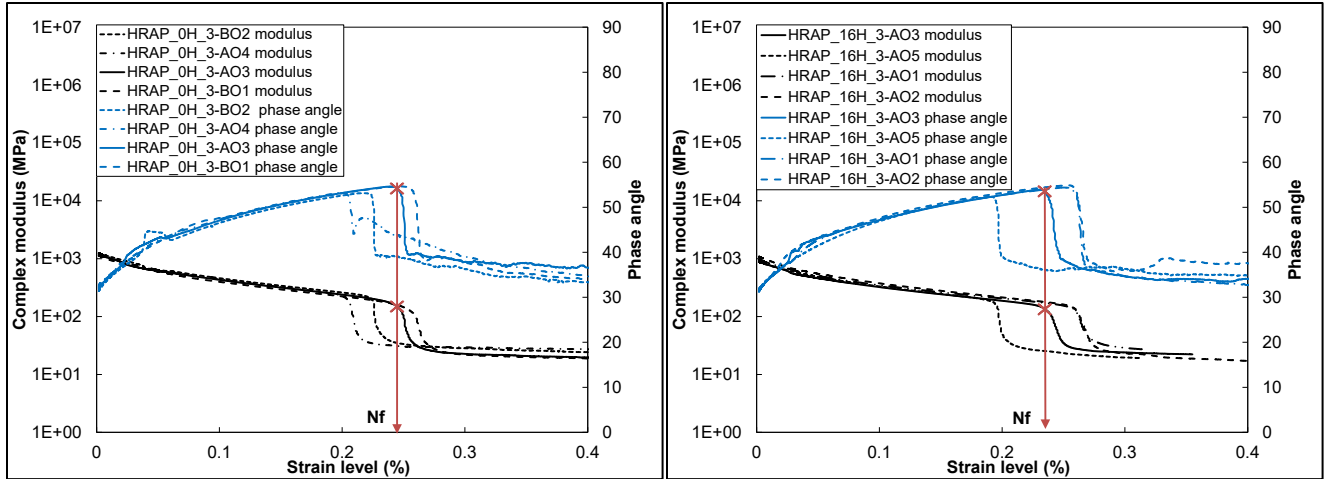


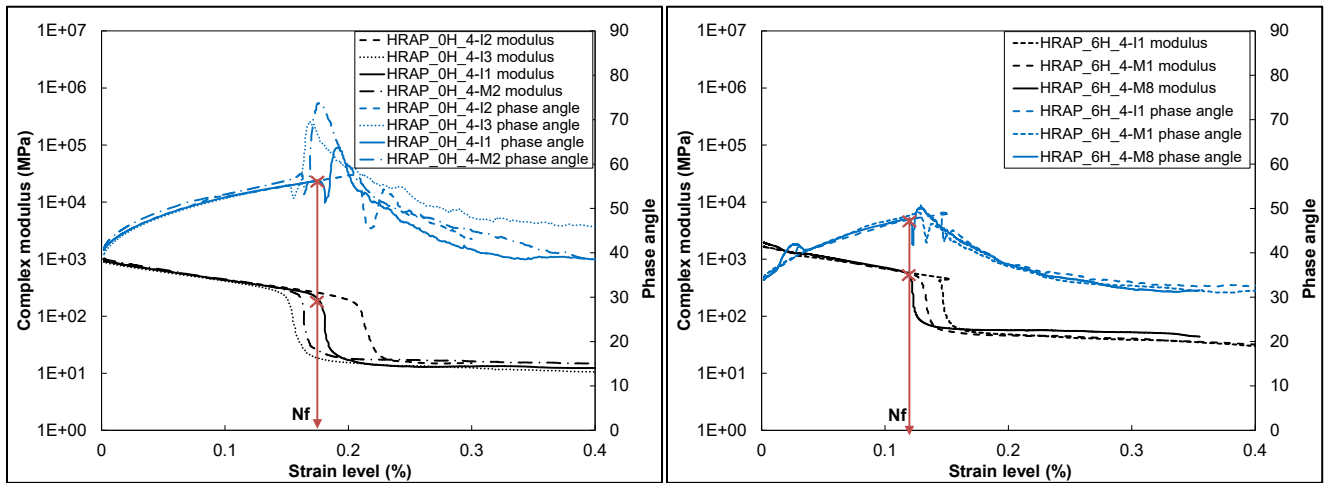
Figure 8.4: LAS testing results for HRAP_2.



(a) HRAP_0H_3

(b) HRAP_16H_3

Figure 8.5: LAS testing results for HRAP_3.



(a) HRAP_0H_4

(b) HRAP_6H_4

Figure 8.6: LAS testing results for HRAP_4.

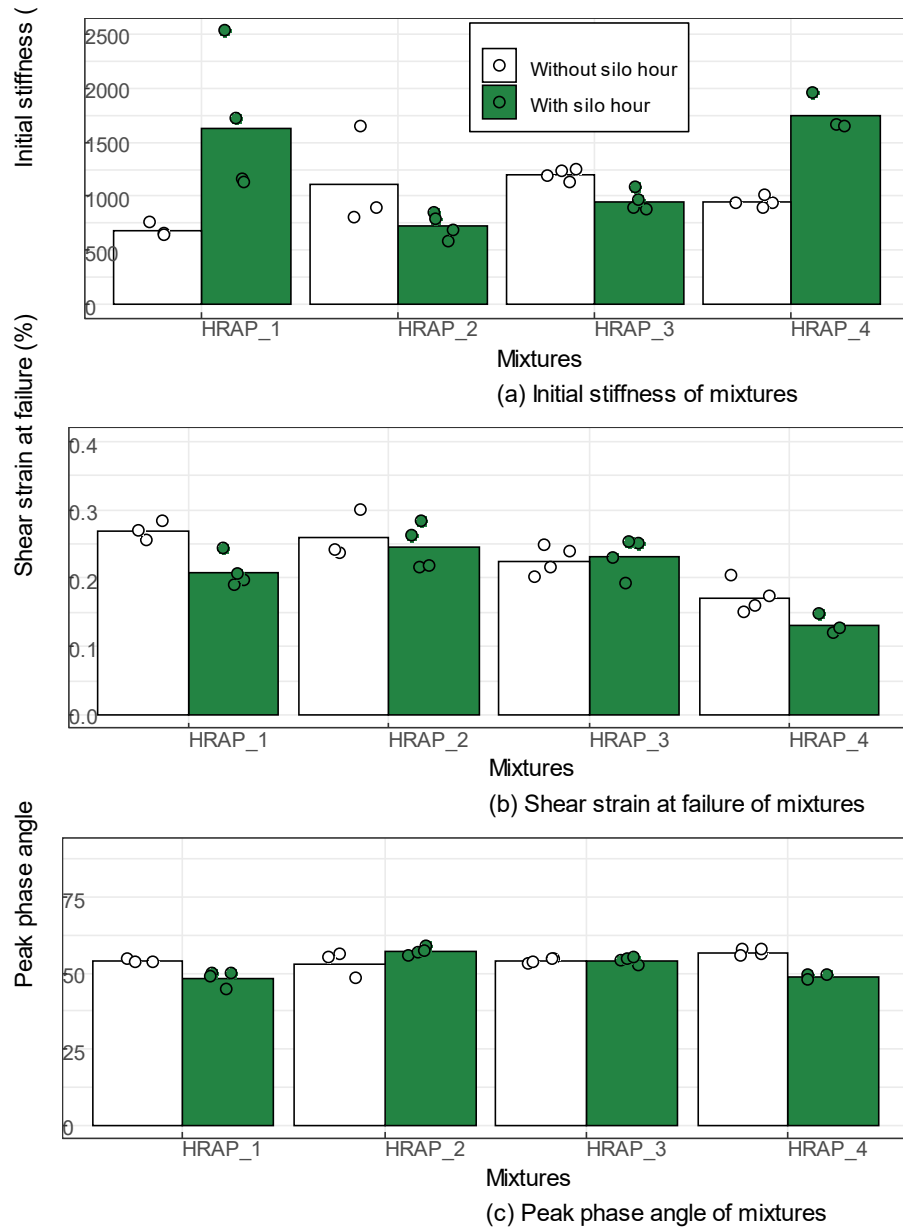


Figure 8.7: Summary of FAM mixes LAS testing results.

The repeatability of LAS testing and the variability of selected fatigue parameters were assessed through the coefficient of variation (COV), shown in Figure 8.8. Most of the parameters—including *E10*, *FailureStrain*, power coefficient *B*, and *DamageLevel*—show low variability, with COV values below 12%, while the coefficient *A* has relatively high variability.

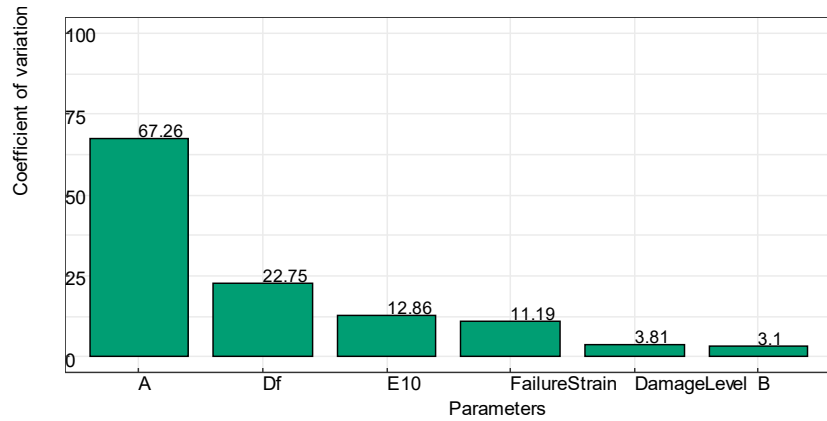


Figure 8.8: Averaged coefficient of variance for fatigue parameters from FAM mixes LAS testing.

8.2 Comparison Between FAM Mixes LAS and I-FIT Tests

The correlation between the FAM mixes LAS test parameters and I-FIT test results is shown in Figure 8.9. The I-FIT results are likely applicable to the LOU-SCB and IDEAL-CT tests based on the strong correlations between the three tests shown in previous chapters. From the correlation matrix, there is a strong linear relationship between coefficients (A and B) from the LAS testing and the fracture energy (G_f) from I-FIT. The coefficient B in the Wohler's law of fatigue equation represents the sensitivity of the applied strain value on fatigue life, and it shows a good correlation with S_{asc} , G_f , S_{pp} , $Strength$, and KIC from the I-FIT test.

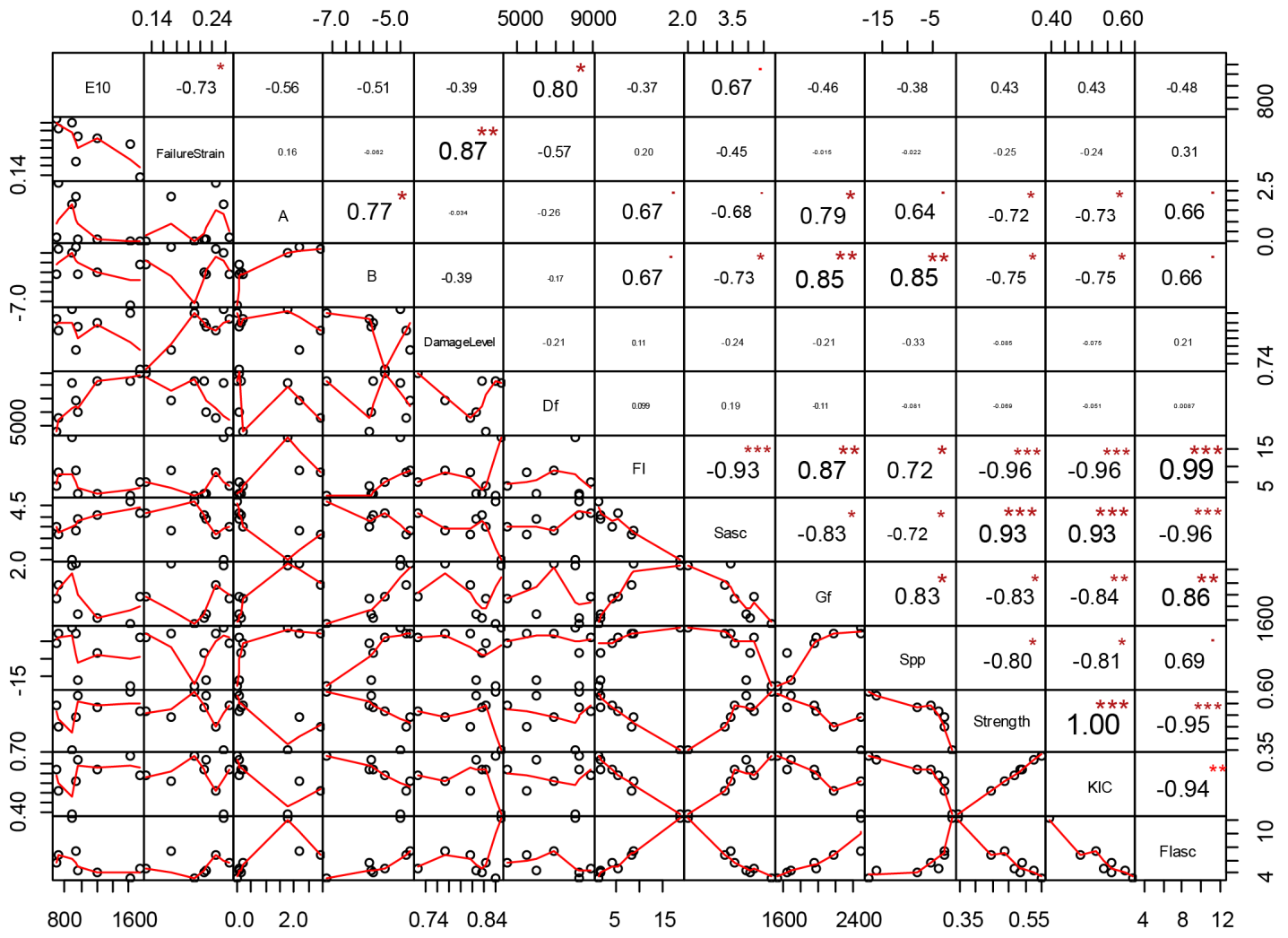
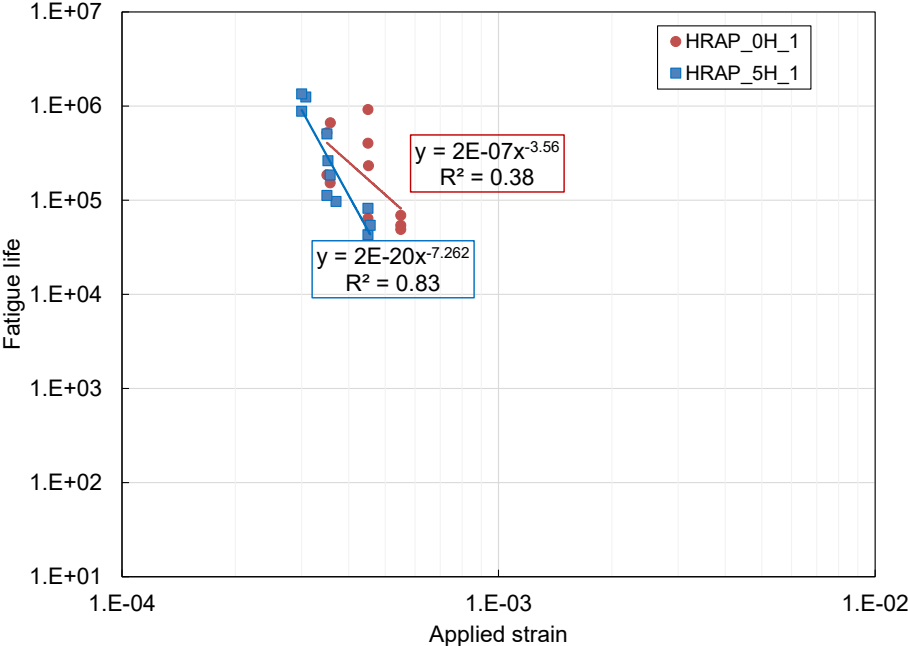


Figure 8.9: Correlation matrix between FAM mixes LAS testing parameters and I-FIT parameters.

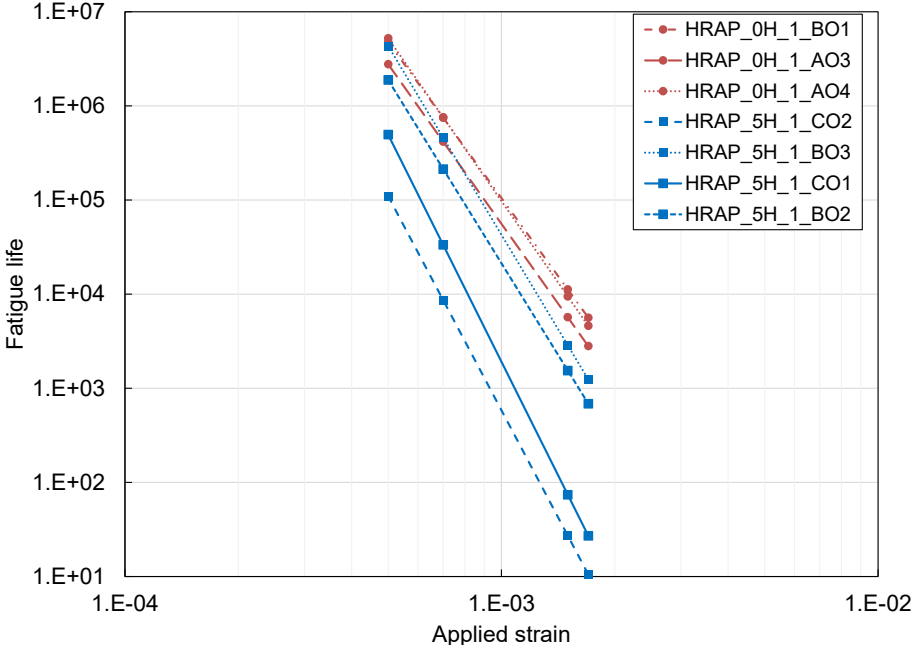
8.3 Comparison Between FAM Mixes LAS and 4PB Tests

The fatigue life obtained from the 4PB tests on full mixtures and LAS testing on FAM mixes were compared for each mix with different silo storage hours. The fatigue life against applied strain values plots are shown in Figure 8.10 to Figure 8.13. For 4PB fatigue testing, the testing data are these scatter points, all of which have been used to fit a power function of the Wohler's law function. The fitted power equation is included in each plot as well as the R^2 value. For LAS testing results, the coefficients (A and B) for the Wohler's law function were obtained directly from the VECD model analysis for each specimen. The fatigue life of each replicate of the FAM mixes, calculated at four selected strain values (0.05%, 0.07%, 0.15%, and 0.17%) using the power law function, are included in the plots.

The fatigue life of the HRAP_1 full mixture in Figure 8.10(a) shows that the material with 5 hours in silo has better fatigue performance at lower strain values while the material without silo hours shows better fatigue life at higher strain values, which is also shown in the Wohler's curves of the FAM mixes in Figure 8.10(b).



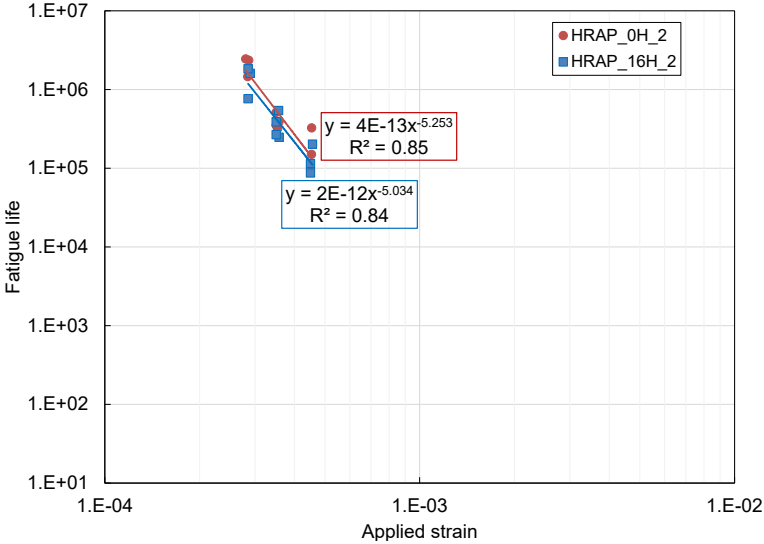
(a) Fatigue life results from 4PB testing



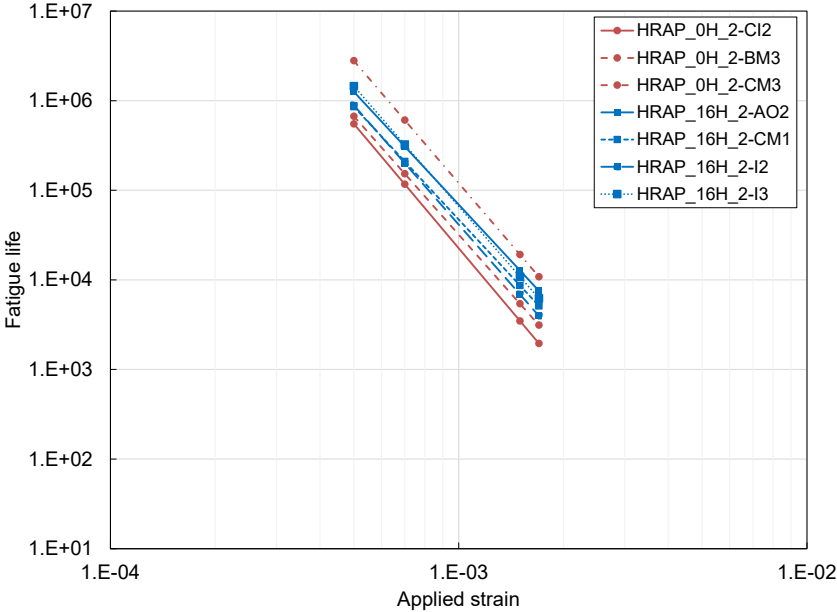
(b) Fatigue life results from FAM mixes LAS testing

Figure 8.10: Wohler's curve for HRAP_0H_1 and HRAP_5H_1.

For the fatigue performance of HRAP_2, the full mix result shown in Figure 8.11(a) indicates that silo storage hours have a negative impact on the fatigue life across multiple strain values. In general, the two fitted lines seem parallel, and the power value (the slope of the fitted curve) in the fitted equation of the mixture without silo hours is slightly higher than the value of the one with silo hours. The power value implies better fatigue performance at lower strain values for the mixture without silo hours and better fatigue performance of the mixture after 16 silo hours at higher strain values. The LAS testing results for the FAM mixes in Figure 8.11(b) show that the FAM mix of HRAP_0H_2 has almost the same fatigue life as HRAP_16H_2 since the fitted lines are overlapping.



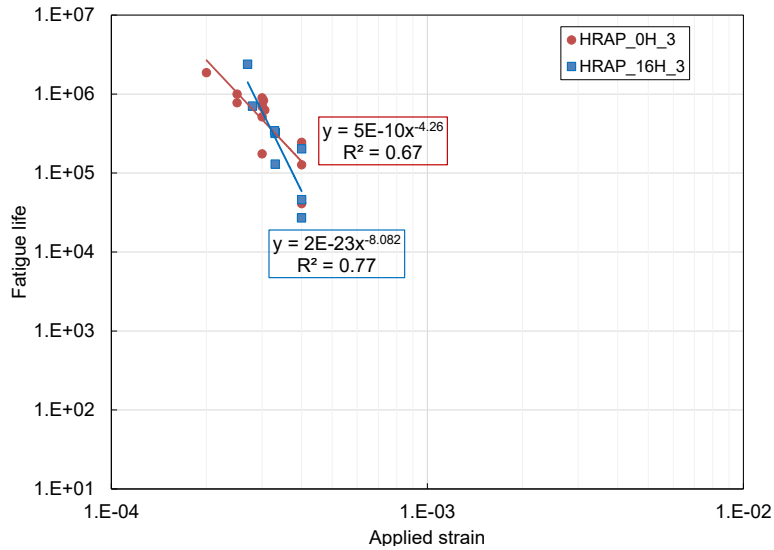
(a) Fatigue life results from 4PB testing



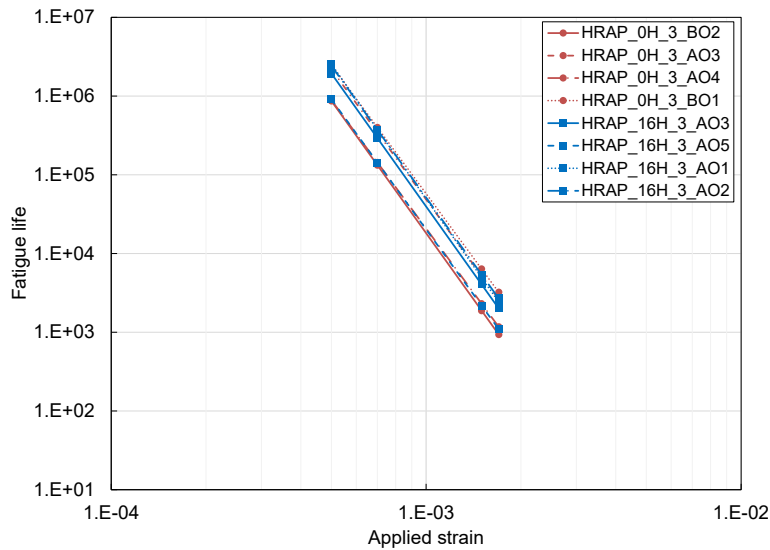
(b) Fatigue life results from FAM mixes LAS testing

Figure 8.11: Wohler’s curve for HRAP_0H_2 and HRAP_16H_2.

The fatigue life versus strain curves of the full mix of HRAP_3 in Figure 8.2 show results consistent with the previous mixtures in terms of the effect of silo hours on fatigue performance: increased sensitivity of fatigue life to strain value after 16 hours in the silo. However, the FAM mixes of HRAP_0H_3 and HRAP_16H_3 show similar fatigue performances with heavily overlapping Wohler's law curves in Figure 8.12(b).



(a) Fatigue life results from 4PB

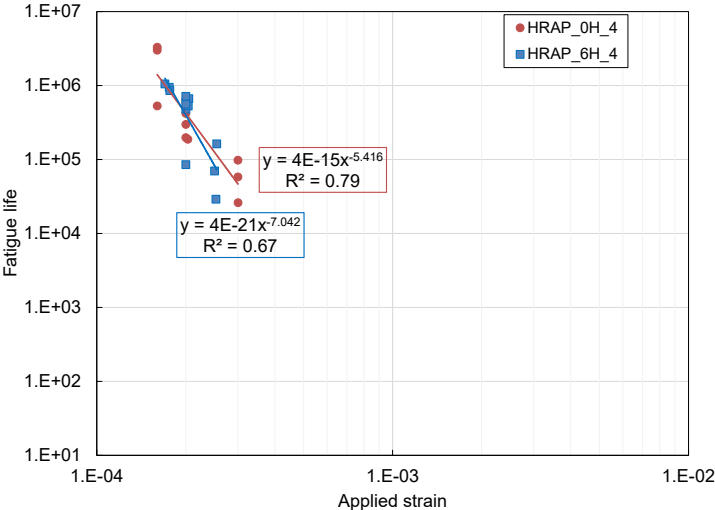


(b) Fatigue life results from FAM mixes LAS testing

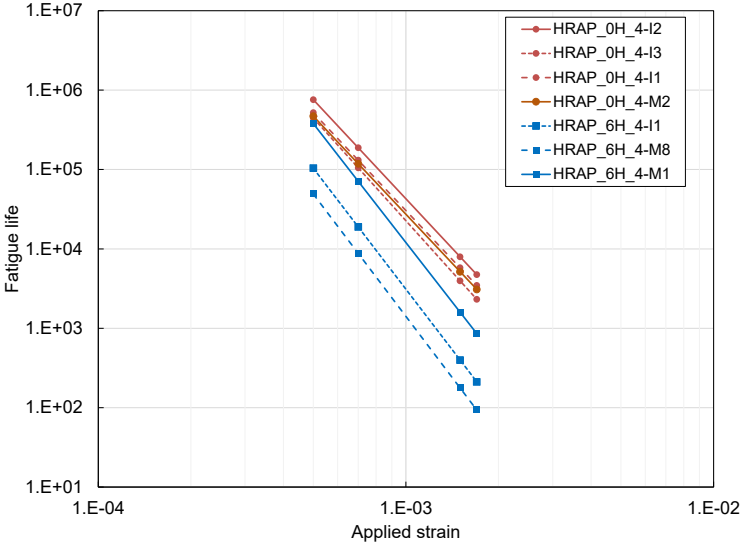
Figure 8.12: Wohler's curve for HRAP_0H_3 and HRAP_16H_3.

The fitted Wohler's curves in Figure 8.13(a) indicate that the full mix material without silo hours has a longer fatigue life at higher strain values than the one with 6 silo hours. However, at lower strain values, the fatigue

performance of HRAP_6H_4 surpassed that of HRAP_0H_4. Figure 8.13(b) shows that for FAM mixes of HRAP_4, 6 hours in the silo reduced the fatigue life compared to HRAP_0H_4 across all strain values and the reduction is more noticeable at high strain values. In addition, the fitted line for the material with silo hours has a sharper slope than the one without silo hours, suggesting a better fatigue life at low strain values for this FAM mix after the short-term silo hours. This finding agrees with the full mix comparison result in Figure 8.13(a).



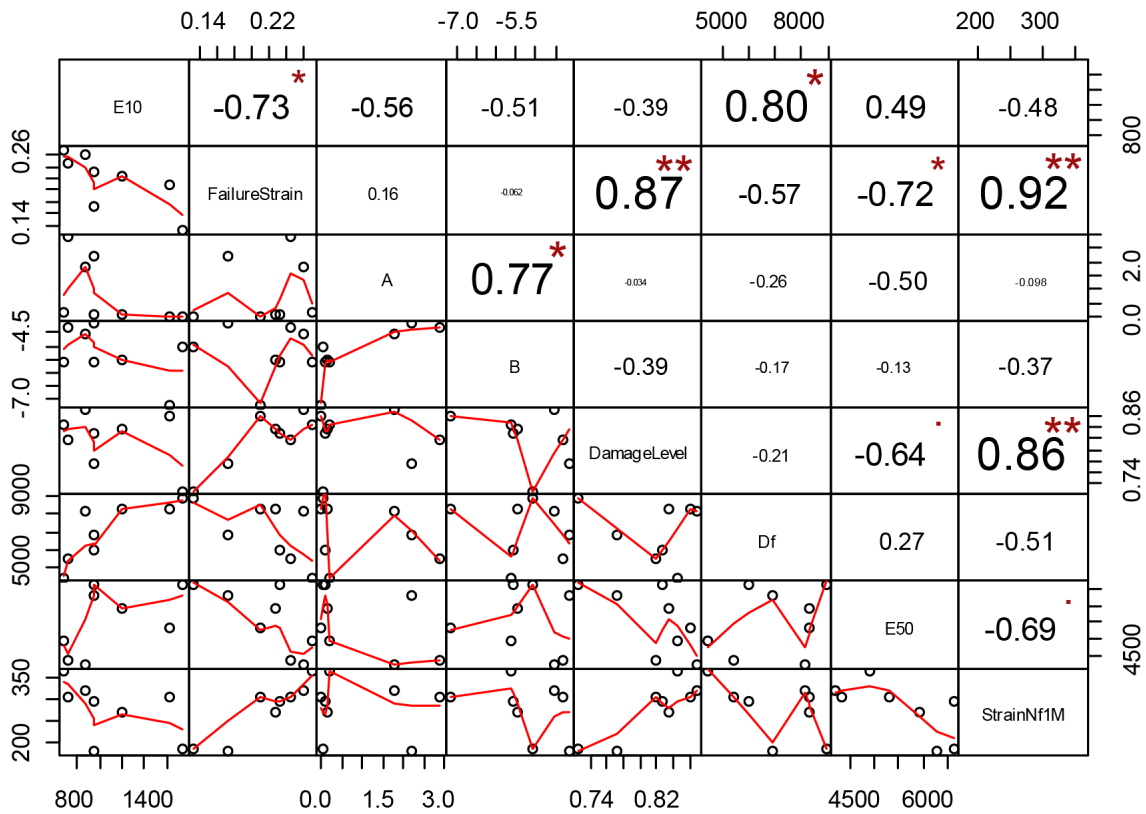
(a) Fatigue life results from 4PB



(b) Fatigue life results from FAM mixes LAS testing

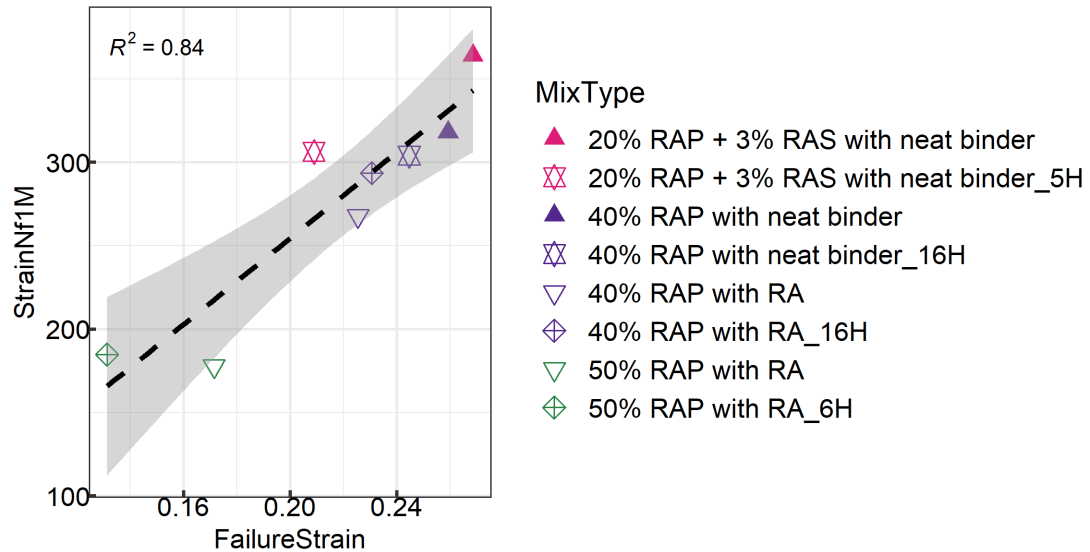
Figure 8.13: Wohler’s curve for HRAP_0H_4 and HRAP_6H_4.

To further study the relationship between FAM mixes LAS testing and full mixes 4PB testing, the correlation between parameters from these two testing methods were plotted, shown in Figure 8.14. The initial stiffness (E_{10}) from the LAS testing represents the intact stiffness of FAM mixes, and E_{50} , from the 4PB testing, represents the intact stiffness of full mixtures. E_{50} is the flexural (tension) stiffness of full asphalt mixtures measured at 10 Hz and 68°F (20°C), and E_{10} is the shear stiffness of the corresponding FAM mixes at 10 Hz and 77°F (25°C). The correlation analysis shows no significant relationship between these two stiffnesses, which may be due to different volumetric portions in the FAM and coarse aggregates for these four types of mixes. The matrix indicates a strong correlation between the strain value at failure in the LAS testing of the FAM mixes ($FailureStrain$) and 4PB testing of the full mixtures ($StrainNf1M$). A linear regression analysis was performed for these two parameters, shown in Figure 8.15, and the R^2 value of 0.84 indicates a strong linear correlation.



Note: E_{50} and $StrainNf1M$ tested at 68°F (20°C), all other parameters at 77°F (25°C).

Figure 8.14: Correlation matrix between FAM mixes LAS testing parameters and 4PB testing parameters.



Note: Gray area indicates 95% confidence interval.

Figure 8.15: Linear regression between *FailureStrain* from FAM mixes fatigue testing and *StrainNf1M* from 4PB testing.

8.4 Summary

The LAS fatigue testing was conducted on FAM mix specimens for four types of asphalt mixtures, all with 20% or more RAP content, and each mixture had two different silo hours. The VECD model was used to analyze the FAM mixes fatigue testing results. The fatigue performance of the FAM mixes was then compared to the I-FIT fracture results (which themselves were found to be highly correlated with the LOU-SCB and IDEAL-CT fracture results) as well as the 4PB fatigue results. The following are conclusions from the findings presented in this chapter:

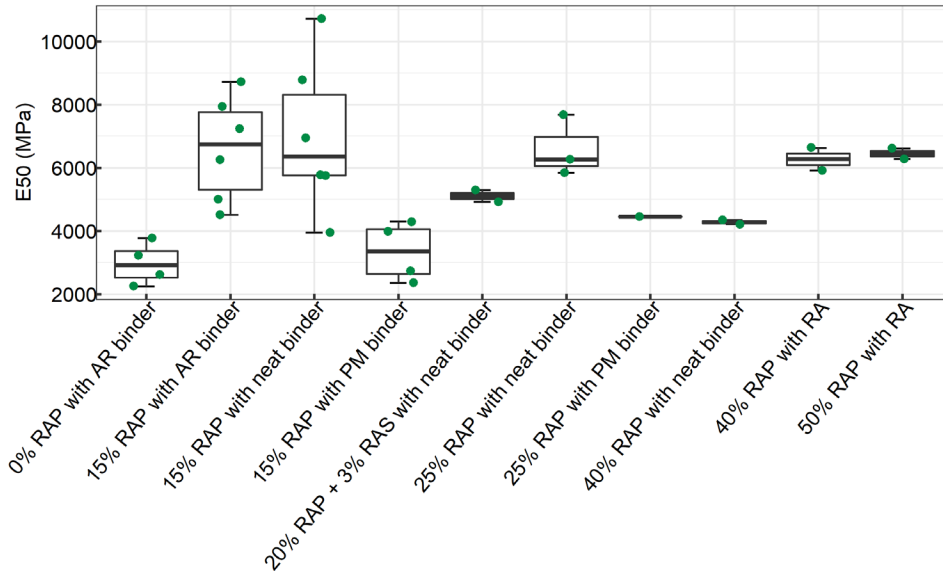
- The variability analysis shows that fatigue parameters from FAM mixes LAS testing—including *E10*, *FailureStrain*, *DamageLevel*, and the power coefficient *B* from Wohler’s law—have low average COV values, indicating low variability of these parameters and good repeatability of the LAS testing on FAM mixes.
- The comparison between FAM mixes LAS testing and I-FIT testing indicates a good relationship between the power coefficient *B* from Wohler’s law of the LAS testing and most of the fracture parameters from the I-FIT testing.
- The correlation study between the FAM mixes LAS fatigue parameters and the 4PB parameters indicates a strong linear correlation between *FailureStrain* from FAM mixes LAS testing and *StrainNf1M* from 4PB testing, with an R^2 value of 0.84. As stated previously, the stiffness of asphalt mixtures plays an important role in determining the fatigue cracking resistance of asphalt pavements and also serves as a key property parameter in the *CalME* fatigue damage model. However, a weak linear relationship exists, with an *r* value of 0.49 between the initial shear stiffness from LAS testing and initial elastic stiffness from 4PB testing for the four high RAP/RAS asphalt materials included in this study.

9 SENSITIVITY OF TESTS TO MATERIAL TYPE

This chapter presents analysis of the sensitivity of the 4PB and I-FIT tests for the different mix types included in the study. The I-FIT test was selected here as the representative fracture test among the three fracture tests as more types of asphalt mixtures have been tested with the I-FIT test.

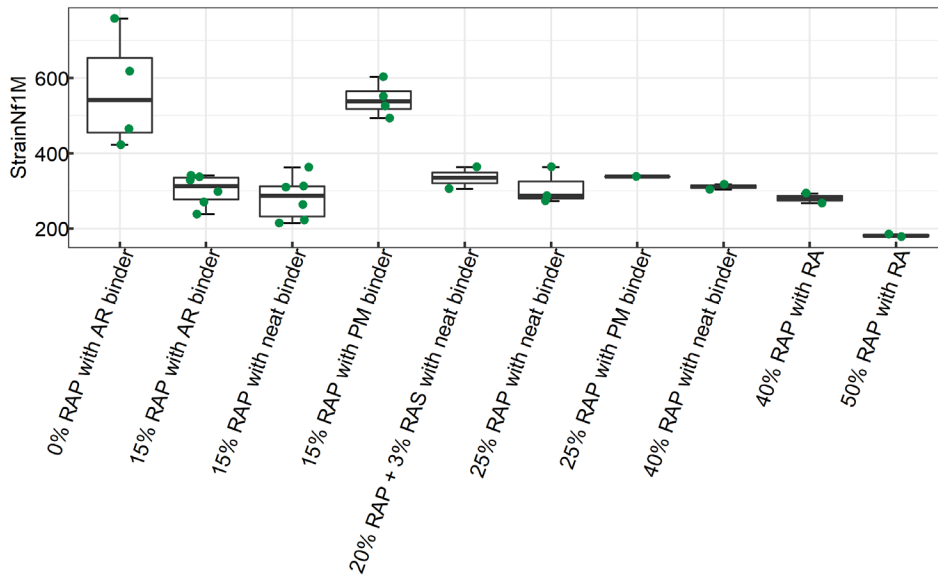
9.1 4PB Testing

The ability of 4PB testing to discern the fatigue cracking performance between asphalt materials is evaluated in this section. The sensitivity to material types is examined through a descriptive analysis and a Tukey's HSD analysis. The boxplot in Figure 9.1 shows the distribution of $E50$ and the boxplot in Figure 9.2 shows the distribution of $StrainNfIM$ for each category of asphalt material types. The $E50$ distribution clearly shows that the gap-graded asphalt mixtures with 0% RAP with AR binder (PG 64-16 + 20% CRM) (meeting Caltrans RHMA-G specifications) and the dense-graded asphalt mixtures with 15% RAP with PM binder have the lowest stiffnesses at 68°F (20°C) and 10 Hz loading frequency compared to the other materials, as expected. However, the increase in RAP content in mixes with conventional binders did not consistently result in higher stiffness, due to other material variables such as softer virgin asphalt binders, the stiffness of the aged RAP binders, and the effects of any recycling agents added to the mix. The $StrainNfIM$ distribution indicates that those same two mix types (0% RAP with AR binder and 15% RAP with PM binder) provide the best fatigue cracking resistance and also have the lowest $E50$ values. In addition, the mixtures in the 50% RAP with RA category have the lowest $StrainNfIM$ and highest $E50$ values—although other mixes that are much stiffer have better fatigue lives, indicating that variables other than stiffness play an important role in fatigue performance.



Note: All mixes are dense graded, except 0% RAP with AR binder, which is gap graded; CRM contents in AR binder are 20% for 0% RAP mixes, 5% or 10% for 15% RAP mixes.

Figure 9.1: E50 sensitivity to material types.



Notes: All mix types are dense graded, except 0% RAP with AR binder which is gap graded; CRM contents in AR binder are 20% for 0% RAP mixes, 5% or 10% for 15% RAP mixes.

Figure 9.2: StrainNf1M sensitivity to material types.

The Tukey's HSD analysis was used to further investigate the sensitivity of fatigue performance by material type, shown in Table 9.1. The mixtures are divided into groups based on either E50 or StrainNf1M parameters. There is no significant difference between mixture types that share the same group letter. Within each grouping, A

represents a higher value of *E50* or *StrainNfIM* than *B*. For example, for *E50*, mixtures of 0% RAP with AR binder (gap graded, 20% CRM) are in Group C because they are softer (lower stiffness values) than mixtures of 15% RAP with neat binder in Group A (higher stiffness values). Table 9.1 has also been color coded to identify distinct groups of mixtures: green cells († symbol) indicate high parameter values while red cells (* symbol) indicate lower parameter values (*E50* and *StrainNfIM*). The mixtures that cannot be differentiated from other mixtures are not in colored cells.

The *E50* groupings in green cells are mixtures of 15% RAP with 5% or 10% rubber in the binder and 15% RAP with neat binder that have the highest initial flexural stiffness, while the ones in red cells are mixtures of 0% RAP with AR binder and 15% RAP with PM binder that are significantly softer than the other materials. The *StrainNfIM* groupings in green cells are mixtures of 0% RAP with AR binder (gap graded, 20% CRM) and 15% RAP with PM binder that show relatively better fatigue performance than the other mixtures, with the Group C mixtures showing significantly inferior fatigue resistance. The *E50* and *StrainNfIM* grouping results imply that mixtures with softer stiffness have better fatigue performance and stiffer mixtures have lower fatigue cracking resistance among the mixtures with low RAP content, as expected in controlled-strain testing. On the other hand, mixtures with RAP content higher than 25% (Group BC and Group C) have noticeably poorer fatigue performance than the mixture with 0% RAP and the mixtures with 15% RAP and polymer-modified binder (Group A and Group AB), based on *StrainNfIM*. However, the parameter *E50* could not distinguish these mixes from the rest of the materials.

Table 9.1: Tukey’s HSD Analysis Result for 4PB Testing

Mix Type	Group by E50	Group by StrainNfIM
0% RAP with AR binder ^a	C*	A†
15% RAP with neat binder	A†	C*
15% RAP with AR binder ^b	AB†	C*
15% RAP with PM binder	BC*	AB†
25% RAP with neat binder	ABC	C*
25% RAP with PM binder	ABC	BC*
20% RAP + 3%RAS with neat binder	ABC	BC*
40% RAP with neat binder	ABC	BC*
40% RAP with RA	ABC	C*
50% RAP with RA	ABC	C*

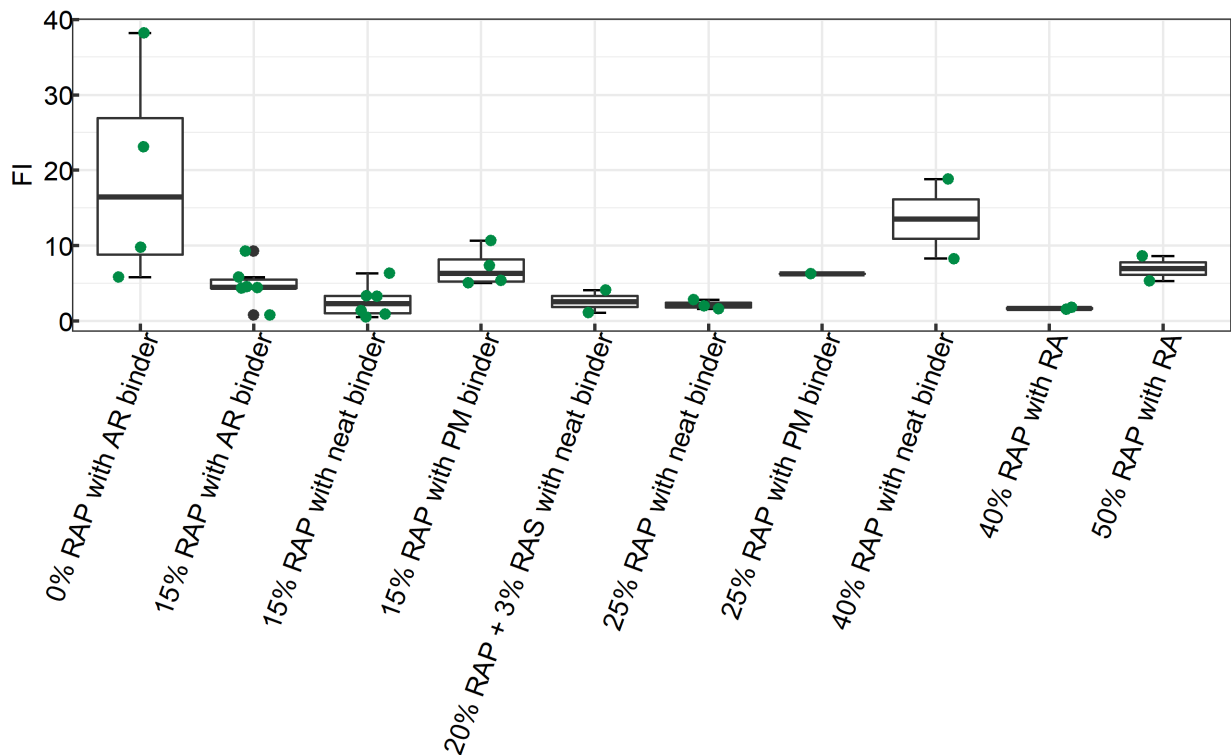
^a Gap-graded, 20% CRM in binder

^b 5% or 10% CRM in binder

Notes: Tukey’s HSD significance level = 0.05. Green (†) indicates high value of parameters, and red (*) indicates lower value of parameters. Groups sharing the same letter are not significantly different (e.g., Group A and Group ABC are not significantly different from each other).

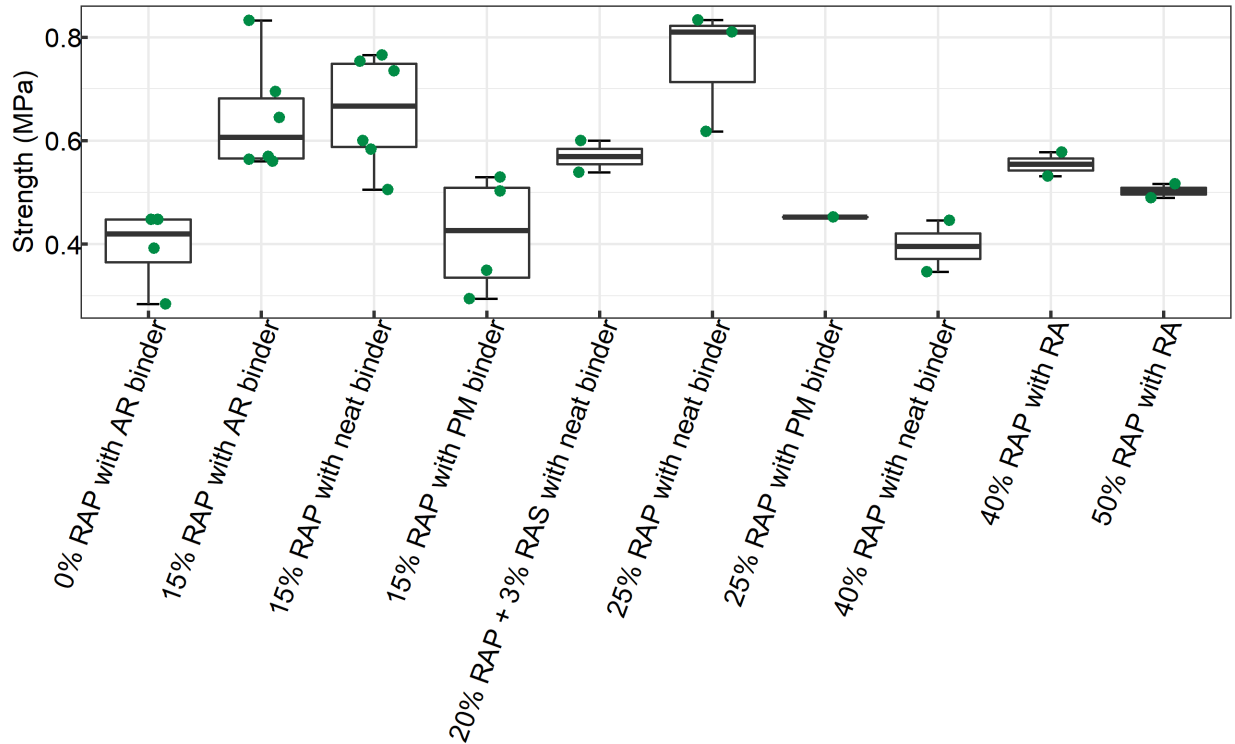
9.2 I-FIT Testing

As more experimental data were obtained from the I-FIT testing, the sensitivity of fracture testing to differentiate between different material types was explored in the case of the I-FIT test. The boxplot in Figure 9.3 displays the flexibility index (*FI*) distribution for 10 mix types. Based on the *FI* values, mixtures of 0% RAP with AR binder and 40% RAP with neat binder are notably different from the rest of the mixtures with the highest *FI* values, but *FI* cannot distinguish among the rest of the mixtures. *Strength* previously showed a good correlation with 4PB flexural stiffness (*E50*), and the sensitivity of *Strength* to material type is assessed in Figure 9.4. The mixtures show distinct differences in strength value except for the overlap of box boundaries between 15% RAP with neat binder and 15% RAP with AR binder mixtures (dense graded, 5% or 10% CRM) and the overlap between the gap graded asphalt mixture of 0% RAP with AR binder (20% CRM) and 40% RAP with neat binder. In addition, the mixtures with 15% RAP with PM binder have the lowest strength, which corresponds with the previous findings for *E50* and *StrainNfIM* from Figure 9.1 and Figure 9.2.



Note: All mix types are dense graded, except 0% RAP with AR binder which is gap graded; CRM contents in AR binder are 20% for 0% RAP mixes, 5% or 10% for 15% RAP mixes.

Figure 9.3: *FI* sensitivity to material types.



Notes: All mix types are dense graded, except 0% RAP with AR binder which is gap graded. CRM contents in AR binder are 20% for 0% RAP mixes, 5% or 10% for 15% RAP mixes.

Figure 9.4: *Strength* sensitivity to material types.

The Tukey's HSD analysis provides a straightforward way to distinguish between mixtures. For better comparison, the previous grouping result from the 4PB test is included in Table 9.2. The *FI* parameter divides these materials into two groups: A and B. Higher *FI* values indicate better fracture resistance. The mixtures in Group A (0% RAP with AR binder [gap graded, 20% CRM]) have the best fracture resistance, as expected. The ones in Group B show secondary fracture performance, and they match with the less favorable fatigue performance of the *StrainNfIM* groupings in Table 9.2. However, for the mixtures containing RAP and PM or the ones with high RAP contents and soft asphalt binders, *FI* fails to distinguish them from the other mixture types. In addition, the fracture energy (G_f) shows no difference among mixtures.

The *Strength* measure from the I-FIT test also divides the materials into two groups. Mixtures in Group B have lower *Strength* values than those in Group A. The mixtures with no RAP content (0% RAP with AR binder [gap graded, 20% CRM]) or lower RAP content with polymer modifier (15% RAP with PM binder) show significantly lower strength values than mixtures with lower RAP content with neat binder or AR binder, which corresponds with the ranking of flexural stiffness (E_{50}). In contrast, *Strength* fails to distinguish mixtures with high RAP

content from the rest of the mixtures (25% RAP with PM, 20% RAP and 3% RAS with neat binder, 40% RAP with RA, and 50% RAP with RA).

In summary, both *FI* and *Strength* display a fair ability for distinguishing between asphalt mixtures. The *FI* grouping results highly agree with the fatigue grouping results of *StrainNfIM*. However, the groupings put the mixes with rubber and polymer-modified binders, which are well known to have excellent fatigue performance, in one group and all other mixes in another group. Meanwhile, the grouping result of *Strength* is consistent with the stiffness *E50* grouping result. Comparison of the color-coding in the *Strength* and *StrainNfIM* categories shows that for asphalt mixtures containing lower RAP content, a higher *Strength* value indicates a lower fatigue life.

Table 9.2: Tukey’s HSD Analysis Result for I-FIT

Mix Type	I-FIT			4PB	
	Group by FI	Group by Gf	Group by Strength	Group by E50	Group by StrainNfIM
0% RAP with AR binder ^a	A [†]	A	B*	C*	A [†]
15% RAP with neat binder	B*	A	A [†]	A [†]	C*
15% RAP with AR binder ^b	B*	A	A [†]	AB [†]	C*
15% RAP with PM binder	AB	A	B*	BC*	AB [†]
25% RAP with neat binder	B*	A	A [†]	ABC	C*
25% RAP with PM binder	AB	A	AB	ABC	BC*
20%RAP + 3%RAS with neat binder	B*	A	AB	ABC	BC*
40% RAP with neat binder	AB	A	B*	ABC	BC*
40% RAP with RA	B*	A	AB	ABC	C*
50% RAP with RA	AB	A	AB	ABC	C*

^a Gap-graded, 20% CRM in binder

^b 5% or 10% CRM in binder

Notes: Tukey’s HSD significance level = 0.05. Green (†) indicates high values of parameters and red (*) indicates lower values of parameter. Groups sharing the same letter are not significantly different. (e.g., Group A and Group ABC are not significantly different from each other).

9.3 Summary

The ability to distinguish the fatigue cracking resistance between asphalt materials is an important criterion when selecting a surrogate stiffness or fatigue performance-related test for the asphalt mix design and QC/QA. The following is a summary of the sensitivity of potential tests and corresponding parameters for asphalt mixtures based on the findings reviewed in this chapter:

- The boxplot of 4PB testing results, including initial stiffness (*E50*) and *StrainNfIM*, provides an overview of the distribution of fatigue properties for different asphalt material types. The distribution of *StrainNfIM* indicates that mixtures of 0% RAP with AR binder (gap graded, 20% CRM) and 15% RAP with PM binder have the best fatigue cracking resistance and also the softest *E50*. In addition, the mixtures in the category of 50% RAP with RA have the lowest *StrainNfIM* values and highest *E50* values—although

some mixtures in other categories that are much stiffer have better fatigue life, indicating that variables other than stiffness play an important role in fatigue performance.

- The Tukey's HSD analysis shows that the softest mixtures have better fatigue performance and that stiffer mixtures have lower fatigue cracking resistance among the mixture types containing low RAP content. However, *StrainNfIM* values show that mixtures with RAP content higher than 25% have noticeably weaker fatigue performance, while *E50* could not distinguish these mixes from the rest of the materials.
- The boxplots of the I-FIT results show that mixtures of 0% RAP with AR binder (gap graded, 20% CRM) and 40% RAP with neat binder have the highest *FI* values and are notably different from the rest of the mixtures, while it is difficult to distinguish between the rest of the mixtures based on the *FI* values. The 15% RAP with PM binder mixtures show the lowest strength, the lowest *E50* value, and the highest *StrainNfIM* value of all the materials.
- The Tukey's HSD grouping results indicate that both *FI* and *Strength* display a fair ability to distinguish between asphalt mixtures. Grouping results of *FI* highly match the fatigue grouping results of *StrainNfIM*, though the grouping primarily separates rubberized and polymer binder mixtures from the rest of the mixtures. Meanwhile, the grouping result of *Strength* is consistent with the *E50* grouping results.
- The analysis of sensitivity to material types using the Tukey's HSD method demonstrates that *Strength* distinguishes between asphalt materials, and the grouping results match the stiffness grouping of asphalt material with low RAP or RAS content.
- In conclusion, among all fracture parameters from the I-FIT test, *Strength* from the I-FIT test is recommended as the representative indicator for fatigue performance because it provides sensitivity to different materials similar to the stiffness (*E50*) and fatigue life (*StrainNfIM*) measured from the 4PB testing.

10 SUMMARY AND PRELIMINARY CRITERIA DEVELOPMENT

10.1 Summary and Comparison of Surrogate Tests

The objective of this study was to develop a surrogate performance-related test to replace 4PB testing that would evaluate the fatigue performance of asphalt pavements and that would be easy to perform, fast to finish, and sufficiently correlated with material stiffness or fatigue performance to provide a useful tool for routine mix design and construction QC/QA. With sufficient correlation to both stiffness and fatigue life, this surrogate test could potentially provide information for the ME designs using *CalME* for routine projects. Candidate testing methods evaluated for this study include the I-FIT, LOU-SCB, IDEAL-CT, and FAM mixes LAS testing. The main aspects of these tests assessed in this study were repeatability of the tests, variability of parameters, and correlation with stiffness and/or fatigue.

Summaries of parameters for each potential surrogate test is presented in Table 10.1 to Table 10.4. Different sets of mixes were used for each pairwise (4PB test versus another test) comparison. These tables show the variability of the main parameters and the correlation with the 4PB testing, including stiffness (E_{50}) and fatigue life ($StrainNf_{IM}$). It should be noted that the correlation analysis was performed between the fatigue parameters obtained from 4PB testing at 68°F (20°C) and 10 Hz while the parameters from surrogate tests were measured at 77°F (25°C). Both temperatures are in the intermediate temperature range associated with fatigue cracking.

Table 10.1: Summary of I-FIT Testing Parameters

Parameters	Variability	Correlation with 4PB-Initial Flexural Stiffness (E_{50})	Correlation with 4PB-StrainNf _{IM}
<i>FI</i>	High (COV = 46.64%)	Weak ($R^2 = 0.27$)	None ($R^2 = 0.082$)
<i>f_{lasc}</i>	Moderate (COV = 30.85%)	Weak ($R^2 = 0.28$)	Weak ($R^2 = 0.11$)
<i>S_{pp}</i>	High (COV = 54.67%)	Moderate ($R^2 = 0.44$)	Weak ($R^2 = 0.17$)
<i>S_{asc}</i>	Moderate (COV = 25.77%)	Moderate ($R^2 = 0.56$)	Weak ($R^2 = 0.25$)
<i>G_f</i>	Low (COV = 15.58%)	None ($R^2 = 0.022$)	None ($R^2 = 0.0019$)
<i>K_{IC}</i>	Low (COV = 11.36%)	Moderate ($R^2 = 0.64$)	Weak ($R^2 = 0.25$)
<i>Strength</i>	Low (COV = 11.32%)	Moderate ($R^2 = 0.64$)	Weak ($R^2 = 0.27$)

Table 10.2: Summary of LOU-SCB Testing Parameters

Parameters	R^2	Correlation with 4PB-Initial Flexural Stiffness (E_{50})	Correlation with 4PB-StrainNf _{IM}
<i>J_c</i>	0.69	Moderate ($R^2 = 0.71$)	Weak ($R^2 = 0.18$)

Note: J_c is obtained through linear regression fitting of testing results of all specimens. Therefore, the R^2 for linear regression fitting is included here instead of variability.

Table 10.3: Summary of IDEAL-CT Parameters

Parameters	Variability	Correlation with 4PB-Initial Flexural Stiffness (E50)	Correlation with 4PB-StrainNf1M
<i>cTindex</i>	Low (COV = 7.81%)	Weak ($R^2 = 0.21$)	Weak ($R^2 = 0.1$)
<i>m75</i>	Low (COV = 6.83%)	Weak ($R^2 = 0.34$)	Weak ($R^2 = 0.20$)
<i>Strength</i>	Low (COV = 2.63%)	Strong ($R^2 = 0.80$)	Moderate ($R^2 = 0.42$)
<i>L75</i>	Low (COV = 2.84%)	Weak ($R^2 = 0.12$)	None ($R^2 = 0.01$)
<i>Gf</i>	Low (COV = 2.19%)	None ($R^2 = 0.07$)	None ($R^2 = 0.06$)

Table 10.4: Summary of FAM Mixes LAS Testing Parameters

Parameters	Variability	Correlation with 4PB Initial Flexural Stiffness (E50)	Correlation with 4PB StrainNf1M
<i>E10</i>	Low (COV = 12.86%)	Weak ($R^2 = 0.24$)	Weak ($R^2 = 0.24$)
<i>FailureStrain</i>	Low (COV = 11.19%)	Moderate ($R^2 = 0.52$)	Strong ($R^2 = 0.85$)
<i>DamageLevel</i>	Low (COV = 3.81%)	Moderate ($R^2 = 0.41$)	Moderate ($R^2 = 0.74$)
Coefficient <i>A</i> in Wohler's law	High (COV = 67.26%)	Weak ($R^2 = 0.25$)	None ($R^2 = 0.00$)
Coefficient <i>B</i> in Wohler's law	Low (COV = 3.1%)	None ($R^2 = 0.02$)	Weak ($R^2 = 0.14$)

A comparison of these tests—including information about the testing procedure, testing equipment, required training for operator, the recommended representative parameter for evaluating the fatigue performance, variability of the recommended parameter, and the relationship to 4PB fatigue testing—is shown in Table 10.5.

Table 10.5: Comparison of Surrogate Tests

Test	Sample Preparation	Test Duration	Test Machine	Training for Technician	Recommended Parameter	Variability of Parameter	Correlation with 4PB-Initial Flexural Stiffness (E50)	Correlation with 4PB-StrainNf1M
I-FIT	<ul style="list-style-type: none"> • Cylinder compaction • 4 cuts and 1 notch 	<10 minutes	Axial loading device with no temperature chamber (about \$10,000)	Median	<i>Strength</i>	Low	Moderate	Weak
LOU-SCB	<ul style="list-style-type: none"> • Cylinder compaction • 4 cuts and 1 notch 	<10 minutes	Axial loading device with no temperature chamber (about \$10,000)	Median	<i>Jc</i>	— ^a	Moderate	Weak
IDEAL-CT	<ul style="list-style-type: none"> • Cylinder compaction • 0 cuts 	<10 minutes	Axial loading device with no temperature chamber (about \$10,000)	Low	<i>Strength</i>	Low	Strong	Moderate
FAM mixes LAS	<ul style="list-style-type: none"> • Cylinder compaction • 2 cuts • 4 small cores from one gyratory specimen 	2 to 3 hours	Dynamic Mechanical Analyzer (about \$100,000)	High	<i>FailureStrain</i>	Low	Moderate	Strong

^a Jc does not have variability as it is obtained from the linear regression fitting results of all specimens.

Fatigue performance in a pavement structure includes two parts, stiffness and fatigue life. Both the SCB and IDEAL-CT testing results show good correlations with stiffness and weak to moderate correlations with fatigue life, indicating that the suggested parameter *Strength* can account for the material stiffness but cannot sufficiently explain fatigue life. Therefore, *Strength* cannot be used directly as a fatigue life indicator, but it can indicate changes in production when used as a QC/QA test. Since SCB and IDEAL-CT testing are highly correlated, the preference would be to use IDEAL-CT testing because of its easier specimen preparation, quicker testing procedure, low variability, and good correlation with stiffness performance from 4PB tests. However, the correlation of *Strength* with fatigue life performance is not sufficient to set mix design parameters.

On the other hand, *FailureStrain* from the FAM mixes LAS testing shows a strong correlation with the fatigue life parameter, *StrainNfIM*, from the 4PB testing, implying that continued development of FAM mixes LAS testing as a fatigue performance-related test for asphalt mix design should be pursued.

In conclusion, the correlation analysis study shows that the properties characterized by monotonic fracture tests (SCB and IDEAL-CT) do not do a good job of capturing the fatigue damage resistance of asphalt material when the material is under repetitive loading at an intermediate temperature. FAM mixes LAS testing simulates the repetitive loading configuration that contributes to fatigue cracking with increasing strain values. Compared to conventional fatigue tests with constant strain values, FAM mixes LAS testing has the advantage of completing a test within a short amount of time. These results indicate that further exploration of the LAS approach for full mix 4PB tests to shorten the testing time for more expensive mix design is worth investigation.

10.2 Preliminary Development of Criteria

This section discusses the preliminary development of acceptable *Strength* criteria from the IDEAL-CT test. Such a criteria development process can be implemented primarily for routine mix design, JMF approval, and potentially for QC/QA for pavement construction to characterize initial stiffness and fatigue performance if the cost of the testing is warranted relative to the cost of the project, and other practical considerations. The proposed criteria will take both the asphalt material stiffness and fatigue cracking resistance into consideration.

Caltrans is now requiring ME design for all rehabilitation projects. Statewide representative stiffness master curves from flexural beam stiffness tests for each mix type (PG grade, binder type, and gradation type) are continually being updated and used for ME design. The values used in rehabilitation designs should provide information for selecting minimum stiffnesses for use in setting PRS for mix stiffness at a single loading rate and temperature. The requirement of minimum stiffness taken from the ME design could be satisfied by meeting a minimum *Strength* value for the IDEAL-CT test result for a given design. A strong linear relationship has been

established between *Strength* and *E50* based on the IDEAL-CT data in Chapter 7. To explain the process for determining the threshold of strength, *Strength* is set as the dependent variable and *E50* is the independent variable, shown in Equation 10.1. The linear regression summary for this equation is shown in Table 10.6

$$IDT_Strength = (0.132) \times E50 + 66.072 \quad (10.1)$$

Where:

IDT_Strength = strength from IDEAL-CT (psi) at 77°F (25°C), and

E50 = initial stiffness from 4PB tests (ksi) at 68°F (20°C).

Table 10.6: Regression Model Summary for Strength from IDEAL-CT at 77°F (25°C) and E50 from 4PB at 68°F (20°C)

Model	R ²	Adjusted R ²	F-statistic	p-value	df
Equation 10.1	0.80	0.79	78.57	2.3e-8	1/20

The relationship between *E50* and *Strength* is shown in Figure 10.1, along with the proposed threshold line for *Strength*. In an effort to be conservative and increase reliability when proposing a pass/fail threshold criterion with the IDEAL-CT test, the 95% confidence interval band was applied to statistically determine the lower bound of *Strength* for the stiffness that must be achieved. The confidence interval around the regression line can be calculated as follows:

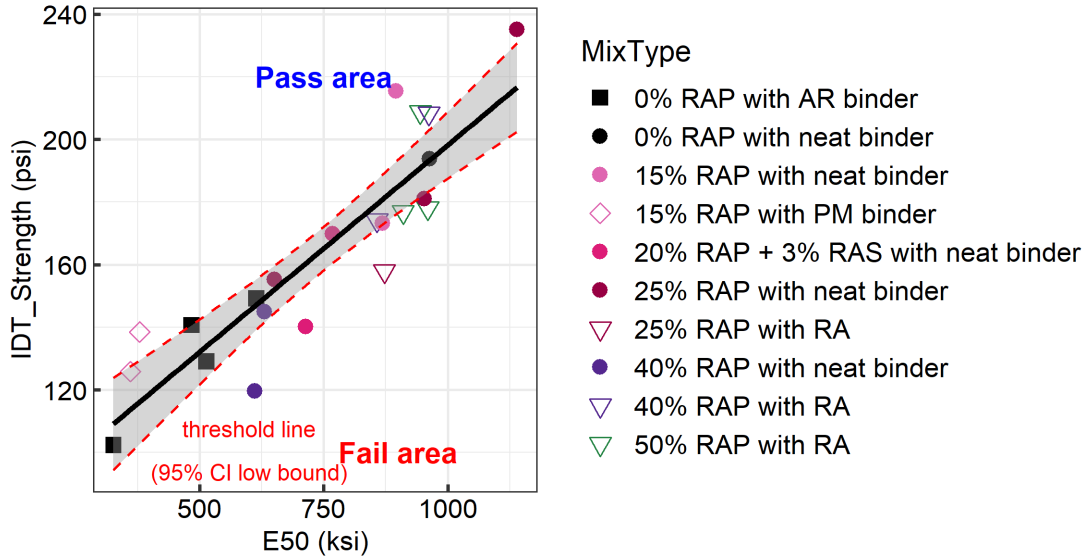
$$\hat{y}_h \pm t_{\frac{\alpha}{2}, n-2} (s.e.)_y \quad (10.2)$$

Where \hat{y}_h is fitted response (*Strength*), and the critical t-value is $t_{\frac{\alpha}{2}, n-2}$ with $n-2$ degrees of freedom and a $(1 - \frac{\alpha}{2})$ percentile.

$(s.e.)_y$ is defined as the standard error of the regression line multiplied by the standard error of the estimate at x_k :

$$(s.e.)_y = \sqrt{\frac{\sum_{i=1}^n (y_i - \hat{y})^2}{n-2}} \sqrt{\frac{1}{n} + \frac{(x_k - \bar{x})^2}{\sum_{i=1}^n (x_i - \bar{x})^2}} \quad (10.3)$$

In Figure 10.1, the 95% confidence interval lower bound is plotted as the threshold line for the criterion of *Strength*. For the stiffness specification, the suggested mean value of strength obtained from replicates of IDEAL-CT should be above the lower bound at the specified stiffness requirement.



Note: 95% confidence interval indicated by red dashed lines.

Figure 10.1: Relationship between *Strength* from IDEAL-CT test and *E50* from 4PB test.

As for the criterion of *Strength* for fatigue life, the testing results of the 4PB test from previous chapters indicate a moderately good relationship between *E50* and *StrainNf1M*. This relationship was built based on the 46 asphalt mixtures tested by 4PB testing in this study, shown in Equation 10.4. The fitted regression summary is presented in Table 10.7 along with the fitted curve, shown in Figure 10.2. Similar moderate inverse nonlinear relationship has also been found between *E50* and *StrainNf0.25M*, shown in Figure 10.3.

$$\ln(\text{StrainNf1M}) = 10.94 - 0.78 * \ln(E50) \tag{10.4}$$

Where:

StrainNf1M = strain value when fatigue life is one million cycles from 4PB tests (microstrain), and

E50 = initial stiffness from 4PB tests (ksi).

Table 10.7: Regression Model Summary for E50 and StrainNf1M from 4PB

Model	R ²	Adjusted R ²	F-statistic	p-value	df
Equation 10.4	0.670	0.66	89.01	3.89e-12	1/44

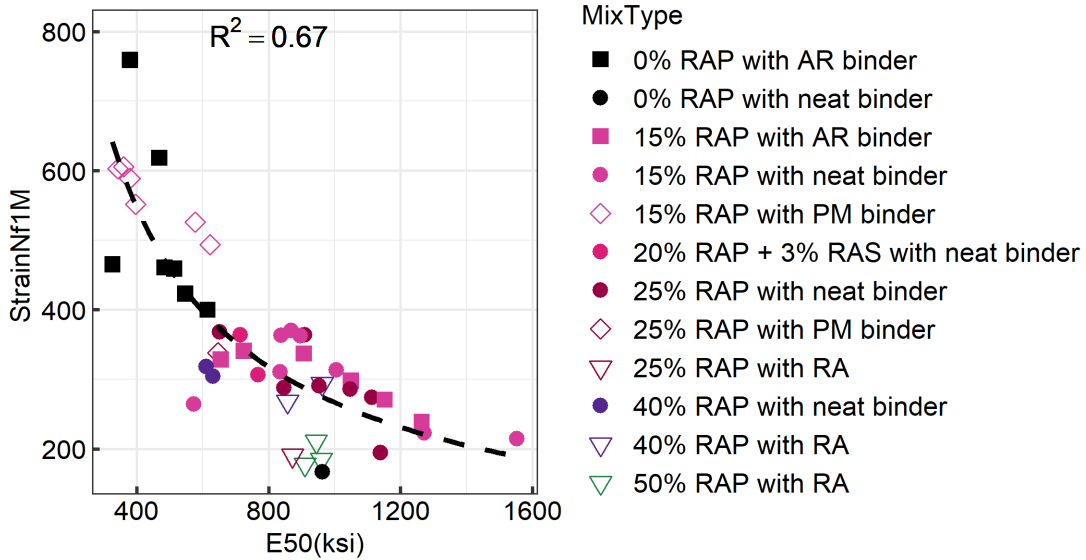


Figure 10.2: Fitted relationship between $E50$ and $StrainNf1M$ from 4PB test.

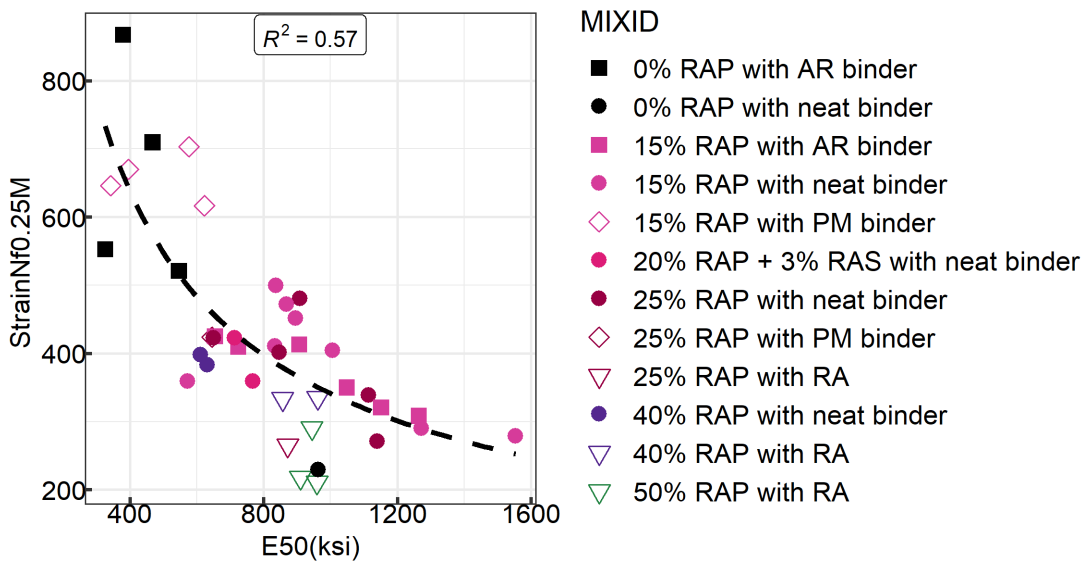


Figure 10.3: Fitted relationship between $E50$ and $StrainNf0.25M$ from 4PB test.

Therefore, the relationship between $Strength$ and $StrainNf1M$ can be constructed based on Equation 10.4, with $Strength$ as the response variable and $StrainNf1M$ as the independent variable, to determine the threshold of $Strength$ that would generally be expected to satisfy the fatigue life requirement based on this relationship, which is shown in Equation 10.5 with the regression model summary shown in Table 10.8. The fitted linear regression between $\ln(IDT_Strength)$ and $\ln(StrainNf1M)$, along with the 95% confidence interval band, is plotted in Figure 10.4. Due to the negative relationship between $StrainNf1M$ and $IDT_Strength$, the upper bound of the

confidence interval is selected as the threshold line for strength. The $IDT_Strength$ needs to be below the upper bound to help control the fatigue performance:

$$\ln(IDT_{Strength}) = 7.12 - 0.353 \times \ln(StrainNf1M) \quad (10.5)$$

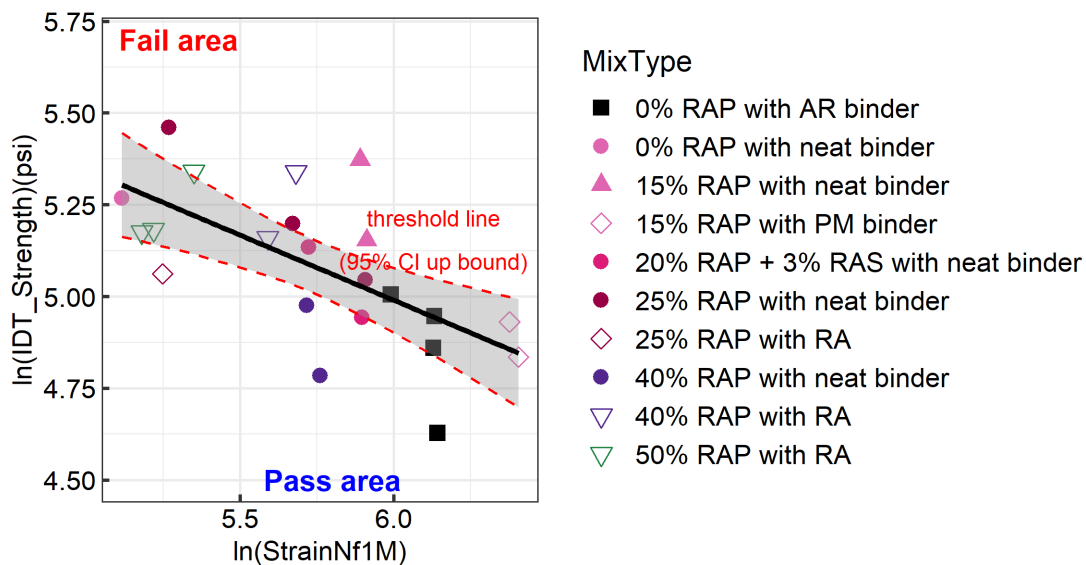
Where:

$IDT_Strength$ = strength from IDEAL-CT (psi), and

$StrainNf1M$ = strain value when fatigue life is one million cycles from 4PB tests (microstrain).

Table 10.8: Regression Model Summary for $IDT_Strength$ and $StrainNf1M$ from 4PB Test

Model	R ²	Adjusted R ²	F-statistic	p-value	df
Equation 10.4	0.42	0.39	14.64	0.001	1/20



Note: 95% confidence interval indicated by red dashed lines.

Figure 10.4: Relationship between $Strength$ from IDEAL-CT with $StrainNf1M$ from 4PB test.

A procedure for determining the criteria value for a specific material to implement the $Strength$ criteria in practice for QC/QA is presented in the flowchart in Figure 10.5. Different criteria for the stiffness and fatigue life of materials need to be satisfied depending on the asphalt material application in the pavement structure—for example, in a thin surface layer or in a thick bottom layer. The general procedure recommended in Figure 10.5 includes the minimum stiffness and the fatigue life (minimum strain value of one million cycles to failure).

Based on the relationship between stiffness and $Strength$ from the IDEAL-CT test, the criterion of $Strength_{min}$ will be determined to meet the minimum stiffness requirement obtained from the stiffness value at the same

temperature and loading rate used in the ME rehabilitation structural design. For maintenance projects where ME design is not used, a reasonable value for each mix type will need to be determined, which will be the lowest value for *Strength*.

The minimum fatigue life requirement will be satisfied by meeting the criterion of $Strength_{max}$, which is the upper bound of *Strength* from the relationship between *Strength* and *StrainNfIM*. To help obtain good fatigue and reflective cracking performance of asphalt pavement, the *Strength* value of asphalt material from the IDEAL-CT test needs to fall in the range of $Strength_{min}$ to $Strength_{max}$.

Appendix A shows a detailed example for deciding the *Strength* range for projects with performance-related specifications (PRSs) along with the validation from the *CalME* simulations. Additionally, Appendix B shows an alternative approach based on mean stiffness for those projects without PRSs to determine the *Strength* criteria range.

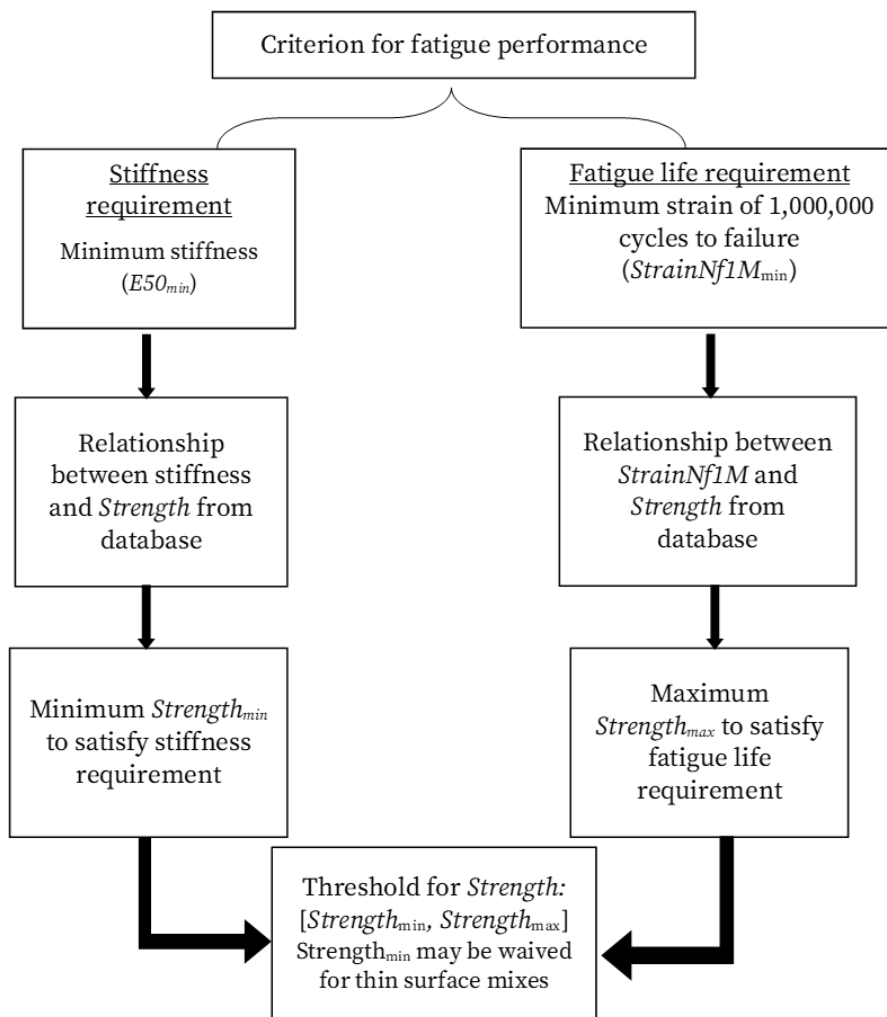


Figure 10.5 : Flowchart for determining criteria for fatigue cracking based on *Strength*.

11 CONCLUSIONS AND RECOMMENDATIONS

The objective of this research is to develop a surrogate performance-related test for cracking performance of asphalt materials. This study evaluated four potential testing methods and investigated the correlation between results of those tests and initial flexural stiffness and fatigue life from the benchmark four-point beam (4PB) test. Representative parameters have been identified for each test that consider variability and the relationship to stiffness and fatigue performance. The following are conclusions from this study:

- The four testing methods included in this study (three monotonic fracture tests: I-FIT [semicircular notched beam], LOU-SCB [semicircular notched beam], and IDEAL-CT [indirect tensile]; one repetitive fatigue test with increasing strain value: fine aggregate mixes [FAM] mixes with linear amplitude sweep [LAS] test) have simple sample preparation processes and testing operations as well as short testing times compared to the benchmark 4PB test.
- The three fracture testing methods (I-FIT, LOU-SCB and IDEAL-CT) showed good correlations with the initial flexural stiffness for the range of asphalt mixes included in the study (conventional, rubberized, polymer-modified, high RAP), while no strong correlation was found between these tests and flexural fatigue life. The results from the three tests are very well correlated linearly with each other for both the strength and fracture parameters. Considering that they produced very similar results, but the IDEAL-CT test is simpler and faster, the IDEAL-CT test is the recommended test among the three.
- The *Strength* parameter obtained from both the I-FIT and IDEAL-CT tests has low variability compared with the respective fracture parameters (*cTindex* from the IDEAL-CT test and *FI* from the I-FIT test) and shows a good positive linear correlation with the initial stiffness from the 4PB test. *Strength* from the IDEAL-CT test also has a moderate negative correlation with the fatigue life (*StrainNfIM*) from the 4PB test. In addition, the initial flexural stiffness from the 4PB fatigue test was found to be nonlinearly well correlated with the fatigue life. Thus, it is proposed that *Strength* be a representative indicator for predicting the initial stiffness of asphalt mixtures. The moderate relationship between *Strength* from the IDEAL-CT test and 4PB fatigue life, and the good inverse nonlinear correlation between 4PB stiffness and 4PB fatigue life—combined with the experience from ME design principles and calculations that mixes with lower stiffness generally perform better than stiffer mixes in thin overlays and thin asphalt layers in new pavements and that mixes with higher stiffness generally perform better than softer mixes in thicker overlays and pavements—leads to a conclusion that mix stiffness as measured through *Strength* from the IDEAL-CT test can be used to indicate the fatigue life based on the stiffness.
- A strong correlation exists between the strain at failure from LAS fatigue testing of FAM mixes and the strain value for fatigue life of one million cycles from 4PB fatigue testing of full mixtures, indicating that FAM mixes LAS testing may serve as a good candidate fatigue test for mix design and QC/QA. However,

due to the limited data set in this study, more experiments on various asphalt materials should be conducted. The FAM mixes LAS test is more expensive, time consuming, and complex than the IDEAL-CT test, but it is less expensive, faster, and simpler than conventional full mix flexural beam testing.

- A procedure for determining the criteria value for a specific material to implement the *Strength* criteria in practice for QC/QA was developed based on the relationships found in this study between flexural stiffness and flexural fatigue, and flexural stiffness and *Strength* from the I-FIT and IDEAL-CT tests:
 - Different criteria for the stiffness and fatigue life of materials need to be satisfied depending on the asphalt material application in the pavement structure—for example, in a thin surface layer or in a thick surface layer, intermediate layer, or bottom layer.
 - The general procedure developed in this study considers both the minimum stiffness to provide resistance to bending and a maximum stiffness to provide adequate fatigue life at a given strain (minimum strain value of one million cycles to failure).
 - The criterion of $Strength_{min}$ will be determined to meet the minimum stiffness requirement obtained from the stiffness value at the same temperature and loading rate used in the ME rehabilitation structural design. For maintenance projects where ME design is not used, a reasonable value for each mix type will need to be determined, which will be the lowest value for *Strength*. Thin overlays on existing asphalt or concrete pavement, and thin layers of new asphalt placed on granular or recycled bases, may not require a minimum stiffness (from $Strength_{min}$), while layers in thicker sections will (generally asphalt layers thicker than about 0.2 to 0.3 ft.).
 - The minimum fatigue life requirement will be satisfied by meeting the criterion of $Strength_{max}$, which is the upper bound of *Strength* from the moderately correlated relationship between *Strength* and *StrainNfIM*. To help obtain good fatigue and reflective cracking performance of asphalt pavement, the *Strength* value of asphalt material from the IDEAL-CT test needs to fall in the range of $Strength_{min}$ to $Strength_{max}$.

The following recommendations are made based on the conclusions of this study:

- Further development of the IDEAL-CT *Strength* parameter is recommended for potential use in routine mix design and QC/QA, where use of a performance-related test is warranted by the value of the project and the cost of testing. The main developments needed are a material aging procedure for preparation of test methods and identification of minimum and maximum values for different applications.
- Further development and potential use in piloting for evaluation for implementation of the procedure developed in this study for determining the criteria value for $Strength_{min}$ and $Strength_{max}$ for different applications (asphalt layer thickness, reflective or fatigue cracking, heavy traffic level) are recommended.

- In parallel with development and piloting, it is recommended that a search be done for mix test records from the AASHTO T 283 testing (similar to IDEAL-CT *Strength*) done over the past 10 years by Caltrans and compared with field cracking performance data in the Caltrans Pavement Management System database. The Automated Pavement Condition Survey (APCS) will not distinguish between top-down age-related and bottom-up reflective cracking from previous age-related cracking, which will mostly be transverse, longitudinal and block cracking. Identification of bottom-up reflective cracking of previous fatigue cracking will be easier to identify because it can only be bottom-up. Consideration will need to be given to new asphalt layer thickness, underlying pavement cracking and thickness, climate, and traffic in analysis of the data, if a sufficient number of mix test results are available.
- Further development of the FAM mixes LAS test for potential application in the practice of routine asphalt mix design or QC/QA is recommended. This work has not been advanced for the past four years at the UCPRC due to other priorities.

REFERENCES

1. California Asphalt Pavement Association. 2020. *Backgrounder: The Asphalt Industry in California*. West Sacramento, CA: California Asphalt Pavement Association.
2. California Department of Transportation, Division of Maintenance, Office of Pavement Management and the Office of Pavement Programming. 2020. *2019 State of the Pavement (SOP) Report*. Sacramento, CA: California Department of Transportation. dot.ca.gov/-/media/dot-media/programs/maintenance/documents/office-of-pavement-management/sop/2019_sop_report-v2_20200928_adacompliant.pdf.
3. Schapery, R. A. 1984. "Correspondence Principles and a Generalized J Integral for Large Deformation and Fracture Analysis of Viscoelastic Media." *International Journal of Fracture* 25: 195–223.
4. Kim, Y. R., and Little, D. N. 1990. "One-Dimensional Constitutive Modeling of Asphalt Concrete." *Journal of Engineering Mechanics* 116, no. 4: 751–772.
5. Di Benedetto, H., Roche, C. L., Baaj, H., Pronk, A., and Lundström, R. 2003. "Fatigue of Bituminous Mixtures : Different Approaches and Rilem Group Contribution." In *6th International RILEM Symposium on Performance Testing and Evaluation of Bituminous Materials*. Zurich, Switzerland April 14-16, 2003.
6. Fujie, Z., Newcomb, D., Gurganus, C., Banihashemrad, S., Park, E. S., Sakhaeifar, M., and Lytton, R. L. 2016. *Experimental Design for Field Validation of Laboratory Tests to Assess Cracking Resistance of Asphalt Mixtures* (NCHRP Report 9-57). Washington, DC: National Cooperative Highway Research Program.
7. Kallas, B.F., and Puzinauskas, V.P. 1972. "Flexure Fatigue Tests on Asphalt Paving Mixtures." In *Fatigue of Compacted Bituminous Aggregate Mixtures*, 47–65. West Conshohocken, PA: ASTM International.
8. Porter, B.W, and Kennedy, T.W. 1975. *Comparison of Fatigue Test Methods for Asphalt Materials* (Research Report 183-4). Austin, Texas: Center for Highway Research, University of Texas at Austin.
9. Deacon, J.A., and Monismith, C.L. 1967. "Laboratory Flexural-Fatigue Testing of Asphalt-Concrete With Emphasis on Compound-Loading Tests." *Highway Research Record* 158: 1–31.
10. Mandapaka, V., Basheer, I., Sahasi, K., Vacura, P., Tsai, B.W., Monismith, C.L., Harvey, J., and Ullidtz, P. 2012. "Application of Four-Point Bending Beam Fatigue Test for the Design and Construction of a Long-Life Asphalt Concrete Rehabilitation Project in Northern California." In *Proceedings of the 3rd Conference on Four-Point Bending*. Davis, California, September 17-18, 2012.
11. Harvey, J., Wu, R.Z., Signore, J., Basheer, I., Holikattie, S., Vacura, P., and Holland, T.J. 2014. "Performance-Based Specifications California Experience to Date." In *Application of Asphalt Mix Performance-Based Specifications* (Transportation Research Circular E-C189). Washington, DC: Transportation Research Board.
12. Bennert, T., Sheehy, E., Blight, R., Gresavage, S., and Fee, F. 2014. "Implementation of Performance-Based

- Specifications for Asphalt Mix Design and Production Quality Control for New Jersey.” In *Application of Asphalt Mix Performance-Based Specifications* (Transportation Research Circular E-C189). Washington, DC: Transportation Research Board.
13. Schütz, W. 1996. “A History of Fatigue.” *Engineering Fracture Mechanics* 54: 263–300.
 14. Deacon, J.A., Tayebali, A.A., Coplantz, J.S., Finn, F.N., and Monismith, C.L. 1994. *Fatigue Response of Asphalt-Aggregate Mixes, Part III—Mix Design and Analysis* (SHRP-A 404). Washington, DC: Strategic Highway Research Program.
 15. Harvey, J., Liu, A., Zhou, J., Signore, J.M., Coleri, E., and He, Y. 2015. *Superpave Implementation Phase II: Comparison of Performance-Related Test Results* (UCPRC-RR-2015-01). Davis, CA: University of California Pavement Research Center. 106cholarshipp.org/uc/item/7vg1c54z.
 16. Fine, M.E., and Chung, Y.W. 1996. “Fatigue Failure in Metals.” *Fatigue and Fracture* 19: 63–72.
 17. Abdulshafi, A.A., and Majidzadeh, K. 1985. “J-Integral and Cyclic Plasticity Approach to Fatigue and Fracture of Asphaltic Mixtures.” *Transportation Research Record* 1034: 112–123.
 18. Shook, J.F., Finn, F.N., Witczak, M.W., and Monismith, C.L. 1982. “Thickness Design of Asphalt Pavements—The Asphalt Institute Method.” In *Proceedings of the 5th International Conference on the Structural Design of Asphalt Pavements*. Delft, the Netherlands, August 23-26, 1982.
 19. Tayebali, A.A., Rowe, G.M., and Sousa, J.B. 1992. “Fatigue Response of Asphalt-Aggregate Mixtures.” *Journal of Association of Asphalt Paving Technologists* 61: 333–360.
 20. Pronk, A.C., Gajewski, M., and Bańkowski, W. 2018. “Application of a Material Fatigue Damage Model in 4PB Tests.” *International Journal of Pavement Engineering* 19, no. 9: 805–814.
 21. Jones, D., Harvey, J., and Bressette, T. 2008. “An Overview of an Accelerated Pavement Testing Experiment to Assess the Use of Modified Binders to Limit Reflective Cracking in Thin Asphalt Concrete Overlays.” In *Proceedings of the 6th RILEM International Conference on Cracking in Pavements*. Chicago, IL, June 16-18, 2008.
 22. Wu, R. 2005. “Finite Element Analyses of Reflective Cracking in Asphalt Concrete Overlays.” PhD diss., University of California, Berkeley. proquest.com/dissertations-theses/finite-element-analyses-reflective-cracking/docview/305032563/se-2?accountid=14505.
 23. Kutay, M.E., and Lanotte, M. 2018. “Viscoelastic Continuum Damage (VECD) Models for Cracking Problems in Asphalt Mixtures.” *International Journal of Pavement Engineering* 19, no. 3: 231–242.
 24. Karki, P., Bhasin, A., and Underwood, B.S. 2016. “Fatigue Performance Prediction of Asphalt Composites Subjected to Cyclic Loading with Intermittent Rest Periods.” *Transportation Research Record: Journal of the Transportation Research Board* 2576: 72–82.
 25. Rowe, G.M., and Brown, S.F. 1997. “Fatigue Life Prediction Using Visco-Elastic Analysis.” In *Proceedings of the International Society of Asphalt Pavements*. Seattle, WA, August 10-14, 1997.

26. Lennon, A.B. 2008. "Fracture Toughness and Fatigue Characteristics of Bone Cements." In *Orthopaedic Bond Cements* 265–295. Sawston, UK: Woodhead Publishing Limited.
27. Saha, G., and Biligiri, K.P. 2016. "Fracture Properties of Asphalt Mixtures Using Semi-Circular Bending Test: A State-of-the-Art Review and Future Research." *Construction and Building Materials* 105: 103–12.
28. Mobasher, B., Mamlouk, M., and Lin, H.M. 1997. "Evaluation Of Crack Propagation Properties Of Asphalt Mixtures." *Journal of Transportation Engineering* 23: 405–13.
29. Rice, J.R. 1968. "A Path Independent Integral and the Approximate Analysis of Strain Concentration by Notches and Cracks." *Journal of Applied Mechanics* 35, no. 2: 379–386.
30. Schapery, R.A. 1973. *A Theory of Crack Growth in Viscoelastic Media* (Report MM 2764-73-1). , College Station, TX: Mechanics and Materials Research Center, Texas A&M University.
31. Majidzadeh, K., Buranarom, C., and Karakouzian, M. 1976. *Application of Fracture Mechanics for Improved Design of Bituminous Concrete* (FHWA-RD-76-9). Washington, DC: Federal Highway Administration.
32. Newman, J.C. 1998. "The Merging of Fatigue and Fracture Mechanics Concepts: A Historic Perspective." *Progress in Aerospace Sciences* 34: 347–390.
33. Kuai, H., Lee, H.J. Zi, G., and Mun, S. 2009. "Application of Generalized J -Integral to Crack Propagation Modeling of Asphalt Concrete Under Repeated Loading." *Transportation Research Record* 2127, no. 1: 72–81.
34. Ullidtz, P., Harvey, J. Tsai, B.W., and Monismith, C. 2008. "Calibration of Mechanistic Empirical Models for Flexible Pavements Using the WesTrack Experiment." *Journal of the Association of Asphalt Paving Technologists* 77: 591–630.
35. Harvey, J., Jones, D., Lea, J.D., Wu, R., Ullidtz, P., and Tsai, B. 2012. "Use of Mechanistic-Empirical Performance Simulations To Adjust and Compare Results From Accelerated Pavement Testing." In *Advances in Pavement Design Through Full-Scale Accelerated Pavement Testing*, edited by Jones, D., 461–470. Boca Raton, FL: CRC Press.
36. Wu, R., Tsai, B.W., Harvey, J., Ullidtz, P., Basheer, I., and Holland, J. 2009. "Using Four-Point Bending Tests in Calibration of the California Mechanistic-Empirical Pavement Design System." In *Four Point Bending: Proceedings of the Second Workshop*. Braga, Portugal, September 24-25, 2009.
37. Gibson, N., Qi, X., Shenoy, A., Al-Khateeb, G., Kutay, M.E., Andriescu, A., Stuart, K., Youthcheff, J. and Harman, T. 2012. *Performance Testing for Superpave and Structural Validation* (FHWA-HRT-11-045). Washington, DC: Federal Highway Administration.
38. Ozer, H., Al-Qadi, I.L., Lambros, J., El-Khatib, A., Singhvi, P., and Doll, B. 2016. "Development of the Fracture-Based Flexibility Index for Asphalt Concrete Cracking Potential Using Modified Semi-Circle Bending Test Parameters." *Construction and Building Materials* 115: 390–401.
39. Chong, K.P., and Kuruppu, M.D. 1984. "New Specimen for Fracture Toughness Determination for Rock and Other Materials." *International Journal of Fracture* 26: 59–62.

40. Mohammad, L.N., Kim, M., and Challa, H. 2016. *Development of Performance Based Specifications for Louisiana Asphalt Mixtures* (FHWA/LA.14/558). Baton Rouge, LA: Louisiana Transportation Research Center.
41. Kim, M., Mohammad, L., and Elseifi, M. 2012. “Characterization of Fracture Properties of Asphalt Mixtures as Measured by Semicircular Bend Test and Indirect Tension Test.” *Transportation Research Record* 2296, no. 1: 115–24.
42. Walubita, L.F., Faruk, A.N., Koochi, Y., Luo, R., and Scullion, T. 2012. *The Overlay Tester (OT): Comparison with Other Crack Test Methods and Recommendations for Surrogate Crack Tests*. (FHWA/TX-13/0-6607-2). College Station, TX: Texas A&M Transportation Institute.
43. Al-Qadi, I., Ozer, H., Lambros, J., Lippert, D., Khatib, A.E., Khan, T., Singh, P., and Rivera-Perez, J.J. 2015. *Testing Protocols to Ensure Performance of High Asphalt Binder Replacement Mixes Using RAP and RAS* (FHWA-ICT-15-017). Rantoul, IL: Illinois Center for Transportation.
44. Mull, M.A., Stuart, K., and Yehia, A. 2002. “Fracture Resistance Characterization of Chemically Modified Crumb Rubber Asphalt Pavement.” *Journal of Materials Science* 37: 557–66.
45. Li, X., Marasteanu, M.O., Williams, R.C., and Clyne, T.R. 2008. “Effect of Reclaimed Asphalt Pavement (Proportion and Type) and Binder Grade on Asphalt Mixtures.” *Transportation Research Record* 2051, no. 1: 90–97.
46. Martin, A.E., Zhou, F., Arambula, E., Park, E.S., Chowdhury, A., Kaseer, F., Yin, F., Munoz, J.C., Rose, A., Hajj, E., Daniel, J., and Glover, C. 2016. *The Effects Of Recycling Agents On Asphalt Mixtures with High RAS and RAP Binder: Phase II Draft Interim Report* (Project No. 9-58). Washington, DC: National Cooperative Highway Research Program.
47. Wu, S., Al-Qadi, I.L., Lippert, D.L., Ozer, H., Espinoza Luque, A.F., and Safi, F.R. 2017. “Early-Age Performance Characterization of Hot-Mix Asphalt Overlay with Varying Amounts of Asphalt Binder Replacement.” *Construction and Building Materials* 153: 294–306.
48. Hakimelahi, H., Saadeh, S., and Harvey, J. 2013. “Investigation of Fracture Properties of California Asphalt Mixtures Using Semicircular Bend and Beam Fatigue Tests.” *Road Materials and Pavement Design* 14: 252–265.
49. Aragão, F.T.S. 2011. “Computational Microstructure Modeling of Asphalt Mixtures Subjected to Rate-Dependent Fracture.” PhD diss., University of Nebraska, Lincoln. digitalcommons.unl.edu/cgi/viewcontent.cgi?article=1020&context=civilengdiss.
50. Kim, Y.R., and Wen, H. 2002. “Fracture Energy from Indirect Tension Testing.” *Asphalt Paving Technology* 71: 779–93.
51. Zhou, F. 2019. *Development of an IDEAL Cracking Test for Asphalt Mix Design, Quality Control and Quality Assurance* (IDEA Project 195). Washington, DC: Transportation Research Board.

52. Aragão, F., Kim, Y., Lee, J., and Allen, D. 2011. "Micromechanical Model for Heterogeneous Asphalt Concrete Mixtures Subjected to Fracture Failure." *Journal of Materials in Civil Engineering* 23: 30–38.
53. Gudipudi, P., and Underwood, B.S. 2015. "Testing and Modeling of Fine Aggregate Matrix and Its Relationship to Asphalt Concrete Mix." *Transportation Research Record* 2507, no. 1: 120–127.
54. Im, S., You, T., Ban, H., and Kim, Y.R. 2017. "Multiscale Testing-Analysis of Asphaltic Materials Considering Viscoelastic and Viscoplastic Deformation." *International Journal of Pavement Engineering* 18: 783–797.
55. Sánchez, D.B., Grenfell, J., Airey, G, and Caro, S. 2017. "Evaluation of the Degradation of Fine Asphalt-Aggregate Mixtures Containing High Reclaimed Asphalt Pavement Contents." *Road Materials and Pavement Design* 18: 91–107.
56. He, Y., Alavi, M.Z., Jones, D., and Harvey, J. 2016. "Proposing a Solvent-Free Approach to Evaluate the Properties of Blended Binders in Asphalt Mixes Containing High Quantities of Reclaimed Asphalt Pavement and Recycled Asphalt Shingles." *Construction and Building Materials* 114: 172–80.
57. Mannan, U.A., Islam, M.R., and Tarefder, R.A. 2015. "Effects of Recycled Asphalt Pavements on the Fatigue Life of Asphalt Under Different Strain Values and Loading Frequencies." *International Journal of Fatigue* 78: 72–80.
58. Glover, C.J., Davison, R.R., Domke, C.H., Ruan, Y., Juristyarini, P., Knorr, D.B., and Jung, S.H. 2005. *Development of a New Method for Assessing Asphalt Binder Durability with Field Evaluation* (FHWA/TX-05/1872-2). College Station, TX: Texas Transportation Institute.
59. Anderson, R.M., King, G.N., Hanson, D.I., and Blankenship, P.B. 2011. "Evaluation of the Relationship Between Asphalt Binder Properties and Non-Load Related Cracking." *Journal of the Association of Asphalt Paving Technologists* 80: 615–664.
60. Rowe, G. 2011. "Prepared Discussion on Evaluation of the Relationship Between Asphalt Binder Properties and Non-Load Related Cracking." *Journal of the Association of Asphalt Paving Technologists* 80: 649–662.
61. Rowe, G.M. 2014. "Interrelationships in Rheology for Asphalt Binder Specifications." In *Proceedings of the Fifty-Ninth Annual Conference of the Canadian Technical Asphalt Association (CTAA)*. Winnipeg, Manitoba, Canada, November 2014.
62. Asphalt Institute Technical Advisory Committee. 2019. *State-of-the-Knowledge: Use of the Delta Tc Parameter to Characterize Asphalt Binder Behavior*. Lexington, KY: Asphalt Institute.
63. Tayebali, A.A., Deacon, J.A., Coplantz, J.S., Finn, F.N., Harvey, J.T., and Monismith, C.L. 1994. *Fatigue Response of Asphalt-Aggregate Mixes* (Report SHRP-A-404). Washington, DC: National Research Council.
64. Ullidtz, P., Harvey, J., Tsai, B.W., and Monismith, C. 2005. *Calibration of Incremental-Recursive Flexible Damage Models in CalME Using HVS Experiments* (Research Report: UCPRC-RR-2005-06). Davis and Berkeley, CA: University of California Pavement Research Center. 109cholarshipp.org/uc/item/59m8m9m1.

65. Ullidtz, P., Harvey, J., Tsai, B.W., and Monismith, C. 2006. *Calibration of CalME Models Using WesTrack Performance Data* (Research Report: UCPRC-RR-2006-14). Davis and Berkeley, CA: University of California Pavement Research Center. escholarship.org/uc/item/49r9d32g.
66. Al-Qadi, I.L., Lippert, D.L., Wu, S., Ozer, H., Renshaw, G., Murphy, T.R., Butt, A., Gundapuneni, S., Trepanier, J.S., Vespa, J.W., and Said, I.M. 2017. *Utilizing Lab Tests to Predict Asphalt Concrete Overlay Performance* (FHWA-ICT-17-020). Rantoul, IL: Illinois Center for Transportation.
67. Ozer, H., Al-Qadi, I.L., Singhvi, P., Bausano, J., Carvalho, R., Li, X., and Gibson, N. 2018. "Prediction of Pavement Fatigue Cracking at an Accelerated Testing Section Using Asphalt Mixture Performance Tests." *International Journal of Pavement Engineering* 19: 264–278.
68. Hashin, Z. 1983. "Analysis of Composite Materials—A Survey." *Journal of Applied Mechanics* 50: 481–505.
69. Weissman, S.L., Harvey, J., Sackman, J.L., and Long, F. 1999. "Selection of Laboratory Test Specimen Dimension for Permanent Deformation of Asphalt Concrete Pavements." *Transportation Research Record* 1681, no. 1: 113–120.
70. Park, S.W., Kim, Y.R., and Schapery, R.A. 1996. "A Viscoelastic Continuum Damage Model and Its Application to Uniaxial Behavior of Asphalt Concrete." *Mechanics of Materials* 24, no. 4: 241–255.
71. Lee, H.J., Daniel, J.S., and Kim, Y.R. 2000. "Continuum Damage Mechanics-Based Fatigue Model of Asphalt Concrete." *Journal of Materials in Civil Engineering* 12, no. 2: 105–112.
72. Underwood, B.S., Baek, C., and Kim, Y.R. 2012. "Simplified Viscoelastic Continuum Damage Model As Platform For Asphalt Concrete Fatigue Analysis." *Transportation Research Record* 2296, no. 1: 36–45.
73. Hintz, C., Velasquez, R., Johnson, C., and Bahia, H. 2011. "Modification and Validation of Linear Amplitude Sweep Test for Binder Fatigue Specification." *Transportation Research Record* 2207, no. 1: 99–106.
74. Rowe, G.M., and Bouldin, M.G. 2000. "Improved Techniques to Evaluate the Fatigue Resistance of Asphaltic Mixes." In *Proceedings of the Congress: 2nd Euraspalt & Eurobitume Congress*. Barcelona, Spain, September 20-22, 2000.
75. Morrison, G.R., Stel, R.V.D., and Hesp, S.A.M. 1995. "Modification of Asphalt Binders and Asphalt Concrete Mixes with Crumb and Chemically Devulcanized Waste Rubber." *Transportation Research Record* 14: 56–63.
76. Hung, S.S., Alavi, M.Z., Jones, D., and Harvey, J.T. 2017. "Influence of Reclaimed Asphalt Pavement on Performance-Related Properties of Gap-Graded Rubberized Hot-Mix Asphalt." *Transportation Research Record* 2633, no. 1: 80–89.
77. He, Y., Alavi, Z., Harvey, J., and Jones, D. 2016. "Evaluating Diffusion And Aging Mechanisms In Blending Of New And Age-Hardened Binders During Mixing And Paving." *Transportation Research Record* 2574, no. 1: 64–73.
78. Hung, S.S. 2018. "Performance Assessment of Asphalt Mixes Containing Reclaimed Asphalt Pavement and

- Tire Rubber.” PhD diss., Univeristy of California, Berkeley. escholarship.org/uc/item/0q97f04p.
79. Mindess, S., Lawrence, F.V., and Kesler, C.E. 1977. The J-Integral as a Fracture Criterion for Fiber Reinforced Concrete. *Cement and Concrete Research* 7, no. 6: 731–42.
80. Elkashef, M., Harvey, J., Jiao, L., and Jones, D. Forthcoming. *Impact of Silo Silo Storage on the Performance of Plant-Produced Mixes Containing High Content of Reclaimed Asphalt Pavement and Reclaimed Asphalt Shingles* (Research Report: UCPRC-RR-2022-04). Davis and Berkeley, CA: University of California Pavement Research Center.

APPENDIX A EXAMPLE FOR DETERMINING STRENGTH CRITERIA FOR USE WITH A PERFORMANCE-RELATED SPECIFICATION BASED ON FLEXURAL BEAM TESTING

A.1 Strength Criteria Range for PRS Projects

This example is based on an AC long life (HMA-LL) project. The requirement for the HMA-LL performance during mix design includes the permanent deformation, flexural stiffness, flexural fatigue, fracture potential from the I-FIT test, and Hamburg wheel-tracking test, and the suggested value for each requirement is listed in Table A.1. The requirements for the beam stiffness and beam fatigue are for the 4PB tests at the testing temperature of 68°F (20°C). The following discussion focuses on the determination of strength criteria based on the correlation analysis results between the IDEAL-CT and 4PB tests, making use of the data set of mix test results that has been developed relating flexural stiffness to IDEAL-CT *Strength*, which have a strong correlation, and the weaker relationship between *Strength* and strain at one million repetitions from the flexural fatigue test.

Table A.1: HMA-LL Performance Requirements

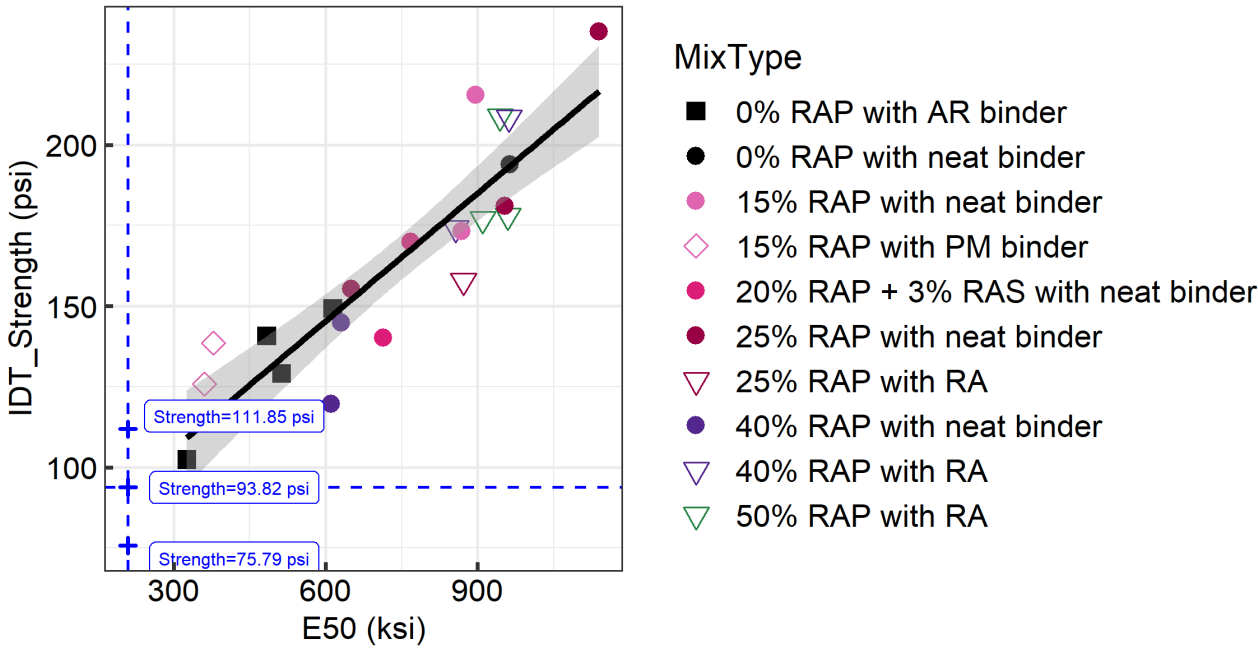
Design Parameter	Test Method	Sample Air Voids	Requirement	Requirement	Requirement
			HMA-LL, Surface	HMA-LL, Intermediate	HMA-LL, Rich Bottom
Permanent deformation ^{a,b} : Minimum number of cycles to 3% permanent axial strain	AASHTO T378 Modified	Mix specific ^c	941	3007	Not required
Beam stiffness (psi) ^b : Minimum stiffness at the 50th cycle at the given testing strain value	AASHTO T321 Modified	Mix specific	210,000 at 893×10 ⁻⁶ in./in.	782,000 at 433×10 ⁻⁶ in./in.	707,000 at 420×10 ⁻⁶ in./in.
Beam fatigue ^b : Minimum of 1,000,000 cycles to failure at this strain Minimum of 250,000 cycles to failure at this strain	AASHTO T321 Modified	Mix specific	495×10 ⁻⁶ in./in. 893×10 ⁻⁶ in./in.	220×10 ⁻⁶ in./in. 443×10 ⁻⁶ in./in.	269×10 ⁻⁶ in./in. 420×10 ⁻⁶ in./in.
Semicircular bend fracture potential ^b : Minimum flexibility index	AASHTO TP 124	Mix specific	3	0.5	0.5
Moisture sensitivity: Minimum repetitions	AASHTO T 324 Modified	Per test method	20,000	20,000	Not required

^a Tested at a temperature of 122°F (50°C), unconfined, 4.4 psi contact stress, and 70 psi repeated axial stress.

^b Average value determined from tests on 3 specimens and calculated as the geometric (not arithmetic) mean.

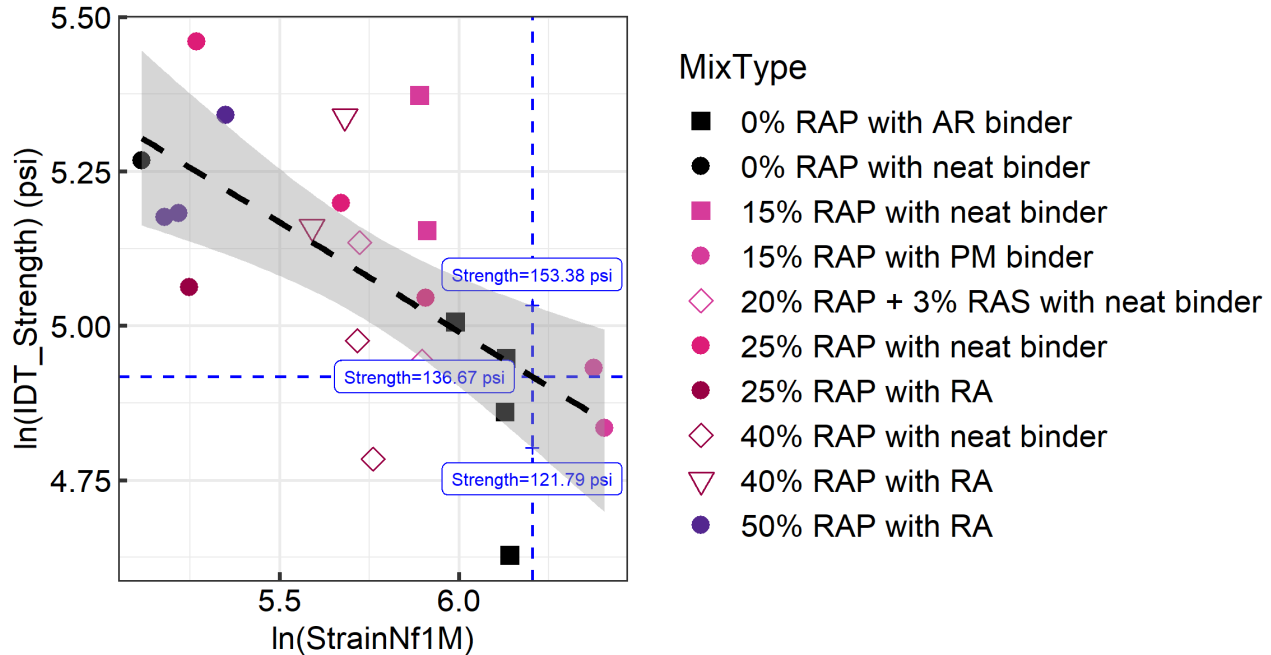
^c 6±0.5% for HMA-LL, Surface and HMA-LL, Intermediate mixes, and 3±0.5% for HMA-LL, Rich Bottom mix all following AASHTO T331.

According to the recommended beam stiffness and beam fatigue in Table A.1, the minimum initial stiffness for the HMA-LL, Surface would be 210,000 psi, and the minimum required $StrainNfIM$ should be 495 microstrain. First, to meet the stiffness requirement based on the threshold line, which is the lower bound of the 95% confidence interval of the regression curve between $E50$ and $Strength$ from the IDEAL-CT test, $Strength_{min}$ was calculated to be 75.79 psi, shown in Figure A.1. Second, for the fatigue life performance, the required minimum $StrainNfIM$ is 495 microstrain ($\ln(StrainNfIM) = 6.2$), from the threshold line (upper bound of 95% confidence interval of the regression curve between $StrainNfIM$ and $Strength$). $Strength_{max}$ was determined to be 153.38 psi, illustrated in Figure A.2. In conclusion, to ensure both the stiffness requirement and fatigue life requirement, the value of strength of the asphalt materials from IDEAL-CT test at the testing temperature of 77°F (25°C) should fall in the range of 76 psi to 153 psi based on the 95% confidence interval. The range will be [94 psi, 137 psi] if the predicted values on the regression lines are used. Based on Figure A.1 and Figure A.2, the asphalt mixtures that fall in the $Strength$ criteria range are listed in Table A.2.



Note: The 95% confidence interval range for strength value is [75.79 psi, 112 psi], the strength value on the regression line is 94 psi; IDT_Strength tested at 77°F [25°C], E50 tested at 68°F [20°C]).

Figure A.1: Determination of $Strength_{min}$ based on the stiffness requirement for surface layer.



Note: The 95% confidence interval range for strength value is [122 psi, 153 psi], the strength value on the regression line is 137 psi; IDT_Strength tested at 77°F (25°C), StrainNf1M tested at 68°F (20°C).

Figure A.2: Determination of $Strength_{max}$ based on the fatigue life requirement for surface layer.

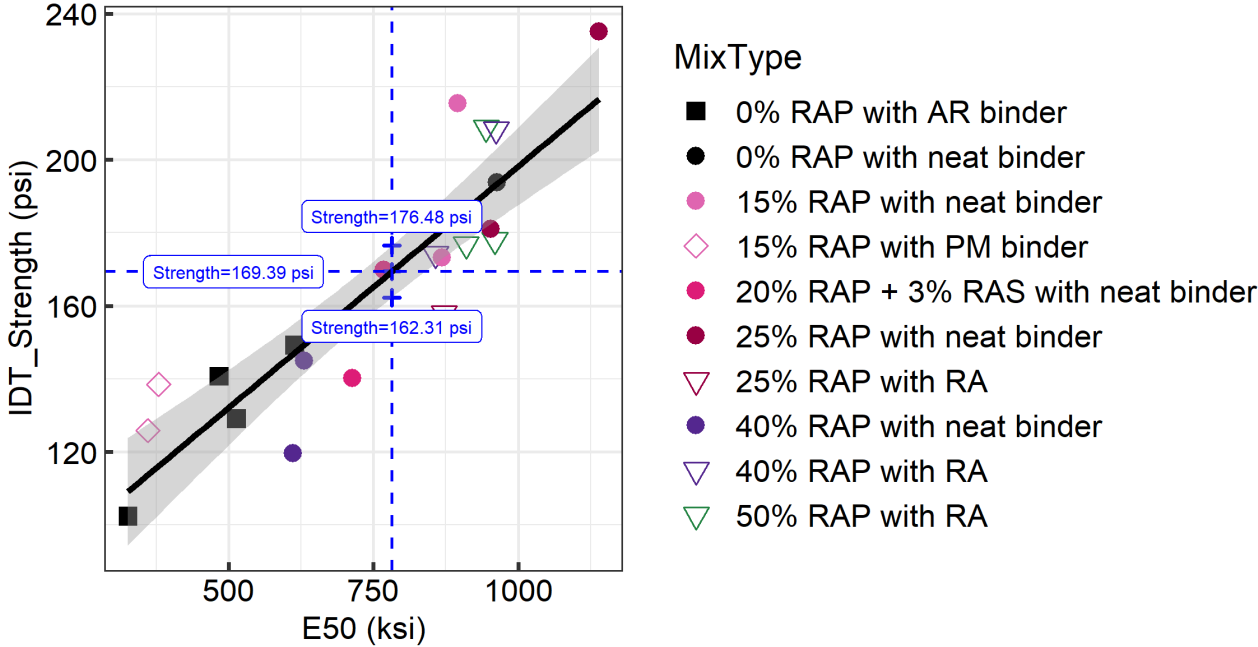
Table A.2: Asphalt Mixtures Passing Strength Criteria Range for HMA-LL Surface Layer

MIXID	Mix Type	Mix Category	Gradation Type	PG + Modifier	Preparation Method	IDT_Strength (psi)
Virgin_2	0% RAP with AR binder	RHMA-G	Gap	PG 64-16 + 20% CRM	FMLC	102.33
HRAP_0H_2	40% RAP with RA	HMA	Dense	PG 64-22	FMLC	119.58
Virgin_5*	0% RAP with AR binder	RHMA-G	Gap	PG 70-10 + CRM	FMLC	149.24
Virgin_6	0% RAP with AR binder	RHMA-G	Gap	PG 64-16 + CRM	FMLC	129.0
Virgin_7*	0% RAP with AR binder	RHMA-G	Gap	PG 64-16 + CRM	FMLC	140.7

Note: * are the mixtures that only meet the 95% CI criteria and not the criteria from regression line.

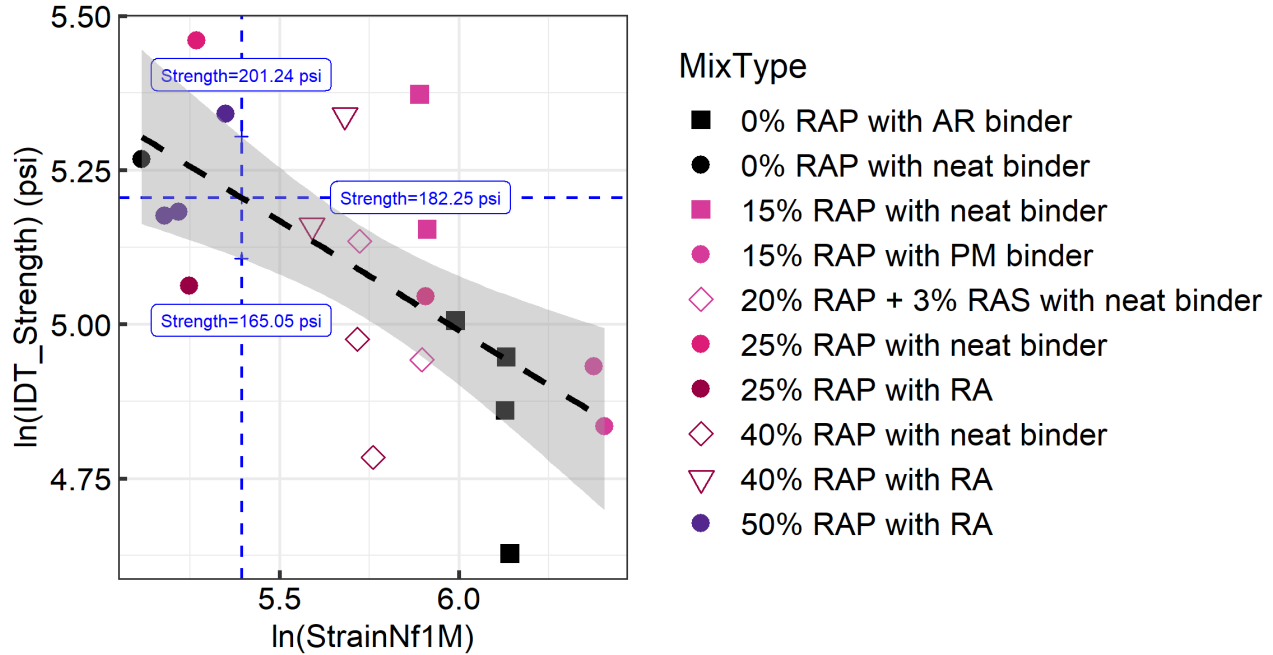
The same procedure can also be applied to the HMA-LL, intermediate layer. The minimum beam stiffness from the PRS requirement is 782,000 psi, and the minimum beam fatigue life is designed to be 220 microstrain ($\ln(\text{StrainNf1M}) = 5.4$) at 1,000,000 cycles. $Strength_{min}$ was calculated to be 162.31 psi based on the 95% confidence interval lower bound of the linear regression between $Strength$ and stiffness. $Strength_{max}$ was determined to be 201.24 psi from the 95% confidence interval upper bound of the linear regression between $Strength$ and $StranNf1M$ in log scale. $Strength_{min}$ and $Strength_{max}$ are displayed in Figure A.3 and Figure A.4

respectively. The asphalt mixtures with a *Strength* value that meets the criteria of *Strength_{min}* and *Strength_{max}* are listed in Table A.3.



Note: The 95% confidence interval range for strength value is [162 psi, 176 psi], the strength value on the regression line is 169 psi; IDT_Strength tested at 77°F (25°C), E50 tested at 68°F (20°C).

Figure A.3: Determination of *Strength_{min}* based on the fatigue stiffness requirement for intermediate layer.



Note: The 95% confidence interval range for strength value is [165.05 psi, 201.24 psi], the strength value on the regression line is 182.25 psi.

Figure A.4: Determination of $Strength_{max}$ based on the fatigue life requirement for intermediate layer.

Table A.3: Asphalt Mixtures Passing Strength Criteria Range for HMA-LL Intermediate Layer

MIXID	Mix Type	Mix Category	Gradation Type	PG + Modifier	Preparation Method	IDT_Strength (psi)
HRAP_5H_1	20% RAP + 3% RAS with neat binder	HMA	Dense	PG 58-22	FMLC	169.76
RAP15%_9	15% RAP with neat binder	HMA	Dense	PG 64-16	FMLC	173.1
RAP25%_6	25% RAP with neat binder	HMA	Dense	PG 64-16	FMLC	180.93

Note: These mixtures meet both the 95% CI criteria and the criteria from regression line.

A.2 Validation of Strength Criteria in CalME

Based on the previous example of the AC long life surface layer strength criteria, the pavement fatigue cracking performance of structures with the two materials that fall in the criteria range and two materials that fail the criteria range were simulated in *CalME*. The simulation was performed using the AC long life project on Interstate 5 in Sacramento County. The input information for pavement structure, traffic, and climate are shown in Table A.4.

Table A.4: Inputs for CalME Simulation with Changing Surface Materials

Structure	Material	Thickness (mm [ft.])	Traffic	Climate Zone
Layer 1	New AC material	61 (0.2)	Design life: 40 years* Growth rate: 5% Traffic index: 14.0 Total ESALs: 41 million	Inland Valley
Layer 2	HMA Type A 25% RAP PG 64-16 I-5 Sacramento AC long life intermedia layer	122 (0.4)		
Layer 3	HMA Type A 15% RAP PG 64-16 I-5 Sacramento AC long life rich bottom layer	61 (0.2)		
Layer 4	Aggregate base	610 (2)		
Layer 5	Subgrade clay soil	Infinite		

The fatigue cracking performance in *CalME* is simulated through the damage caused by tensile strain at the bottom of the asphalt layer. *CalME* implements an incremental-recursive approach to update damage on the material stiffness curve during the loading cycles. The fatigue life is defined when the fatigue cracking reaches 5% of the surface area. The simulation results for the surface layer are shown in Table A.5. Two asphalt mixtures (Virgin_5 and Virgin_6) were selected as representative mixtures that passed the *Strength* criteria. Virgin_5 satisfies the criteria determined from 95% CI (above the 95% CI lower bound representing pass for minimum stiffness requirement and below the 95% CI upper bound representing pass for minimum *StrainNfIM* requirement) while Virgin_6 meets the criteria determined directly from the regression line (above the regression line is pass for minimum stiffness requirement and below the regression line is pass for minimum *StranNfIM*). The criteria based on the 95% CI would allow a larger range of strength for selecting asphalt materials. Meanwhile, two asphalt mixtures (RAP25%_6 and HRAP_16H_3) were included for comparison as they fail the maximum *Strength* criterion. As all the asphalt mixtures in the current *CalME* database meet the minimum *Strength* criterion, no simulation was performed for mixtures failing the minimum strength requirement. The simulated fatigue cracking results for these four mixtures showed that Virgin_5 meeting the *Strength* criteria from 95% CI has the longest fatigue life while the rest of the materials which pass the minimum *Strength* criterion show slightly lower fatigue lives.

Table A.5: Fatigue Cracking Simulation in CalME for Surface Layer

Asphalt Mixture for Layer 1	Strength (psi)	Passing Strength Criteria (Yes/No)		Fatigue Life Nf (Year)
		Minimum	Maximum	
Virgin_5 (0% RAP with AR binder, PG 70-10 + CRM)	141	Yes	Yes	38.7
Virgin_6* (0% RAP with AR binder, PG 64-16 + CRM)	129	Yes	Yes	8.7
RAP25%_6 (25% RAP with neat binder, PG 64-16)	208	Yes	No	14.7
HRAP_16H_3 (40% RAP with neat binder, PG 64-10)	215	Yes	No	25.8

As for validating the strength criteria of the intermediate layer, the same *CalME* inputs—including structure thickness, traffic, and climate zone—were used. The material in layer 2 for this case was selected from those asphalt mixtures passing the strength criterion and compared with those that do not pass. Table A.5 provides the *CalME* simulation results for two materials that meet the *Strength* criteria for the intermediate layer (HRAP_5H_1 and RAP25%_6), two materials that fail the minimum *Strength* criterion (HRAP_0H_2 and RAP25%_7) and one material that fails the maximum *Strength* criterion (RAP15%_10). The fatigue lives of pavement with RAP25%_7 and HRAP_0H_2, which fail the minimum *Strength* criterion are slightly lower than the ones passing criteria. However, the fatigue life of RAP15%_10, which passes the minimum *Strength* but fails the maximum *Strength*, is close to the two mixtures passing the criteria. There were insufficient test results for rich bottom mixes to do a similar analysis for that layer.

Table A.6: Inputs for CalME Simulation with Changing Intermediate Materials

Structure	Material	Thickness (mm [ft.])	Traffic	Climate Zone
Layer 1	HMA Type A 15% RAP PG 64-28 PM I-5 Sacramento AC long life surface layer	61 (0.2)	Design life: 40 years Growth rate: 5% Traffic index: 16.0 Total ESALs: 126 million	Inland Valley
Layer 2	New AC material for Intermediate layer	122 (0.4)		
Layer 3	HMA Type A 15% RAP PG 64-16 I-5 Sacramento AC long life rich bottom layer	61 (0.2)		
Layer 4	Aggregate base	610 (2)		
Layer 5	Subgrade clay soil	Infinite		

Note: A 20 year design life was assumed for the simulation, while the actual Sacramento I-5 project had a 40 year design life.

Table A.7: Fatigue Cracking Simulation in CalME for Intermediate Layer

Asphalt Mixture for Layer 1	Strength (psi)	Passing Strength Criteria (Yes/No)		Fatigue Life Nf (Year)
		Minimum	Maximum	
HRAP_5H_1 (20% RAP + 3% RAS with neat binder, PG 58-22)	170	Yes	Yes	11.6
RAP25%_6 (25% RAP with neat binder, PG 64-16)	173	Yes	Yes	11
HRAP_0H_2 (40% RAP with neat binder, PG 58-22)	120	No	Yes	7.5
RAP25%_7 (25% RAP with neat binder, PG 64-16)	155	No	Yes	10.5
RAP15%_10 (15% RAP with neat binder, PG 64-16)	215	Yes	No	11.6

APPENDIX B EXAMPLE FOR DETERMINING STRENGTH CRITERIA FOR PROJECTS WITH NO PERFORMANCE-RELATED SPECIFICATION

For those asphalt pavement projects that do not have performance-related testing requirements developed from testing of mixes in a region specifically for the given project, an alternative approach is based on the mean value of HMA stiffnesses in the *CalME* standard materials library. The distribution of stiffnesses of HMA at 10 Hz and 68°F (20°C) from the flexural beam frequency sweep tests is shown in Figure B.1, with a mean value of 1,028 ksi. In California, base asphalt binders with different PGs are required based on the climate zones. Therefore, the detailed stiffnesses distribution of each PG base binder was plotted separately in Figure B.2, along with the mean value.

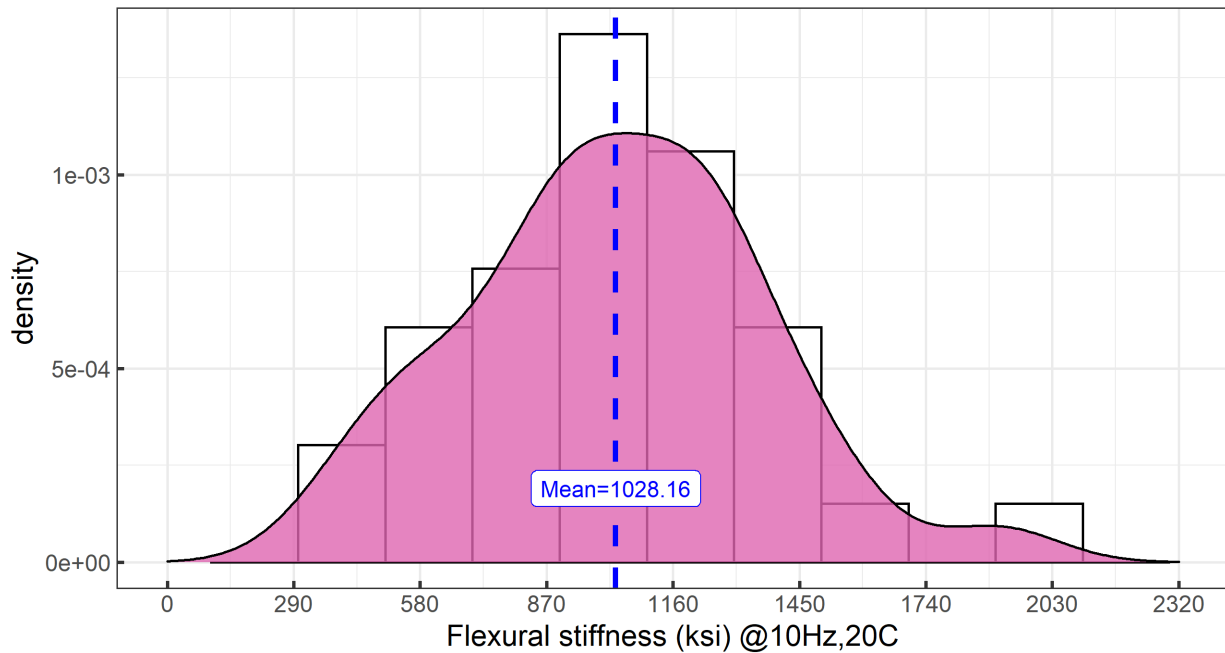
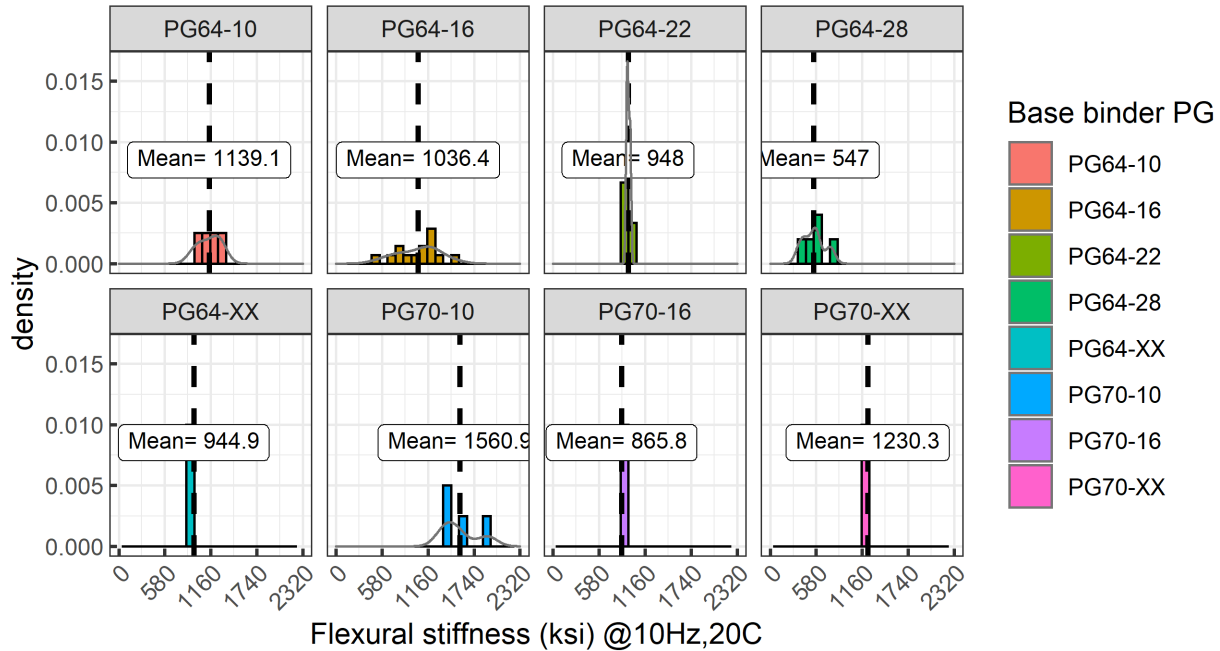


Figure B.1 Histogram of HMA stiffness from *CalME* material library.

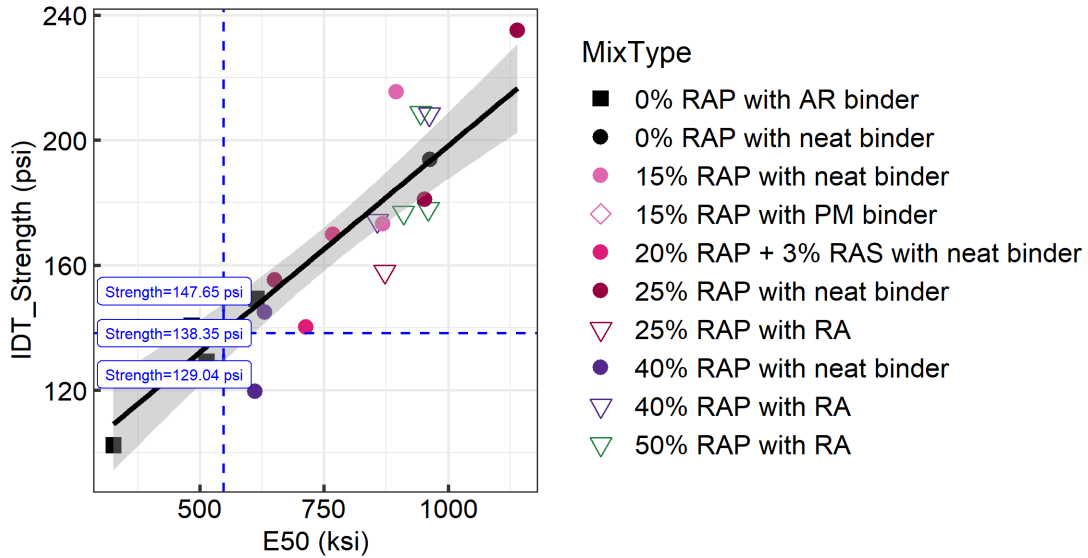


Note: PG 64-XX and PG 70-XX indicate mean results for all PG 64 and PG 70 mixes, respectively.

Figure B.2 Histograms of HMA stiffness (ksi) with different base binder PGs from CalME material library.

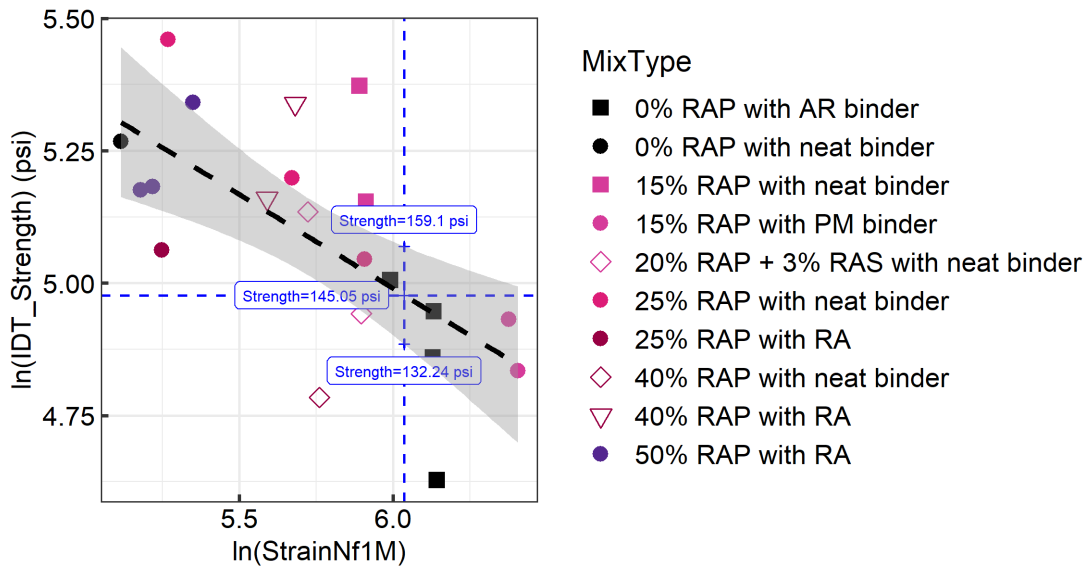
To ensure a reasonable range of strength criterion, the $Strength_{min}$ value needs to be lower than the $Strength_{max}$. According to the equations between initial flexural stiffness ($E50$) and $Strength$, $E50$ and $StrainNfIM$, and $StrainNfIM$ and $Strength$, $E50$ is the primary variable controlling both the minimum and maximum value of $Strength$ for the projects with no PRS. The correlations used were between flexural stiffness and fatigue life tests at 68°F (20°C) and IDEAL-CT tests at 77°F (25°C). If the selected $E50$ is too high or too low, there is a chance that the minimum strength calculated based on the positive relationship between $E50$ and $Strength$ would be larger than the maximum strength obtained from the negative relationship between strength and $StrainNfIM$.

After trial and error, it was found that when $E50$ is larger than 950 ksi, the $Strength_{min}$ will be larger than the $Strength_{max}$. Therefore, the base binder of PG 64-28 was selected as an example here to verify this alternative approach due to relatively lower mean flexural stiffness. The mean stiffness for materials with PG 64-28 binder is 547 ksi. The corresponding $StrainNfIM$ was then calculated as 418.6 microstrain. The maximum $Strength$ value could be obtained based on the upper bound of the 95% confidence interval for the linear relationship between $Strength$ from the IDEAL-CT test and $StrainNfIM$ from 4PB test, and the minimum $Strength$ was obtained from the lower bound of the 95% confidence interval for the linear relationship between $Strength$ from the IDEAL-CT test and initial stiffness from the 4PB test, shown previously in Figure 10.1 and Figure 10.4. As a result, the $Strength$ criteria range was determined to be $Strength_{min} = 129$ psi and $Strength_{max} = 159$ psi using Equation 10.1 and Equation 10.5, shown in Figure B.3 and Figure B.4.



Note: The 95% confidence interval range for strength value is [129 psi, 148 psi], and the strength value on the regression line is 138 psi.

Figure B.3 Determination of $Strength_{min}$.



Note: The 95% confidence interval range for strength value is [132 psi, 159 psi], and the strength value on the regression line is 145 psi.

Figure B.4 Determination of $Strength_{max}$.

The detailed simulation input information is given in Table B.1. Because the binder PG 64-28 is required for the High Mountain (or High Desert) climate region, this region was selected for the simulation of a new AC pavement. The fatigue life obtained from the *CalME* fatigue cracking simulation results is listed in Table B.2. The asphalt mixtures that meet the *Strength* criteria based on the mean stiffness value had highest fatigue lives. The

HRAP_16H_3 mix exceeded the upper limit of the *Strength* criteria range, and it offered a slightly lower fatigue life, while the HRAP_0H_2 and Virgin_6 mixes failed the *Strength_{min}* requirement and lasted less than one year in the *CalME* simulation before fatigue failure.

Table B.1: Inputs for CalME Simulation of New AC Pavement

Structure	Material	Thickness [mm (ft.)]	Traffic	Climate Zone
Layer 1	New AC material	244 (0.8)	Design life: 20 years Growth rate: 5.2% Traffic index: 16.0 Total ESALs: 126 million	High Mountain
Layer 2	Aggregate base	305 (1)		
Layer 3	Subgrade clay soil	Infinite		

Table B.2: Fatigue Cracking Simulation Results from CalME of New AC Pavement

Asphalt Mixture for Layer 1	Strength (psi)	Passing Strength Criteria (Yes/No)		Fatigue life Nf (Year)
		Minimum	Maximum	
Virgin_5* (0% RAP with AR binder, PG 70-10 + CRM)	149	Yes	Yes	9.4
Virgin_7 (0% RAP with AR binder, PG 64-16 + CRM)	141	Yes	Yes	6.5
HRAP_16H_3 (40% RAP with RA, PG 64-10)	208	Yes	No	5.2
Virgin_6 (0% RAP with AR binder, PG 64-16 + CRM)	129	No	Yes	0.8
HRAP_0H_2 (40% RAP with neat binder, PG 58-22)	120	No	Yes	0.5

Another simulation case of rehabilitation pavement structure of AC overlay on an existing cracked AC layer was also included to investigate the application of mean stiffness as the criteria for evaluating the reflective cracking of non-PRS projects. The stiffness distribution of RHMA, which is a commonly used as an AC overlay material at a frequency of 10 Hz and temperature of 68°F (20°C) in the *CalME* library, is shown in Figure B.5, with a mean value of 598 ksi. Following the procedure proposed in Figure 10.5, the *Strength* criteria range was determined to be 137 to 161 psi, shown in Figure B.6 and Figure B.7.

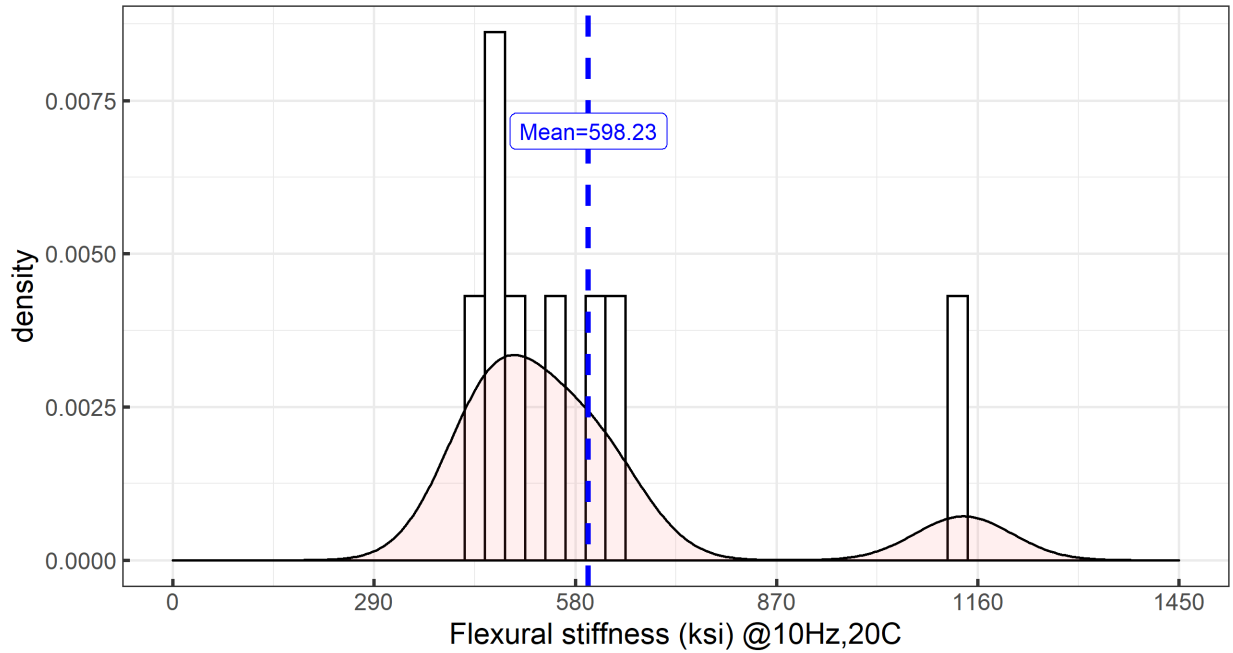
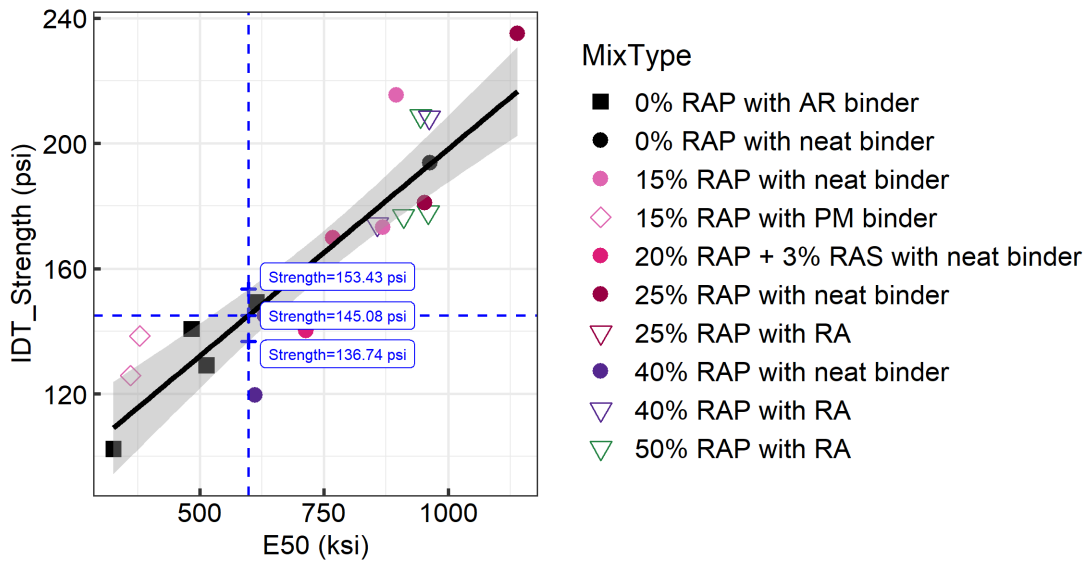
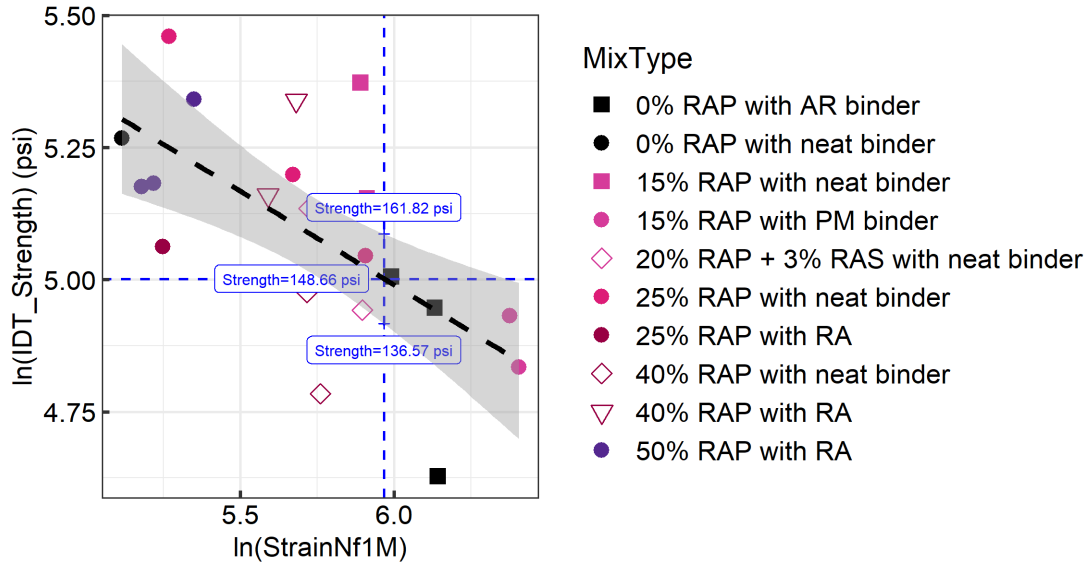


Figure B.5 Histogram of RHMA stiffness from *CalME* material library.



Note: The 95% confidence interval range for strength value is [137 psi, 153 psi], and the strength value on the regression line is 145 psi.

Figure B.6 Determination of $Strength_{min}$ based on mean stiffness of RHMA.



Note: The 95% confidence interval range for strength value is [137 psi, 162 psi], and the strength value on the regression line is 137 psi.

Figure B.7 Determination of $Strength_{max}$ based on mean stiffness of RHMA.

The reflective cracking simulations were then performed in *CalME*, with two materials passing the *Strength* criteria and two materials failing the *Strength* criteria. The inputs for the *CalME* reflective cracking simulation are shown in Table B.3. Given the selected structure information, traffic, and climate zone, the simulated reflective cracking results of two materials passing the *Strength* criteria and two materials outside the *Strength* criteria range are shown in Table B.4. The materials satisfying the *Strength* requirement have better reflective cracking performance, and the material that fails the minimum strength requirement has much lower fatigue life while the one that fails the maximum strength requirement shows comparable reflective cracking resistance with the ones that pass the criteria.

Table B.3: Inputs for *CalME* Simulation of RHMA Over Cracked AC Pavement

Structure	Material	Thickness (mm [ft.])	Traffic	Climate Zone
Layer 1	New AC material	61 [0.2]	Design life: 20 years Growth rate: 5.2% Traffic index: 10.0 Total ESALs: 2 million	North Coast
Layer 2	Cracked old AC	107 [0.35]		
Layer 3	Aggregate base	305 [1]		
Layer 4	Subgrade clay soil	Infinite		

Table B.4: Reflective Cracking Simulation Results from CalME of RHMA Over Cracked AC Pavement

Asphalt Mixture for Layer 1	Strength (psi)	Passing Strength Criteria (Yes/No)		Fatigue Life Nf (Year)
		Minimum	Maximum	
Virgin_5 (0% RAP with AR binder, PG 70-10+ 20% CRM)	141	Yes	Yes	6.7
Virgin_7* (0% RAP with AR binder, PG 64-16 + 20%CRM)	149	Yes	Yes	6.9
HRAP_0H_2 (40% RAP with neat binder, PG 58-22)	120	No	Yes	2.3
HRAP_5H_1 (20% RAP + 3% RAS with neat binder, PG 58-22)	170	Yes	No	7.0

Notes: * is the mixture that only meets the 95% CI criteria and not the criteria from regression line. HRAP_0H_2 fails the minimum *Strength* criterion. HRAP_5H_1 fails the maximum *Strength* criterion.